Green Chemistry

Cutting-edge research for a greener sustainable future

www.rsc.org/greenchem

Volume 9 | Number 2 | February 2007 | Pages 101–192

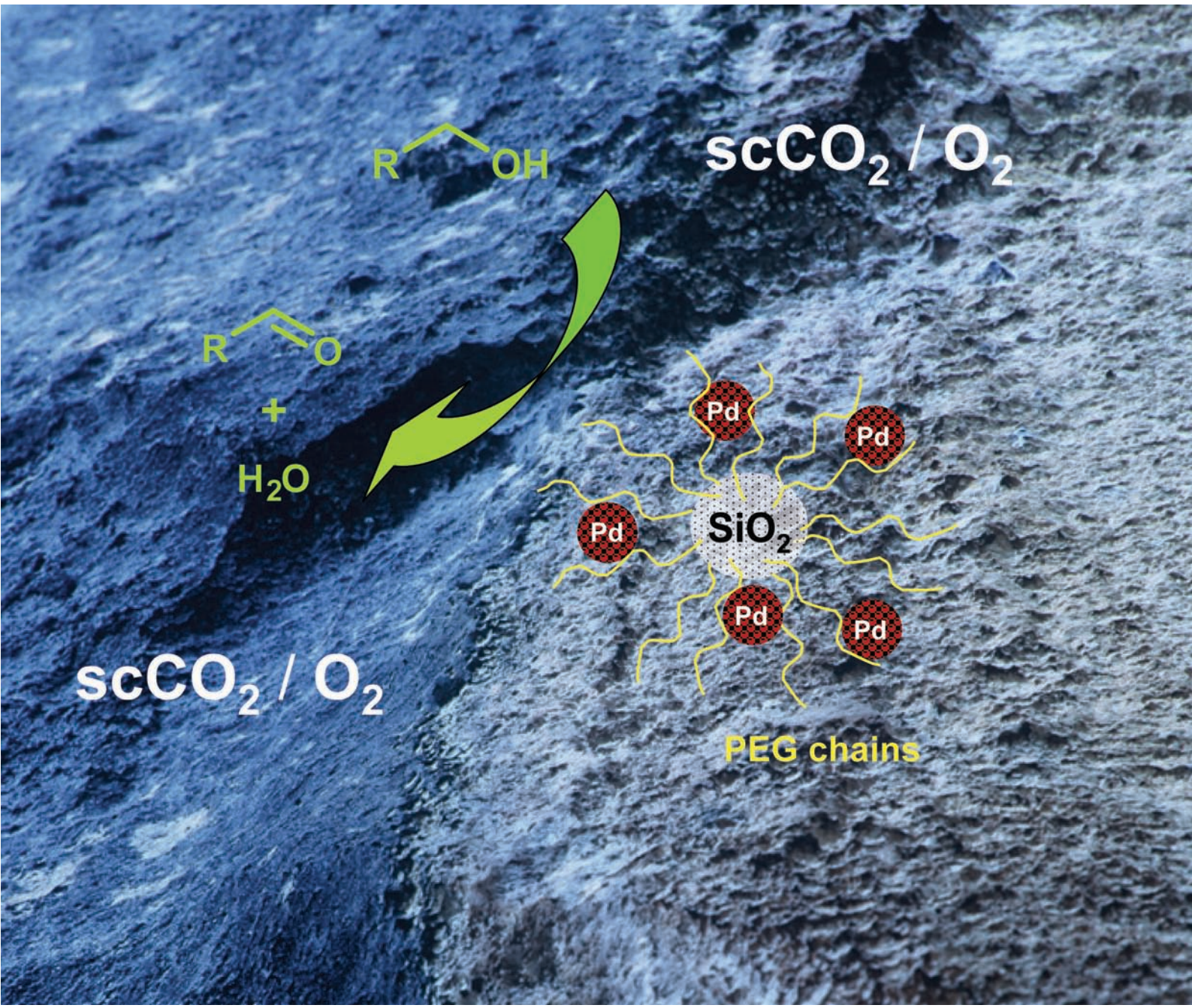

ISSN 1463-9262

RSC Publishing

1463-9262(2007)9:2;1-A

Green Chemistry

Cutting-edge research for a greener sustainable future

www.rsc.org/greenchem

RSC Publishing is a not-for-profit publisher and a division of the Royal Society of Chemistry. Any surplus made is used to support charitable activities aimed at advancing the chemical sciences. Full details are available from www.rsc.org

IN THIS ISSUE

ISSN 1463-9262 CODEN GRCHFJ 9(2) 101–192 (2007)

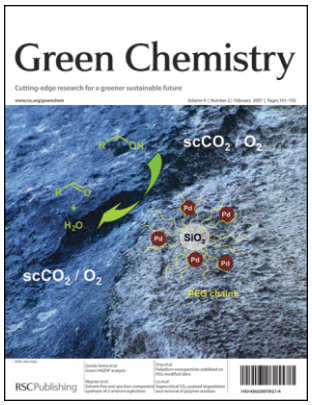

Cover
Palladium nanoparticles stabilised by hybrid materials based on PEG-modified silica are efficient and stable catalysts for the selective aerobic oxidation of alcohols to aldehydes using $scCO_2$ as the mobile phase in continuous-flow processes. Image reproduced by permission of Nils Theyssen from *Green Chem.*, 2007, **9**(2), 127.

CHEMICAL TECHNOLOGY

Chemical Technology highlights the latest applications and technological aspects of research across the chemical sciences.

Chemical Technology
February 2007/Volume 4/Issue 2
www.rsc.org/chemicaltechnology

TUTORIAL REVIEW

Green Chemistry (print: ISSN 1463-9262; electronic: ISSN 1463-9270) is published 12 times a year by the Royal Society of Chemistry, Thomas Graham House, Science Park, Milton Road, Cambridge, UK CB4 0WF.

All orders, with cheques made payable to the Royal Society of Chemistry, should be sent to RSC Distribution Services, c/o Portland Customer Services, Commerce Way, Colchester, Essex, UK CO2 8HP. Tel +44 (0) 1206 226050; E-mail sales@rscdistribution.org

2007 Annual (print + electronic) subscription price: £902; US$1705. 2007 Annual (electronic) subscription price: £812; US$1534. Customers in Canada will be subject to a surcharge to cover GST. Customers in the EU subscribing to the electronic version only will be charged VAT.

If you take an institutional subscription to any RSC journal you are entitled to free, site-wide web access to that journal. You can arrange access via Internet Protocol (IP) address at www.rsc.org/ip. Customers should make payments by cheque in sterling payable on a UK clearing bank or in US dollars payable on a US clearing bank. Periodicals postage paid at Rahway, NJ, USA and at additional mailing offices. Airfreight and mailing in the USA by Mercury Airfreight International Ltd., 365 Blair Road, Avenel, NJ 07001, USA.

US Postmaster: send address changes to Green Chemistry, c/o Mercury Airfreight International Ltd., 365 Blair Road, Avenel, NJ 07001. All despatches outside the UK by Consolidated Airfreight.

PRINTED IN THE UK

Advertisement sales: Tel +44 (0) 1223 432246; Fax +44 (0) 1223 426017; E-mail advertising@rsc.org

Green Chemistry

Cutting-edge research for a greener sustainable future

www.rsc.org/greenchem

Green Chemistry focuses on cutting-edge research that attempts to reduce the environmental impact of the chemical enterprise by developing a technology base that is inherently non-toxic to living things and the environment.

INFORMATION FOR AUTHORS

Full details of how to submit material for publication in Green Chemistry are given in the Instructions for Authors (available from http://www.rsc.org/authors). Submissions should be sent *via* ReSourCe: http://www.rsc.org/resource.

Authors may reproduce/republish portions of their published contribution without seeking permission from the RSC, provided that any such republication is accompanied by an acknowledgement in the form: (Original citation) – Reproduced by permission of the Royal Society of Chemistry.

♾ The paper used in this publication meets the requirements of ANSI/NISO Z39.48-1992 (Permanence of Paper).

Royal Society of Chemistry: Registered Charity No. 207890

COMMUNICATION

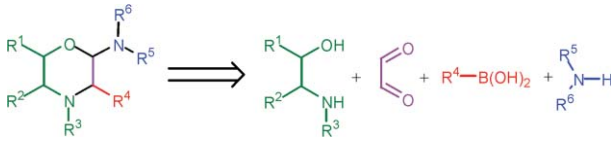

PAPERS

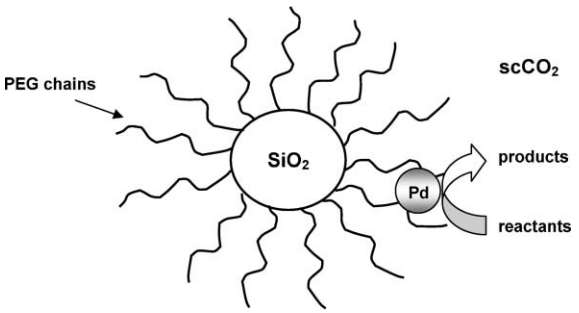

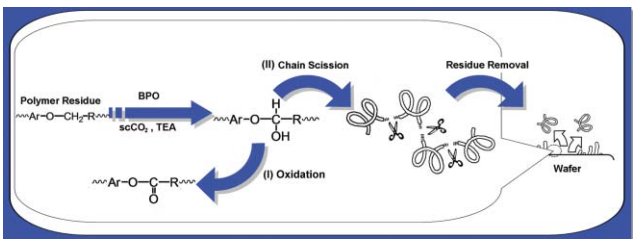

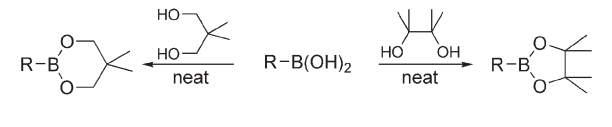

146

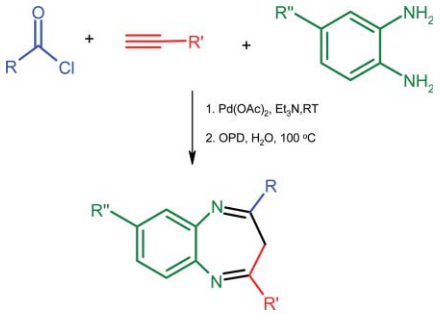

A novel one-pot three-component synthesis of 2,4-disubstituted-3*H*-benzo[*b*][1,4]diazepines in water

Sanjay S. Palimkar, Rajgopal J. Lahoti and Kumar V. Srinivasan*

A novel green and efficient one-pot three-component synthesis of 2,4-disubstituted-3*H*-benzo[*b*][1,4]diazepines in excellent isolated yields has been reported.

153

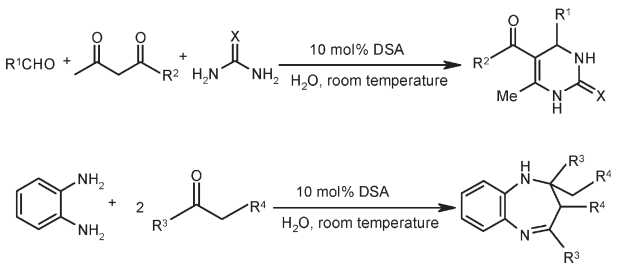

A highly efficient and green method for the synthesis of 3,4-dihydropyrimidin-2-ones and 1,5-benzodiazepines catalyzed by dodecyl sulfonic acid in water

Saikat Das Sharma, Pranjal Gogoi and Dilip Konwar*

A green method for the synthesis of 3,4-dihydropyrimidin-2-ones and 1,5-benzodiazepines employing dodecyl sulfonic acid in water at room temperature is described.

158

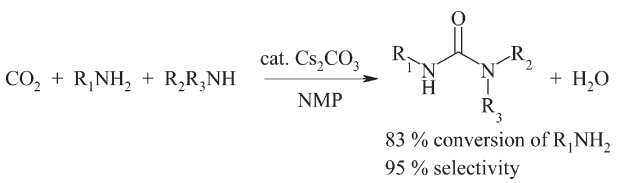

Synthesis of symmetrical or asymmetrical urea compounds from CO_2 *via* base catalysis

Angelica Ion, Vasile Parvulescu, Pierre Jacobs and Dirk De Vos*

Symmetrical or asymmetrical urea derivatives can be prepared from carbon dioxide in good yields using Cs catalysts in NMP, even in the absence of dehydrating agents.

162

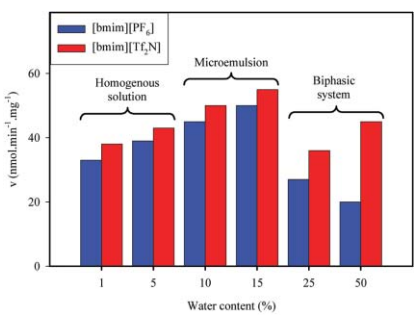

Effect of ionic liquids on epoxide hydrolase-catalyzed synthesis of chiral 1,2-diols

Cinzia Chiappe,* Elsa Leandri, Bruce D. Hammock* and Christophe Morisseau

Effect of water on the csEH catalyzed hydrolysis of β-methylstyrene oxide in IL–water mixtures.

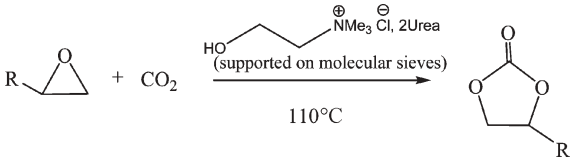

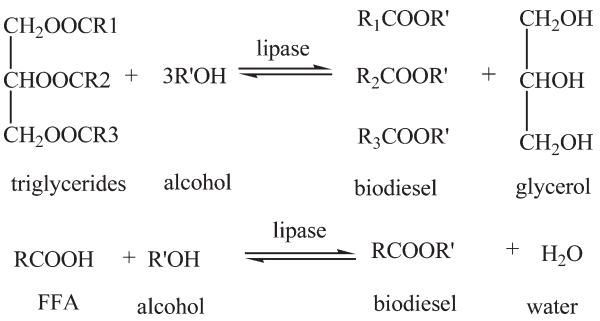

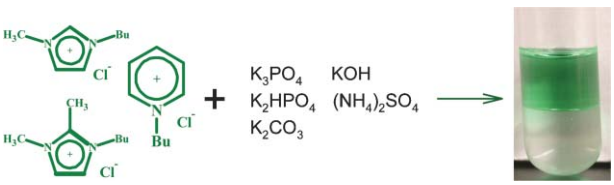

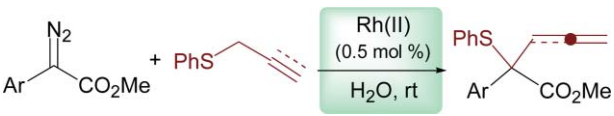

AUTHOR INDEX

FREE E-MAIL ALERTS AND RSS FEEDS

Contents lists in advance of publication are available on the web *via* www.rsc.org/greenchem - or take advantage of our free e-mail alerting service (www.rsc.org/ej_alert) to receive notification each time a new list becomes available.

Try our RSS feeds for up-to-the-minute news of the latest research. By setting up RSS feeds, preferably using feed reader software, you can be alerted to the latest Advance Articles published on the RSC web site. Visit www.rsc.org/publishing/technology/rss.asp for details.

ADVANCE ARTICLES AND ELECTRONIC JOURNAL

Free site-wide access to Advance Articles and the electronic form of this journal is provided with a full-rate institutional subscription. See www.rsc.org/ejs for more information.

* Indicates the author for correspondence: see article for details.

Electronic supplementary information (ESI) is available *via* the online article (see http://www.rsc.org/esi for general information about ESI).

Green HAZOP analysis: incorporating green engineering into design, assessment and implementation of chemical processes

Juan García-Serna,*[a] Jose Luis Martínez[b] and María José Cocero[c]

Received 20th December 2005, Accepted 25th October 2006
First published as an Advance Article on the web 16th November 2006
DOI: 10.1039/b518092a

The expression 'sustainable development' has become a catchphrase in chemical engineering design and operation. There have been several successful attempts for the inherently safer design of processes. There is still a need of guidance tools for design, assessment and implementation of processes using green engineering criteria. Green HAZOP presents a systematic tool based on HAZOP analysis for the incorporation of green engineering criteria within detailed design, commissioning and operation stages. It is aimed at discovering how deviations from the green design intent can occur during the different phases of a project realisation in equipment, actions or materials, and whether the consequences of these deviations can result in a non-green or non-sustainable process. A comprehensive industrial example about Bhopal's pesticide plant and the dramatic accident is presented in text.

Introduction

The severe and tragic accidents that have occurred at chemical and process plants within the last half century have shifted the method of conceptual design towards a more healthy and environmentally friendly safety design process. Learning from accidents is a costly end-point analysis of the problem. However, important lessons can be learnt from these accidents for the prevention and improvement of current and future designs.

Some authors and engineers consider the design of a process a hierarchical procedure where, like an onion, the design process is divided in different layers, starting from an irreducible structure, usually the reaction, continuing with the separation and recycling system, then with the heat exchanger network and finally with the utilities and facilities. This approach is an iterative sequence of steps focused on optimizing the design from both process and economic criteria.[1]

Currently, process, safety and economic reasons are conditions *sine qua non* for a feasible and reliable final design. Environmental considerations are integrated in the sequence to comply with the legal framework of the region in which the plant is going to be installed. Future design guidelines will turn the traditional design scheme into a new one, which combines four main aspects: process, safety, greenness and economics. In other words, the ideal final design will be a jigsaw where all the pieces, *i.e.* process, safety, greenness and economics will fit together.

[a]*c/Prado de la Magdalena s/n, Dpto. Ing. Química y Tecn. Medio Ambiente, University of Valladolid, Valladolid, 47014, Spain. E-mail: jgserna@gmail.com; Fax: (+34) 983423013; Tel: (+34) 983423174*
[b]*Refinería C.I. Puertollano REPSOL-YPF, Carretera de Calzada s/n, Puertollano, Ciudad Real, 13500, Spain. E-mail: jlmartinezgon@repsolypf.com*
[c]*c/Prado de la Magdalena s/n, Dpto. Ing. Química y Tecn. Medio Ambiente, University of Valladolid, Valladolid, 47014, Spain. E-mail: mjcocero@iq.uva.es; Fax: (+34) 983423013; Tel: (+34) 983423174*

Early in 1978, Trevor Kletz suggested that the chemical industry should re-direct its efforts toward elimination of hazards where feasible—by minimization, material substitution, alternative reaction routes, modified storage arrangements ('what you don't have can't leak') and energy limitation—rather than devoting extensive resources to safety systems and procedures to manage the risks associated with the hazards.[2] This novel approach to design was called 'Inherently Safer Design'. ISD means that hazards are eliminated, not controlled, and the means by which the hazards are eliminated are so fundamental to the design of the process that they cannot be changed or defeated without changing the process.[3]

Green engineering (GE), as defined during and after the Sandestin Conference,[4] transforms existing engineering disciplines and practices to those that promote sustainability.[5] It is not aimed at substituting but at transforming the already existing disciplines towards more sustainable practices, by incorporating development and implementation of technologically viable products, processes and production systems (PPSs) that promote human welfare, while protecting human health and elevating the protection of the biosphere as an indispensable criterion in these engineering solutions (see also Table 1).

With regards to GE, there are still a number of questions to answer: what can a chemical engineer do to ensure that a product, a process or a production system is sustainable? What are the metrics and the tools to determine the 'greenness' of a product, a process or a system? Is/Are there any useful industrial guidance tool/s for the design, assessment or implementation of PPSs within the scope of GE? In that case, is/are this/these tool/s universal, unique, easy-to-use, cost-effective and reliable?

Unfortunately, due to the novelty of GE as a discipline there is a lack of material and more specifically of appropriate industrial guidance tools on this topic in the literature. As an example, Agenda 21, the Program of Action adopted at the

Table 1 Draft of green engineering principles (Sandestin)[a,2]

1. Engineer processes and products holistically, use systems analysis, and integrate environmental impact assessment tools.
2. Conserve and improve natural ecosystems while protecting human health and well-being.
3. Use life-cycle thinking in all engineering activities.
4. Ensure that all material and energy inputs and outputs are as inherently safe and benign as possible.
5. Minimize depletion of natural resources.
6. Strive to prevent waste.
7. Develop and apply engineering solutions, while being cognizant of local geography, aspirations, and cultures.
8. Create engineering solutions beyond current or dominant technologies; improve, innovate and invent (technologies) to achieve sustainability.
9. Actively engage communities and stakeholders in development of engineering solutions.

[a] There is a duty to inform society of the practice of green engineering.

Earth Summit in Rio de Janeiro in 1992, requires finding new methods to analyse products, processes and production systems, suggesting the necessity of new ideas and data types for GE, and considers that GE assessment should be developed at both national and international levels.[6]

One of the existing tools was developed within EC Environment Programme 1990–94 co-funded research "Major Industrial Hazards" within the INSIDE project. The INSET Toolkit provides chemists, engineers and managers with the framework and 18 different tools (named using letters from A to R) to systematically identify, evaluate, optimize and select inherently Safety Health Environment (SHE) processes and designs. The proposed tools are applicable at different stages of the design, namely, (1) chemistry route selection, (2) chemistry route evaluation, (3) process design optimization and (4) process plant design.

Another set of tools have been created by Britest Limited, which is composed of a group of companies in the fine chemical and pharmaceutical sectors together with a team of academics, since 1998.[7] The Britest method comprises a set of proprietary tools developed in a structured logical way to fully define the project objective, analyse the transformation and determine how to best, most economically, achieve the objective. These tools provide a logical basis for all stages of the analysis of process design and equipment selection.

The Environmental Health and Safety Committee, EHSC, of the RSC reviewed an assessment procedure called 'Guideword Led Hazard Identification Method', LHI, proposed within a HSE project.[8] This procedure analyses each process combining guidewords, from two lists. The first list is: minimize, substitute, eliminate, moderate and simplify, and the second list is: inventory, pressure, temperature, energy release, process equipment and unwanted reaction.

As Ashforda and Zwetsloot indicated, the willingness of companies to adopt and implement inherently safer options is different for new installations, existing installations that will remain in production for several years (retrofit cases), and for installations that are more or less at the end of their life-cycle (transitional stage).[9] In the same way the willingness of companies to incorporate sustainable solutions will depend on the type of the project as well.

In the last three decades a number of different procedures (set of various steps with applicable techniques) have been proposed to carry out the detailed risk analysis. Among these procedures HAZOP[10] and LHI[8] methodologies have been used to develop a tool incorporating green engineering into design and operation stages. In particular, a modification of HAZOP presented by Khan and Abbasi,[11] which optimizes the HAZOP method, reducing the time spent in doing the analysis by *ca.* 50%, is considered. Also, a multilevel HAZOP introduced by Cagno *et al.*[12] that broke down the methodology into two dimensions: vertical (sequence of operations) and horizontal (operator, control system and plant/process level) is very important.

In this work, green HAZOP is discussed in detail. Firstly, the technique and its scope of application are defined. Then, some useful definitions are listed with regards to clarifying the methodology presented next. The methodology has been subdivided into six different tasks, definition of the problem, selection of the team, preparation for the study, preparation of the data, the systematic analysis and the subsequent trade-off-interpretation of the results. A final case study combining both safety and green analysis based on the Bhopal accident of a carbaryl plant is presented.

Green HAZOP analysis (g-HAZOP)

g-HAZOP is a structured technique in which an interdisciplinary team conducts a systematic study of a process using guidewords to discover how deviations from the green design intent can occur in equipment, actions, or materials, and whether the consequences of these deviations can result in a non-green or non-sustainable process. The results of the g-HAZOP are the team's recommendations, which include the identification of threats to the greenness of the process or, in other words: 'threats to its sustainability', and the recommendations for changes in chemicals, design and procedures to ensure the sustainability of the system. Deviations during normal, start-up, shutdown, and maintenance operations are discussed by the team and are included in the g-HAZOP.

Scope of application

Among the different phases of the realisation of a project, there are three phases in which g-HAZOP can be applied with a high probability of success and effectiveness (see Fig. 1).

• *Basic Engineering*. Normally, the best time to conduct a g-HAZOP is when the design is fairly firm. At this point, the design is well enough defined to allow meaningful answers to the questions raised in the g-HAZOP process. Also, at this point it is still possible to change the design without a major cost. As commented before, g-HAZOP will normally, and it is extremely recommended that it does, come after a safety analysis (HAZOP followed by g-HAZOP). However, depending on the project and its circumstances, g-HAZOP can always be conducted alone

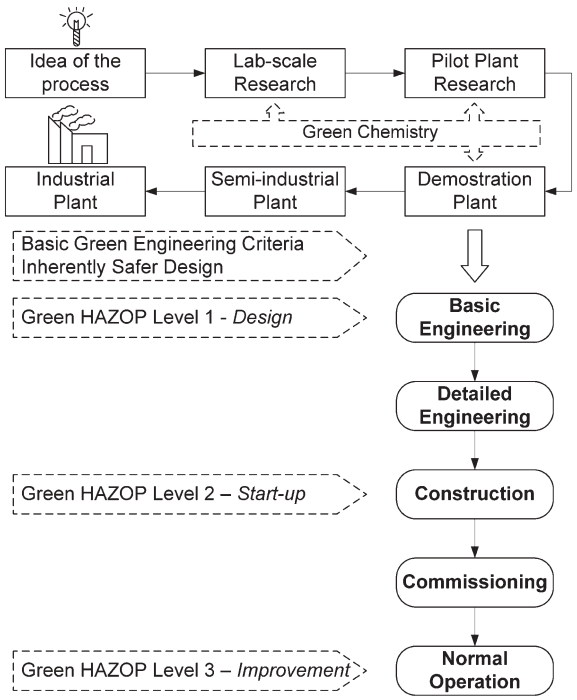

Fig. 1 Phases of a project realisation.

• *Construction*. Commissioning begins after plant construction and concerns its start-up. It is one of the most critical phases of the project as it demands greater specific knowledge, judgement and managerial skill, and as it is followed by a complex uncertainty in events, getting worse with the pressure of time. Added to that, engineering companies cannot risk paying penalties because of not accomplishing with project's guarantees. During construction, several periods can be established, when feasible, to carry out a g-HAZOP analysis applied to the commissioning just before it starts.

• *Normal operation*. The application of g-HAZOP during the normal operation of the plant is enormously convenient for the continuous improvement of the process. Chemical plants experience continuous modifications, like 'living organisms', as a result of day-by-day requirements and even per recommendation in previous HAZOP and g-HAZOP analyses. Accordingly, a major g-HAZOP analysis can be conducted several months before each scheduled stop for maintenance of the plant while minor g-HAZOP analyses can be conducted in the meantime.

To sum up, aspects that will last for the whole project are defined during basic engineering (level 1, design), 'as built' aspects are studied during commissioning (level 2, start-up) and 'process weaknesses' are studied during operation (level 3, continuous improvement).

Useful concepts and main parts of a g-HAZOP

The following terms are used in the g-HAZOP process:

• *Study nodes*: the locations (on piping and instrumentation drawings and procedures) at which the process parameters are investigated for deviations.

• *Design intention*: the way in which a process is intended to function.

• *Guideword*: simple words that are used to modify the green design intention and to guide and stimulate the brainstorming process for identifying process hazards. The library-based approach was used, in which the most appropriate guidewords for the process were selected from the total list of possible guidewords (see Table 3 also).

• *Deviation*: a departure from the green design intent discovered by systematically applying guidewords to process parameters (deviation = guideword + process variable).

• *Cause*: the reason why a deviation might occur.

• *Consequence*: the results of a deviation.

• *Greenness guard*: all the means that, being already installed in the system, may help in the prevention of the causes, or mitigate the consequences, of deviations from sustainability (*e.g.* the insulation of a pipe which is already installed for winterizing but also works for heat conservation).

• *Recommendations*: team's recommendations for chemical substitution, design changes, procedural changes or for further study.

• *Green expert information base (GEIB)*: an expert knowledge base consisting of information of causes of process deviations and their consequences for various components aimed at simplifying and saving time in the analysis of new components. It can be an Excel file, a Word file or a relational database collecting the experience from previous analyses.

• *Green cost trade-off simplified analysis* (g-TOSA): an instrument used to quantify the relationship between key economic and some indicators of the 'greenness' and safety of a product, a process or a production system. It measures these indicators at the level of the node analysed during the g-HAZOP and then aggregates the results from individual fields to area, unit or chemical plant levels.

Some examples that may help in the understanding of these concepts can be found within the case study presented later in the text.

Sequence of activities and methodology

How to structure the g-HAZOP analysis as a systematic task is presented in this section. The normal way of conducting the g-HAZOP is in a linear way, in which the main steps are: firstly, the definition of the purpose, objectives and the scope of the study; secondly, the selection of the team; thirdly, the preparation of the documentation for the study; next, carrying out the team reviews (this step includes different steps), and finally recording the results. This is a linear procedure which relies on the experience of the persons participating in the g-HAZOP at that time. The full list of activities is presented in Table 2 (activities without a prime) and their sequence in Fig. 2 and 3 (algorithm detailed explanation). It is important to note that some of these steps can take place at the same time. For example, the team reviews the design, records the findings, and follows up on the findings continuously. Thus, working with some steps in parallel will notably reduce the time spent in the whole process. How and when this reduction is going to be effective relies on the expertise of the team leader.

Green expert information base (GEIB). In order to optimize g-HAZOP a 'green expert information base' (GEIB) can be

Table 2 List of activities pre, during and post g-HAZOP analysis

Item[a]	Description
1	Define the purpose.
2	Select the team.
3	Collect data and information from plant and GEIB.
4	Identify nodes. Plan for discussion sessions.
5	Generate deviations (guideword + variable).
5′	Use GEIB for causes.
6	Find causes.
6′	Use GEIB for consequences prediction.
7	Consult data and discuss in the meeting.
7′	Examine greenness guards and compare those in GEIB.
8	Develop consequences.
8′	Generate preliminary recommendation report.
9	Examine greenness guards.
9′	Generate a rough g-HAZOP report.
10	Manage all the constraints.
11	Develop final recommendations.
12	Generate the final g-HAZOP report.

[a] Steps without apostrophe refers to the normal g-HAZOP and steps with a prime (*e.g.* 3′) refer to an optimised g-HAZOP (GEIB).

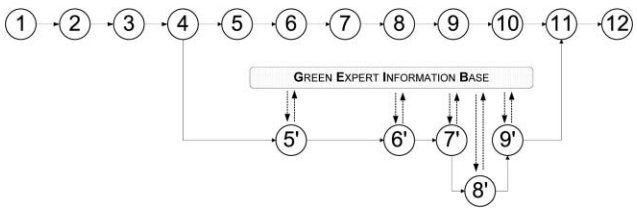

Fig. 2 Green HAZOP sequence of activities.

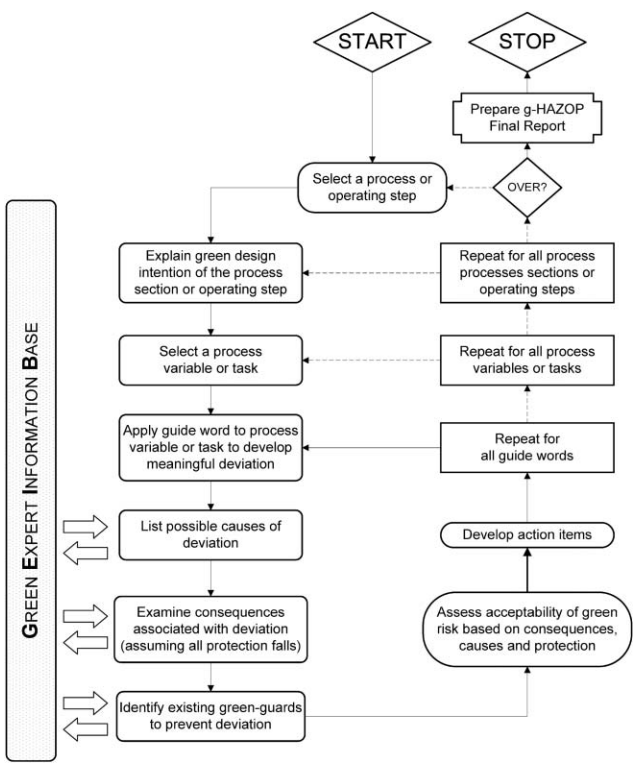

Fig. 3 Green HAZOP algorithm flow.

included in the process (see activities with a prime in Table 2 and Fig. 2). In this case, the identification of causes and consequences is imported from an expert database, which accumulates previous knowledge on other processes. As already defined, GEIB is an expert knowledge base consisting of information for process deviations, their causes, and their immediate consequences for various components (process/equipment/pipeline/systems, *etc.*) within the scope of green engineering. The GEIB aids in the realisation of the g-HAZOP analysis and at the same time it gets a feedback from the analysis (see Fig. 2 and 3).

Define the purpose, objectives, and scope of the study

The purpose, objectives and scope of the study should be made as explicit as possible. A clear green engineering point of view is essential for this analysis. For guidance on what others do to be green, the nine draft recommendations resulting from the Sandestin Conference have been transcribed in Table 1. The main objectives will be set between the person responsible of the plant and the g-HAZOP leader (typically a chemical engineer with founded knowledge on GE) before the analysis. It is important that this interaction take place to provide the proper authority to the study and to ensure that the study is focused. Also, even though the general objective is to identify green risks and sustainability problems, the team should focus on the underlying purpose or reason for the study. Example reasons for a study might be to check the green design or improve an existing one, to develop a list of questions to ask a supplier, to check operating and green procedures or to verify if instrumentation or equipment is working properly at the maximum efficiency. It is also important to define what specific consequences to consider, such as employee safety and comfort (in plant or neighbouring research centre), the loss of sustainability indicators (*i.e.* loss of an ecolabel), the reliability and the potential environmental impacts.

Select the team

Ideally, the team consists of five to seven members, although a smaller team could be sufficient for a smaller plant. The size of the team should optimize the use of time and promote the creation of ideas. The team leader should have experience in leading a g-HAZOP. The team leader has critical responsibility in the g-HAZOP study; he should arrange all documents and essential information, and decide about discussion sessions

Table 3 g-HAZOP guidewords and their significance

Guidewords[a]	Application
No	Negation of the design intent
Less	Quantitative decrease
More	Quantitative increase
Part of[b]	Qualitative decrease
As well as[b]	Qualitative increase
Reverse	Logical opposite of the intent
Other	Complete or partial substitution

[a] Guidewords are shared with those of HAZOP analysis with regards to establish as many analogies as possible between both methods. [b] Limited use. Use 'less' and 'more' instead.

according to requirements of the project and the ability and aptitudes of the team members. The discussion sessions should be conducted in a relaxed atmosphere so that everyone should feel free to contribute in the study. The leader should introduce the team into a suitable 'atmosphere', for instance, remembering the main aspects of green engineering and its principles and some previous successful examples. During the discussion, the leader should also take care that no-one should dominate the discussion, and discussion should not deviate from the main goal. A very important point to be remembered during the discussions is that more emphasis should be given to the problem identification and assessment (non-green situations) rather than problem solving (non-green problem management). The fact is that the whole group should be sensitive to green goals. It is recommended that if a previous HAZOP analysis has been conducted, part of the team that has participated in the HAZOP also participate in the green HAZOP. When feasible, the team must integrate the gender dimension, having equal number of men and women.

A team should include: a team leader (chemical engineer specialised in green engineering), a process/control engineer, a plant operating engineer, a maintenance specialist (one of these should be selected by the team leader: instrumentation, static equipment, dynamic equipment, inspection and verification depending on the case), a chemist (researcher specialised in green chemistry), a safety engineer (extremely important), plant operator chief (they know how plants run on a day-to-day basis, their experience is invaluable). Among them one should act as a coordinator/secretary taking notes. The team leader's most important job is to keep the team focused on the key task: to identify problems, not necessarily to solve them. In other words, the aim is not to identify and solve a green problem at the same time but to identify as many problems as the team can (causes identification this is the most creative phase).

Prepare for the study

The amount of preparation depends upon the size and complexity of the plant. The preparative work consists of three stages: obtaining the necessary data; converting the data into a suitable form and planning the study sequence; and arranging the meetings.

Obtain the necessary data. Typically, the data consist of various drawings in the form of: line diagrams, flowsheets, plant layouts and isometric and fabrication drawings. More specifically, for a g-HAZOP, the additional information required would be: the safety data sheets with environmental data, the issues of the life cycle of the main products, a green area classification of the plant and any other data that can be relevant for this purpose (this data will be selected and analysed by the leader).

Prepare the data. Data must be inspected to make sure they pertain to the defined area of study and contain no discrepancies or ambiguities. In addition to this, data must be converted into a suitable form for the analysis. The study sequence must be planned at this stage.

Arrange the necessary meetings. The team leader is in a position to plan meetings. The first requirement is to estimate the team-hours needed for the study. The ideal rate is 4 nodes per session. A g-HAZOP session should be limited to 3–4 h and hourly breaks are recommended. Thus, for instance, a g-HAZOP for the study of 8 to 20 nodes will last between 2 and 5 days, approximately. The total number of nodes will be determined at the beginning by the team leader after the g-HAZOP objectives has been defined. Nevertheless, when an external consultant or consultancy is hired to conduct the analysis these figures can be increased.

Carry out the team review

The main objective, scope of the g-HAZOP, available information, date and duration of the meeting, and team members and their position should be written down before starting the analysis. The g-HAZOP concept aims to review the plant in a series of meetings, during which an interdisciplinary team methodically 'brainstorms' the plant design, following the structure provided by the guidewords and the team leader's experience.

The team focuses on specific points of the design (called 'study nodes'), one at a time. At each of these study nodes, deviations in the process parameters are examined using the guidewords. It should be done node by node to be as systematic as possible. The guidewords are used to ensure that the design is explored in every conceivable way. Thus, the team must identify a fairly large number of deviations, each of which must then be considered so that their potential green causes and consequences can be identified. This brainstorming stimulates creativity and generates ideas. The iterative procedure is presented in Fig. 3 and 4.

Guidewords are simple words which are used to qualify or quantify the intention in order to guide and stimulate the brainstorming process, thereby discovering deviations. The chosen guidewords are the same as the guidewords used in HAZOP.[5] Nevertheless, some specific words have been added. Each guideword is applied to the process variables at the

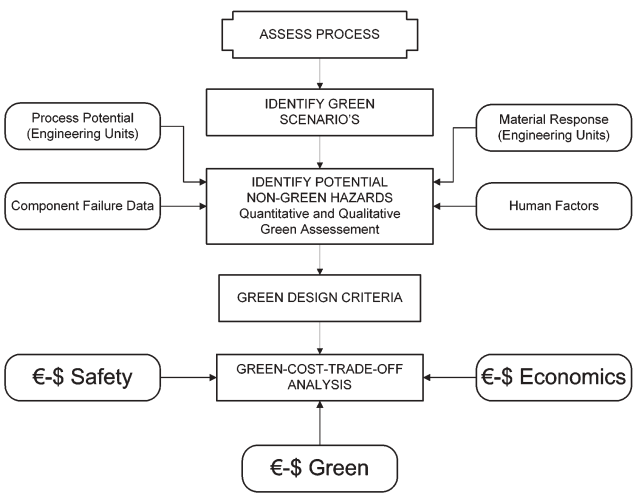

Fig. 4 Green HAZOP concept flow diagram and cost–trade-off analysis.

Table 4 Parameters and their physical significance in g-HAZOP

Area	Pre-parameter	Parameter	Notes[a]
Raw materials and products	Material	Renewable	Material source renewable or depleting.
	Energy		Energy source renewable or depleting.
	Material	Diversity	Minimum number of substances or parts.
	Energy		Minimum number of energy sources.
		Entropy/preserve function	Preserve the function as long as possible.
	Material	Minimization	Minimum use of material flows.
	Energy		Minimum use of energy flows.
	Space		Minimum use of space.
	Time		As quick as possible.
	Material	Toxicity	Use substances inherently non hazardous.
Process	Material	Over-design/over-capacity	Use the exact amount of materials.
	Energy		Use the exact amount of energy.
	Material	On demand	Material flows should be better output pulled than input pushed.
	Energy		Energy flows should be better output pulled than input pushed.
	Volume		Equipment over-design.
		Gaseous or liquid emissions	Reduce gaseous emissions (CO_2, CO, NO_x, SO_x, *etc.*).
		Waste generation	Waste should not exist. Reuse and recycle.
Efficiency	Material	Efficiency	Efficient processes in terms of mass balance
	Energy		Efficient processes in terms of energy balance
	Space		Efficient processes in terms of space.
	Time		Efficient processes in terms of time. For batch operation and start-up period.
Integration	Material	Integration and interconnectivity	Integrate material flows avoiding waste.
	Energy		Integrate energy flows avoiding heat loss and energy quality loss (pinch).
	Environment		Improve the environment with the construction.
Controllability		Controllability	Controllability of material flows and equipment.
		Operability	Operability of material flows and equipment.
			Controllability of energy flows and equipment.
Life cycle		Immortality	Targeted durability, not immortality, design goal. Biodegradability.
		Performance in 'afterlife'	What is going to happen after the product is used?

[a] See the twelve principles of green engineering for more information about the green philosophy.[13,14]

point in the plant (study node) which is being examined. The parameters to study in g-HAZOP are listed in Table 4, but not limited to them; depending on the case other parameters can also be evaluated. These parameters are based on the twelve engineering principles.[13,14]

Compile the results

The process of compiling the results is an important part of the g-HAZOP, because it is going to be the visible part of the work. So, it is very important that all the ideas are included in the final report, although it is impossible to record manually all that is said during the meetings. It is very useful to have the team members review the final report writing and then come together for a report review meeting. The process of reviewing key findings will often fine-tune these findings and uncover others. The success of this process demands a good recording scheme. g-HAZOP model forms should be filled in during the meeting.

Green-cost trade-off simplified analysis (g-TOSA)

How to decide whether one g-HAZOP recommendation is feasible or not, a crucial point for decision makers, is not always easy to solve. This step comes right after the final g-HAZOP report is generated (Fig. 4). g-TOSA is simpler than conventional trade-off analysis (TOA). Economic, safety and green aspects must be considered at the same time for the final decision to be credible. In the g-TOSA these three aspects are evaluated from 1 to 5 to help on the final decision of carrying out the results of the g-HAZOP (team's recommendations) in that node, area or plant unit. Evaluation scales are shown in Table 5. Results are presented in a 3D vector, called SGE vector: [safety, greenness, economics]. Thus, depending on the

Table 5 g-TOSA qualitative evaluation scale

Severity scale (safety)

Value	Evaluation	Description
1	Very high	Several victims
2	High	One victim or hospitalised
3	Medium	Injured people
4	Low	First Aid required
5	Very low	Non observable effects

$$|SGE| = (w_1 \cdot S^2 + w_2 \cdot G^2 + w \cdot_3 E^2)^{1/2} \quad (1)$$

Non-greenness scale (greenness)

Value	Evaluation	Description
1	Brown	It damages the environment very seriously
2	Light brown	It damages the environment seriously
3	Yellow	It neither damages nor improves
4	Light green	It improves the environment slightly
5	Green	It improves the environment enormously

Cost scale (economics)

Value	Evaluation	Description
1	Very high	Major modification of the whole process
2	High	Major modification of the process unit
3	Medium	Modification or addition of major equipment
4	Low	Modification or addition of minor equipment
5	Inexpensive	Very low cost

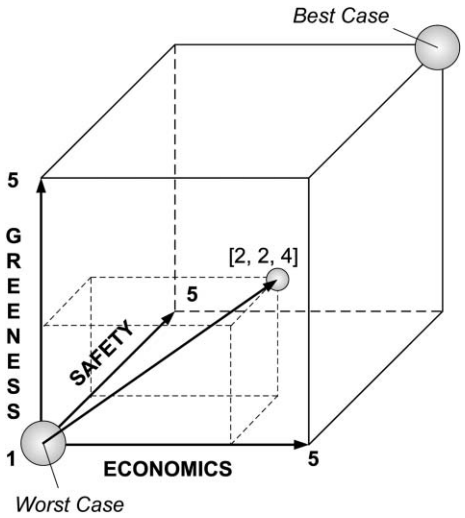

Fig. 5 Green TOSA analysis.

case, the three different components are differently weighted, w_1, w_2 and w_3, as presented in eqn 1. SGE modulus, |SGE| is used to compare and contrast different alternatives. These results can also be plotted as spheres within a 3D-cube, as shown in Fig. 5.

Generally, carrying out a team's recommendation favours one aspect against the other two, although this is not necessarily true. How to organize and when to include the g-TOSA to help in the g-HAZOP analysis is presented in Fig. 6. BASF has created two useful tools, namely, Eco-efficiency™ analysis and SEE™ balance that use this methodology to evaluate societal-environmental and economic aspects related to the sustainability of a project.[15]

The main factors on which the success or failure of g-HAZOP analysis rely

• The correct delimitation of the scope of study going from the previous recommended safety study to the depth of green engineering analysis.

• The completeness and accuracy of drawings and other data used as a basis for the study.

• The technical skills and insights of the team about green engineering and sustainability.

• The ability of the team to use the approach as an aid to their imagination in visualizing deviations, causes, and consequences and possible greenness guards.

• The ability of the team to concentrate on the more serious green hazards or potential which are identified (maximum efficiency).

• The availability and quality of the green expert information base.

Lack of experience of the team leader and of other members seems to be the most evident reason for the failure of g-HAZOP, providing GE is one of the most challenging disciplines of present science. The mistake of making the plant just safe and not going beyond to making it sustainable during the g-HAZOP analysis is going to be one of the most complicated challenges.

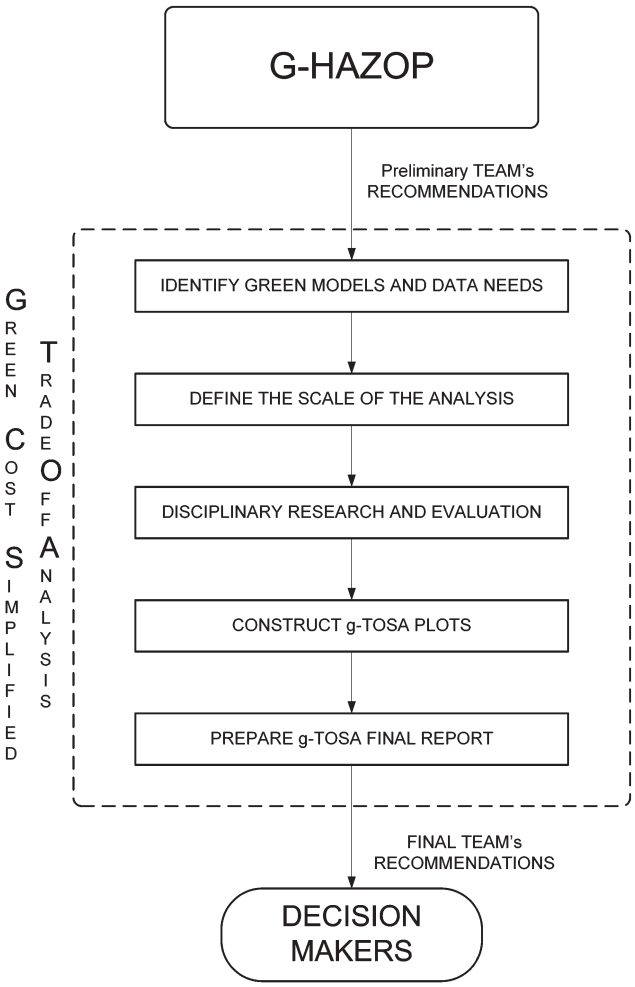

Fig. 6 Overview of the green TOSA.

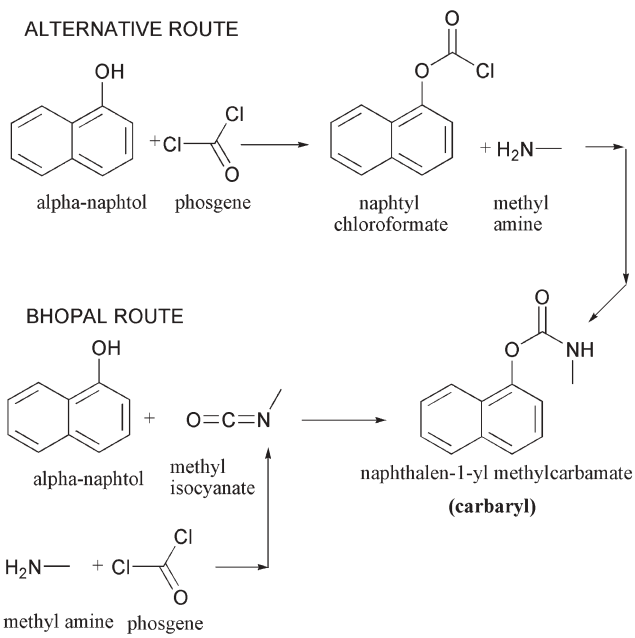

Scheme 1 Production of the insecticide carbaryl.

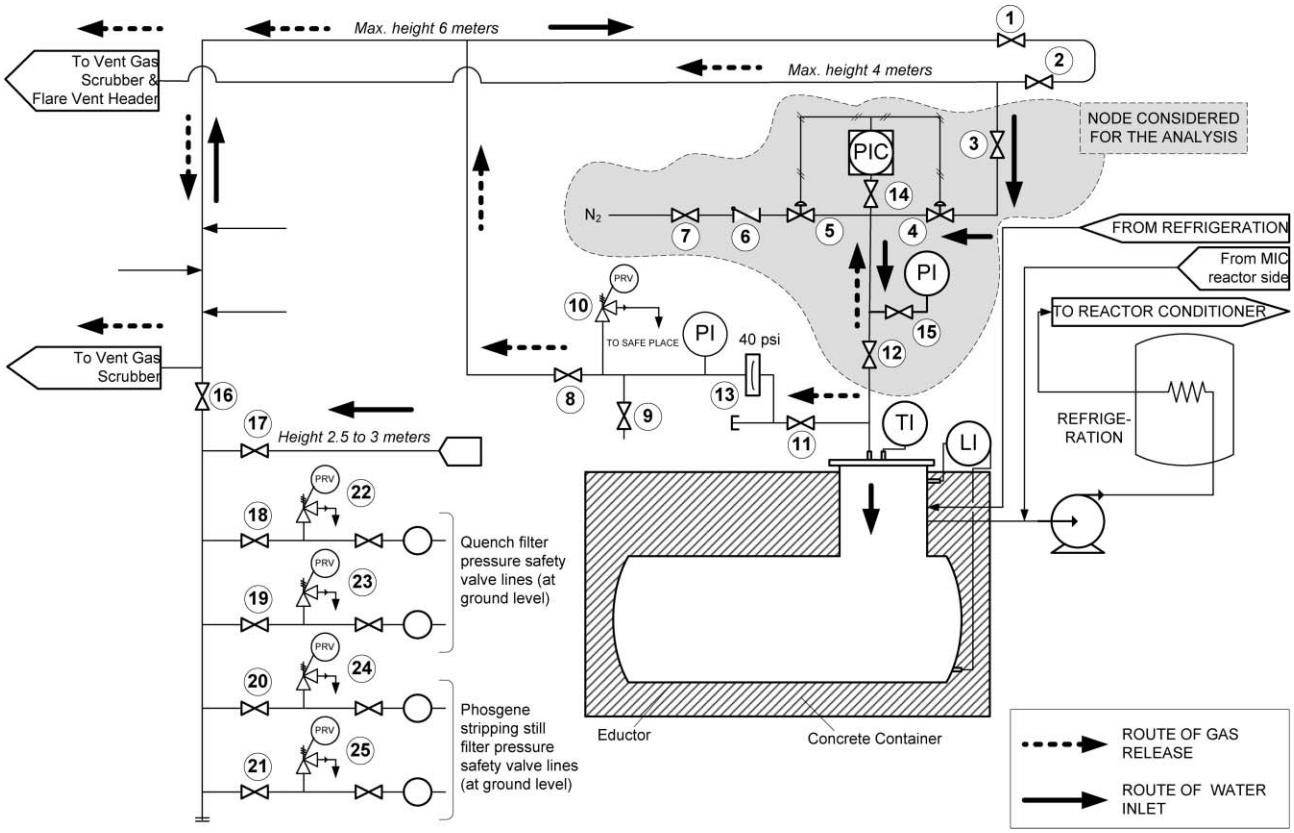

Fig. 7 Process and instrumentation diagram of tank no. 610 of the Bhopal accident plant.[13] (1) Interconnection isolation valve. (2) Interconnection PVH isolation valve. (3) PVH isolation valve. (4) Vent control valve. (5) Nitrogen control valve. (6) Check valve for nitrogen line. (7) Nitrogen header isolation valve. (8) RVVH isolation valve. (9) RVVH bleeder valve. (10) Relief valve for MIC tank. (11) First RVVH isolation valve for MIC tank. (12) First PVH isolation valve for MIC tank. (13) Rupture disk. (14) PIC isolation valve. (15) PI isolation valve. (16) RVVH isolation valve. (17) Valve from which water for flushing was apparently let in. (18)–(21) Down-stream isolation valves for filters. (22)–(25) Bleeder valves. RVVH, relief valve vent header; PVH, process valve vent header; VGS, vent gas scrubber; FVH, flare vent header; MRS, MIC reactor side.

Case study

One of the worst accidents in the history of the chemical industry occurred in the Union Carbide plant at Bhopal, India on 3 December 1984. This example has been selected for three main reasons: first, it illustrates quite well how essential safety is in chemical industry, secondly, it is a well known example and engineering details of the accident can be easily found in the literature, *e.g.* between 1984 and 2003 thirty-five books based on the Bhopal gas tragedy and 400 papers containing 'Bhopal' as a keyword have been published;[16] and finally, it is a good model to show how green engineering can improve the operation and design of a plant in order to achieve sustainability.

Description

At this plant an insecticide called carbaryl (*n*-methyl carbamate) was produced. Carbamates are the third major group of synthetic organic insecticides, developed after organochlorine and organophosphorus compounds. Because of their high degree of biodegradability, they are free from the persistence and bioaccumulation associated with organochlorines. Carbamates, although often highly toxic to humans and higher animals, are reversible inhibitors of acetylcholinesterase and much safer to use than the irreversible organophosphorus inhibitors. Carbamates became widely used for soil insects and in foliar application to field and vegetable crops as feasible substitutes of DDT.[17] Carbaryl was produced at Bhopal's plant by reacting in one step phosgene with methyl amine to produce methyl isocyanate, and in a second step reacting this methyl isocyanate with alpha-naphthol (see Scheme 1). Methyl isocyanate (MIC) is an intermediate of the reaction and it was stored in a buried tank. MIC is an extremely toxic (LC_{50} mice 29 mg m^{-3}), highly volatile (vapor pressure 348 mmHg at 20 °C, boiling temperature 43–45 °C) liquid, and it reacts with water in an exothermic reaction producing methylamine and carbon dioxide, both gases.

What happened at the Bhopal plant

The most extended explanation of the catastrophe indicates that the Bhopal tragedy started when one of the three buried tanks of MIC became contaminated with water and a runaway reaction occurred.[18] The temperature and pressure rose rapidly, the rupture disc and pressure safety valve lifted and MIC vapour went to the scrubber, but as the scrubber was not working properly the toxic gas got past it and it was discharged into the atmosphere through a vent situated at

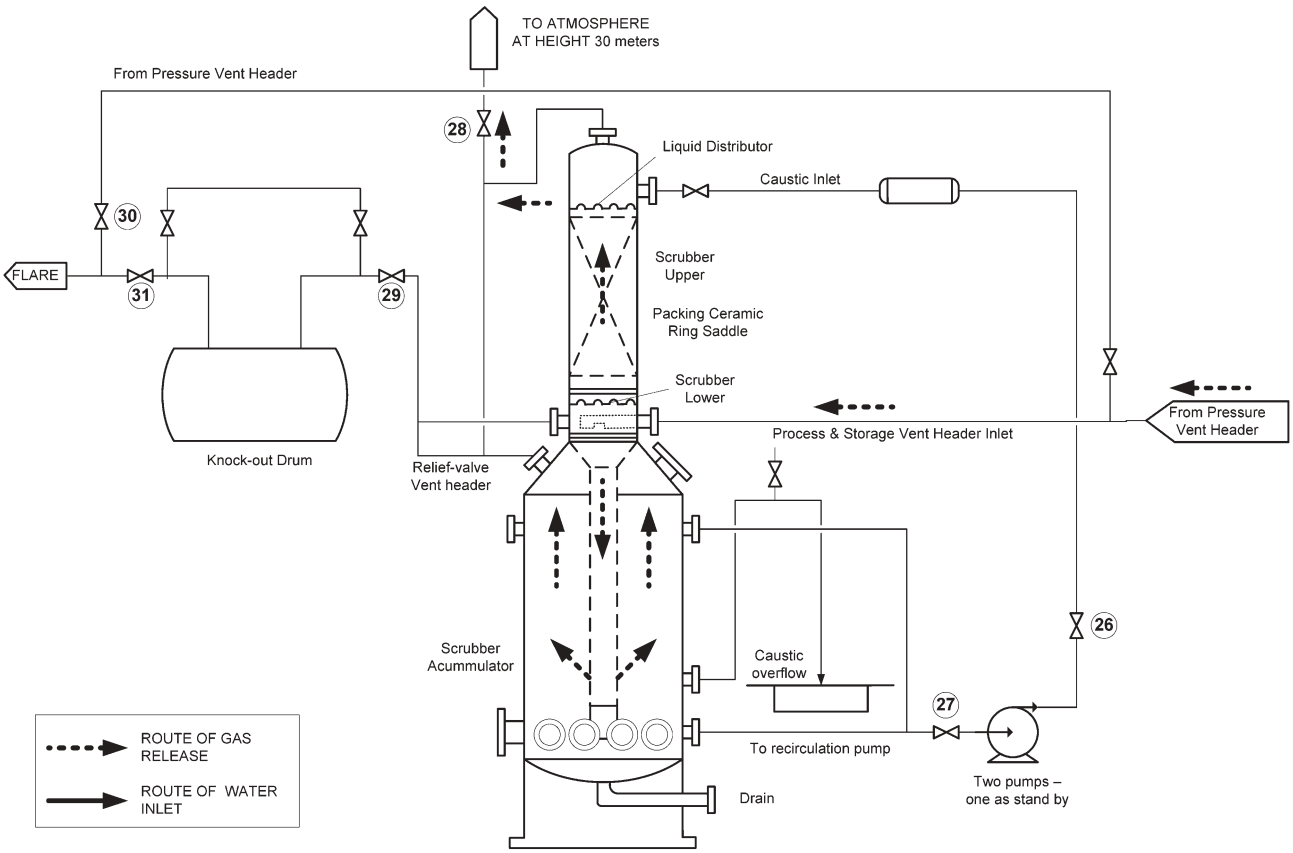

Fig. 8 Process and instrumentation diagram of the scrubbing system and flare of the Bhopal accident plant.[13]

30 metres from the ground. Several problems occurred at the same time: the refrigeration system to cool down the storage tank was also shut down, the scrubbing system which should have absorbed the vapour was not immediately available and the flare system, which should have burnt any vapour which got past the scrubbing system, was out of use.

Simplified process and instrumentation diagrams of the system are given in Fig. 7 and 8. These diagrams have been obtained from the Trade Union Report on Bhopal.[19]

HAZOP analysis

A hazards and operability (HAZOP) analysis has been conducted to the most critical node of the Tank No. 610, the blanketing line (see Fig. 7), targeted at identifying the main safety problems, their causes and consequences. The complete analysis is presented in Table 6, the main conclusions are detailed next. 'Less flow' in the tank vent line can cause low pressure in the vessel during emptying and should be solved by installing a low pressure interlock system, which stops the pump, and some alarms related to it. The problem of 'no flow' is easily solved by establishing 'lock open' in all the isolation valves of the line. A critical problem has been found in 'reverse flow', which may allow any compound, water included, to enter the MIC tank; a check valve must be installed after valve no. 4 (see Fig. 7 and Table 6, Recommendations 8.1.1.1 and 17.1.1.1). In addition to this, water must not be permitted near the tanks (Table 6, 17.1.1.2) and in the vent lines (Table 6, 17.1.1.3). The official point of view of the disaster pointed out that the entering of water in the tank was the most probable cause of the accident. It should be stressed that simple recommendations, such as 17.1.1.1, 17.1.1.2 and 17.1.1.3, could have averted the toxic cloud release.

Green HAZOP analysis

Once the HAZOP analysis is finished, the main safety features are fullfilled. Then, a g-HAZOP has been conducted aimed at improving the plant from the green engineering viewpoint. Table 7 shows detailed results of this study, which are summarised below.

For the case of 'more entropy' the authors find that, first, the nitrogen vent causes a continuous MIC release into the scrubber, which is retained within the caustic reservoir, causing a loss in product and an increase in entropy. This cannot be avoided easily to assure a safer operation. However, in the case of an emergency, when the rupture disc opens the system is depressurised completely, which implies a serious hazard and loss of product. For this case the substitution of the rupture disc by a pressure safety valve is recommended (see Table 7, Recommendation 3.1.1.1). 'More toxicity' is one of the key deviations of the g-HAZOP. MIC is extremely toxic and volatile, therefore its substitution is highly recommended. There are two possibilities, one route using methyl formamide (MFA) which implies the co-production of hydrogen and another route using the same reagents but reacting alpha-naphthol with phosgene first (see Scheme 1 and Table 7, 7.1.1.1). The loss of product can be minimised by

Table 6 HAZOP analysis for the selected case study

Guideword	Deviation	Causes	Consequences	Safety guards	Recommendations
More	Flow	1. Pressure in tank increases.	1.1. Pressure in the line increases up to control valve.	1.1.1. Lines are designed to support that pressure. No consequences for safety (NCFS).	
		2. Control system fail.	2.1. More vent gas to scrubber. Scrubber pressure increases. Scrubber cannot clear all the vented gas. Gases containing methyl isocyanate (MIC) are vented to atmosphere. Gases containing MIC are vented to the flare system.	2.1.1. Pressure safety valves (PSV) connected to the flare. 2.1.2. Bypass line direct to the flare. Rupture disk.	
		3. Nitrogen excessive inlet or fail open or 'less nitrogen'.	3.1. More pressure in the vessel and line until the rupture disc. Rupture disc discharges to the scrubbing system and to the flare.	3.1.1. *Idem* 1.1.1 and 2.1.1.	
Less	Flow	4. Control valve closes.	4.1. *Idem* 1.1. 4.2. *Idem* 3.1.	4.1.1. *Idem* 1.1.1.	
		5. Nitrogen valve closes.	5.1. Low pressure in vessel during emptying.	5.1.1. Possibility of backward pressurization through the scrubber line.	5.1.1.1. Install an low pressure interlock that stops the feed pump. 5.1.1.2. Add low alarm to the PIC. 5.1.1.3. Install a bypass line in the control valve for manual control in case of fail.
No	Flow	6. *Idem* 'less flow'.	6.1. *Idem* 4.1 and 4.2.	6.1.1. *Idem* 4.1.1.	
		7. Any isolation valve of the circuit is manually closed.	7.1. *Idem* 'less flow'.	7.1.1. *Idem* 4.1.1.	7.1.1.1. Establish 'car seal open (CSO)' and 'lock open (LO)' in all the isolation valves of this circuit.
Reverse	Flow	8. More pressure downstream of the line than in the vessel.	8.1. Other gas and liquid products enter the vessel. If water it will react with MIC increasing pressure and temperature of the vessel.	8.1.1. No safety guard.	8.1.1.1. Install check valve in the gas discharge line after PIC.
			8.2. Vaporization of MIC. Gases to scrubbing system and flare.	8.2.1. Scrubber's PSV connected to flare.	
More	Pressure	9. *Idem* 'more flow 1 and 2'.	9.1. *Idem* 1.1 and 2.1.	9.1.1. *Idem* 1.1.1, 2.1.1 and 2.1.2.	*Idem* 2.1.1.1.
Less	Pressure	10. *Idem* 'less flow 4'.			
More	Temperature	11. Refrigeration system fails.	11.1. *Idem* 'more pressure' 9.1.	11.1.1. Gases sent to the flare from scrubbing system.	
			11.2. *Idem* 8.2.	11.2.1. *Idem* 8.2.1.	
		12. MIC product enters hotter.	12.1. *Idem* 9.1.		
		13. Temperature indicator fails measuring less temperature than existing.	13.1. Refrigeration system does not refrigerate enough and MIC is vaporised.	13.1.1. No safety guard	13.1.1.1. Duplicate and install reliable temperature indicators.
		14. Higher external temperature (*e.g.* summer).	14.1. *Idem* 13.1.	14.1.1. Tank buried.	14.1.1.1. Insulate the tank properly.
Less	Temperature	15. Lower external temperature (*e.g.* winter).	15.1. Product is cooled.		
		16. Temp. indicator fails measuring + temp. than real.	16.1. *Idem* 15.1.	16.1.1. NCFS.	
Other	Composition	17. Water enters the vessel.	17.1. MIC is contaminated. Water reacts with MIC producing CO_2 and methylamine. Pressure and temperature increases due to highly exothermic reaction.	17.1.1. No safety guard.	17.1.1.1. Install check valve in the blanketing line. 17.1.1.2. Water must not be permitted near the tank. 17.1.1.3. Establish 'car seal close CSC' and 'lock close (LC)' in the valve-17. Install a blind disk.
		18. Phosgene enters the vessel.	18.1. MIC is contaminated. NCFS.		

Table 6 HAZOP analysis for the selected case study (*Continued*)

Guideword	Deviation	Causes	Consequences	Safety guards	Recommendations
19. Refrigeration system failure			19.1. Tank's temperature rises. *Idem* 'more temperature'.		
20. General electric power failure			20.1. Stop of the refrigeration pumps. See 'more temperature'.		
			20.2. General plant stop.	20.2.1. Valve to their safety position. 20.2.2. Interlock systems working. 20.2.3. Emergency stop systems working.	
21. Instrumentation air failure			21.1. Control valves to their safety position. See 'less pressure' and 'more flow'.		
22. Nitrogen failure			22.1. *Idem* 'less pressure'.		

Table 7 Green HAZOP analysis for the selected case study

Guideword	Deviation	Causes	Consequences	Greenness guards	Recommendations
	Material renewable	N/A			
	Energy renewable	N/A			
Other	Material diversity	1. Use of NaOH in an auxiliary system.	1.1. Different substance not for the process but for safety. Contamination of products.		
	Energy diversity	N/A			
More	Entropy	2. Continuous vent of N_2 + MIC.	2.1. MIC reacts in the scrubber	2.1.1. MIC—Na^+ can be recovered from the spent caustic solution. Only for controlled releases.	
		3. Rupture disc discharges.	3.1. MIC is burnt at the flare tip. The system is depressurised.	3.1.1. No greenness guard.	3.1.1.1. Substitute the rupture disc by a pressure safety valve (PSV). 3.1.1.2. Study the option of installing a high integrity protection system (HIPS) SIL = 2.
More	Material minimization	4. Continuous vent of nitrogen with MIC.	4.1. Loss of product.	4.1.1. Refrigeration system.	4.1.1.1. Study the optimum storage temperature for refrigeration and vent
				4.1.2. Set point of the control valve to minimize vent. Split range installed.	4.1.2.1. Study the optimum pressure set point to minimize vent assuring safety.
Less	Energy minimization	5. Decrease in external temperature.	5.1. Heat loss from vessel to ambient. No green conseq.	5.1.1. Tank buried.	
Less	Energy minimization	6. Increase in external temperature.	6.1. Cold loss from vessel to ambient. More refrigerant consumption.	6.1.1. Current refrigeration system. Tank buried.	6.1.1.1. Insulate tank with glass wool.
	Space minimization	N/A			
	Time minimization	N/A			

Table 7 Green HAZOP analysis for the selected case study (*Continued*)

Guideword	Deviation	Causes	Consequences	Greenness guards	Recommendations
More	Toxicity	7. Increasing of MIC in vent gases due to increase in temperature or pressure or insufficient scrubbing system.	7.1. Toxic gas emission.	7.1.1. Scrubbing system and flare system.	7.1.1.1. Study the substitution of MIC with methyl formamide (MFA).[a] 7.1.1.2. Study the substitution of the Bhopal route by an alternative route (see Scheme 1).
			7.2. Loss of product.	7.2.1. Flare system.	7.2.1.1. Study the installation a blow-down cooled system with liquid ring pumps at flare's know-out drum to recover the product for further use.
		8. Leakage, uncontrolled or undetected of MIC to grade.	8.1. Soil contamination and MIC release direct to atmosphere.	8.1.1. Concrete containing vessel.	8.1.1.1. Substitute the vessel by a non-buried vessel with a leakage preventing vessel (container specially designed for product recovery).
No/less	On-demand material	9. MIC storage.	9.1. Risk of contamination and poisoning.	9.1.1. No greenness guards.	9.1.1.1. Produce MIC on-line. 9.1.1.2. Minimize the MIC storage.
			9.2. Consumption of nitrogen.	9.2.1. No greenness guards.	9.2.1.1. *Idem* 9.1.1.1. and 9.1.1.2.
No/less	On-demand energy	10. MIC storage at a low temperature.	10.1. Consumption of energy in refrigeration. Continuous cold loss.	10.1.1. No greenness guards.	10.1.1.1. *Idem* 9.1.1.1. and 9.1.1.2.
More	Material (over-design)	11. See 'no/less on-demand material'.			
More	Energy (over-design)	12. See 'no/less on-demand energy'.			
		13. Refrigeration system too large.	13.1. Loss of efficiency.	13.1.1. No greenness guards.	13.1.1.1. Study optimum size of the refrigeration system. 13.1.1.2. Better temperature controller.
			13.2. Increase in utility consumption.	13.2.1. No greenness guards.	13.2.1.1. *Idem* 13.1.1.2.
More	Emission	14. Nitrogen flowrate. See 'more entropy 2'.			
		15. NaOH consumption in scrubbing system. See 'other material 1'.	15.1. Spent caustic emission.	15.1.1. Spent caustic is collected and treated off-site by external company (author's assumption).	15.1.1.1. Evaluate the installation of spent caustic treatment plant on-site.
More	Waste generation	16. MIC is released in the rupture disc.	16.1. Production of MIC^{-}-Na^{+}.	16.1.1. *Idem* 15.1.1.	*Idem* 15.1.1.1.
Less	Material efficiency	17. Excessive nitrogen vent to the atmosphere.	17.1. *Idem* 'more entropy (2)' and 'less material minimization (4)'.	17.1.1. No greenness guards.	
Less	Energy efficiency	18. *Idem* 'energy minimization (6)'.			
Less	Space efficiency	19. Apply recommendation 8.1.1.1. Un-bury vessel.	19.1. More land is used. Need of equipment reorder. Piping and material costs.	19.1.1. No greenness guards.	19.1.1.1. Hold. Study this recommendation in combination with 8.1.1.1.
Less	Time efficiency	Only applicable for start-up for this node.			
Less	Material integration	20. Continuous nitrogen vent.	20.1. Loss of nitrogen with MIC.	20.1.1. Pressure control of the vessel.	20.1.1.1. Study the possibility of minimising nitrogen for the flare headers purge using this vent for purging them.
Less	Energy integration	21. Independent refrigeration system (non integrated).	21.1. More energy consumption.	21.1.1. Apparently does not exist. Need more data.	21.1.1.1. Study the increase in storage pressure.
More	Environ. integration	22. Buried tank.	22.1. Equipment not visible from the outside.	22.1.1. Currently it is buried.	
Other	Environ. integration	23. Apply recommendation 8.1.1.1. Un-bury vessel.	23.1. *Idem* 8.1.	23.1.1. *Idem* 8.1.1.	23.1.1.1. Minimize the visual impact of the new vessel.

Table 7 Green HAZOP analysis for the selected case study (*Continued*)

Guideword	Deviation	Causes	Consequences	Greenness guards	Recommendations
No	Environ. integration	24. Purge to atmosphere in valve-28 at 100 ft. is opened.	24.1. Toxic gas release to atmosphere.	24.1.1. No greenness guards.	24.1.1.1. Remove vent. 24.1.1.2. Indicate 'car seal close (CSC)' or 'lock close (LC)' in the valve
			24.2. Visual impact of the vent at 100 ft.	24.2.1. Need more data.	
Less	Controllability	25. No temperature controller installed in the vessel. Any disturbance will lead in temperature changes because of manual control.	25.1. Excessive refrigeration.	25.1.1. No greenness guard.	25.1.1.1. Install an automatic temperature controller connected to the control panel.
			25.2. No refrigeration if any isolation valve is closed (safety consequences).	25.2.1. No safety guard. No greenness guard.	25.2.1.1. *Idem* 25.1.1.1.
		26. No pressure controller installed in scrubber.	26.1. Loss efficiency in gas removal. Gas release to flare.	26.1.1. No greenness guard.	261.1.1. Install an automatic pressure controller.
			26.2. Nitrogen blanketing control works worse.	26.2.1. No greenness guard.	262.1.1. *Idem* 25.1.1.1.
	Operability	Not applicable for this node.			
More	Immortality	27. Vessel buried in concrete.	27.1. It cannot be easily dismantled.	27.1.1. No greenness guard.	27.1.1.1. *Idem* 8.1.1.1.
			27.2. Toxic emission due to uncontrolled leakage.	27.2.1. Concrete container.	27.2.1.1. Install a leak-detection system in container.
		28. MIC highly toxic and not very biodegradable.	28.1. Contamination and poisoning if a leak occur.	28.1.1. No greenness guard.	28.1.1.1. *Idem* 7.1.1.1.
Other	Performance in afterlife	Need more data to take decisions about further applicability'.			

[a] Methyl formamide, MFA, is less toxic, less volatile and reacts with alpha-naphthol to produce carbaryl + hydrogen. MFA does not react with water.

the installation of a recovery system before the flare using cooled liquid ring pumps (Table 7, 7.2.1.1). In addition to this, the vessel should be un-buried to avoid uncontrolled leakages and to facilitate its dismantling and future after-use (Table 7, 8.1.1.1). Different studies for refrigeration minimisation and storage minimisation are suggested.

Conclusions

In conclusion, the g-HAZOP methodology presents the following fundamental features:

First, it is the first systematic green engineering guidance tool for engineers to design, assess and implement processes within the highest industrial standards of environment improvement.

Second, the main g-HAZOP structure and methodology is based on the widespread HAZOP analysis. This guarantees its ease of use and therefore its future implementation within engineering companies design procedures. In addition to this, this tool has been prepared by chemical engineers and tested by different process engineers experts in design and evaluation of processes. They have found in g-HAZOP a promising tool applicable to their working areas.

Thirdly, g-HAZOP methodology is explained in detail in the text, and it has been illustrated by a striking example, the carbaryl plant at Bhopal, which caused the most dramatic chemical disaster ever. This example combines, in an intriguing manner, both safety engineering and green engineering guidelines.

Finally, g-HAZOP is a powerful tool for finding problems and non-green situations in chemical plants. A g-HAZOP analysis conducted by a well-prepared engineer can help in tackling non-green problems, not just mitigating their consequences but eliminating their causes. This is the best way to reach the highest design standards for the millennia.

Acknowledgements

The authors wish to thank the Spanish Ministry of Science and Technology for the financial support, PPQ 2003-07209.

References

1 R. Smith, *Chemical Process Design and Integration*, McGraw-Hill, New York, 2005.
2 T. A. Kletz, What You Don't Have, Can't Leak, *Chem. Ind.*, 1978, 287–292.
3 T. A. Kletz, *Process Plants: A Handbook for Inherently Safer Design*, Taylor and Francis, Bristol, PA, USA, 1998.
4 M. A. Abraham and N. Nguyen, Green Engineering: Defining the Principles – Results from the Sandestin Conference, *Environ. Prog.*, 2003, **22**(4), 233–236.
5 G. H. Brundtland, *For World Commission on Environment and Development, Our Common Future*, Oxford University Press, Oxford, UK, 1987.
6 Agenda 21, Conference on Environment and Development (UNCED) held in Rio de Janeiro, Brazil, 3 to 14 June 1992.
7 Britest method, www.britest.co.uk, available on line July 2006.
8 EHSC, Environmental Health and Safety Committee, Note on Inherently Safer Chemical Processes, Royal Society of Chemistry, www.rsc.org, 2000.
9 N. A. Ashforda and G. Zwetsloot, Special Issue on Risk Assessment and Environmental Decision Making, Encouraging Inherently Safer Production in European firms: a report from the field, *J. Hazard. Mater.*, 1999, 123–144.

10 British Standard IEC 61882:2001, Hazard and Operability studies (HAZOP studies) – Application Guide, 2001.
11 F. I. Khan and S. A. Abbasi, OptHAZOP—an effective and optimum approach for HAZOP study, *J. Loss Prev. Process Ind.*, 1997, **10**(3), 191–204.
12 E. Cagno, F. Caron and M. Mancini, Risk analysis in plant commissioning: the Multilevel Hazop, *Reliab. Eng. Syst. Saf.*, 2002, **77**, 309–323.
13 W. McDonough, M. Braungart, P. T. Anastas and J. B. Zimmerman, Applying the Principles of Green Engineering to Cradle-to-Cradle Design, *Environ. Sci. Technol.*, 2003, **37**(23), 434A–441A.
14 P. T. Anastas and J. B. Zimmerman, Design through the 12 principles of green engineering, *Environ. Sci. Technol.*, 2003, **37**(5), 94A–101A.
15 I. Schmidt, M. Meurer, P. Saling, A. Kicherer, W. Reuter and C. Gensch, SEEbalance – Managing Sustainability of Products and Processes with the Socio-Eco-Efficiency, *Analysis by BASF*, ed. S. Seuring, Greener Management International, Greenleaf Publishing, vol. 45, 2004, 79–94.
16 S. Saraf and M. Karanjikar, Literary and economic impact of the Bhopal gas tragedy, *J. Loss Prev. Process Ind.*, 2005, **18**(4–6), 274–282.
17 *Ullmann's Encyclopedia of Industrial Chemistry*, Wiley-VCH, Weinheim, 6th edn, 2002.
18 T. Kletz, *Learning from Accidents*, Gulf Professional Publishing, Oxford, 3rd edn, 2001.
19 *Trade Union Report on Bhopal*, Semcosh, http://www.semcosh.org/bhopal.htm, 2004.

Solvent-free one-pot four-component synthesis of 2-aminomorpholines. Access to related diaminoalcohols†

Thomas Régnier, Fabienne Berrée,* Olivier Lavastre and Bertrand Carboni

Received 14th September 2006, Accepted 19th December 2006
First published as an Advance Article on the web 22nd December 2006
DOI: 10.1039/b613395a

Under microwave irradiation, a series of 2-aminomorpholines were readily produced in a straightforward four-component process from commercially available 1,2-aminoalcohols, glyoxal, boronic acids and aliphatic or aromatic amines. Further reduction furnished the corresponding diaminoalcohols.

Morpholine derivatives attract special attention as pharmaceutical drug candidates and are amply represented in patent literature.[1] Some of these heterocyclic molecules show promising properties, including antidepressant, anticancer and anti-inflammatory activities, that explain the constant interest of synthetic chemists.[2] In this context, the utilisation of a multi-component approach for the generation of this drug-like scaffold is of special utility for the rapid production of a wide range of compounds, which is highly desirable in the context of lead finding and lead optimisation.[3] In parallel, the development of environmentally benign solvent-free reactions is becoming an area of growing interest, as well as microwave assisted reactions that often allow rate enhancement, higher yields and, sometimes, better selectivity in respect to the conventional heating.[4] We herein describe a straightforward synthesis of 2-aminomorpholines *via* a one-pot four-component process that involves first a Petasis reaction, followed by a microwave-promoted amine condensation (Scheme 1). In addition to the access to morpholine libraries, this sequence can be also considered as an efficient, rapid and versatile method for the modular decoration of an amino-substituted pharmacophore, for example, in order to modify the pharmacokinetic properties.

Results and discussion

On the basis of the reaction discovered by N. Petasis and coworkers,[5] we previously reported the solution phase synthesis of 2-hydroxymorpholines and their conversion to polysubstituted aminodiols. Our initial experiments were carried out in ethanol.[6] To improve yields and purity, and therefore to minimise chromatographic purifications, the effects of several parameters (without solvent or solvent: toluene, ethanol, methylene chloride, acetonitrile, reagent concentrations: 0.2 and 1 mol L^{-1}, addition order, number of equivalents of boronic acid: 1 or 3, temperature: ambient or 50 °C) were studied using a Buchi Syncore® reactor. *N*-methyl-aminoethanol **1a**, phenyl boronic acid **3a** and glyoxal were chosen as model compounds. The best results were obtained when the reaction was conducted in the absence of solvent. A quasi-quantitative condensation then occurred, giving 4-methyl-3-phenylmorpholin-2-ol as the only product detected in the ^{1}H NMR spectrum (Scheme 2).

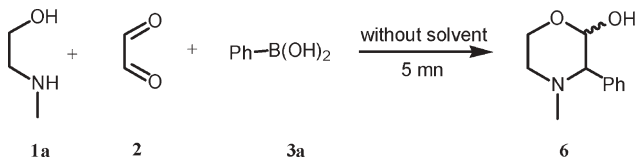

Scheme 2 Synthesis of 4-methyl-3-phenylmorpholin-2-ol in a one-pot solvent-free process.

These observations were confirmed with other aryl or vinyl boronic acids and aminoalcohols, except in the case of 2-(methylamino)-2-phenylethanol and 1-(allylamino)propan-2-ol, where the best results were observed in ethanol. We then envisaged the transformation of these heterocycles to the corresponding amino derivatives by simply adding a supplementary amine component. This second condensation reaction was carried out in a one-pot process without any purification of the crude 2-hydroxymorpholine intermediates (**6**), except for **1b** and **1c**. First attempts were conducted under thermal conditions in refluxing toluene. If the expected products were effectively present, this method was unsatisfactory in terms of yields and purity. When neat reagents are submitted to microwave irradiation during 15 min at a regulated temperature of 110 °C, the required products are obtained cleaner, with higher yield and after shorter reaction times. With optimal experimental conditions identified, a variety of 1,2-aminoalcohols, boronic acids and amines were used to access to diversely substituted 2-aminomorpholines in good to moderate yields (Scheme 1, Table 1). *N*-Alkylaminoethanol associated with aryl boronic acids gave best results with a decrease in yield in the case of a primary aliphatic or aromatic amines compared to a secondary one (entries c and d). A similar observation was made with styrylboronic acid (entry h) while the presence of substituents was best tolerated in position 2 on the aminoalcohol than in position 1 (entries k and l). In all cases, the *trans*-morpholine

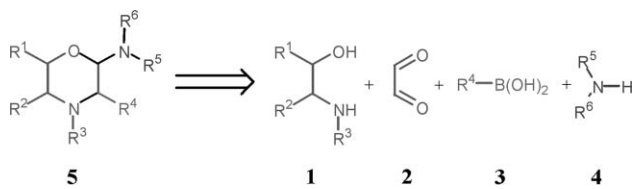

Scheme 1 2-Aminomorpholines from four building blocks.

Sciences Chimiques de Rennes, UMR 6226 CNRS-Université de Rennes 1, Bat 10 A, Campus de Beaulieu, 35042, Rennes Cedex, France. E-mail: fabienne.berree@univ-rennes1.fr; Fax: (33) 0223236227; Tel: (33) 0223235735

† Electronic supplementary information (ESI) available: Experimental procedures and spectroscopic data for new compounds. See DOI: 10.1039/b613395a

Table 1 Preparation of various 2-aminomorpholines (**5**) and diaminoalcohols (**8**)

Entry	R^1	R^2	R^3	R^4	R^5	R^6	Yield (%)[a] **5**	**8**
a	H	H	Me	Ph	Me	$PhCH_2$	76	87
b	H	H	Me	Ph	Piperidino		77	95
c	H	H	Me	Ph	C_5H_{11}	H	55	—
d	H	H	Me	Ph	Ph	H	50	86
e	H	H	Me	Ph	4-Br–C_6H_4–	H	63	73
f	H	H	Me	Ph	Et	Ph	62	—
g	H	H	Me	4-MeO–C_6H_4–	Me	$PhCH_2$	76	68
h	H	H	Me	–CHCH–Ph	Piperidino		43	—
i	H	H	$PhCH_2$	Ph	Piperidino		65	82
j	H	H	$PhCH_2$	Ph	-Furylmethyl	$PhCH_2$	52	30[c]
k	H	Ph	Me	Ph	Me	$PhCH_2$	63[b]	61
l	Me	H	$–CH_2–CHCH_2$	Ph	Morpholino		42[b]	78

[a] After silica gel chromatography. [b] From isolated 2-hydroxymorpholine. [c] Due to a partial decomposition during the purification step.

diastereoisomer was the sole or the major product (>90%) with respect to the coupling constant (J = 8–9 Hz), compared to those of the minor *cis* isomers (J = 2–3 Hz).[7] The mechanism of this amination reaction can be rationalised by the presence of an equilibrium between the 2-hydroxymorpholine and the corresponding δ-hydroxyaldehyde. Addition of the amine to the CHO moiety was followed by an intramolecular cyclisation with loss of water to afford the desired 2-aminomorpholines (**5**).

In the absence of amine, a dehydration of the 2-hydrohydroxymorpholine intermediate occurred. In best experimental conditions (30 min, 110 °C), *N*-methylaminoethanol, glyoxal and phenyl boronic afforded a 3,4-dihydro-2*H*-1,4-oxazine in 85% yield, that could open a new route to this class of heterocycles (Scheme 3).[8]

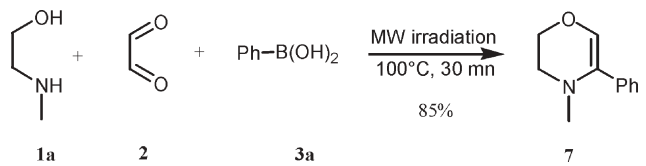

1a **2** **3a** **7**

Scheme 3 Synthesis of 4-methyl-5-phenyl-3,4-dihydro-2*H*-1,4-oxazine, **7**.

In addition, we were also interested into the conversion of **5** to diaminoalcohols (**8**), used as structural cores in binucleating ligands,[9] as piperazines[10] or squaraines precursors.[11] They were readily synthesised by $LiAlH_4$ reduction of 2-aminomorpholines (**6**) in good to moderate yields (Scheme 4, Table 1). In the case of **5k**, a mixture of diastereoisomers (6/3/1) was obtained. The major compound can be separated by chromatography and submitted to $LiAlH_4$ reduction, giving **8k** as a single enantiomer.

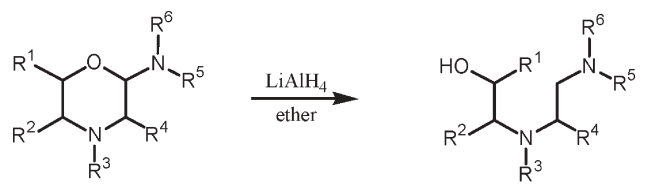

5 **8**

Scheme 4 Synthesis of diaminoalcohols (**8**).

In conclusion, we have developed an efficient one-pot synthesis of novel 2-aminomorpholines *via* a microwave-assisted solvent-free four component process. A dehydration product is cleanly produced in the absence of amine and the morpholine derivatives were easily converted to diaminoalcohols. Further investigations are on going to study the scope and limitations of this 3,4-dihydro-2*H*-1,4-oxazine synthesis, as well as the use of *in-situ* generated 2-hydroxymorpholines as α-amino-aldehydes equivalents in other environmentally benign processes.

Notes and references

1 For some recent patents, see: K. K. Murthi, R. Koestler, C. Smith, T. Brandstetter and A. F. Kluge, 2006, EP 1674457 20041223; Y. Tanaka, S. Takeda, H. Higashi, M. Matsuura, F. Kobayashi, M. Hamada and M. Tanaka, 2006, WO 2006028284; V. P. Palle, A. K. Verma, M. Salman, R. K. Singh, Y. B. Waman, G. Sharma and A. Ray, 2006, WO 2006016237; M. Cik, G. S. Diels and G. R. Van Lommen, 2006, WO 2006008259; T. B. Durham, P. J. Hahn, T. J. Kohn, J. R. McCarthy, H. B. Broughton, R. D. Dally, M. R. Gonzalez-Garcia, K. J. Henry, T. A. Shepherd, J. A. Erickson and A. B. Bueno-Melendo, 2006, WO 2006034093.
2 R. Witjmans, M. K. Vink, H. E. Schoemaker, F. L. van Delft, R. H. Blaauw and F. P. Rutjes, *Synthesis*, 2004, 641; A. Amantana and P. L. Iversen, *Curr. Opin. Pharmacol.*, 2005, **5**, 550.
3 *Multicomponent Reactions*, ed. J. Zhu and H. Bienaymé, Wiley-VCH, Weinheim, 2005.
4 *Microwaves in Organic Synthesis*, ed. A. Loupy, Wiley-VCH, Weinheim, 2006; R. S. Varma, *Pure Appl. Chem.*, 2001, **73**, 193.
5 N. A. Petasis and I. A. Zavialov, *J. Am. Chem. Soc.*, 1997, **119**, 445; N. A. Petasis and I. A. Zavialov, *J. Am. Chem. Soc.*, 1998, **120**, 11798. For some recent references, see: Y. M. Chang, S. H. Lee, M. H. Nam, M. Y. Cho, Y. S. Park and C. M. Yoon, *Tetrahedron Letters*, 2005, **46**, 3053; M. Follmann, F. Graul, T. Schafer, S. Kopec and P. Hamley, *Synlett*, 2005, 1009; H. Jourdan, G. Gouhier, L. Van Hijfte, P. Angibaud and S. R. Piettre, *Tetrahedron Lett.*, 2005, **46**, 8027; K. K. Nanda and B. W. Trotter, *Tetrahedron Lett.*, 2005, **46**, 2025; S. Sugiyama, S. Arai, M. Kiriyama and K. Ishii, *Chem. Pharm. Bull.*, 2005, **53**, 100; T. J. Southwood, M. C. Curry and C. A. Hutton, *Tetrahedron*, 2006, **62**, 236.
6 F. Berrée, A. Debache, Y. Marsac, B. Collet, P. Girard-Le Bleiz and B. Carboni, *Tetrahedron*, 2006, **62**, 4027.
7 J. J. Hale, S. G. Mills, M. MacCoss, S. K. Shah, H. Qi, D. J. Mathre, M. A. Cascieri, S. Sadowski, C. D. Strader, D. E. MacIntyre and J. M. Metzger, *J. Med. Chem.*, 1996, **39**, 1760.
8 A. Zulys, M. Dochnahl, D. Hollmann, K. Löhnwitz, J.-S. Hermann, P. W. Roesky and S. Blechert, *Angew. Chem., Int. Ed.*, 2005, **44**, 7794.
9 C. Incarvito, M. Lam, B. Rhatigan, A. L. Rheingold, C. Jin Qin, A. L. Gavrilova and B. Bosnich, *J. Chem. Soc., Dalton Trans.*, 2001, 3478.
10 C. N. Filer, F. E. Granchelli, A. H. Soloway and J. L. Neumeyer Boston, *J. Med. Chem.*, 1977, **20**, 1508.
11 G. Dileck and E. U. Akkaya, *Tetrahedron Lett.*, 2000, **41**, 3721.

Palladium nanoparticles stabilised on PEG-modified silica as catalysts for the aerobic alcohol oxidation in supercritical carbon dioxide†

Zhenshan Hou,[a] Nils Theyssen[a] and Walter Leitner*[ab]

Received 12th May 2006, Accepted 31st October 2006
First published as an Advance Article on the web 9th November 2006
DOI: 10.1039/b606740a

PEG-modified (PEG = polyethylene glycol) silica surfaces are able to effectively stabilize and immobilize palladium nanoparticles for their use as selective oxidation catalysts in combination with $scCO_2$ as reaction medium under mild conditions. These catalysts show high activity and excellent stability under continuous-flow operation.

Introduction

The development of clean and efficient oxidation methods for fine chemicals synthesis is a major goal of Green Chemistry.[1] The selective aerobic oxidation of alcohols to aldehydes and ketones has found particular interest in this context.[2] Catalysts based on palladium nanoparticles are highly promising systems for this transformation, but their application is limited by aggregation and formation of less active and selective Pd-black.[3,4] In addition, the oxidation state of the surface atoms has been identified as an important control factor for catalyst activity.[4a,j] Therefore, there is a continuing need for new catalytically active materials and corresponding reaction engineering approaches to clean alcohol oxidation.

Recently, we have developed an efficient system for continuous-flow aerobic alcohol oxidation using palladium nanoclusters that were stabilized and immobilized in a liquid polyethylene glycol (PEG) matrix in combination with supercritical carbon dioxide ($scCO_2$) as the mobile phase.[5] Although this approach has the potential to solve some of the above mentioned problems associated with the use of Pd-nanoparticle catalysts in oxidation, a stable and well-defined catalyst based on a solid and mainly inorganic matrix seems even more desirable, as it would allow the use of simple and highly efficient fixed-bed technology, reducing at the same time the risk of depletion or oxidative degradation of a pure PEG-matrix. We report here that PEG-modified silica surfaces are able to effectively stabilize and immobilize palladium nanoparticles for their use as selective oxidation catalysts in combination with $scCO_2$ as reaction medium under mild conditions. This concept is expected to be of general utility for catalysis with supported metal nanoparticles.

The rational of our approach is schematically depicted in Fig. 1. The metal nanoparticles, in this particular case palladium particles with diameters in the 3 nm range, are deposited or generated on the surfaces of silica particles that have been modified with covalently attached PEG chains of moderate length (average molecular weight M_w = 750 g mol^{-1}). The stabilizing effect of polyethers is well documented for nanoparticles in solution phase.[6] Catalysts stabilised on PEG-modified silica should be ideally combined with a reaction medium that allows for high mass transfer without wetting the surface and increasing the particle mobility on the surface. Supercritical carbon dioxide ($scCO_2$, T_c = 31.0 °C, p_c = 7.4 MPa) combines liquid like solvent properties with typical gas phase properties such as rapid mass transfer and negligible surface tension.[7,8] Thus, $scCO_2$ should be able to transport dissolved substrates to and products from the active nanoparticles in a gas-like manner at temperatures that are far below the regular boiling temperatures of the organic compounds. This scenario allows rapid chemical transformation at the active centre, ensures efficient removal of the products from the surface, and minimizes the mobility of solid-supported catalytically active species.[9]

Results and discussion

For the preparation of a covalently anchored PEG-phase, compound **1** was reacted with polyethene glycol monomethyl ether (M = 750 g mol^{-1}) in the presence of NaH in THF under refluxing conditions (Scheme 1). The resulting PEG-modified triethoxysilane **2** was copolymerised in acetone and water with

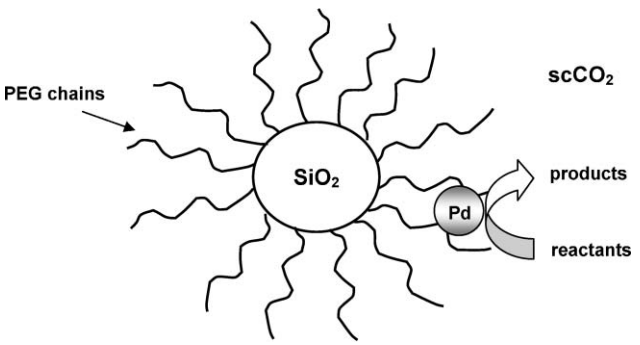

Fig. 1 Palladium nanoparticles stabilised on PEG-modified silica for catalytic transformations using supercritical carbon dioxide ($scCO_2$) as mobile phase for reactants and products.

[a]*Max-Planck-Institut für Kohlenforschung, Kaiser-Wilhelm-Platz 1, D-45468 Mülheim an der Ruhr, Germany*
[b]*Institut für Technische und Makromolekulare Chemie, Lehrstuhl für Technische Chemie und Petrolchemie, RWTH Aachen, Worringerweg 1, D-52064 Aachen, Germany. E-mail: leitner@itmc.rwth-aachen.de*

† Electronic supplementary information (ESI) available: Technical parameters of the solid state analytical measurements, XRD-pattern of **4a**, IR-spectra of **4a** and **8**, ^{29}Si MAS NMR of **3a** spectra and TEM pictures of samples **5** and **8** before and after the oxidation. See DOI: 10.1039/b606740a

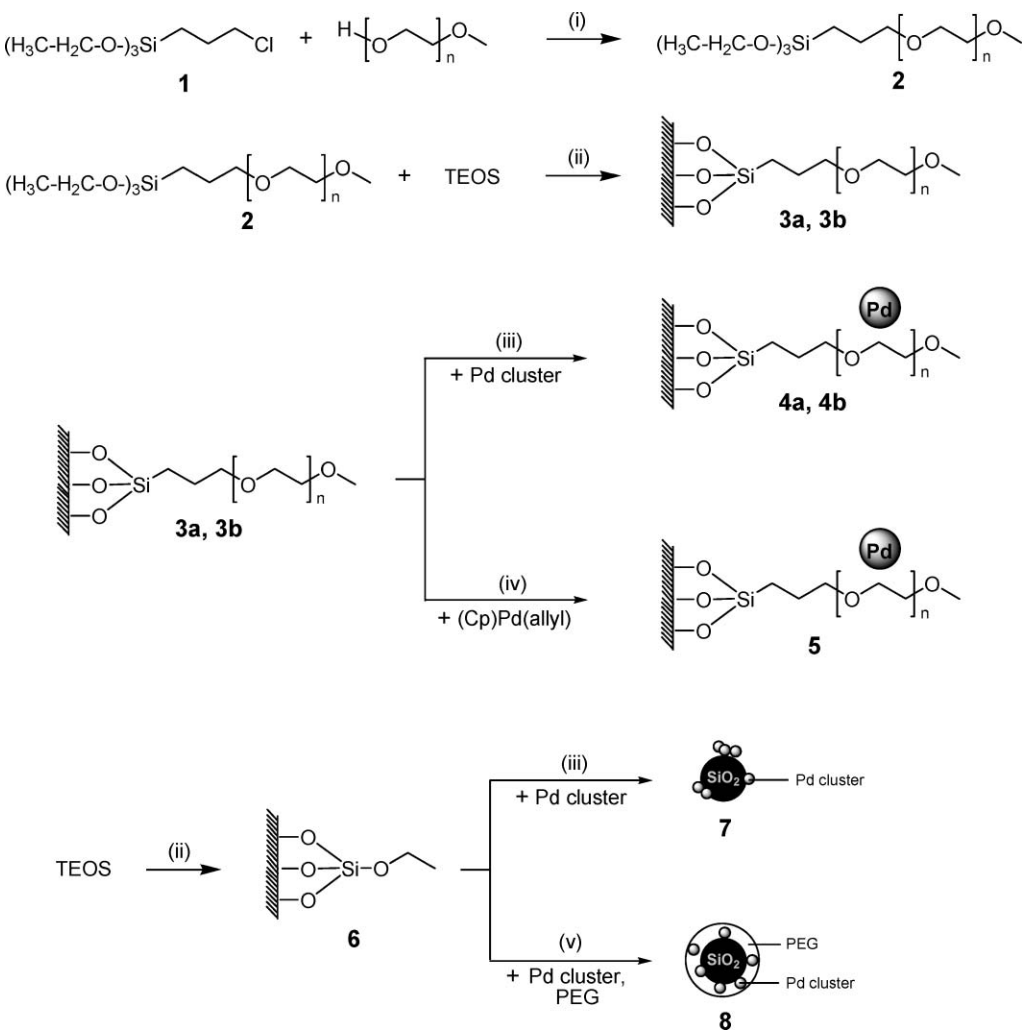

Scheme 1 Preparation of catalyst materials based on Pd-nanoparticles on different silica supports—*Reagents and reaction conditions*: (i) 1 equiv. NaH, dry THF, reflux, 10 h; (ii) TEOS : **2** = 4 : 1 (mol/mol) for **3a**; TEOS : **2** = 2 : 1 (mol/mol) for **3b**, and pure TEOS for **6**; acetone and water (8 equiv.), dibutyltin dilaurate (0.02 equiv.) as catalyst for initiating polymerization, stirring first at 60 °C for 5 h and then at room temperature for 24 h; (iii) impregnation with Pd cluster $[Pd_{561}phen_{60}(OAc)_{180}]$ from acetic acid solution at room temperature. (iv) impregnation with complex $[Pd(\eta^3\text{-}C_3H_5)(\eta^5\text{-}C_5H_5)]$ in *n*-pentane, evaporating *n*-pentane at low temperature (0 °C), followed by thermal decomposition of the Pd complex under argon at 60 °C for 6 h. (v) simultaneous impregnation with PEG_{750} and palladium cluster from acetic acid solution.

tetraethoxysilane (TEOS) in a molar ratio of 4 : 1 and 2 : 1 to form the two corresponding PEG-modified silica supports **3a** and **3b**, respectively. The reference silica material **6** was prepared in an analogous manner for comparison. The materials were found to possess low BET areas in the range and even below 1 $m^2\ g^{-1}$ associated with largely non-porous structures[10] and XRD measurements indicate the formation of amorphous silica. These results imply that the PEG chains are accessible mainly on the external surface of the generated silica particles.

Catalyst materials based on this PEG-modified silica were generated by the wet-impregnation method as well as by generation of nanoparticles *via* decomposition of molecular palladium precursors on the surface. Reference catalysts lacking the covalently bound PEG chains were also prepared (Scheme 1). Firstly, PEG-modified silica **3a**, **3b** were impregnated with a solution of the Pd cluster $[Pd_{561}phen_{60}(OAc)_{180}]$[11] in acetic acid to obtain catalyst **4a** and **4b**, respectively. Alternatively, impregnation of **3a** with the molecular precursor $[Pd(\eta^3\text{-}C_3H_5)(\eta^5\text{-}C_5H_5)]$ and subsequent thermal decomposition at 60 °C on the surface gave catalyst **5**. For the purpose of comparison, the Pd cluster $[Pd_{561}phen_{60}(OAc)_{180}]$ was impregnated on reference material **6** comprising ethoxy groups at the silica surface. The cluster was directly adsorbed on the support **6** to form catalyst **7** or embedded in a thin PEG film to give catalyst **8**.

In a first set of experiments, the performance of the different catalysts for cinnamyl alcohol aerobic alcohol oxidation have been compared under previously reported batch-wise conditions using materials with a Pd-loading of 5 weight-% in all cases.[5] In the preliminary screening, catalysts **4a–b** and **5** showed a similar behaviour which was distinct from materials **7–8**. Fig. 2 shows typical conversion/time profiles obtained by online GC analysis[12] for material **4a** *vs.* **7** and **8** containing the same Pd-species impregnated on different supports. This comparison reveals significantly longer induction periods for the non-covalently modified supports, indicating that the

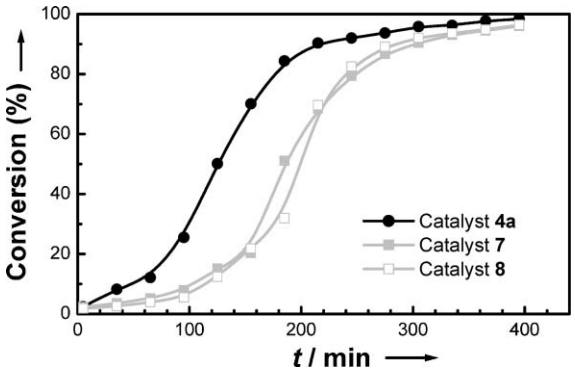

Fig. 2 Reaction profiles of cinnamyl alcohol aerobic oxidation with different catalysts under supercritical carbon dioxide conditions. Reaction conditions: 80 °C, catalysts: 90 mg (Pd-loading: 5 wt%, total Pd-amount: 2 mol%); substrate: 1.95 mmol; O_2: 36 mmol; d (CO_2/O_2) = 0.55 g ml^{-1}, molar ratio CO_2 : O_2 = 92 : 8.

covalently PEG-modified surface provides the best environment for the catalysts formed on basis of the Pd_{561} cluster. Therefore, catalyst material **4a** was selected for further evaluation of the scope of the oxidation with various substrates under a set of benchmark conditions (Table 1).

As can be seen from the screening results in Table 1, benzylic and allylic alcohols were very rapidly and selectively converted into the corresponding carbonyl compounds in $scCO_2$ under mild conditions (entries 1, 2 and 4). Secondary alcohols like 1-phenylethanol and cyclooctanol were also efficiently transformed into the corresponding ketones, albeit the transformation occured markedly slower (entries 3 and 5). The primary alkyl alcohol butanol gave poor conversion yielding mainly the acid and corresponding ester (entry 6). Overall, the trends in reactivity are very similar to those observed with the Pd_{561} cluster in liquid PEG as stabilizing matrix.[5]

Table 1 Results of batch-wise aerobic alcohol oxidation in $scCO_2$ using catalyst **4a**[a]

Entry	Substrate	Product	t/h	Conv. (%)	Sel. (%)	TON[b]
1	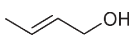	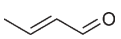	4	98.9	98.0	45
2	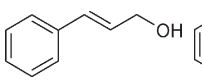	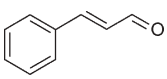	5	96.8	98.5	47
3	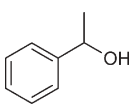	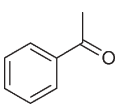	12	58.8	99.5	29
4	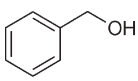	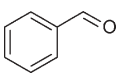	16	96.5	98.8	45
5	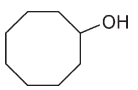	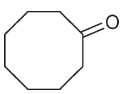	18	46.4	98.2	22
6	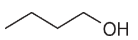	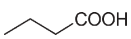	8	12.3	47.8	3[c]

[a] Reaction conditions: T = 80 °C; V(reactor) = 36 mL; **4a** = 90 mg, substrate = 1.95 mmol; d (CO_2/O_2) = 0.55 g ml^{-1}, molar ratio CO_2 : O_2 = 92:8; [b] Total turnover number (TON) = mol product/mol Pd; [c] acid butyl ester is formed as a second product, together with small amounts of butanal.

Finally, the newly synthesized catalysts were tested for continuous-flow fixed-bed oxidation of benzyl alcohol under supercritical conditions. The periphery of the apparatus was identical to a previously described set-up,[5] but the central continuously stirred tank reactor could now be replaced with a tubular fixed-bed reactor. The solid catalysts were held in place by small plugs of quartz on both ends of the metal tube (inner diameter: 7.5 mm, total length: 50 cm). As shown in Fig. 3, initial single pass conversions in the range of 50–60% were obtained with all catalysts. The average residence time in the catalyst bed of the flow reactor is estimated to be about 1.2 h.[13] A selectivity to benzaldehyde >98% was achieved in all cases. These values compare well with performance observed under batch-wise operation, where relatively long reaction times (~5 h) are required to achieve similar conversions. The productivity in mol of product divided by reaction time and catalyst weight is about a factor of 9 better for the flow reactor as compared to the batch-wise set-up.

Significant differences were, however, observed especially for the long term stability of the tested catalysts. Catalyst **7**, which contains only adsorbed Pd clusters without any stabilizing matrix, shows the lowest initial activity and a continuous and fairly rapid deactivation occurs leading to only 30% single pass conversion after 30 h on stream. The non-covalently bound PEG film leads to a slightly higher activity, but deactivation is still significant within the investigated time frame. In contrast, the covalently bound PEG chains lead to an excellent activity and stabilization of the Pd cluster in materials **4a** and **4b**. After 30 h catalyst **4a** showed a total turnover number (TON) of 1750 corresponding to an average turnover frequency (TOF) of 58 h^{-1}, based on the total Pd-loading as the most conservative basis.[14] The similar behaviour of catalyst **5** formed by thermal decomposition of a molecular precursor indicates that the beneficial stabilising

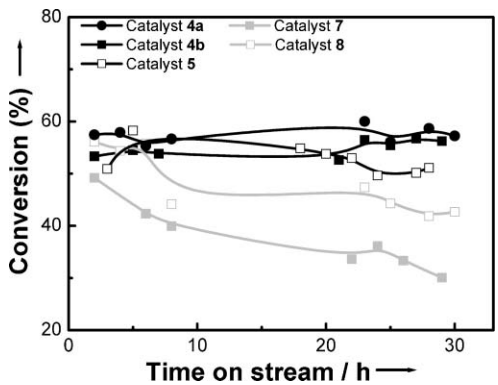

Fig. 3 Continuous-flow fixed-bed aerobic oxidation of benzyl alcohol in $scCO_2$ with different catalysts (0.20 g catalyst, T = 80 °C, p (CO_2/O_2: 92/8) = 15 MPa, flow rate: 1 ml h^{-1}, exit flow: 7.5 L h^{-1}).

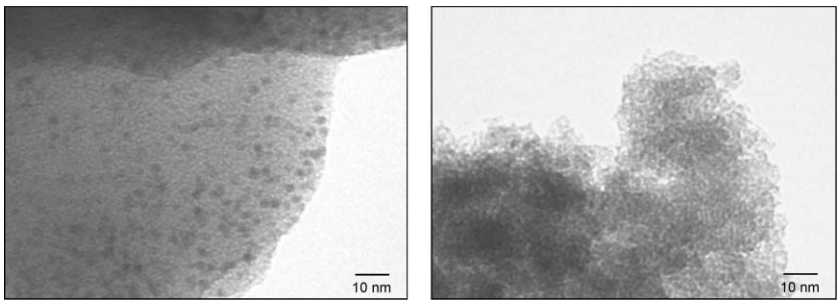

Fig. 4 TEM micrographs of the PEG-stabilised catalyst **4a** before (left) and after (right, 30 h time on stream) oxidation of phenylethanol.

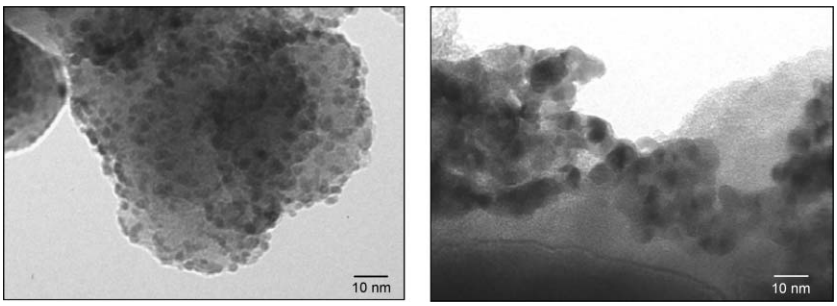

Fig. 5 TEM micrographs of catalysts **7** before (left) and after (right, 30 h time on stream) oxidation of phenylethanol.

effect of the covalently bound PEG phase might be of more general applicability.

TEM micrographs taken before and after reaction confirm that the covalently bound PEG-chains effectively prevent agglomeration of the Pd nanoparticles on the surface during the catalytic process. Before reaction, all catalysts prepared in this study showed highly dispersed Pd-nanoparticles with average sizes in the 3 nm range on the various supports, as exemplified for **4a** and **7** in Fig. 4 and 5, respectively. Significant agglomeration during the reaction occurred on catalyst **7** where no stabilizing matrix was present. In contrast, sample **4a** showed very little aggregation after reaction, indicating that the bound PEG-chains effectively reduced the mobility of the Pd clusters on the surface. The materials **5** and **8** showed intermediate levels of agglomeration between these two extreme situations (see ESI†). Although other factors such as Pd-leaching or over-oxidation on the particle surface cannot be ruled out completely as factors contributing to catalyst deactivation at this stage, these findings clearly demonstrate the potential of the PEG-modified silica as stabilizing support for metal nanoparticles.

Conclusion

In conclusion we have shown that palladium nanoparticles stabilised by PEG-modified silica are efficient and stable catalysts for the selective aerobic oxidation of alcohols to aldehydes and ketones using $scCO_2$ as the mobile phase in continuous-flow processes. The metal nanoparticles are efficiently stabilized on the surface of this hybrid material and agglomeration under the reaction conditions is reduced as compared to other methods of support tested in this study. The covalently bound PEG phase supports described herein are readily available and easily converted into catalyst materials. The combination with well-established fixed-bed technology using $scCO_2$[8] demonstrates the potential of this methodology for general applicability.

Experimental

General

Polyethylene glycol 750 monomethyl ether and sodium hydride (95%) were obtained from Aldrich and 3-chloropropyltriethoxysilane (97%) from ABCR. Palladium cluster $[Pd_{561}phen_{60}(OAc)_{180}]$[10a] and the complex $[Pd(\eta^3\text{-}C_3H_5)(\eta^5\text{-}C_5H_5)]$[15] were synthesized according to previous published procedures. All organic solvents used in this work were dried by standard procedures and the synthesis of catalyst materials was performed under argon.

Synthesis of 2

Commercially available polyethylene glycol 750 monomethyl ether (dried at 35 °C under high vacuum for 12 h prior to use; 17.5 g, 23.5 mmol) was dissolved in 10 mL of THF. This solution was added to a suspension of NaH (0.56 g, 23.5 mmol) in 20 mL of THF at room temperature, and then the mixture was stirred for 2 h at 80 °C. After cooling down the reaction mixture to room temperature, 3-chloropropyltriethoxysilane (5.8 g, 24.1 mmol) in 15 mL THF was added drop-wise at room temperature and stirred for another 16 h at 60 °C. The reaction mixture was allowed to cool down to room temperature. After filtering the suspension over a short path of NH_4Cl,[16] THF was removed under vacuum. The residue was washed with *n*-pentane (10 mL × 3) to remove a small amount of excess 3-chloropropyltriethoxysilane. After evaporating *n*-pentane, the final product was obtained as colorless waxy solid (19.2 g, 85.8%). ^1H NMR (δ, 300 MHz, CD_2Cl_2):

0.48–0.58 (m, 2H, CH_2Si), 1.63–1.89 (m, 2H, CH_2), 3.74 (6H, OCH_2), 1.12 (t, 9H, CH_2CH_3), 3.25 (s, 3H, OCH_3), 3.35–3.66 (m, OCH_2CH_2); ^{13}C NMR (δ, 75 MHz, CD_2Cl_2): 7.03 (CH_2Si), 23.72 (CH_2), 58.84 (OCH_2), 18.57 (CH_2CH_3), 58.45 (OCH_3), 70–72 (OCH_2CH_2). Elemental analysis: C 52.74%, H 9.08%, Si 3.07%.

Synthesis of 3a and 3b

5 g of **2** (5.24 mmol) and TEOS (4.35 g, 20.97 mmol) was dissolved in 50 mL acetone and stirred vigorously to form a homogeneous solution at room temperature. Then 5.5 mL water and three drops of dibutyl tin laurate were added to initiate the copolymerization. The solution was refluxed at 60 °C for 6 h and then stirred for another 24 h at RT. After filtering the suspension, the resulting solid was washed sequentially with large amounts of acetone, ethanol and water. The white solid was dried at 100 °C for 12 h to get **3a**. Similarly, **3b** (10.48 mmol TEOS) and **6** (without **2**) were also prepared according the above procedures. Elemental analysis: **3a**: C 23.71%, Si 26.57, H 5.17%; **3b**: C 35.65%, Si 19.59%, H 6.66%.

Preparation of 4a and 4b

0.5 g of **3a** was mixed with 2.36 mL of a solution of the Pd_{561}-cluster in acetic acid (0.10 mmol ml^{-1}) and stirred for 4 h at RT. Slow evaporation of the solvent gave **4a** as brown powder. Similarly, material **4b** was obtained as brown powder starting from **3b**. Pd contents of the samples were adjusted to 5 wt% in all cases and confirmed by elemental analysis.

Preparation of 5

0.5 g of **3a** was added to a solution of 55 mg of complex $[Pd(\eta^3\text{-}C_3H_5)(\eta^5\text{-}C_5H_5)]$ in 10 mL *n*-pentane and stirred for 4 h. Then the solvent was evaporated at 0 °C. The remaining solid was thermally decomposed at 60 °C for 6 h leading to material **5** as black powder. Elemental analysis: Pd 5.15%.

Preparation of 7

0.5 g of the reference material **6** was mixed with a solution of the Pd_{561}-cluster as described above for **4a** to adjust a Pd-loading of 5 wt%. Stirring at RT for 4 h and slow evaporation of the solvent gave **7** as a brown powder.

Preparation of 8

0.25 g of PEG-750 (monomethyl ether) was mixed homogeneously with 2.74 mL of an acetic acid solution of the Pd cluster (c = 0.1 mmol ml^{-1}). Material **6** (0.32 g) was added and the suspension was stirred at RT for 4 h. **8** was obtained as brown powder after evaporating the solvent and the Pd content of the sample was determined to be 5.02 wt%.

Batch-wise catalytic oxidation of alcohols in $scCO_2$

90 mg of catalyst **4a** and 1.95 mmol alcohol were placed in a 36 mL stainless-steel high pressure reactor. The reactor was pressurised with a defined CO_2/O_2 mixture (19.5 g, $c(O_2)$ = 8 mol%) and heated under vigorous stirring to the desired temperature for a given time (see Fig. 2 and Table 1). The total pressure was 18 MPa. After reaction, CO_2 was released slowly through two serial cold traps at −35 °C. The products were collected from the cold traps and the autoclave using diethyl ether as a solvent. The combined fractions were then analysed by ^1H NMR and GC.

Continuous-flow fixed-bed catalytic oxidation of benzyl alcohol in $scCO_2$

The reactions have been performed in a fixed-bed stainless steel tubular reactor with an inner diameter of 7.5 mm. The temperature of the catalyst bed was controlled by a pumped thermal oil fluid which kept the reactor at a temperature of 80 °C. Pure quartz (80 mesh, 3.5 g) was used to dilute the catalyst bed (0.2 g catalyst in powder form). The catalyst bed was fixed in the tube with a small plug of quartz beads on both ends of the catalyst bed. A pre-warmed (50 °C) continuous stream CO_2/O_2 ($c(O_2)$ = 8 mol%) was passed through the tubular reactor at a flow rate of approximately 7.5 L h^{-1} (exit flow at ambient conditions including reactant and products, total pressure of 15 MPa). The substrate was fed into the CO_2 stream before entering the reactor with a HPLC pump at a rate of 1.0 mL h^{-1}. The reaction mixture was isolated in two sequential cold traps at −35 °C from the exit flow upon depressurization of the supercritical solvent. The cold traps were replaced periodically after about 2 h and their combined content was analysed by ^1H NMR and GC.

Acknowledgements

We thank the Max-Planck-Society, the BMBF (WING project "NanoSelox") and the Fonds der Chemischen Industrie for financial support of this research. Inevitable technical assistance by Axel Brinkmann (MPI für Kohlenforschung) is gratefully acknowledged. We thank Axel Dreier (MPI für Kohlenforschung) for measuring the TEM-pictures.

References

1 (*a*) P. T. Anastas and J. C. Warner, *Green Chemistry: Theory and Practice*, Oxford University Press, Oxford, UK, 1998; (*b*) P. T. Anastas and M. M. Kirchhoff, *Acc. Chem. Res.*, 2002, **35**, 686–694; (*c*) P. T. Anastas and R. L. Lankey, *Green Chem.*, 2000, **2**, 289–295.
2 R. A. Sheldon, I. W. C. E. Arends, G.-J. T. Brink and A. Dijksman, *Acc. Chem. Res.*, 2002, **35**, 774–781.
3 T. Mallat and A. Baiker, *Chem. Rev.*, 2004, **104**, 3037–3058.
4 For recent examples of aerobic alcohol oxidation catalysed by palladium nanoparticles, see: (*a*) A. F. Lee, S. F. J. Hackett, J. S. J. Hargreaves and K. Wilson, *Green Chem.*, 2006, **8**, 549–555; (*b*) J.-D. Grunwaldt, M. Caravati and A. Baiker, *J. Phys. Chem. B*, 2006, **110**, 9916–9922; (*c*) M. Caravati, D. M. Meier, J.-D. Grunwaldt and A. Baiker, *J. Catal.*, 2006, **240**, 126–136; (*d*) H. L. Wu, Q. H. Zhang and Y. Wang, *Adv. Synth. Catal.*, 2005, **347**, 1356–1360; (*e*) A. Corma, H. Garcia and A. Leyva, *J. Mol. Catal. A: Chem.*, 2005, **230**, 97–105; (*f*) M. S. Kwon, N. Kim, C. M. Park, J. S. Lee, K. Y. Kang and J. Park, *Org. Lett.*, 2005, **7**, 1077–1079; (*g*) K. Mori, T. Hara, T. Mizugaki, K. Ebitani and K. Kaneda, *J. Am. Chem. Soc.*, 2004, **126**, 10657–10666; (*h*) K.-M. Choi, T. Akita, T. Mizugaki, K. Ebitani and K. Kaneda, *New J. Chem.*, 2003, **27**, 324–328; (*i*) Y. Uozumi and R. Nakao, *Angew. Chem., Int. Ed.*, 2003, **42**, 194–197; (*j*) J.-D. Grunwaldt, M. Caratati, M. Ramin and A. Baiker, *Catal. Lett.*, 2003, **90**, 221–229; (*k*) G. Kovtun, T. Kameneva, S. L. Hladyi, M. Starchevsky, Y. Pazdersky, I. Stoarov, M. Vargaftik and I. Moiseev, *Adv. Synth. Catal.*, 2002, **344**, 957–964.

5 Z. Hou, N. Theyssen, A. Brinkmann and W. Leitner, *Angew. Chem., Int. Ed.*, 2005, **44**, 1346–1349.
6 (*a*) L. Longenberger and G. Mills, *J. Phys. Chem.*, 1995, **99**, 475–478; (*b*) H. Bönnemann, G. Braun, W. Brijoux, R. Brinkmann, A. Schulze Tilling, K. Seevogel and K. Siepen, *J. Organomet. Chem.*, 1996, **520**, 143–162.
7 *Chemical Synthesis Using Supercritical Fluids*, ed. P. G. Jessop and W. Leitner, Wiley-VCH, Weinheim, 1999.
8 (*a*) A. Baiker, *Chem. Rev.*, 1999, **99**, 453–474; (*b*) W. Leitner, *Acc. Chem. Res.*, 2002, **35**, 746–756; (*c*) P. Licence, J. Ke, M. Sokolova, S. K. Ross and M. Poliakoff, *Green Chem.*, 2003, **5**, 99–104.
9 These properties of $scCO_2$ were exploited recently also with site-isolated molecular ruthenium alcohol oxidation catalysts: S. Campestrini, M. Carraro, R. Ciriminna, M. Pagliaro and U. Tonellato, *Adv. Synth. Catal.*, 2005, **347**, 825–832.
10 For precise BET measurements on these materials of very low surface area much larger amount of substances would have been needed ($\sim$40 g).
11 (*a*) M. N. Vargaftik, V. P. Zagorodnikov, I. P. Stolarov and I. I. Moiseev, *J. Mol. Catal.*, 1989, **53**, 315–348; (*b*) G. Schmid, *Chem. Rev.*, 1992, **92**, 1709–1727.
12 D. Koch and W. Leitner, *J. Am. Chem. Soc.*, 1998, **120**, 13398–13404.
13 The effective volume of the catalyst bed was calcuated from the following values: *m* (catalyst, diluted in quartz) = 3.7 g, bed density (catalyst, diluted in quartz) = 1.4 g mL^{-1}, density (solid quartz) = 2.6 g mL^{-1}; $V_{eff} = V_{bed} - V_{solid}$ = 1.2 mL. The average residence time was then calculated by the following equation: average residence time = V_{eff}/substrate flow rate = 1.2 h.
14 TON and TOF values would be considerably higher if only Pd-atoms on the surface of the nanoparticles would be considered as potentially catalytically active centers.
15 Y. Tatsuno, T. Yoshida and Seiotsuka, *Inorg. Synth.*, 1979, **19**, 221–223.
16 J. Büchele, M. Marzini and H. A. Mayer, *J. Chem. Soc., Dalton. Trans.*, 2003, 4107–4114.

Supercritical carbon dioxide-assisted oxidative degradation and removal of polymer residue after reactive ion etching of photoresist

Bertrand Lo,[a] ChuChun Tai,[a] JiaYaw Chang,[a] ChienHui Wu,[a] BoJung Chen,[a] Tzu-Chen Kuo,[b] Pei-Jung Lian[b] and YongChien Ling*[a]

Received 24th February 2006, Accepted 18th October 2006
First published as an Advance Article on the web 27th October 2006
DOI: 10.1039/b602885c

A green cleaning method involving oxidative degradation in supercritical carbon dioxide ($scCO_2$) to remove the polymer residue from chlorine reactive ion etching (RIE) and ashing of photoresist was developed. Benzoyl peroxide dissolved in pentane-2,4-dione was used as an oxidizing reagent to degrade the polymer residue. Random chain scission products from oxidative degradation were removed by $scCO_2$. Surface characterization and microscopic examination were conducted to investigate the polymer residue. The results indicate that oxidative degradation by benzoyl peroxide in $scCO_2$ provides an effective alternative route to remove post-RIE polymer residue in semiconductor devices.

Introduction

With growing demand for faster computation and lower energy consuming IC devices, the developing process for smaller feature size and higher device density is regarded as being the route of choice. The challenge for advanced exposure techniques such as photoresist stripping and etch residue removal is becoming the critical process. Dry etching such as reactive ion etching (RIE) is the most commonly used method for photoresist stripping. Using an oxygen plasma, most photoresist was ashed and removed *via* oxidation and dehydrogenation by active oxygen species.[1] A two-step stripping process consisting of oxygen plasma ashing and hydrogen plasma cleaning effectively removed residual carbon and polymer.[2] An alternative wet stripping technique using ozone and deionized (DI) water removed hard-baked resist by free radicals *via* oxidative reactions and random chain scission.[3] The oxidation efficiency of the ozonated DI-water was reported to increase with increasing temperature.[4] However, the oxidation efficiency was still restricted by the dramatically low solubility of ozone in water at higher temperature. Besides, the restriction of boundary layer and poor transportation of radicals to the polymer residue might retard the overall oxidation efficiency.

Supercritical carbon dioxide ($scCO_2$) possesses the attractive characteristics of absence of surface tension, excellent mass-transfer efficiency, and controllable solvent ability. In conjunction with its environmentally friendly merits of non-toxic, easily recyclable nature and low critical temperature, $scCO_2$ has become the impetus for many innovative applications, *i.e.*, green processes, in the microelectronics industry.[5] Two recent reviews have detailed the utilization of $scCO_2$ in integrated circuit manufacturing.[6,7] There are few reports about using $scCO_2$ to remove etch residue after photoresist stripping, presumably due to the inert characteristics of $scCO_2$.[8–11] The shortcoming of inadequate solubility was generally resolved by adding co-solvents (modifiers) to enhance the $scCO_2$ solvent strength or surfactants to form microemulsions to enable solute solubilization. Co-solvents such as tetramethylammonium hydroxide (TMAH) a in methanol–water mixture and tetramethylammonium bicarbonate (TMAB) in methanol[7] have been used to remove post-fluorocarbon plasma etch residue. Water-in-CO_2 microemulsion has been successfully used to remove porous low-*k* dielectrics post C_4F_8 etching and O_2 etching.[8] The hydroxyl ion from the TMAH was proposed to attack the interconnection between the residue and substrate, and repeating pressure variation induced the swelling and removal of polymer residue. We have previously attempted to remove the polymer residue after chlorine reactive ion etching (RIE) of photoresist using TMAB in methanol as co-solvent with $scCO_2$. The cleaning efficiency is not as expected even under extended cleaning time.[12]

The free radical generator was considered a candidate for the oxidative degradation of polymer residue.[13–15] 2,2′-Azobis(isobutyronitrile) (AIBN) and benzoyl peroxide (BPO) are the prevalent free radical generators used to initiate polymerization.[16] BPO has also been used to degrade polymer targeted for treatment and recycling.[13,17] Degradation in solution has been proposed to possess better oxidation efficiency, presumably due to improved mass transportation and heat conducting.[18] The poor solubility of BPO in $scCO_2$ is the key problem. The trace amount of dissolved BPO is sufficient to initiate the polymerization but insufficient to effectively degrade the polymer residue. The difficulty encountered with inherent poor solubility could be overcome by either mixing a polar co-solvent, like methanol, with the reagent to improve its solubility or by dissolving the reagent in a suitable amount of selected solvent (better solubility for the reagent) to improve the transportation efficiency *via* emulsion. The latter approach of forming droplets can overcome the limitation of mass transfer between heterophases and the boiling of solvent, presumably caused by the heat released by the oxidative

[a]*Department of Chemistry, National Tsing Hua University, HsinChu 30013, Taiwan*
[b]*Metals Industry Research & Development Center, KaoHsiung 81160, Taiwan*

reaction. In this study, we present a novel green cleaning route using $scCO_2$-assisted oxidative degradation to remove the post-RIE polymer residue based on the droplet formation concept. Preliminary results indicate that $scCO_2$-assisted oxidative degradation may extend the opportunity of using $scCO_2$ processing in semiconductor manufacturing, and substitute for traditional wet chemical methods.

Experimental

The *p*-type 4-inch silicon wafers (Wafer Works Corp., HsinChu, Taiwan) were cleaned by the traditional RCA process before the Al metallization process. The preparation processes of the post-RIE sample with polymer residue are illustrated in Fig. 1. A 5000 Å thick Al film was first deposited onto the cleaned Si substrate using thermal evaporation. The 1 μm thick polyhydroxystyrene-based photoresist film (FH-6400L, Fuji-Hunt Electronics Technology Corp., Tokyo, Japan) was coated thereafter by spin-coating. After exposure and developing, the uncovered Al layer was etched by Cl_2–BCl_3 RIE (ICP 750 W, bias 120 W, Cl_2 and BCl_3 at 35 sccm flow rate, 10 mtorr, 10 min) to prepare the post-CE sample. After O_2 plasma ashing (ICP 500 W, bias 100 W, O_2 at 40 sccm flow rate, 100 mtorr, 2 min) of the resist, the wafer was cut into chips (0.7 mm × 0.7 mm) to prepare the post-OA sample. The oxidative reagent was prepared by sonicating 2.5 g of benzoyl peroxide (Aldrich, 97%) dissolved in 25 ml of pentane-2,4-dione (Merck, GR grade) for 10 min. After BPO was completely dissolved, 2 ml of triethylamine (Riedel-deHaën, 99%) was added to the solution. The $scCO_2$-assisted cleaning process was performed using the home-made system shown in Fig. 2. A high pressure syringe pump (ISCO Inc., Lincoln, Nebraska, USA) was used to supply the liquid CO_2 at the specified pressure. Liquid CO_2 passed through the mixer containing the desired amount of reagent at a flow rate of 0.5 ml min^{-1}. The reactor was modified from a 3.5 ml extraction vessel (Keystone Scientific Inc., Bellefonte, PA, USA) with an internal diameter of 1.0 cm. The Teflon-made holder was placed inside the reactor to position die with plane

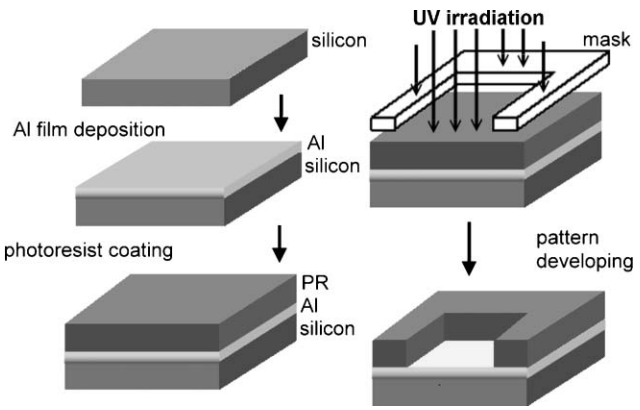

Fig. 1 The preparation processes of post-RIE sample with polymer residue. After RCA cleaning, the aluminium film was deposited on the silicon wafer. Then, the positive photoresist (PR) was coated on the top of aluminium film. After PR baking, the mask with desired patterns was used to protect the specific zone from the UV irradiation. After developing, the mask patterns were cloned on the aluminium film.

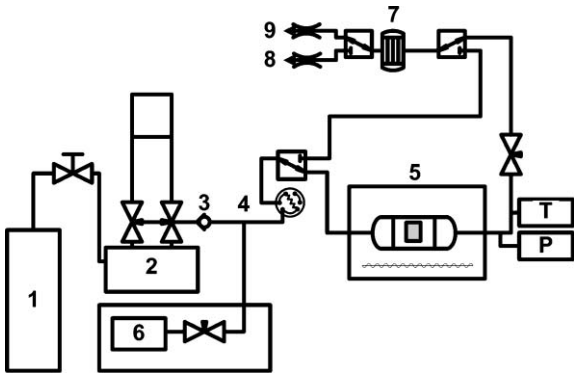

Fig. 2 Schematic diagram of the experimental apparatus: (1) CO_2 cylinder, (2) syringe pump, (3) check valve, (4) mixer, (5) heater, (6) high-pressure pump, (7) back-pressure regulator, (8) vent, (9) trap, T thermometer, P pressure gauge.

oriented nearly parallel to the flow direction. The needle valve (HIP Inc., Erie, PA, USA) and the back pressure regulator (Go Regulator Inc., Spartanburg, USA) were used to regulate the pressure variation. The tubing between injection valve and reactor was pre-heated. In addition, the reactor was also heated by a home-made oven to the chosen operating temperature. The reactor was initially pressurized and kept at the required temperature for 30 min. The flow rate was regulated, held stable at 0.5 ml min^{-1}, and the co-solvent was sequentially injected at a 50 μl min^{-1} flow rate. After 20 min of operation at a constant flow rate, the pressurized reactor was vented.

The identity of the polymer residue was characterized using various spectroscopic techniques. Fourier transform infrared (FT-IR) analysis was conducted on a DA8.3 FT-IR spectrometer (Bomem, CA). Time-of-flight secondary ion mass analysis was carried out on a Tof-SIMS spectrometer (ION-TOF ToF-SIMS IV, Münster, Germany) with a 25 keV Ga^+ primary ion source (0.7 pA pulse current). X-ray photoelectron spectroscopy (XPS) analysis was conducted on an XPS spectrometer (ULVAC-PHI Model PHI Quantera SXM, USA) with an Al K_α source (25 W, 15 kV). All spectra were obtained from an area away from the pattern edges. Microscopic images were obtained with a scanning electron microscope (SEM, JEOL Model JSM-6330F, Japan).

Results and discussion

Microscopic examination and FT-IR characterization

SEM microscopic examination of the post-CE sample (Fig. 3(a)) revealed the absence of polymer residue on the Si

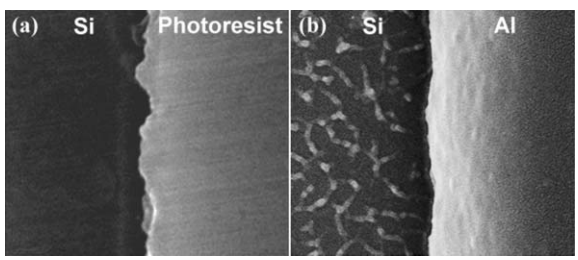

Fig. 3 SEM images of (a) post-CE, and (b) post-OA sample.

substrate. The formation of a rod-like residue was observed on the Si substrate in the post-OA sample (Fig. 3(b)). The novolak-based resist polymer has been reported to form phenolic string *via* intramolecular hydrogen bonding during deposition.[19] During O_2 plasma ashing, the intermediate products would absorb on the surface of native Si oxide and transform into polymer residue. We speculate that the carbonyl radical formed during O_2 plasma ashing induced partial dehydration-polymerization between polymers, *i.e.*, when the arrangement of polymers was dominated by the phenolic strings.

FTIR results reveal the changes to functional groups caused by O_2 plasma ashing. Features such as a C–O–C absorption band and a C–Cl absorption band are present in post-OA samples. These functional groups indicated that the residue was composed of ether and carbon–chlorine features. The presence of ether structure in the residue implies that ether might be an origin for degradation, *i.e.*, if the polymer residue was formed by polymer-to-polymer linking *via* C–O–C formation. The anisotropic plasma etching induced partial cross-linking between polymers, enhanced their mechanical strength, and obstructed subsequent ashing.

Cleaning efficiency and XPS characterization

The reported temperature for the generation of free radicals from BPO was over 70 °C.[13] To accommodate temperature lowering caused by the dynamic flowing operation used in this study, the temperature of the injected reactant must be higher than 70 °C to make the oxidative degradation efficiency (or cleaning efficiency, CLE) compatible with the static mode. In order to study the effect of operational temperature on CLE, XPS was used to measure the C1s peak of polymer residue and the measured results were used to calculate the C_{1s} ratio as the area sum of C_{1s} peaks normalized to the total peak area sum. The relative difference of the C_{1s} ratios of $scCO_2$-cleaned sample and RCA-cleaned sample was used as an index of CLE. Fig. 4 shows the C_{1s} ratio and CLE as a function of operational temperature ranging from 60 to 140 °C. The changing trend of C_{1s} peak is the reverse of that of CLE. The CLE expectedly increased with higher temperature and the best efficiency was obtained at a temperature of *ca.* 120 °C. The numerical results listed in Table 1 indicate that $scCO_2$ cleaning provides better CLE than traditional RCA cleaning.

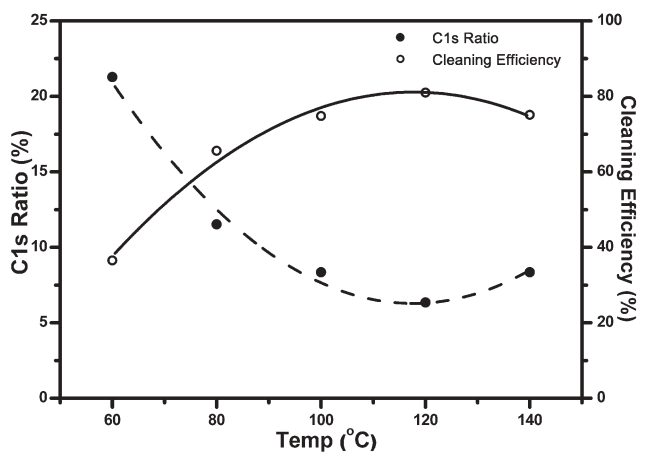

Fig. 4 C_{1s} ratio of polymer residue in XPS spectra and cleaning efficiency (CLE) as a function of temperature.

Table 1 Relative intensity of XPS C_{1s} peak and Tof-SIMS ion *m/z* 107 and *m/z* 221 from polymer residue in samples subjected to different cleaning process

	C_{1s} peak[b]			Ion fragment[c]		
Sample	C–C	C–O	O–C=O	*m/z* 107	*m/z* 221	CLE (%)
RCA-Cleaning	79.5	13.7	6.8	1.2	0.4	—
SC-60[a]	48.6	41.0	10.4	2.4	0.5	36.5
SC-80[a]	43.5	47.5	9.0	1.5	0.2	65.6
SC-100[a]	65.8	26.5	7.7	0.5	<0.1	74.8
SC-120[a]	70.7	23.7	5.6	0.4	<0.1	81.0
SC-140[a]	72.3	22.2	5.5	0.3	<0.1	75.1

[a] SC-number. SC stands for $scCO_2$ cleaning, the number is the operating temperature. [b] Percentage of C_{1s} peak sum in XPS spectra. [c] Percentage relative to Si *m/z* 28 ion intensity in Tof-SIMS spectra.

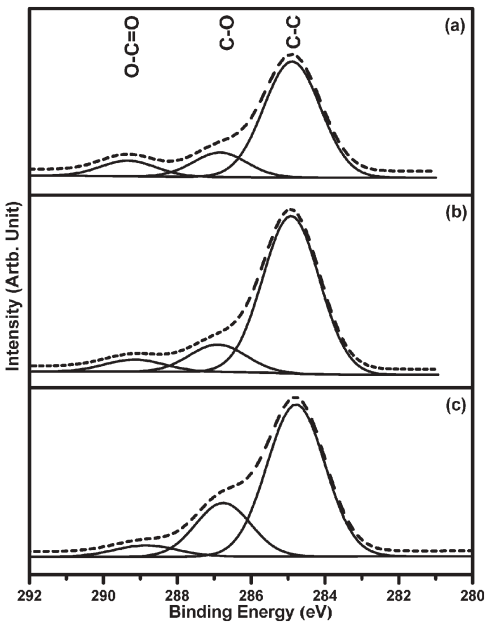

Fig. 5 C_{1s} XPS spectra of: (a) RCA cleaning, (b) $scCO_2$ cleaning at 60 °C, (c) $scCO_2$ cleaning at 120 °C.

To further study the oxidative degradation, the C_{1s} peak was fitted with three peaks of increasing binding energy, such as C–C, C–O and O–C=O (Fig. 5). Their relative peak intensities in RCA-cleaned sample and $scCO_2$-cleaned samples at 60 °C and 120 °C are apparently different. The increment in C–O and C=O peak intensity provides a clue about the reaction pathway. These results imply that post-RIE residue can be removed by the $scCO_2$-assisted cleaning *via* oxidative degradation.

Tof-SIMS and SEM confirmation

To further study oxidative degradation, Tof-SIMS[20] was used to measure and compare the composition of polymer residue in RCA-cleaned and $scCO_2$-cleaned samples. Table 1 lists the numerical results based on two characteristic fragment ions *m/z* 107 and 221. The composition of *m/z* 107 ion is the

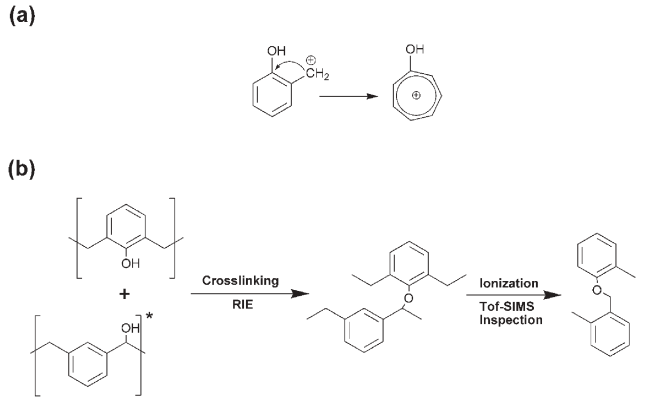

Fig. 6 Characteristic ion fragment structure: (a) *m*/*z* 107 hydroxyltropylium ion fragment, (b) *m*/*z* 221 aromatic ether ion fragment.

hydroxyltropylium ion (Fig. 6(a)), a representative fragment of a hydroxylbenzyl unit. A similar changing tendency of ion intensity *versus* temperature as C_{1s} ratio implies that hydroxyltropylium ion intensity can be used to estimate the amount of polymer residue, presumably because photoresist consists mainly of a phenol-based structure. The composition of *m*/*z* 221 ion (Fig. 6(b)) containing an ether linkage is an adduct ion, which was formed during the O_2 plasma ashing process. The σ bond between the aromatic ether oxygen atom and aromatic carbon atom was *via* sp^2 hybridization. The unhybridized p orbital of the aromatic ether oxygen atom can additionally overlap with the π system of the aromatic ring *via* p-π conjugation, forming a more stable conformation. The *m*/*z* 221 ion intensity can therefore also be used to estimate the amount of polymer residue. Detailed inspection of the ion intensity as a function of temperature indicates that the best CLE can be obtained at a temperature of 120–140 °C.

The spatial distribution of polymer residue on a surface might also provide a clue about the formation mechanism. We therefore used SEM to examine the surface morphology of $scCO_2$-cleaned samples. The results (Fig. 7) indicate that rod-like residues are predominant in both RCA-clean (Fig. 7(a)) and $scCO_2$-clean at 60 °C (Fig. 7(b)) samples, indicating that 60 °C temperature was too low to induce effective oxidative degradation of residue. The morphology of the residue started to change into the spherical residue (Fig. 7(c)) at 80 °C, indicating apparent degradation of polymer residue. At temperatures above 100 °C (Fig. 7(d), 7(e), and 7(f)) the spherical residue became dim, indicating enhancement of oxidative degradation and removal of polymer residue. The SEM results agree well with XPS and Tof-SIMS results, indicating that oxidative degradation mechanism is plausible.

Oxidative degradation mechanism

The proposed oxidative degradation based on a literature work[21] indicates that the reaction was initiated by the abstraction of the α-methylene hydrogen atoms in the polymer residue (Fig. 8a) by the benzoyloxy radical. Combination of the chain radical with a benzoyloxy radical formed a hemiacetal, which oxidized to an ester (Fig. 8b). The ester containing a carbonyl group functioned as a Lewis base (LB) and interacted with $scCO_2$ functioning as a Lewis acid (LA).[19]

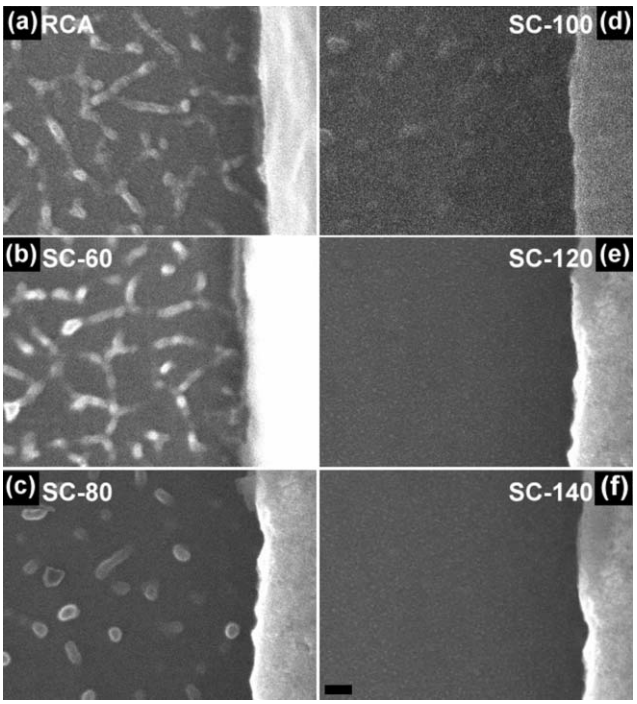

Fig. 7 SEM images of polymer residue: (a) RCA cleaning only; $scCO_2$ cleaning at (b) 60 °C, (c) 80 °C, (d) 100 °C, (e) 120 °C, (f) 140 °C. The scale bar is 100 nm.

The formation of LA–LB conjugate might enhance the solubility of an ester. In addition, the hydrolysis reaction might provide another possible pathway for the chain scission (Fig. 8c). After acid hydrolysis the low molecular-weight degradation products (mixture I in Fig. 8c) would also be readily removed due to improved solubility and higher volatility properties. A smaller portion of the chain radicals might crosslink to each other (Fig. 8d). The crosslinked polymer might be subject to a similar degradation and removal process as the hemiacetal. The LA–LB conjugate (mixture II in Fig. 8c) might be eluted out by solvation with $scCO_2$, whereas the low molecular-weight degradation products might be eluted out by either the co-solvent droplets or the $scCO_2$ flowing over the surface of the chip.

BPO was reported to play a critical role in the oxidative degradation of polymers. The successful application of BPO in biphasic oxidative degradation of the polymer in solution was attributed to efficient heat and mass transfer.[11] The limitation of mass transfer between the free radicals and polymer residue may be alleviated by the lower viscosity and smaller radius of emulsion droplets. The anti-solvent effect of $scCO_2$ promoted precipitation of the $scCO_2$-phobic compounds like BPO in the co-solvent droplets when flowing through the pre-heated tubing.[22] The inter-droplet interaction, like coalescence and reassembling, in the emulsion would release BPO from droplet core. The effective interaction area between BPO and residue was therefore improved by the emulsion dispersion. Consequently, mass transportation between heterophases and the interface area would dominate oxidative degradation in $scCO_2$. Our preliminary results indicate that oxidative degradation in $scCO_2$ seems to overcome the heat and mass

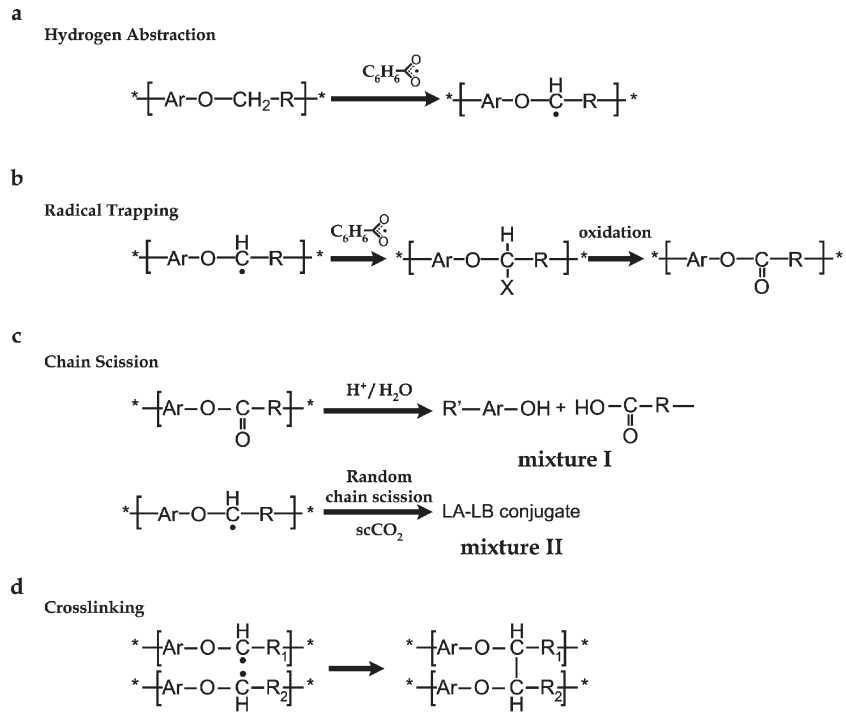

Fig. 8 Oxidative degradation mechanism of polymer residue in CO_2: (a) hydrogen abstraction; (b) radical trapping; (c) chain scission; (d) crosslinking.

transfer limitations in the liquid phase. To our best knowledge, this is the first report describing the formation of pentane-2,4-dione emulsion droplets in $scCO_2$. One possible explanation for incomplete removal of the spherical residue might be that the binding between some of the polymer residue and Si substrate is too strong to be broken by chain scission. The degradation by free radical also became difficult when the chain was sequentially excised until the α-methylene hydrogens were exhausted.

Considering the amount of pentane-2,4-dione added in this study, the expected phase separation of emulsions can arise from either inter-droplet interactions or interface tension-driven combination.[23] The successful oxidative degradation result implies that the phase separation might improve the transportation and dispersion of BPO in pentane-2,4-dione and $scCO_2$ mixture. The result also indicates that the reactant transported by the droplets (co-solvent pool) after phase separation might compensate for the solute–solvent clustering effect, *i.e.*, for the excessive addition of co-solvent, which might function as a micro-reactor to dissolve BPO. Research to confirm this presumption is currently under way.

Conclusions

In conclusion, this study shows that the free radicals generated by benzoyl peroxide dissolved in pentane-2,4-dione can degrade the post-RIE polymer residue and facilitate its removal in $scCO_2$. The influences of $scCO_2$ temperature (60–140 °C) on the removal of polymer residue were also investigated. A droplet transportation model was proposed to explain the difference in removal yield under the chosen pressure. The oxidative degradation yield observed by XPS and Tof-SIMS showed useful results. Oxidative degradation of polymer residue in $scCO_2$ is advantageous over a conventional solvent-based method, which used an enormous amount of water and toxic solvents. This advantage makes the $scCO_2$-based process an ideal candidate method for the technology roadmap for semiconductors.[24] The proposed oxidative degradation mechanism is discussable, nevertheless. To elucidate further the proposed mechanism, the interfacing of an on-line HPLC system to the $scCO_2$ system for on-line monitoring of intermediate products is currently under way.

Acknowledgements

Financial support by National Science of the Republic of China (NSC 92-2113-M007-058), Metals Industry Research and Development Center (93-EC-17-A-04-R7-0180), and National Tsing Hua University is gratefully acknowledged.

References

1 M. A. Hartney, D. W. Hess and D. S. Soane, *J. Vac. Sci. Technol., B*, 1989, **7**, 1–13.
2 H. Seo, S. B. Kim, J. Song, Y. Kim, H. Soh, Y. C. Kim and H. Jeon, *J. Vac. Sci. Technol., B*, 2002, **20**, 1548–1555.
3 I. I. Kashkoush, R. Matthews and R. E. Novak, in *1997 IEEE International Symposium on Semiconductor Manufacturing Conference Proceedings*, San Francisco, CA, USA, 1997, pp. 81–85.
4 S. De Gendt, P. Snee, I. Cornelissen, M. Lux, R. Vos, P. W. Mertens, D. M. Knotter, M. M. Meuris and M. Heyns, *Diffus. Defect Data, Pt. B*, 1999, **65–6**, 165–168.
5 A. O'Neil and J. J. Watkins, *Green Chem.*, 2004, **6**, 363–368.
6 G. L. Weibel and C. K. Ober, *Microelectron. Eng.*, 2003, **65**, 145–152.
7 J. W. King and L. L. Williams, *Curr. Opin. Solid State Mater. Sci.*, 2003, **7**, 413–424.

8 G. Levitin, S. Myneni and D. W. Hess, *J. Electrochem. Soc.*, 2004, **151**, G380–G386.
9 S. Myneni and D. W. Hess, *J. Electrochem. Soc.*, 2003, **150**, G744–G750.
10 X. G. Zhang, J. Q. Pham, H. J. Martinez, P. J. Wolf, P. F. Green and K. P. Johnston, *J. Vac. Sci. Technol., B*, 2003, **21**, 2590–2598.
11 G. Asai, Y. Muraoka, K. Saito, I. Mizobata, T. Iwata, K. Masuda, K. Iijima, T. Yoshikawa and D. Peters, in *Ultra Clean Processing of Silicon Surfaces V*, 2003, pp. 297–300.
12 Y. C. Ling, B. Lo, A. Ghule, K. Y. Hsu, W. Y. Chen, C. C. Tai, T. C. Kuo and P. J. Lien, in *The 3rd International Symposium on Supercritical Fluid Technology for Energy and Environment Applications*, Tianjin, China, 2004, p. 15.
13 G. Madras and S. Chattopadhyay, *Chem. Eng. Sci.*, 2001, **56**, 5085–5089.
14 Y. C. Kim and B. J. McCoy, *Ind. Eng. Chem. Res.*, 2000, **39**, 2811–2816.
15 E. J. Beckman, *Environ. Sci. Technol.*, 2003, **37**, 5289–5296.
16 D. Li, B. X. Han and Z. M. Liu, *Macromol. Chem. Phys.*, 2001, **202**, 2187–2194.
17 G. Sivalingam and G. Madras, *Chem. Eng. Sci.*, 2004, **59**, 1577–1587.
18 S. Sato, T. Murakata, S. Baba, Y. Saito and S. Watanabe, *J. Appl. Polym. Sci.*, 1990, **40**, 2065–2071.
19 A. Reiser, *J. Imaging Sci. Technol.*, 1998, **42**, 15–22.
20 C. Y. Chen, A. V. Ghule, W. Y. Chen, C. C. Wang, Y. S. Chiang and Y. C. Ling, *Appl. Surf. Sci.*, 2004, **231–2**, 447–451.
21 E. M. Christenson, J. M. Anderson and A. Hiltner, *J. Biomed. Mater. Res., Part A*, 2004, **70A**, 245–255.
22 Y. Enokida, O. Tomioka, S. C. Lee, A. Rustenholtz and C. M. Wai, *Ind. Eng. Chem. Res.*, 2003, **42**, 5037–5041.
23 W. Ryoo, S. E. Webber and K. P. Johnston, *Ind. Eng. Chem. Res.*, 2003, **42**, 6348–6358.
24 *The International Technology Roadmap for Semiconductors*, Semiconductor Industry Association, San Jose, CA, USA, 2005.

A facile and green synthetic route to boronic acid esters utilizing mechanochemistry

Michael Schnürch,* Markus Holzweber, Marko D. Mihovilovic and Peter Stanetty*

Received 8th August 2006, Accepted 18th October 2006
First published as an Advance Article on the web 1st November 2006
DOI: 10.1039/b611424e

A facile and environmentally benign method for the formation of boronic acid esters from corresponding boronic acids is reported. Simple grinding of a 1 : 1 mixture of the boronic acid (alkyl, aryl, or heteroaryl boronic acid) and the diol (pinacol or 2,2-dimethylpropane-1,2-diol) without a solvent gave the boronic acid esters. A subsequent simple work-up step gave the title compounds in excellent yield and purity.

Introduction

Boronic acids and esters are nowadays important building blocks in synthetic organic chemistry due to their application in Suzuki–Miyaura[1] cross-coupling reactions. They are regularly used in C–C and also C–N and C–O bond forming cross-coupling processes known in the literature.[2] A great advantage of the Suzuki–Miyaura reaction over other cross-coupling methods is, in many cases, the possibility to avoid organic solvents and perform the reaction in aqueous media, making this cross-coupling reaction the ''greenest'' of all methods. Besides their importance to cross-coupling chemistry, boronic acids have also been used as protecting group for diols, diamines, anthranilic acid, and polyols.[3,4] Initially, such protection reactions were carried out in solution or at functionalized surfaces.[3] Kaupp *et al.* reported recently that these cyclizations proceed quantitatively in the solid state (grinding and ball mill) or in stoichiometric melts.[4] In their work, only phenylboronic acid was used as a protecting group, and excellent results were obtained. Inspired by these findings we investigated the potential of this method for a general and solvent-free entry towards a wide range of boronic acid esters superior to current techniques by its simplicity.

The usefulness of boronic acid esters is based on various properties. Some reactions do not tolerate acidic protons and therefore boronic esters have to be applied in cross-coupling reactions rather than the corresponding acids. Boronic acid esters are often more stable than the corresponding acids. In particular, deboronation of unstable boronic acids can often be avoided or at least considerably decreased when they are transformed into the ester.[5] However, the esters tend to react slower in Suzuki–Miyaura cross-coupling reactions. Apart from cross-coupling chemistry, boronic acid esters have also been useful substrates in other reactions: boronic acid pinacol esters were used as components in the Petasis reaction.[6] Additionally, boric or boronic acid esters sometimes show certain biological activities, *e.g.* boron-containing amino-acids are potent inhibitors of the serine proteases chymotrypsin and subtilisin.[7] Since boronic acid esters are of such great importance in synthetic organic chemistry nowadays, we aimed at the development of an efficient and environmentally benign method for their preparation.

The formation of boronic acids usually proceeds *via* metalation of the most acidic position of a molecule and a subsequent electrophilic quench with boron reagents such as $B(OMe)_3$ or $B(O\text{-}i\text{Pr})_3$.[8] The corresponding boronic acids are obtained after hydrolysis. For boronic acid esters, on the other hand, several preparation methods have been reported and various starting materials can be applied. A very common method generates the boronic acid esters from the boronic acid. This is either achieved *via* a transesterification step with a diol after the metalation and electrophilic quench with $B(OMe)_3$ or $B(O\text{-}i\text{Pr})_3$,[9] or by esterification of an already isolated boronic acid.[6b,10] These esterification reactions are typically carried out under reflux by azeotropic distillation (*e.g.* with benzene or toluene) to remove the formed water. Similarly, stirring the boronic acid and the diol in the presence of molecular sieves in a suitable solvent (*e.g.* CH_2Cl_2) was reported.[11] These methods usually require several hours or even days of reaction time. The necessity to use hazardous solvents and the low energy efficiency are additional drawbacks of these methods. However, this strategy is generally applicable to a wide range of different boronic acids.

Pd-catalyzed methods have also been reported for the direct formation of arylboronic acid esters from aryl halides or triflates, however, with some limitations.[12] Most commonly, pinacolborane (HBpin)[13] or bis(pinacolato)diboron (B_2pin_2)[14] are the reagents of choice for these reactions. HBpin is very sensitive to moisture and air, it is difficult to handle as oil, and it often provides lower yields compared to B_2pin_2. B_2pin_2 on the other hand is an easy to handle colorless solid but much more expensive compared to HBpin. Additionally, homo-coupling products are often obtained as by-products, since the boronic acid ester is introduced under cross-coupling conditions. Consequently, the expensive reagents have to be used in excess (up to 5 equiv.!). The reactions usually require several hours (1–24 h) and often special catalyst–ligand systems of limited accessibility are required. The reported yields vary (0–99%) depending on the applied method and the properties of the starting material. As is often the case with cross-coupling methods, substantial optimization work has to be

Institute of Applied Synthetic Chemistry, Vienna University of Technology, Getreidemarkt 9/163-OC, A-1060 Vienna, Austria. E-mail: peter.stanetty@tuwien.ac.at; Fax: +43-1-58801-15499

invested in order to obtain good results. Therefore, no general reaction conditions are available for the formation of a wide range of different boronic acid esters. However, the possibility to form boronic acid esters directly from aryl halides remains a major advantage, but the method is not applicable for simple alkyl halides (with the exception of allylic halides).[15]

Simple alkanes can also be converted to boronic acid esters at the end of the chain using either photochemical[16] or thermal[17] methods.

Recently, another method was reported by Snieckus *et al.*, who described the formation of boronic acid esters by an *ipso* substitution of the TMS group with BX_3 (X = F, Cl) with subsequent esterification with pinacol.[18]

Another possibility is the use of electrochemical methods.[19] Aryl iodides, bromides, and even chlorides can be used to form boronic acid esters with HBpin. Magnesium or aluminum anodes in combination with nickel foam or stainless steel cathodes were used and the boronic acid esters were obtained in varying yields (19–79%).[20] Inert techniques have to be applied and the reaction was carried out in dry THF, requiring 3 equiv. of HBpin. The biggest disadvantage of this method is the need for special equipment for electrochemical synthesis.

Arylboronic acid esters were also prepared by cyclization of alkyneboronic acid esters with suitable dienes.[21]

The activation of chemical reactions can be achieved by various methods. Usually thermochemistry, electrochemistry, photochemistry and ultrasound are the main methods of interest, with the fifth option for chemical activation, mechanochemistry,[22] often being neglected. While this technique is widely applied in the chemistry of metals, alloys, polymers, and ceramics, the method plays a minor role in organic synthesis and is only used in very special cases. Selected successful examples of applying mechanochemistry in synthesis include the preparation of fullerenes[23] and the oxidation of olefins to carbonic acids with potassium permanganate in a solvent-free environment.[24] Grinding of crystalline organic acids and amines leads to proton transfer with ammonium salt formation or to hydrogen bonded complexes.[25] A major advantage of mechanochemistry are reaction conditions in the absence of a solvent, which is a crucial aspect in the development of clean, environmentally benign, and economical processes.

Results and discussion

Within this contribution we report a general method for the formation of alkyl, aryl, and heteroaryl boronic acid esters from boronic acids using mechanochemistry. Inspired by the preceding work of Kaupp[4] on the utilization of phenylboronic acid as a protecting group for diols, diamines, anthranilic acid, and polyols using solid state or stoichiometric melt synthesis, we investigated the general applicability of this method for the formation of a diverse range of boronic acid esters.

Initially, pinacol was used as the diol component. The applied procedure was kept as simple as possible: preliminary experiments were carried out mixing equimolar amounts of boronic acid and pinacol in a grinding bowl with concomitant mechanochemical conversion. Optimized results were obtained by reacting the starting materials in a ball mill for one hour. The resulting slurry was washed from the ball mill with small amounts of solvent (EtOH or Et_2O, depending on the solubility of the obtained material), dried over Na_2SO_4, filtered and the solvent was evaporated. We identified this protocol as exceptionally suitable for the preparation of almost all investigated boronic acids, usually providing yields in the range of 90% and higher. The purity after the drying step was usually sufficient for further reactions and no column chromatography was required. In some cases, Kugelrohr distillation was used to finally purify the crude material. The obtained results are compiled in Table 1.

The parent phenylboronic acid **1a** was converted to pinacol ester **5a** in 96% yield (Table 1, entry 1). Both, electron withdrawing and electron donating substituents at the boronic acid substrate did not significantly affect the yield. Electron withdrawing examples included 4-fluorophenylboronic acid (**1b**, entry 2) as well as 2- and 3-formylphenylboronic acids (**1d**, entry 4 and **1e**, entry 5) and gave similar results to electron donating 3-methoxyphenylboronic acid **1c** (Table 1, entry 3). As expected, the sterically hindered 2,6-dimethylphenylboronic acid **1f** afforded a lower yield of 60% of **5f**. Additionally, heterocyclic boronic acids have been investigated. Substituted thiopheneboronic acids **1h** and **1i** were converted smoothly to the desired esters **5h** and **5i** in 83% and 80% yield, respectively (Table 1, entries 8 and 9). 2-Fluoropyridine-4-boronic acid **1g** was also converted in 89% to the desired ester **5g** (Table 1, entry 7). Compound **1g** was freshly prepared in our laboratory according to the literature.[26]

In a further extension of our methodology, we applied the mechanochemical protocol to a commercially available aliphatic boronic acid: 2-phenylethylboronic acid **1j** was smoothly converted to the ester **5j** in an excellent 95% yield (Table 1, entry 10).

Generally, we calculated our reaction batches for 500 mg of the expected product. In order to evaluate the scale-up possibilities we chose the reaction of phenylboronic acid as an example since it is the cheapest of the commercially available boronic acids and increased the reaction size by a factor of 20. In this reaction we obtained 9.6 g of phenylboronic acid pinacol ester, which corresponds to 96% yield.

Additionally, we demonstrated that no ball mill is necessary in small scale experiments and grinding the components for 5 minutes in a grinding bowl also gave quantitative conversion to the desired boronic acid esters **5a** and **5b** in comparable purities and yields (entries 1 and 2).[27]

Since the reactions with pinacol worked exceptionally well, we also tried to use another diol in this procedure. 2,2-Dimethylpropan-1,3-diol was used since the resulting boronic acid esters are also often applied in Suzuki–Miyaura cross-coupling reactions. Seven examples of boronic acids were submitted to the mechanochemical esterification process, again covering examples of aryl, heteroaryl, and alkyl boronic acids. As expected, excellent results were obtained for this set of compounds. The phenylboronic acids **1a**, **1c**, and **1f** gave isolated yields >90% of the corresponding esters **6a** (99%), **6b** (91%), and **6d** (97%) (Table 1, entries 11, 12 and 14). Only 3-formylphenylboronic acid **1e** gave a lower but still acceptable 76% yield of **6c** (Table 1, entry 13). The two heterocyclic examples, 2-fluoropyridine-4-boronic acid **1g** and

Table 1 Boronic acid esters

Entry	Diol	Product	Yield (%)
1	**2**	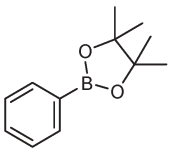 **5a**	96[a]
2	**2**	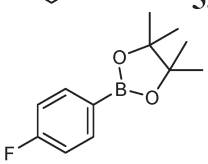 **5b**	86[a]
3	**2**	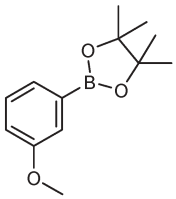 **5c**	86[a]
4	**2**	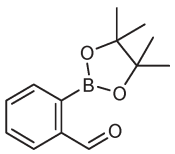 **5d**	88[a]
5	**2**	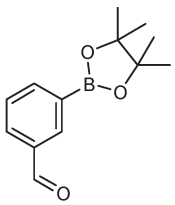 **5e**	96[b]
6	**2**	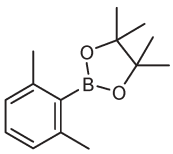 **5f**	60[b]
7	**2**	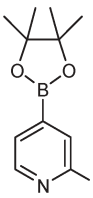 **5g**	89[a]
8	**2**	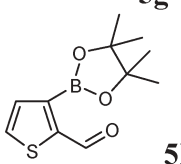 **5h**	83[a]
9	**2**	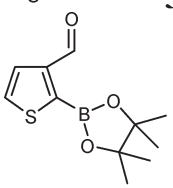 **5i**	80[a]
10	**2**	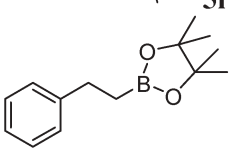 **5j**	95[b]

Table 1 Boronic acid esters (*Continued*)

Entry	Diol	Product	Yield (%)
11	**3**	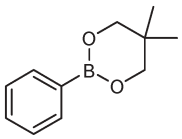 **6a**	99[a]
12	**3**	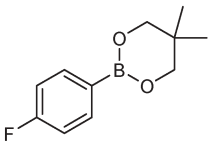 **6b**	85[a]
13	**3**	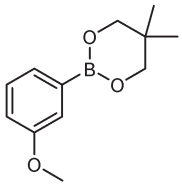 **6c**	91[a]
14	**3**	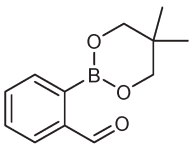 **6d**	82[a]
15	**3**	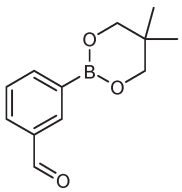 **6e**	76[a]
16	**3**	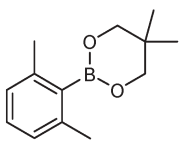 **6f**	97[a]
17	**3**	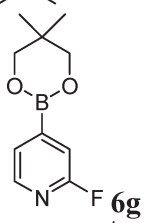 **6g**	90[b]
18	**3**	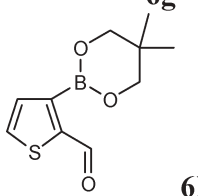 **6h**	92[a]
19	**3**	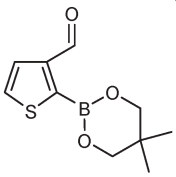 **6i**	84[a]
20	**3**	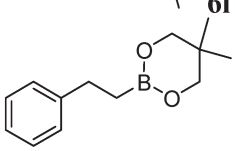 **6j**	95[b]

[a] Kugelrohr distilled. [b] Crude (NMR pure).

3-formylthiophene-2-boronic acid **1i** were converted to the corresponding esters **6e** (90%) and **6f** (86%) in slightly better yields compared to the pinacol examples (Table 1, entries 15 and 16). The alkylboronic acid **1j** also gave 95% of the ester **6g**, as it was in the case for **5j** (Table 1, entry 17).

The reported method has a number of advantages compared to existing methods. First of all, the atom efficiency is excellent since the starting materials are applied as 1 : 1 mixtures and only water is eliminated as a by-product. The reaction itself can therefore be considered as waste-free. Additionally, no solvent is necessary during the reaction and only small amounts of non-toxic solvents (Et_2O, EtOH) were used in the isolation process to transfer the product from the ball mill. The relative amounts of solvent required can be minimized with increasing size of reaction batches. Compared with other methods this mechanochemical approach is also much faster. As mentioned earlier, the classical methods to form boronic acid esters from boronic acids using azeotropic distillation usually require several hours or even days, whereas this reaction is complete within a maximum of 60 minutes.

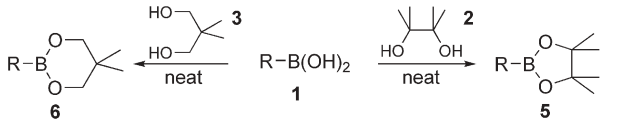

Conclusion

We have developed a facile and high-yielding mechanochemical protocol for the preparation of boronic acid esters. All different types of boronic acids investigated (aryl, heteroaryl, alkyl) reacted smoothly in this process and gave products in excellent yields (comparable or superior to previous references) and purities. It is therefore a more general method than Pd-catalyzed reactions, which have not, so far, been investigated for alkylhalides, and frequently suffer from homo-coupling by-products. In summary, our method is a very efficient process, which requires no elaborate equipment, as the reaction can even be carried out in a grinding bowl. Short reaction times (maximum 1 hour) and simple work-up conditions (filtration, evaporation and eventually Kugelrohr distillation) allow the isolation of boronic acid esters in a short period of time.[28] Mechanochemistry is therefore a powerful alternative to the classical esterification reaction of boronic acids and complements nicely to other methods starting from alternative substrates (*e.g.* Pd-catalyzed methods starting from halides). Additionally, our protocol represents an environmentally benign, atom efficient, and waste free process, since the reaction is carried out under solvent free conditions with equimolar amounts of reagents.

Experimental

Melting points were determined using a Kofler-type Leica Galen III micro hot stage microscope and are uncorrected. Combustion analysis was carried out in the Microanalytical Laboratory, Institute of Physical Chemistry, University of Vienna. Small-scale experiments were carried out on a Retsch MM2 swing mill and the scale-up transformation was performed on a Fritsch Analysette 3 PRO ball mill. Kugelrohr distillation was carried out on a BÜCHI GKR-51 apparatus. NMR-spectra were recorded from $CDCl_3$ or d_6-DMSO solutions on a Bruker AC 200 (200 MHz) or Bruker Avance UltraShield 400 (400 MHz) spectrometer and chemical shifts are reported in ppm using TMS as internal standard.

General procedure

Boronic acid (1 equiv.) and pinacol (1 equiv.) or 2,2-dimethylpropane-1,3-diol (1 equiv.) were ground in a swing mill for 1 hour at 70% of max. capacity. The resulting product was dissolved in diethyl ether (approx. 5 ml) or, in case of a solid product, in ethanol (approx. 5 ml). The solution was dried over sodium sulfate, filtered, and evaporated under reduced pressure. The resulting boronic acid ester can be used for cross-coupling reactions without further purification in most cases. If necessary, esters can be purified by Kugelrohr distillation under reduced pressure. Spectral properties of the obtained products matched with reported literature data.

4,4,5,5-Tetramethyl-2-phenyl-1,3,2-dioxaborolane[29] (5a)

Phenylboronic acid (299 mg, 2.45 mmol, 1 equiv.) and pinacol (290 mg, 2.45 mmol, 1 equiv.) gave the ester as a colorless liquid. Purification: Kugelrohr distillation, 170 °C, 11 mbar. Yield: 456 mg, 2.23 mmol, 91% (lit.:[29] 87%).

The scale-up (phenylboronic acid: 5.97 g, 49 mmol, 1 equiv.; pinacol: 5.79 g, 49 mmol, 1 equiv.) was performed on a Fritsch Analysette 3 PRO ball mill to give a colorless liquid. Purification: Kugelrohr distillation, 110 °C, 0.32 mbar. Yield: 9.56 g, 47 mmol, 96% (lit.:[29] 87%).

2-(4-Fluorophenyl)-4,4,5,5-tetramethyl-1,3,2-dioxaborolane[20] (5b)

4-Fluorophenylboronic acid (315 mg, 2.25 mmol, 1 equiv.) and pinacol (266 mg, 2.25 mmol, 1 equiv.) gave the ester as a colorless liquid. Purification: Kugelrohr distillation, 200 °C, 11 mbar. Yield: 430 mg, 1.94 mmol, 86% (lit.:[20] 25%).

2-(3-Methoxyphenyl)-4,4,5,5-tetramethyl-1,3,2-dioxaborolane[30] (5c)

3-Methoxyphenylboronic acid (324 mg, 2.13 mmol, 1 equiv.) and pinacol (253 mg, 2.13 mmol, 1 equiv.) gave the ester as a pale yellow liquid. Purification: Kugelrohr distillation, 220 °C, 11 mbar. Yield: 430 mg, 1.84 mmol, 86% (lit.:[30] 92%).

2-(4,4,5,5-Tetramethyl-1,3,2-dioxaborolan-2-yl)benzaldehyde[11] (5d)

2-Formylphenylboronic acid (323 mg, 2.15 mmol, 1 equiv.) and pinacol (255 mg, 2.15 mmol, 1 equiv.) gave the ester as a beige liquid. Yield: 441 mg, 1.90 mmol, 88% (lit.:[11] 68%).

3-(4,4,5,5-Tetramethyl-1,3,2-dioxaborolan-2-yl)benzaldehyde[11] (5e)

3-Formylphenylboronic acid (323 mg, 2.15 mmol, 1 equiv.) and pinacol (255 mg, 2.15 mmol, 1 equiv.) gave the ester as a yellow liquid. Yield: 481 mg, 2.07 mmol, 96% (lit.:[11] 77%).

4,4,5,5-Tetramethyl-2-(2,6-dimethylphenyl)-1,3,2-dioxaborolane[31] (5f)

2,6-Dimethylphenylboronic acid (323 mg, 2.15 mmol, 1 equiv.) and pinacol (255 mg, 2.15 mmol, 1 equiv.) gave the ester as a yellow solid. Purification: Kugelrohr distillation, 220 °C, 0.43 mbar. Mp.: 54–57 °C (lit.:[29,31] n. a.). Yield: 294 mg, 1.27 mmol, 59% (lit.:[29] 63%).

2-Fluoro-4-(4,4,5,5-tetramethyl-1,3,2-dioxaborolan-2-yl) pyridine[26] (5g)

2-Fluoropyridine-4-boronic acid (300 mg, 2.13 mmol, 1 equiv.) and pinacol (252 mg, 2.13 mmol, 1 equiv.) gave the ester as a colorless liquid which crystallized slowly. Purification: Kugelrohr distillation, 140 °C, 0.38 mbar. Mp.: 37–45 °C (lit.:[26] 60 °C). Yield: 421 mg, 1.88 mmol, 89% (lit.:[26] 62%).

3-(4,4,5,5-Tetramethyl-1,3,2-dioxaborolan-2-yl)thiophene-2-carbaldehyde[32] (5h)

2-Formylthiophene-3-boronic acid (313 mg, 2.27 mmol, 1 equiv.) and pinacol (268 mg, 2.27 mmol, 1 equiv.) gave the ester as a yellow solid. Purification: Kugelrohr distillation, 150 °C, 0.4 mbar. Mp.: 40–45 °C (lit.:[32] n. a.). Yield: 450 mg, 1.89 mmol, 83% (lit.:[32] n. a.).

δ_H(200 MHz; $CDCl_3$) 1.36 (12 H, s, 4 × CH_3), 7.48 (1 H, d, *J* 4.9, CH), 7.69 (1 H, dd, *J* 4.9 and 1.2, CH), 10.44 (1 H, d, *J* 1.2, CHO)

δ_C(50 MHz, $CDCl_3$) 24.8 (4 × q), 84.4 (2 × s), 133.4 (d), 134.9 (d), 152.6 (s), 186.0 (d)

2-(4,4,5,5-Tetramethyl-1,3,2-dioxaborolan-2-yl)thiophene-3-carbaldehyde[33] (5i)

3-Formylthiophene-2-boronic acid (313 mg, 2.27 mmol, 1 equiv.) and pinacol (268 mg, 2.27 mmol, 1 equiv.) gave the ester as a yellow liquid which crystallized slowly. Purification: Kugelrohr distillation, 150 °C, 0.4 mbar. Mp.: 54–61 °C (lit.:[33] 65.3–68.3 °C). Yield: 432 mg, 1.81 mmol, 80% (lit.:[33] 49%).

4,4,5,5-Tetramethyl-2-phenylethyl-1,3,2-dioxaborolane[34] (5j)

2-Phenylethylboronic acid (323 mg, 2.15 mmol, 1 equiv.) and pinacol (255 mg, 2.15 mmol, 1 equiv.) gave the ester as a colorless solid. Mp.: 38–40 °C (lit:[34] n. a). Yield: 475 mg, 2.05 mmol, 95% (lit.:[34a] quant).

5,5-Dimethyl-2-phenyl-1,3,2-dioxaborinane[35] (6a)

Phenylboronic acid (321 mg, 2.63 mmol, 1 equiv.) and 2,2-dimethylpropan-1,3-diol (274 mg, 2.63 mmol, 1 equiv.) gave the ester as a colorless solid. Purification: Kugelrohr distillation, 150 °C, 0.36 mbar. Mp.: 59–62 °C (lit.:[35] 62 °C). Yield: 495 mg, 2.60 mmol, 99% (lit.:[35] 82%).

2-(4-Fluorophenyl)-5,5-dimethyl-1,3,2-dioxaborinane (6b)

4-Fluorophenylboronic acid (336 mg, 2.40 mmol, 1 equiv.) and 2,2-dimethylpropan-1,3-diol (250 mg, 2.40 mmol, 1 equiv.) gave the ester as a colorless solid. Purification: Kugelrohr distillation, 140 °C, 0.68 mbar. Mp.: 61–65 °C (lit.:[36] 64–68 °C). Yield: 425 mg, 2.04 mmol, 85%.

δ_H(200 MHz; $CDCl_3$; Me_4Si) 1.02 (6 H, s, 2 × CH_3), 3.76 (4 H, s, 2 × OCH_2), 7.04 (2 H, t, *J* 8.9, 2 × CH), 7.79 (2 H, t, *J* 7.4, 2 × CH)

δ_C(50 MHz; $CDCl_3$; Me_4Si) 21.9 (2 × q), 31.84 (s), 72.3 (2 × t), 114.5 (dd, *J* 20.1), 136.0(dd, *J* 7.8), 164.8 (ds, *J* 164.8)

2-(3-Methoxyphenyl)-5,5-dimethyl-1,3,2-dioxaborinane (6c)

3-Methoxyphenylboronic acid (345 mg, 2.27 mmol, 1 equiv.) and 2,2-dimethylpropan-1,3-diol (237 mg, 2.27 mmol, 1 equiv.) gave the ester as a colorless solid. Purification: Kugelrohr distillation, 140 °C, 0.32 mbar. Mp.: 68–71 °C. Yield: 453 mg, 2.06 mmol, 91% (Found: C, 65.41; H, 7.84. $C_{12}H_{17}BO_3$ requires C, 65.49, H, 7.84%).

δ_H(200 MHz; $CDCl_3$; Me_4Si) 1.02 (6 H, s, 2 × CH_3), 3.77 (4 H, s, 2 × OCH_2), 3.83 (3 H, s, OCH_3), 6.98 (1 H, ddd, *J* 8.1 and 2.8 and 1.2, CH), 7.23–7.44 (3 H, m, 3 × CH)

δ_C(50 MHz; $CDCl_3$; Me_4Si) 21.9 (2 × q), 31.9 (s), 55.1 (q), 72.3 (2 × t), 117.2 (d), 117.9 (d), 126.2 (d), 128.7 (d), 159.0 (s)

2-(5,5-Dimethyl-1,3,2-dioxaborinan-2-yl)benzaldehyde[35] (6d)

2-Formylphenylboronic acid (344 mg, 2.29 mmol, 1 equiv.) and 2,2-dimethylpropan-1,3-diol (238 mg, 2.29 mmol, 1 equiv.) gave the ester as a colorless liquid. Purification: Kugelrohr distillation, 170 °C, 0.67 mbar. Yield: 411 mg, 1.88 mmol, 82% (lit.:[35] 99%).

3-(5,5-Dimethyl-1,3,2-dioxaborinan-2-yl)benzaldehyde[37] (6e)

3-Formylphenylboronic acid (344 mg, 2.29 mmol, 1 equiv.) and 2,2-dimethylpropan-1,3-diol (238 mg, 2.29 mmol, 1 equiv.) gave the ester as a yellow liquid. Purification: Kugelrohr distillation, 150 °C, 0.32 mbar. Yield: 382 mg, 1.75 mmol, 76% (lit.:[37] 65%).

5,5-Dimethyl-2-(2,6-dimethylphenyl)-1,3,2-dioxaborinane (6f)

2,6-Dimethyphenylboronic acid (344 mg, 2.29 mmol, 1 equiv.) and 2,2-dimethylpropan-1,3-diol (239 mg, 2.29 mmol, 1 equiv.) gave the ester as a pale yellow liquid which crystallized slowly. Purification: Kugelrohr distillation, 150 °C, 0.36 mbar. Mp.: 49–54 °C. Yield: 485 mg, 2.22 mmol, 97% (Found C, 71.43; H, 8.84%. $C_{13}H_{19}BO_2$ requires C, 71.59, H, 8.78%).

δ_H(200 MHz; $CDCl_3$; Me_4Si) 1.13 (6 H, s, 2 × CH_3), 2.43 (6 H, s, 2 × CH_3), 3.82 (4 H, s, 2 × OCH_2), 6.98 (2 H, d, *J* 7.4, 2 × CH), 7.09–7.19 (1 H, m, CH)

δ_C(50 MHz; $CDCl_3$; Me_4Si) 22.2 (4 × q), 31.5 (s), 72.2 (2 × t), 126.3 (2 × d), 128.4 (d), 140.4 (2 × s)

2-Fluoro-4-(5,5-dimethyl-1,3,2-dioxaborinan-2-yl)pyridine (6g)

2-Fluoropyridine-4-boronic acid (300 mg, 2.13 mmol, 1 equiv.) and 2,2-dimethylpropan-1,3-diol (221 mg, 2.13 mmol, 1 equiv.) gave the ester as a colorless liquid. Purification: Kugelrohr distillation, 140 °C, 0.38 mbar. Yield: 399 mg, 1.91 mmol, 90% (Found C, 57.19, H, 6.29, N, 6.40%. $C_{10}H_{13}BFNO_2$ requires C, 57.46, H, 6.27, N, 6.70%).

δ_H(200 MHz; $CDCl_3$; Me_4Si) 1.03 (6 H, s, 2 × CH_3), 3.78 (4 H, s, 2 × OCH_2), 7.27 (1 H, d, *J* 2.0, CH), 7.49 (1 H, dd, *J* 4.5 and 3.1, CH), 8.21 (1 H, d, *J* 4.9, CH).

δ_C(50 MHz; $CDCl_3$; Me_4Si) 21.71 (2 × q), 31.83 (s), 72.37 (2 × t), 113.88 (dd, *J* 35), 125.37 (dd, *J* 3.9), 146.81 (d, *J* 13.4), 163.68 (d, *J* 240.2)

3-(5,5-Dimethyl-1,3,2-dioxaborinan-2-yl)thiophene-2-carbaldehyde (6h)

2-Formylthiophene-3-boronic acid (348 mg, 2.23 mmol, 1 equiv.) and 2,2-dimethylpropan-1,3-diol (232 mg, 2.23 mmol, 1 equiv.) gave the ester as a yellow liquid. Purification: Kugelrohr distillation, 160 °C, 0.87 mbar. Yield: 462 mg, 2.06 mmol, 92%.

δ_H(200 MHz; $CDCl_3$; Me_4Si) 1.02 (6 H, s, 2 × CH_3), 3.77 (4 H, s, 2 × OCH_2), 7.43 (1 H, d, *J* 4.9, CH), 7.62 (1 H, dd, *J* 4.9 and 1.2, CH), 10.42 (1 H, d, *J* 1.2 CHO)

δ_C(50 MHz; $CDCl_3$; Me_4Si) 21.69 (2 × q), 31.74 (s), 72.26 (2 × t), 132.90 (d), 134.79 (d), 151.52 (s), 186.32 (d)

2-(5,5-Dimethyl-1,3,2-dioxaborinan-2-yl)thiophene-3-carbaldehyde (6i)

3-Formylthiophene-2-boronic acid (348 mg, 2.23 mmol, 1 equiv.) and 2,2-dimethylpropan-1,3-diol (232 mg, 2.23 mmol, 1 equiv.) gave the ester as a yellow liquid. Purification: Kugelrohr distillation, 180 °C, 0.86 mbar. Yield: 421 mg, 1.88 mmol, 84%.

δ_H(200 MHz; $CDCl_3$; Me_4Si) 1.04 (6 H, s, 2 × CH_3), 3.80 (4 H, s, 2 × OCH_2), 7.47 (1 H, dd, *J* 4.9 and 0.8, CH), 7.64 (1 H, d, *J* 4.9, CH), 10.40 (1 H, s, CHO)

δ_C(50 MHz; $CDCl_3$; Me_4Si) 21.76 (2 × q), 31.95 (s), 72.52 (2 × t), 127.10 (d), 131.05 (d), 149.22 (s), 188.31 (d)

5,5-Dimethyl-2-phenylethyl-1,3,2-dioxaborinane[38] (6j)

2-Phenylethylboronic acid (343 mg, 2.28 mmol, 1 equiv.) and 2,2-dimethylpropan-1,3-diol (238 mg, 2.28 mmol, 1 equiv.) gave the ester as a colorless liquid. Yield: 485 mg, 2.22 mmol, 95% (lit.:[38] 70%).

Acknowledgements

We are grateful to Prof. G. Kickelbick, Institute of Materials Chemistry, Vienna University of Technology for giving us the possibility to use his Retsch MM2 swing mill.

References

1 (*a*) N. Miyaura and A. Suzuki, *J. Chem. Soc., Chem. Commun.*, 1979, 866–867; (*b*) N. Miyaura, K. Yamada and A. Suzuki, *Tetrahedron Lett.*, 1979, 3437–3440; (*c*) N. Miyaura and A. Suzuki, *Chem. Rev.*, 1995, **95**, 2457–2483; (*d*) A. Suzuki, *J. Organomet. Chem.*, 1999, **576**, 147–168; (*e*) S. Kotha, K. Lahiri and D. Kashinath, *Tetrahedron*, 2002, **58**, 9633–9695; (*f*) A. R. Martin and Y. Yang, *Acta Chem. Scand.*, 1993, **47**, 221–230; (*g*) A. Suzuki, *Chem. Commun.*, 2005, **38**, 4759–4763.

2 (*a*) D. M. T. Chan, K. L. Monaco, R.–P. Wang and M. P. Winters, *Tetrahedron Lett.*, 1998, **39**, 2933–2936; (*b*) D. M. T. Chan, K. L. Monaco, R. Li, D. Bonne, C. G. Clark and P. Y. S. Lam, *Tetrahedron Lett.*, 2003, **44**, 3863–3865.

3 (*a*) J. M. Sugihara and C. M. Bowman, *J. Am. Chem. Soc.*, 1958, **80**, 2443–2446; (*b*) M. Pailer and W. Fenzel, *Monatsh. Chem.*, 1961, **92**, 1294–1299.

4 G. Kaupp, M. R. Naimi-Jamal and V. Stepanenko, *Chem.–Eur. J.*, 2003, **9**, 4156–4160.

5 A. J. Roche and B. Canturk, *Org. Biomol. Chem.*, 2005, **3**, 515–519.

6 (*a*) A. A. Kolomeitsev, A. A. Kadyrov, J. Szczepkowska-Sztolcman, M. Milewska, H. Koroniak, G. Bissky, J. A. Barten and G.-V. Röschenthaler, *Tetrahedron Lett.*, 2003, **44**, 8273–8277; (*b*) T. Koolmeister, M. Södergren and M. Scobie, *Tetrahedron Lett.*, 2002, **43**, 5965–5968.

7 C. A. Kettner and A. B. Shenvi, *J. Biol. Chem.*, 1984, **259**, 15106–15114.

8 (*a*) W. J. Thompson and J. Gaudino, *J. Org. Chem.*, 1984, **49**, 5237–5243; (*b*) Y. Tokunaga, H. Ueno, Y. Shimomura and T. Seo, *Heterocycles*, 2002, **57**, 787–790.

9 (*a*) C. Coudret, *Synth. Commun.*, 1996, **26**, 3543–3547; (*b*) P. Stanetty, M. Schnuerch and M. D. Mihovilovic, *J. Org. Chem.*, 2006, **71**, 3754–3761; (*c*) C. Coudret, *Synth. Commun.*, 1996, **26**, 3543–3547; (*d*) W. Li, D. P. Nelson, M. S. Jensen, R. S. Hoermer, D. Cai and R. D. Larsen, *Org. Synth.*, 2005, **81**, 89–97.

10 (*a*) A. Mendoza and D. S. Matteson, *J. Org. Chem.*, 1979, **44**, 1352–1354; (*b*) H. C. Brown, N. G. Bhat and V. Somayaji, *Organometallics*, 1983, **2**, 1311–1316.

11 C. M. Vogels, L. G. Nikolcheva, D. W. Norman, H. A. Spinney, A. Decken, M. O. Baerlocher, F. J. Baerlocher and S. A. Wescott, *Can. J. Chem.*, 2001, **79**, 1115–1123.

12 J. A. Marshall, *Chemtracts*, 2000, **13**, 219–222.

13 (*a*) M. Murata, S. Wanatabe and Y. Masuda, *J. Org. Chem.*, 1997, **62**, 6458–6459; (*b*) M. Murata, T. Oyama, S. Wanatabe and Y. Masuda, *J. Org. Chem.*, 2000, **65**, 164–168; (*c*) M. Melaimi, F. Mathey and P. Le Floch, *J. Organomet. Chem.*, 2001, **640**, 197–199.

14 (*a*) T. Ishiyama, Y. Itoh, T. Kitano and N. Miyaura, *Tetrahedron Lett.*, 1997, **38**, 3447–3450; (*b*) T. Ishiyama, N. Matsuda, N. Miyaura and A. Suzuki, *J. Am. Chem. Soc.*, 1993, **115**, 11018–11019; (*c*) X. Liu, *Synlett*, 2003, 2442–2443; (*d*) T. Ishiyama, M. Murata and N. Miyaura, *J. Org. Chem.*, 1995, **60**, 7508–7510.

15 (*a*) M. Murata, S. Wanatabe and Y. Masuda, *Tetrahedron Lett.*, 2000, **41**, 5877–5880; (*b*) K. Takahashi, T. Ishiyama and N. Miyaura, *J. Organomet. Chem.*, 2001, **625**, 47–53.

16 H. Chen and J. F. Hartwig, *Angew. Chem., Int. Ed.*, 1999, **38**, 3391–3393.

17 (*a*) H. Chen, S. Schlecht, T. C. Semple and J. F. Hartwig, *Science*, 2000, **287**, 1995–1997; (*b*) D. H. Woodmansee, X. Bu and G. C. Bazan, *Chem. Commun.*, 2001, 619–620.

18 Z. Zhao and V. Snieckus, *Org. Lett.*, 2005, **7**, 2523–2526.

19 (*a*) C. Laza, C. Pintaric, S. Olivero and E. Dunach, *Electrochim. Acta*, 2005, **50**, 4897–4901; (*b*) C. Laza and E. Dunach, *C. R. Chim.*, 2003, **6**, 185–187.

20 C. Laza and E. Dunach, *Adv. Synth. Catal.*, 2003, **345**, 580–583.

21 J. E. Moore, M. York and J. P. A. Harrity, *Synlett*, 2005, 860–862.

22 (*a*) M. K. Beyer and H. Clausen-Schaumann, *Chem. Rev.*, 2005, **105**, 2921–2948; (*b*) S. Kipp, V. Sepelak and K. D. Becker, *Chem. Unserer Zeit*, 2005, **39**, 384–392; (*c*) P. Balaz, W. S. Choi, M. Fabian and E. Godocikova, *Acta Montan. Slovaca*, 2006, **11**, 122–129; (*d*) Z. V. Todres, *Organic Mechanochemistry and Its Practical Application*, CRC Press, Boca Raton, FL, USA, 2006.

23 Selected examples: (*a*) T. Braun, A. Buvaribarcza, L. Barcza, I. Konkolythege, M. Fodor and B. Migali, *Solid State Ionics*, 1994, **74**, 47–51; (*b*) G. W. Wang, K. Komatsu, Y. Murata and M. Shiro, *Nature*, 1997, **387**, 583–586; (*c*) F. Constabel and K. E. Geckler, *Tetrahedron Lett.*, 2004, **45**, 2071–2073.

24 M. Nüchter, B. Ondruschka and R. Trotzki, *J. Prakt. Chem.*, 2000, **342**, 720–724.

25 (*a*) A. V. Trask, D. A. Haynes, W. D. S. Motherwell and W. Jones, *Chem. Commun.*, 2006, 51–53; (*b*) J. Fernandez-Bertran, J. C. Alvarez and E. Reguera, *Solid State Ionics*, 1998, **106**, 129–135.

26 A. Buillon, J.-C. Lancelot, V. Collot, P. R. Bovy and S. Rault, *Tetrahedron*, 2002, **58**, 4369–4373.

27 Equimolar amounts of the boronic acid and the diol were grinded in a grinding bowl until the material became completely liquid. Completion of the reaction was confirmed by ^{1}H-NMR.

28 Application of the reported boronic esters in Suzuki cross-coupling reactions will be published elsewhere.

29 Y. Ma, C. Song, W. Jiang, G. Xue, J. F. Cannon, X. Wang and M. B. Andrus, *Org. Lett.*, 2003, **5**, 4635–4638.

30 T. Ishiyama, K. Ishida and N. Miyaura, *Tetrahedron*, 2001, **57**, 9813–9816.

31 O. Baudoin, D. Guénard and F. Guéritte, *J. Org. Chem.*, 2000, **65**, 9268–9271.

32 M. Lautens and J. Mancuso, *J. Org. Chem.*, 2004, **69**, 3478–3487.
33 C. Christopherson, M. Begtrup, S. Ebdrup, H. Petersen and P. Vedso, *J. Org. Chem.*, 2003, **68**, 9513–9516.
34 (*a*) C. M. Crudden, Y. B. Hleba and A. C. Chem, *J. Am. Chem. Soc.*, 2004, **126**, 9200–9201; (*b*) A. V. Kalinin, S. Scherer and V. Snieckus, *Angew. Chem., Int. Ed.*, 2003, **42**, 3399–3404.
35 H. Chaumeil, S. Signorella and C. Le Drian, *Tetrahedron*, 2000, **56**, 9655–9662.
36 Aldrich, product no: 632686.
37 B. Shi and R. W. Boyle, *J. Chem. Soc., Perkin Trans. 1*, 2002, 1397–1400.
38 P. R. Blackmore, S. P. Marsden and H. D. Vater, *Org. Lett.*, 2006, **10**, 773–776.

A novel one-pot three-component synthesis of 2,4-disubstituted-3*H*-benzo[*b*][1,4]diazepines in water

Sanjay S. Palimkar, Rajgopal J. Lahoti and Kumar V. Srinivasan*

Received 21st July 2006, Accepted 30th October 2006
First published as an Advance Article on the web 8th November 2006
DOI: 10.1039/b610523h

A novel green and efficient one-pot three-component synthesis of 2,4-disubstituted-3*H*-benzo[*b*][1,4]diazepines in excellent isolated yields has been reported. The methodology initially involves the formation of ynones *via* coupling of a wide range of acid chlorides with terminal alkynes catalysed by $Pd(OAc)_2$ under copper-, ligand- and solvent-free conditions in just 10 min at rt followed by the Michael addition and cyclocondensation of *o*-phenylenediamines added *in situ* using water as a solvent at reflux temprature. In addition, the structure of the benzodiazepine was confirmed to be the diimino molecule and not the enamine by X-ray crystallographic analysis of the benzodiazepine **4b**. The methodology is suitable for the operation in combi-chem mode to generate libraries of a diverse array of benzodiazepines. The methodology has been successful in achieving the twin green chemistry objectives of a solvent and ligand free operation and the use of water as a non-hazardous, inexpensive and readily available solvent in the sequential reaction steps performed *in situ*, thus combining the features of both economic and environmental advantages.

Introduction

The chemical industry is one of the major contributors to the environmental pollution, owing to the use of hazardous chemicals and in particular large amounts of flammable, volatile and often toxic organic solvents. With increasing interest in green chemistry concept, such volatile organic solvents are being replaced by alternative non-toxic, non-flammable and non-volatile media such as ionic liquids, supercritical fluids and water or alternatively, the reactions are carried out under solvent free conditions.[1] Water is a readily available, safe, cheap and environmentally benign solvent. It is in this context, significant interest has been evinced in the development of organic reactions in water in recent times.[2]

Sequential transformations and multi-component one-pot reactions are always resource effective and environmentally acceptable and thus greener as compared to multi-step reactions.[3] They offer significant advantages over conventional linear step syntheses, by reducing time, saving money, energy and raw-materials thus resulting in both economical and environmental benefits. At the same time, diversity can be achieved for building up libraries by simply varying each component.[4]

Benzodiazepines and their polycyclic derivatives, target molecules of the present work are a very important class of bioactive compounds, widely used as anticonvulsant, anti-inflammatory, analgesic, hypnotic, sedative and anti-depressive agents.[5] In addition to this, 2,4-disubstituted-3*H*-1,4-benzodizepines[6] are especially useful synthons for the rapid construction of polyheterocyclic systems due to the presence of two possible dipolarophile sites. This structural feature could allow the diversity-oriented synthesis[7] of small libraries of benzodiazepine-based compounds for pharmacological testing on a wide range of biological targets.[8] Among several methodologies presented in literature, the synthesis of 2,4-disubstituted-3*H*-benzo[*b*][1,4]diazepine has been reported both by Ried and Koeing[9] and by Andreichikov and co-workers,[10] by the reaction of *o*-phenylenediamines with ynones. This method has been extended to the synthesis of variously substituted 2,4-diphenyl-3*H*-benzo[*b*][1,4]diazepines.[11] The reactions have been carried out in boiling ethanol,[11*a*] methanol, or mixture of ethanol and acetic acid,[11*b*,*c*] the volatile solvents contributing to environmental pollution.

As part of our continuing interest to develop more efficient and environmentally benign methods in organic synthesis, our investigations include, for instance copper-, ligand- and amine-free one-pot synthesis of indole,[12] ionic liquid promoted regiospecific synthesis of quinoline,[13] ultrasound promoted acetylation of alcohols and three-component synthesis of dihydropyrimidones by the Biginelli reaction in room temperature ionic liquids.[14] In continuation, herein, we wish to report for the first time, a novel one-pot three-component synthesis of 2,4-disubstituted-3*H*-benzo[*b*][1,4]diazepines *via* the coupling of acid chlorides with terminal alkynes followed by the *in situ* Michael addition and cyclocondensation of the resulting ynones with substituted *o*-phenylenediamines (OPDs) using water as a solvent (Scheme 1).

Results and discussion

Initially, the coupling of benzoyl chloride with phenyl acetylene was achieved under copper-, ligand- and solvent-free condition using $Pd(OAc)_2$ (0.2 mol%) as a catalyst and one equivalent of triethylamine as the base. After complete formation of the product ynone as monitored by TLC (in all the

Division of Organic Chemistry: Technology, National Chemical Laboratory, Dr. Homi Bhabha Road, Pune, 411 008, India. E-mail: kv.srinivasan@ncl.res.in; Fax: +91 20 25902629; Tel: +91 20 25902098

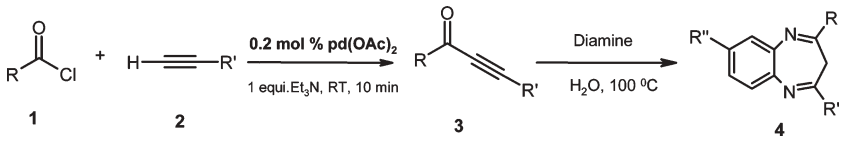

Scheme 1

cases the reaction time is just 10 min), OPD was added along with water as solvent and reaction was carried out reflux at temperature 100 °C for 2 h to afford the 2,4-diphenyl-3*H*-benzo[*b*][1,4]diazepine in excellent isolated yield. To survey the generality and scope of this one-pot three-component protocol, the methodology was applied to the synthesis of a variety of benzodiazepine derivatives. The results are summarized in Table 1.

We investigated further the electronic effect of different substituents present on each component of the coupling partners. We observed that a wide range of acid chlorides having both electron-donating and electron-withdrawing groups were equally facile for the reaction resulting in the formation of benzodiazepine derivatives in excellent isolated yields.

Even the hetro-aryl acid chlorides such as 2-thiophene carbonyl chloride (entries 10, 17) and 2-furoyl chloride (entry 11) reacted smoothly to give the heterodiazepine derivatives in excellent yields.

For a comparative study, the various terminal alkynes including different substituents such as methyl, methoxy, fluoro and trifluoromethyl were used. Among these, it was found that a relatively low yield in the case of trifluoromethyl substituted terminal alkyne was obtained as compared to other substituted terminal alkynes (entry 5). Moreover, both the unsubstituted OPD and the substituted OPDs having electron-donating group on the aromatic moiety gave benzodiazepienes in excellent yields. However in the case of OPD having an electron-withdrawing group such as $-NO_2$, no reaction was observed even after refluxing for a prolonged period (24 h).

All the benzodiazepine derivatives synthesized were well characterized by ^{1}H, ^{13}C NMR, IR, and elemental analyses. The benzodiazepine derivatives **4b**, **4g** and **4c**, **4h** obtained from the isomeric ynone intermediates are identical. Furthermore, the structure of benzodiazepine **4** was confirmed by an X-ray crystal structure analysis of the compound **4b** (Fig. 1). X-ray crystallographic data confirm the structure of the benzodiazepine **4** to be in the diimine form as indicated rather than the enamine form, additional evidence for which is obtained by the presence of CH_2 protons (chemical shift 3.65) as a broad singlet in the ^{1}H-NMR spectra and the absence of –NH stretching frequency at 3300–3400 cm^{-1} in the IR spectra.

Conclusion

In summary, we have developed a novel, efficient and environment friendly one-pot three-component method for the synthesis of 2,4-disubstituted-3*H*-benzo[*b*][1,4]diazepines in excellent isolated yields using water as a non-hazardous, inexpensive and readily available solvent. The methodology does not require the use of any organic solvent or a ligand thus eminently meeting green chemistry objectives. Although the various substituents (electron-donating and electron-withdrawing) on each component of the coupling partner were well tolerated, the reaction became very sluggish when a strongly electron-withdrawing functionality such as a CF_3 or a NO_2 was present either in the terminal alkyne or OPD, respectively. The combination of the relatively fast reaction times, easy work-up procedures and the features stated above mean that the methodology can be operated in a combi-chem mode to generate libraries constituting a diverse array of benzodiazepine derivatives.

Experimental

General

Melting points were recorded in open capillary using Buchi melting point B540 apparatus. Column chromatography was performed using silica gel (60–120 mesh size), and TLC was carried out using aluminum sheets precoated with silica gel 60F254. All chemicals used were reagent grade procured commercially and used without further purification. ^{1}H NMR and ^{13}C NMR spectra were recorded on a Bruker Avance DPX 200 spectrometer in $CDCl_3$ using TMS as internal standard. Infrared spectra were recorded with an ATI MATTSON RS-1 FTIR spectrometer. Elemental analysis was performed on a Flash EA 1112 Thermo Finnigan instrument. The reactions were carried out in a RB flask of 10 mL capacity. Triethyl amine was dried over calcium hydride.

General procedure for the one-pot syntheses of 2,4-disubstituted-3*H*-benzo[*b*][1,4]diazepines. A mixture of acid chloride (1 mmol), terminal alkyne (1 mmol), triethyl amine (1 mmol) and $Pd(OAc)_2$ (0.2 mol%) was stirred at room temperature for 10 min under an atmosphere of argon. After the completion of reaction monitored by TLC, diamine (1.2 mmol) and water (5 ml) were added to the same reaction flask. The resulting reaction mixture was further subjected to heating at 100 °C for the time indicated in Table 1. After the completion of reaction, the reaction mixture was extracted with ethyl acetate. The organic layer was separated and dried over anhydrous magnesium sulfate, followed by the evaporation of solvent to obtain the crude product. The crude product was further purified by column chromatography using ethyl acetate/petroleum ether as eluent to afford the desired product.

Crystallographic data

(1*E*,4*E*)-2-Phenyl-4-*p*-tolyl-3*H*-benzo[*b*][1,4]diazepine (4b), $C_{22}H_{18}N_2$. A single crystal suitable for structural analysis was grown from a mixture of petroleum ether–dichloromethane (9 : 1) as a colorless needle.† See also Table 2.

† CCDC reference number 622178. For crystallographic data in CIF or other electronic format see DOI: 10.1039/b610523h

Table 1 One-pot three-component synthesis of benzodiazepines in water[a]

Entry	Acid chloride **1**	1-Alkyne **2**	Diamine **3**	Product **4**	Reaction time/h[b]	Yield[c] (%)
1	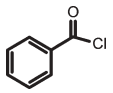 **1a**	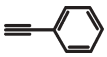 **2a**	 **3a**	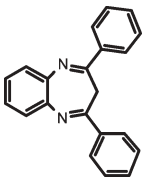 **4a**	2	80
2	**1a**	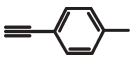 **2b**	**3a**	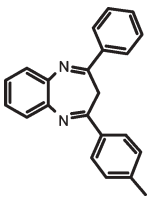 **4b**	2	81
3	**1a**	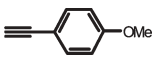 **2c**	**3a**	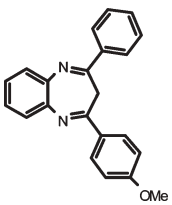 **4c**	2	72
4	**1a**	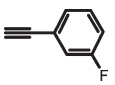 **2d**	**3a**	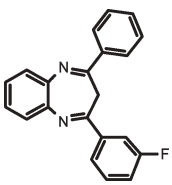 **4d**	2	85
5	**1a**	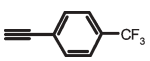 **2e**	**3a**	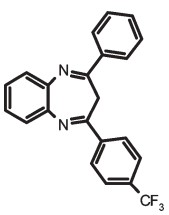 **4e**	2	60
6	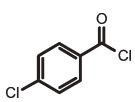 **1b**	**2a**	**3a**	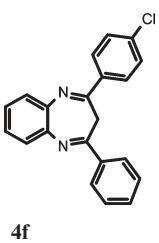 **4f**	2	82
7	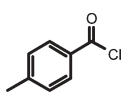 **1c**	**2a**	**3a**	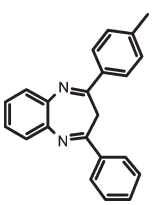 **4g**	4	75

Table 1 One-pot three-component synthesis of benzodiazepines in water[a] (*Continued*)

Entry	Acid chloride **1**	1-Alkyne **2**	Diamine **3**	Product **4**	Reaction time/h[b]	Yield[c] (%)
8	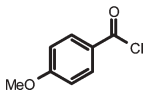 **1d**	**2a**	**3a**	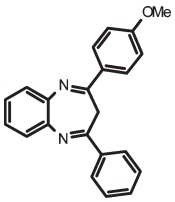 **4h**	4	85
9	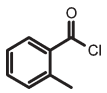 **1e**	**2a**	**3a**	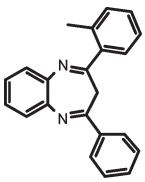 **4i**	4	60
10	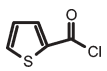 **1f**	**2a**	**3a**	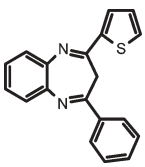 **4j**	2	82
11	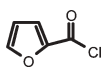 **1g**	**2a**	**3a**	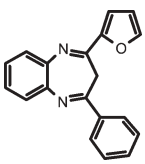 **4k**	2	89
12	**1a**	**2a**	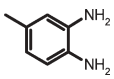 **3b**	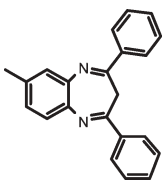 **4l**	2	85
13	**1a**	**2b**	**3b**	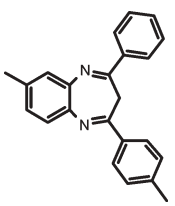	2	76
14	**1b**	**2a**	**3b**	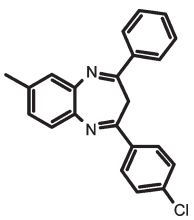 **4n**	2	90

Table 1 One-pot three-component synthesis of benzodiazepines in water[a] (*Continued*)

Entry	Acid chloride **1**	1-Alkyne **2**	Diamine **3**	Product **4**	Reaction time/h[b]	Yield[c] (%)
15	**1c**	**2a**	**3b**	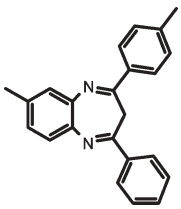 **4o**	4	89
16	**1d**	**2a**	**3b**	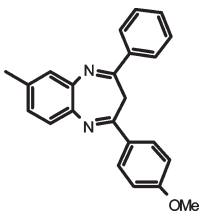 **4p**	4	90
17	**1e**	**2a**	**3b**	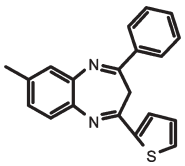 **4q**	2	83

[a] 1 mmol acid chloride, 1 mmol 1-alkyne, 1 mmol Et_3N, 0.2 mol% $pd(OAc)_2$, 1.2 mmol diamine, 5 ml water at 100 °C. [b] Time of reflux. [c] Isolated yields after column chromatography.

Characterization data for the benzodiazepines 4a–q

(1*E*,4*E*)-2,4-Diphenyl-3*H*-benzo[*b*][1,4]diazepine (4a). Colorless solid, mp 139 °C (lit.,[9] 140–141 °C), (found: C, 84.75; H, 5.30; N, 9.46. $C_{21}H_{16}N_2$ requires C, 85.11; H, 5.44; N, 9.45%); ν_{max}(film)/cm^{-1} 3018, 2400, 1602, 1447, 1216, 692 and 668; δ_H (200 MHz; $CDCl_3$; TMS) 3.64 (br s, 2H, CH_2), 7.31–7.44 (m, 8H, H Ar), 7.57–7.63 (m, 2H, H Ar) and 7.93–7.98 (m, 4H, H Ar); δ_C (50 MHz; $CDCl_3$; TMS) 34.9, 125.4, 128.1, 128.6,128.7, 130.5, 137.2, 140.7 and 154.1.

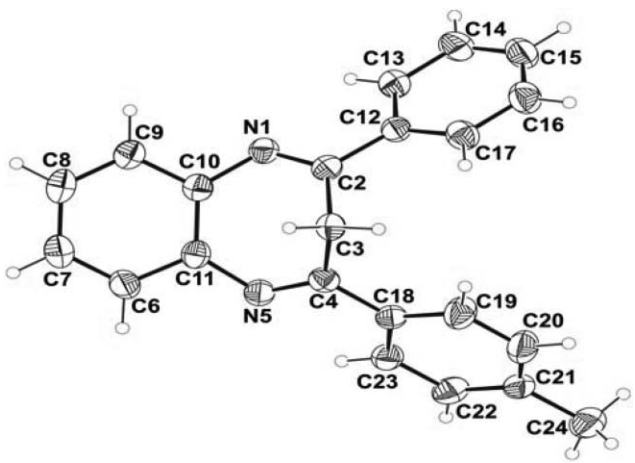

Fig. 1 X-ray single crystal structure of compound **4b**.

(1*E*,4*E*)-2-Phenyl-4-*p*-tolyl-3*H*-benzo[*b*][1,4]diazepine (4b and 4g). Colorless solid, mp 160–162 °C (lit.,[11a] 160–161 °C), (found: C, 84.95; H, 5.68; N, 9.37. $C_{22}H_{18}N_2$ requires C, 85.13; H, 5.85; N, 9.03%); ν_{max}(film)/cm^{-1} 3018, 2400, 1595, 1215,

Table 2 X-Ray crystallographic data for compound **4b**

Empirical formula	C_{22} H_{18} N_2
Formula weight	310.38
Temperature	297(2) K
Wavelength	0.71073 mm^{-1}
Crystal system, space group	Monoclinic, $P2_1/n$
Unit cell dimensions	a = 17.3650(17) Å, α = 90° b = 9.9287(10) Å, β = 113.400(2)° c = 20.981(2) Å, γ = 90°
Volume	3319.9(6) Å^3
Z, calculated density	8, 1.242 Mg m^{-3}
Absorption coefficient	0.073 mm^{-1}
F(000)	1312
Crystal size	0.49 × 0.10 × 0.03 mm
Theta range for data collection	2.12–25.00°
Limiting indices	$-20 \leqslant h \leqslant 20$, $-11 \leqslant k \leqslant 11$, $-24 \leqslant l \leqslant 24$
Reflections collected/unique	23493/5837 [R(int) = 0.0691]
Completeness to θ = 25.00	99.8%
Absorption correction	Semi-empirical from equivalents
Max. and min. transmission	0.9978 and 0.9651
Refinement method	Full-matrix least-squares on F^2
Data/restraints/parameters	5837/0/436
Goodness-of-fit on F^2	1.042
Final R indices [$I > 2\sigma(I)$]	$R1$ = 0.0771, w$R2$ = 0.1717
R indices (all data)	$R1$ = 0.1434, w$R2$ = 0.2055
Extinction coefficient	0.0005(5)
Largest diff. peak and hole	0.577 and −0.257 e A^{-3}

691, and 668; δ_H (200 MHz, $CDCl_3$; TMS) 2.36 (s, 3H, CH_3), 3.65 (br s, 2H, CH_2), 7.19–7.25 (m, 2H, H Ar), 7.30–7.35 (m, 2H, H Ar), 7.39–7.44 (m, 3H, H Ar), 7.57–7.62 (m, 2H, H Ar), 7.87 (dt, *J* 8.33 and 1.93 Hz, 2H, H Ar) and 7.94–7.99 (m, 2H, H Ar); δ_C (50 Hz, $CDCl_3$; TMS) 21.3, 34.8, 125.2, 125.3, 128.0, 128.1, 128.6, 128.7, 129.4, 130.5, 134.5, 137.3, 140.7, 140.8, 140.9, 154.0, and 154.2.

(1*E*,4*E*)-2-(4-Methoxyphenyl)-4-phenyl-3*H*-benzo [*b*][1,4] diazepine (4c and 4h). Colorless solid, mp 148–150 °C, (found: C, 81.23; H, 5.54; N, 8.34. $C_{22}H_{18}N_2O$ requires C, 80.96; H, 5.56; N, 8.58%); ν_{max}(film)/cm^{-1} 3019, 2400, 1606, 1215, 692, and 668; δ_H (200 MHz, $CDCl_3$; TMS) 3.82 (s, 3H, OCH_3), 8.91 (dt, *J* 8.97 and 2.04 Hz, 2H, H Ar), 7.25–7.43 (m, 2H, H Ar), 7.39–7.43 (m, 3H, H Ar), 7.56–7.62 (m, 2H, H Ar), and 7.92–7.99 (m, 4H, H Ar); δ_C (50 Hz, $CDCl_3$; TMS) 34.7, 55.3, 113.9, 125.4, 128.1, 128.6, 129.9, 130.5, 137.4, 140.6, 140.9, 153.5, 154.2, and 161.6.

(1*E*,4*E*)-2-(3-Fluorophenyl)-4-phenyl-3*H*-benzo[*b*][1,4]diazepine (4d). Colorless solid, mp 138–140 °C, (found: C, 80.18; H, 4.52; N, 8.70. $C_{21}H_{15}FN_2$ requires C, 80.24; H, 4.81; N, 8.91%); ν_{max}(film)/cm^{-1} 3018, 2400, 1587, 1446, 1215, 690, and 668; δ_H (200 MHz, $CDCl_3$; TMS) 3.66 (br s, 2H, CH_2), 7.06–7.16 (m, 1H, H Ar), 7.31–7.46 (m, 6H, H Ar), 7.55–7.74 (m, 4H, H Ar), and 7.93–8.00 (m, 2H, H Ar); δ_C (50 Hz, $CDCl_3$; TMS) 34.9, 114.8, 115.3, 117.4, 117.8, 123.5, 123.6, 125.5, 125.7, 128.1, 128.7, 130.7, 137.1, 139.5, 140.3, 140.8, 152.6, 153.9, 160.5, and 165.4.

(1*E*,4*E*)-2-(4-(Trifluoromethyl)phenyl)-4-phenyl-3*H*-benzo[*b*]-[1,4]diazepine (4e). Colorless solid, mp 107–108 °C, (found: C, 72.32; H, 4.21; N, 7.64. $C_{22}H_{15}F_3N_2$ requires C, 72.52; H, 4.15; F, 15.64, N, 7.69%); ν_{max}(film)/cm^{-1} 3019, 2400, 1601, 1318, 1215, 759, and 669; δ_H (200 MHz, $CDCl_3$; TMS) 3.79 (br s, 2H, CH_2), 7.32–7.49 (m, 5H, H Ar), 7.57–7.68 (m, 4H, H Ar), 7.94–7.99 (m, 2H, H Ar), and 8.07 (d, *J* 8.13 Hz, 2H, H Ar); δ_C (50 Hz, $CDCl_3$; TMS) 34.9, 125.6, 126.0, 128.2, 128.3, 128.8, 130.9, 137.0, 140.2, 140.8, 152.4, and 153.8.

(1*E*,4*E*)-2-(4-Chlorophenyl)-4-phenyl-3*H*-benzo [*b*][1,4] diazepine (4f). Colorless solid, mp 172–174 °C, (found: C, 76.12; H, 4.71; N, 8.50. $C_{21}H_{15}ClN_2$ requires C, 76.24; H, 4.57; Cl, 10.72; N, 8.47%); ν_{max}(film)/cm^{-1} 3019, 2400, 1593, 1215, 700 and 668; δ_H (200 MHz; $CDCl_3$; TMS) 3.66 (br s, 2H, CH_2), 7.30–7.46 (m, 7H, H Ar), 7.54–7.63 (m, 2H, H Ar) and 7.87–7.99 (m, 4H, H Ar); δ_C (50 Hz, $CDCl_3$; TMS) 34.8, 125.5, 128.1, 128.7, 129.4, 130.7, 135.6, 137.1, 140.4, 140.7, 152.6 and 153.9.

(1*E*,4*E*)-2-Phenyl-4-*o*-tolyl-3*H*-benzo[*b*][1,4]diazepine (4i). Colorless solid, mp 117–118 °C, (found: C, 84.95; H, 6.08; N, 9.20. $C_{22}H_{18}N_2$ requires C, 85.13; H, 5.85; N, 9.03%); ν_{max}(film)/cm^{-1} 3016, 1602, 1215, 759, 692 and 666; δ_H (200 MHz; $CDCl_3$; TMS) δ 2.26 (s, 3H, CH_3), 3.55 (br s, 2H, CH_2), 7.20–7.27 (m, 3H, H Ar), 7.29–7.39 (m, 6H, H Ar), 7.55–7.64 (m, 2H, H Ar) and 7.77–7.82 (m, 2H, H Ar); δ_C (50 Hz, $CDCl_3$; TMS) 20.9, 35.1, 126.8, 126.9, 127.6, 127.9, 128.5, 128.7, 130.4, 130.8, 131.0, 135.4, 137.1, 137.8, 138.7, 139.8, 140.7, 143.9, 147.7, 148.2, 153.1 and 153.6.

(1*E*,4*E*)-2-Phenyl-4-(thiophen-2-yl)-3*H*-benzo[*b*][1,4]diazepine (4j). Colorless solid, mp 130–131 °C, (found: C, 75.58; H, 4.83; N, 9.46. $C_{19}H_{14}N_2S$ requires C, 75.47; H, 4.67; N, 9.26; S, 10.60%); ν_{max}(film)/cm^{-1} 3019, 2400, 1596 and 692; δ_H (200 MHz; $CDCl_3$; TMS) 3.66 (br s, 2H, CH_2), 6.99–7.03 (m, 1H, H Ar), 7.26–7.35 (m, 2H, H Ar), 7.38–7.46 (m, 4H, H Ar), 7.52–7.60 (m, 3H, H Ar) and 7.98–8.05 (m, 2H, H Ar); δ_C (50 Hz, $CDCl_3$; TMS) 35.2, 125.4, 127.7, 128.1, 128.6, 128.8, 131.2, 137.0, 140.1, 140.9, 143.9, 148.6 and 154.1.

(1*E*,4*E*)-2(Furan-2-yl)-4-phenyl-3*H*-benzo[*b*][1,4]diazepine (4k). Dark liquid, (found: C, 79.68; H, 4.91; N, 9.74. $C_{19}H_{14}N_2O$ requires C, 79.70; H, 4.93; N, 9.78%); ν_{max}(film)/cm^{-1} 3019, 2399, 1596, 1261 and 669; δ_H (200 MHz; $CDCl_3$; TMS) 3.55 (br s, 2H, CH_2), 6.41–6.44 (m, 1H, H Ar), 7.02 (dd, *J* 3.53 and 0.75 Hz, 1H, H Ar), 7.20–7.29 (m, 2H, H Ar), 7.33–7.41 (m, 3H, H Ar), 7.48–7.55 (m, 3H, H Ar) and 7.99–8.08 (m, 2H, H Ar); δ_C (50 Hz, $CDCl_3$; TMS) 33.9, 112.4, 113.8, 125.4, 128.1, 128.5, 128.7, 130.6, 136.9, 140.2, 140.9, 144.9, 145.3, 152.0 and 154.1.

(1*E*,4*E*)-7-Methyl-2, 4-diphenyl-3*H*-benzo[*b*][1,4]diazepine (4l). Colorless solid, mp 112–114 °C (lit.,[15] 111 °C), (found: C, 85.09; H, 5.77; N, 8.78. $C_{22}H_{18}N_2$ requires C, 85.13; H, 5.85; N, 9.03%); ν_{max}(film)/cm^{-1} 3019, 2400, 1602, 1215, 758 and 669; δ_H (200 MHz; $CDCl_3$; TMS) 2.46 (s, 3H, CH_3), 3.70 (br s, 2H, CH_2), 7.17 (dd, *J* 8.20 and 1.63 Hz, 1H, H Ar), 7.37–7.44 (m, 7H, H Ar), 7.50 (d, *J* 8.21 Hz, 1H, H Ar) and 7.93–7.97 (m, 4H, H Ar); δ_C (50 Hz, $CDCl_3$; TMS) 21.1, 34.9, 126.8, 127.9, 128.6, 130.4, 135.3, 137.4, 138.5, 140.5, 153.3 and 153.7.

(1*E*,4*E*)-7-Methyl-4-phenyl-2-*p*-tolyl-3*H*-benzo[*b*][1,4]diazepine (4m). Colorless solid, mp 124–126 °C, (found: C, 84.87; H, 6.30; N, 8.86. $C_{23}H_{20}N_2$ requires C, 85.15; H, 6.21; N, 8.63%); ν_{max}(film)/cm^{-1} 3018, 2400, 1655, 1215, 758, 691 and 667; δ_H (200 MHz; $CDCl_3$; TMS) 2.23 (s, 3H, CH_3), 2.34 (s, 3H, CH_3), 3.55 (br s, 2H, CH_2), 7.02–7.12 (m, 3H, H Ar), 7.25–7.29 (m, 4H, H Ar), 7.40 (d, *J* 8.34 Hz, 1H, H Ar), 7.75 (d, *J* 8.21 Hz, 2H, H Ar) and 7.82–7.87 (m, 2H, H Ar); δ_C (50 Hz, $CDCl_3$; TMS) 21.0, 21.2, 34.7, 126.7, 127.9, 128.5, 129.3, 130.4, 134.6, 134.9, 135.2, 137.3, 138.6, 140.4, 140.7, 153.1, 153.6 and 153.7.

(1*E*,4*E*)-2-(4-Chlorophenyl)-7-methyl-4-phenyl-3*H*-benzo[*b*][1,4]diazepine (4n). Colorless solid, mp 125–127 °C, (found: C, 76,61; H, 4.89; N, 8.11. $C_{22}H_{17}ClN_2$ requires C, 76.63; H, 4.97; Cl, 10.28; N, 8.12%); ν_{max}(film)/cm^{-1} 3019, 2400, 1593, 1215, 758 and 669; δ_H (200 MHz; $CDCl_3$; TMS) 2.46 (s, 3H, CH_3), 3.63 (br s, 2H, CH_2), 7.17 (dd, *J* 8.22 and 1.39 Hz, 1H, H Ar), 7.34–7.52 (m, 7H, H Ar) and 7.87–7.95 (m, 4H, H Ar); δ_C (50 Hz, $CDCl_3$; TMS) 21.1, 34.8, 127.1, 128.1, 128.5, 128.6, 128.7, 128.9, 129.4, 130.6, 135.5, 135.7, 136.8, 137.2, 138.5, 140.2, 152.2 and 153.0.

(1*E*,4*E*)-7-Methyl-2-phenyl-4-*p*-tolyl-3*H*-benzo [*b*][1,4] diazepine (4o). Colorless solid, mp 111–113 °C, (found: C, 84.97; H, 6.32; N, 8.66. $C_{23}H_{20}N_2$ requires C, 85.15; H, 6.21; N, 8.63%); ν_{max}(film)/cm^{-1} 3019, 2400, 1595, 1216, 757, 692 and 668; δ_H (200 MHz; $CDCl_3$; TMS) 2.31 (s, 3H, CH_3), 2.42 (s, 3H, CH_3), 3.62 (br s, 2H, CH_2), 7.10–7.18 (m, 3H, H Ar), 7.34–7.39 (m,

4H, H Ar), 7.49 (d, *J* 8.20 Hz, 1H, H Ar), 7.84 (d, *J* 8.07 Hz, 2H, H Ar) and 7.90–7.95 (m, 2H, H Ar); δ_C (50 Hz, $CDCl_3$; TMS) 21.0, 21.2, 34.7, 126.6, 127.9, 128.5, 129.3, 130.3, 134.4, 134.9, 135.1, 137.4, 138.4, 140.5, 140.8, 153.3 and 153.5.

(1*E*,4*E*)-2-(4-Methoxyphenyl)-7-methyl-4-phenyl-3*H*-benzo[*b*][1,4]diazepine (4p). Colorless solid, mp 155–157 °C, (found: C, 81.10; H, 5.90; N, 8.20. $C_{23}H_{20}N_2O$ requires C, 81.15; H, 5.92; N, 8.23%); ν_{max}(film)/cm^{-1} 3018, 2400, 1606, 1513, 1215, 692 and 668; δ_H (200 MHz; $CDCl_3$; TMS) 2.44 (s, 3H, CH_3), 3.78 (s, 3H, OCH_3), 6.89 (d, *J* 8.85 Hz, 2H, H Ar), 7.13 (dt, *J* 8.33 and 1.51 Hz, 1H, H Ar), 7.37–7.40 (m, 4H, H Ar), 7.49 (dd, *J* 8.21, 2.40 Hz, 1H, H Ar) and 7.90–7.96 (m, 4H, H Ar); δ_C (50 Hz, $CDCl_3$; TMS) 21.0, 34.6, 55.2, 113.9, 126.4, 126.7, 127.9, 128.5, 129.8, 130.3, 134.8, 135.2, 137.4, 138.4, 140.7, 153.0, 153.3 and 161.5.

(1*E*,4*E*)- 7-Methyl-4-phenyl-2-(thiophen-2-yl)-3*H*-benzo[*b*][1,4]diazepine (4q). Colorless solid, mp 115–117 °C, (found: C, 75.69; H, 5.12; N, 8.75. $C_{20}H_{16}N_2S$ requires C, 75.92; H, 5.10; N, 8.85%); ν_{max}(film)/cm^{-1} 3018, 2400, 1576, 1432, 1215, 757 and 668; δ_H (200 MHz; $CDCl_3$; TMS) 2.45 (s, 3H, CH_3), 3.67 (br s, 2H, CH_2), 7.04 (m, 1H, H Ar), 7.15 (dd, *J* 8.20, 1.49 Hz, 1H, H Ar), 7.38–7.50 (m, 6H, H Ar), 7.59–7.69 (m, 1H, H Ar) and 8.01–8.06 (m, 2H, H Ar); δ_C (50 Hz, $CDCl_3$; TMS) 20.2, 39.5, 125.2, 125.4, 125.9, 127.8, 128.2, 128.3, 128.5, 129.3, 130.4, 131.0, 136.3, 137.4, 138.8, 140.3, 153.4 and 156.9.

Acknowledgements

S.S.P. thanks CSIR, New Delhi for providing the Research Fellowship and Mr Rajesh G. Gonade, Centre for Material Characterization for carrying out the X-ray crystallographic analysis.

References

1 (*a*) For general references on green chemistry, see: P. T. Anastas and J. C. Warner, *Green Chemistry: Theory and Practice*, Oxford University Press, Oxford, 1998; *Green Chemistry: Designing Chemistry for the Environment*, American Chemical Society Symposium Series, No. 626, ed. P. T. Anastas and T. C. Williamson, Washington, DC, 1996; (*b*) *Ionic Liquids in Synthesis*, ed. P. Wasserscheid and T. Welton, Wiley-VCH, Weinheim, 2003; (*c*) *Chemical Synthesis Using Supercritical Fluids*, ed. P. G. Jessop and W. Leitner, Wiley-VCH, Weinheim, 1999; (*d*) P. A. Grieco, *Organic Synthesis in Water*, ed. P. A. Grieco, Blackie Academic and Professional, London, 1998; (*e*) C.-J. Li, *Chem. Rev.*, 1993, **93**, 2023; (*f*) K. Tanaka, *Solvent-free Organic Synthesis*, Wiley-VCH, Weinheim, 2003.

2 (*a*) N. Azizi, F. Aryanasab, L. Torkiyan, A. Ziyaei and M. R. Saidi, *J. Org. Chem.*, 2006, **71**, 3634; (*b*) U. K. Roy and S. Roy, *Tetrahedron*, 2006, **62**, 678.

3 (*a*) For a review see: A. Domling and I. Ugi, *Angew. Chem., Int. Ed.*, 2000, **39**, 3168; (*b*) N. K. Terret, M. Gardener, D. W. Gordon, R. J. Kobylecki and J. Steele, *Tetrahedron*, 1995, **51**, 8135; (*c*) L. A. Thomson and J. A. Ellman, *Chem. Rev.*, 1996, **96**, 555; (*d*) J. A. Ellman, *Acc. Chem. Res.*, 1996, **29**, 132.

4 (*a*) A. Dömling, E. Herdtweck and I. Ugi, *Acta Chem. Scand.*, 1998, **52**, 107; (*b*) M. Lombardo and C. Trombini, in *Proceedings of the XXIII Summer School "A. Corbella" Seminars in Organic Synthesis, Gargnano (BS), 1998, June 15–19*, 7.

5 (*a*) H. Schutz, *Benzodiazepines*, Springer, Heidelberg, 1982; (*b*) J. K. Landquist, in *Comprehensive Heterocyclic Chemistry*, ed. A. R. Katritzky and C. W. Rees, Pergamon, Oxford, 1984, vol. 1, p. 166; (*c*) L. O. Randall and B. Kamel, in *Benzodiazepines*, ed. S. Garattini, E. Mussini and L. O. Randall, Raven Press, New York, 1973, p. 27 and references cited therein.

6 J. A. Barltrop, C. G. Richards, D. M. Russel and G. J. Ryback, *J. Chem. Soc.*, 1959, 1132.

7 S. L. Schreiber, *Science*, 2000, **287**, 1964.

8 It has been shown that the addition of fused 5-membered heterocycles onto benzodiazepines increases their CNS depressant activity: J. B. Hester, Jr., A. D. Rudzik and B. V. Kamdar, *J. Med. Chem.*, 1971, **14**, 1078.

9 W. Ried and E. Koenig, *Justus Liebigs Ann. Chem.*, 1972, **24**, 755.

10 Yu. S. Andreichikov, S. G. Pitirimova, S. P. Tendryakoya, R. F. Saraeya and T. N. Tokmakova, *Zh. Org. Khim.*, 1978, **14**, 169; Yu. S. Andreichikov, S. G. Pitirimova, S. P. Tendryakoya, R. F. Saraeya and T. N. Tokmakova, *J. Org. Chem. USSR*, 1978, **14**, 156.

11 (*a*) S. P. Korshunov, V. M. Kazantseva, L. A. Vopilina, V. S. Pisareva and N. V. Utekhina, *Khim. Geterotsikl. Soedin.*, 1973, **9**, 1421; S. P. Korshunov, V. M. Kazantseva, L. A. Vopilina, V. S. Pisareva and N. V. Utekhina, *Chem. Heterocycl. Compd.*, 1973, **9**, 1287; (*b*) R. L. Amey and N. D. Heindel, *Org. Prep. Proced. Int.*, 1976, **8**, 306; (*c*) W. Ried and R. Teubner, *Justus Liebigs Ann. Chem.*, 1978, 741.

12 S. S. Palimkar, P. Harish Kumar, R. J. Lahoti and K. V. Srinivasan, *Tetrahedron*, 2006, **62**, 5109.

13 S. S. Palimkar, S. A. Siddiqui, T. Daniel, R. J. Lahoti and K. V. Srinivasan, *J. Org. Chem.*, 2003, **68**, 9371.

14 (*a*) A. R. Gholap, K. Venkatesan, T. Daniel, R. J. Lahoti and K. V. Srinivasan, *Green Chem.*, 2003, **6**, 693; (*b*) A. R. Gholap, K. Venkatesan, T. Daniel, R. J. Lahoti and K. V. Srinivasan, *Green Chem.*, 2004, **3**, 147.

15 This compound was originally isolated as a rearrangement product of an isoxazolone which was itself prepared in a multi-step synthesis: W. Muller, U. Kraatz and F. Korte, *Chem. Ber.*, 1973, **106**, 332.

A highly efficient and green method for the synthesis of 3,4-dihydropyrimidin-2-ones and 1,5-benzodiazepines catalyzed by dodecyl sulfonic acid in water†

Saikat Das Sharma, Pranjal Gogoi and Dilip Konwar*

Received 7th August 2006, Accepted 26th October 2006
First published as an Advance Article on the web 9th November 2006
DOI: 10.1039/b611327c

A simple, efficient, mild and green method has been developed for the synthesis of 3,4-dihydropyrimidin-2-ones employing dodecyl sulfonic acid as an excellent surfactant-type Brønsted acid catalyst in aqueous media at room temperature. The catalyst was shown to be equally effective for the synthesis of 1,5-benzodiazepines under the same reaction condition.

Introduction

Development of non-hazardous synthetic methodologies for organic reactions are one of the latest challenge to the organic chemists. Recently, organic reactions conducted in aqueous media have received much attention[1] because water is non-toxic, cheap, abundantly available and benign to the environment. Although water not only increased the rate and the yield of a reaction but also, enhanced enantioselectivity in chiral synthesis,[2] the major drawbacks of using water as a solvent are its poor ability to solubilize organic reactants and unsuitability for use with moisture sensitive organic compounds and catalysts. In this connection, a surfactant plays an appreciable role to overcome the solubility problems of organic molecules in water. A surfactant not only solubilizes the organic compounds but also protects them from moisture by forming micelles. A surfactant-type Brønsted acid[3] forms stable dispersion systems with organic substrates and thus acts both as a catalyst to activate the molecule and as a protector to create a hydrophobic environment within the micelle.

Dihydropyrimidinones[4] and benzodiazepines[5] are both classes of biologically important organic molecules. The dihydropyrimidinone (DHPM) scaffold is featured in a wide variety of bioactive molecules. A number of marine alkaloids with broad spectrum of biological activities contain DHPM framework as a part of their structures.[6] Appropriately functionalized DHPMs have emerged as antihypertensive agents due to their metabolism *in vivo* to the potent calcium channel blockers,[7a] α_{1a} adrenoceptor antagonists for the treatment of benign prostatic hyperlasia[7b] and neuropeptide Y antagonist.[7c] Monastrol is the only cell-permeable molecule currently known to block mitosis by specifically inhibiting the motor activity of the mitotic kinesis Eg5 and can therefore be considered as a lead for the development of new anticancer drugs.[7d] The benzodiazepines are extensively used clinically as CNS drugs, *e.g.*, diazepam, lorazepam, parazepam, oxazepam are used as anxiolytics, flurazepam is a hypnotic, clonazepam is an antiepileptic,[8a] tifluadom is an effective opioid analgesic with preference for opiate k-receptors.[8b] Furthermore, benzodiazepine derivatives have been shown to be potent inhibitors of HIV-1 reverse transcriptase.[8c] These ubiquitous applications of DHPMs and benzodiazepines stimulated several groups to develop new and efficient synthetic protocols for the synthesis of these two bioactive units.

The syntheses of DHPMs are carried out by venerable Biginelli reaction involving acid catalyzed three-component condensation of 1,3-dicarbonyl compound, aldehyde and urea. Several improved Lewis and Brønsted acid catalysts,[9a–k] polymer supported reagents,[9l–n] triflates,[9o–q] microwave-assisted methodologies and ultrasonic methods[9r–s] have been employed for the synthesis of DHPMs. Whereas benzodiazepines are generally synthesized by acid catalyzed condensation of *o*-phenylenediamine with ketones. This transformation is also catalyzed by a plethora of reagents including BF_3–OEt_2,[10a] $NaBH_4$,[10b] MgO–$POCl_3$,[10c] Al_2O_3–P_2O_5,[10d] AcOH-microwave,[10e] I_2,[10f] $Ag_3PW_{12}O_{40}$,[10g] $InBr_3$,[10h] (bromodimethyl) sulfonium bromide,[10i] CAN,[10j] $ZnCl_2$,[10k] $AgNO_3$,[10l] triflates,[10m,n] and ionic liquid.[10o] However, despite the potential utility of these catalysts, many of these methodologies for the synthesis of DHPMs and benzodiazepines are associated with several shortcomings such as long reaction time, high temperature, harsh reaction conditions, use of expensive reagents, low yields, occurrence of several side products, high sensitivity to ambient air and moisture, use of organic solvents and toxic and hazardous transition metals. So gaps still remain in terms of the search for economical and environmentally benign methods. As a part of our continual efforts to utilize water as a reaction medium in various organic transformation[11] herein we wish to report the synthesis of DHPMs (Scheme 1) and benzodiazepines (Scheme 2) by a surfactant-type Brønsted acid catalyst in water at room temperature.

Results and discussion

Our initial efforts focused on the search of a catalyst, which is stable enough in aqueous media to carry out the synthesis of DHPM in water at ambient temperature. In this connection,

Synthetic Organic Chemistry Division, Regional Research Laboratory, Jorhat, 785006, Assam, India. E-mail: dkonwar@yahoo.co.uk; Fax: +9103763370011; Tel: +91-9435351864

† Electronic supplementary information (ESI) available: Experimental procedures and characterization data of all the compounds. See DOI: 10.1039/b611327c

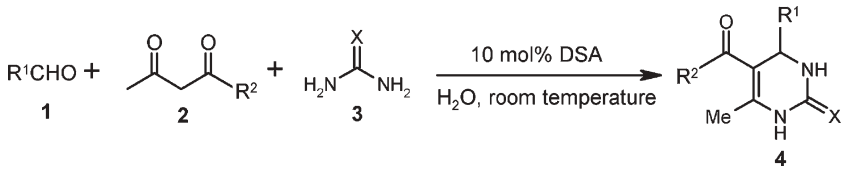

Scheme 1

dodecyl sulfonic acid (DSA) was choosen as the catalyst to carry out the Biginelli reaction in water. To find the efficacy of this surfactant-type Brønsted acid catalyst, we carried out the Biginelli reaction with benzaldehyde, ethyl acetoacetate and urea in the presence of DSA in water at room temperature which gave the corresponding DHPM derivative in excellent yield. The optimized reaction conditions were screened by conducting the reaction in different solvents and catalyst loadings at room temperature. The results are summarized in Table 1. It was found that the yield was good even in solvent less condition (entry 7) in the presence of DSA. In the absence of a catalyst, the reaction did not proceed at all in water at room temperature (entry 14). DSA catalyzed the reaction very efficiently producing high yield of products in a much shorter time (entry 8). It was found that 10 mol% of DSA is sufficient to carry out the Biginelli reaction successfully. An increase in the amount of DSA to more than 10 mol% showed no substantial improvement in the yield, whereas the yield is reduced by decreasing the amount of DSA to 5 mol%.

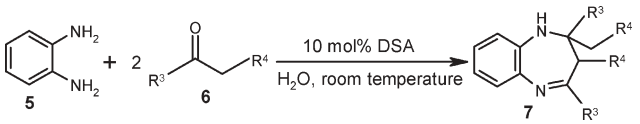

Scheme 2

Under these optimized reaction condition the scope of the reaction was then explored. A broad range of structurally diverse 1,3-dicarbonyl compounds, aldehydes and urea were subjected under this protocol to produce the corresponding DHPMs (Table 2). Many of the pharmacologically significant substitution patterns can be introduced with efficiency. Aromatic aldehydes produced high yield of DHPMs irrespective of electronic effects. Aliphatic aldehydes also worked well with this protocol. A wide range of functional groups were tolerated under the reaction condition. A variety of dicarbonyl compounds could be used successfully. Thiourea was also used with similar success. In a typical procedure, a 2 mmol quantitity of aldehyde, a 2 mmol quantity of 1,3-dicarbonyl compound and a 3 mmol quantity of urea or thiourea were mixed in water (10 ml) in the presence of 10 mol% of DSA, and the reaction mixture was stirred for the stipulated time at 25–30 °C; after work-up, it produced the corresponding DHPM with very good to excellent yield (Scheme 1).

After the successful application of DSA as a catalyst in the synthesis of DHPMs we next wished to further explore the potentiality of the catalyst. So, DSA was used as a Brønsted acid catalyst in the condensation reaction of *o*-phenylenediamine with a ketone having an α-hydrogen leading to the product 1,5-benzodiazepine in water medium at ambient temperature (Scheme 2). To our delight, even the synthesis of 1,5-benzodiazepines was catalyzed efficiently by DSA

Table 1 Condensation of benzaldehyde, ethyl acetoacetate and urea under different catalysts and solvent systems

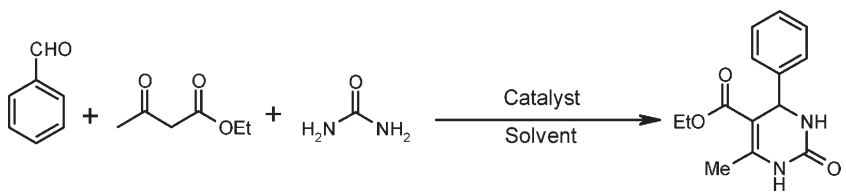

Entry	Catalysts	Catalyst load (mol%)	Solvents	Time/h	Yield (%)[a]
1	DSA	10	MeOH	4.0	68
2	DSA	10	EtOH	4.0	71
3	DSA	10	$CHCl_3$	7	39
4	DSA	10	CH_2Cl_2	7	36
5	DSA	10	Toluene	10	51
6	DSA	10	Acetonitrile	4.3	79
7	DSA	10	Neat	3.5	84
8	DSA	10	H_2O	2.3	91
9	DSA	20	H_2O	2.4	91
10	DSA	5	H_2O	6	78
11	AcOH	10	H_2O	12	5
12	H_3BO_3	10	H_2O	12	39
13	SDS[d]	10	H_2O	14	NR[e]
14	No catalyst	10	H_2O	20	NR[e]

[a] Isolated yield. [b] stirring at 25–30 °C. [c] The structure of the compound was determined by using ^{1}H NMR, FT-IR, MS (*m*/*z*) and elemental analyses. [d] Sodium dodecyl sulfate. [e] No reaction.

Table 2 Dodecyl sulfonic acid catalyzed synthesis of dihydropyrimidin-2(1H)-ones and thiones

Entry	Aldehydes **1a–p**	β-Dicarbonyls **2a–p**	X	Time/h	Yield (%)[a]
a	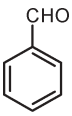	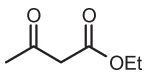	O	2.4	91
b	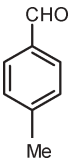	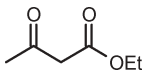	O	3.0	88
c	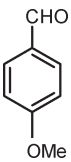	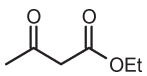	O	3.1	87
d	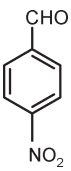	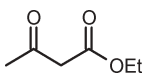	O	2.3	90
e	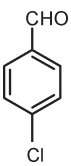	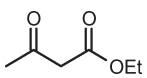	O	2.5	88
f	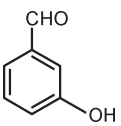	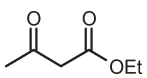	O	3.2	85
g	$CH_3CH_2CH_2CHO$	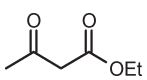	O	4.0	81
h	$(CH_3)_2CHCHO$	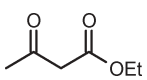	O	4.0	83
i	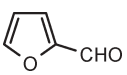	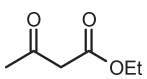	O	3.4	82
j	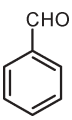	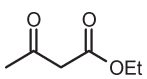	S	3.1	90
k	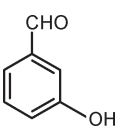	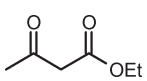	S	3.5	83
l	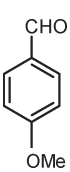	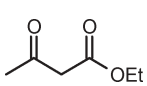	S	3.2	88
m	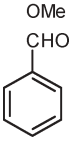	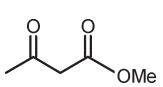	O	3.3	89
n	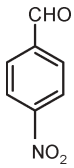	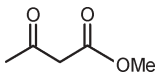	O	3.5	87
o	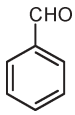	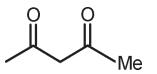	O	3.2	91
p	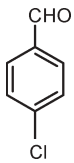	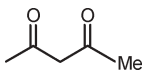	O	3.5	86

[a] Isolated yield. [b] stirring at 25–30 °C. [c] The structures of all the compounds were determined by using ^{1}H NMR, FT-IR, MS (*m*/*z*) and elemental analyses and they are in good agreement with the authentic samples.[9]

leading to high yields of products. The scope of this protocol was examined with respect to the different ketones and *o*-phenylenediamines. Both aliphatic (acyclic and cyclic) and aromatic ketones are suitable and give substituted 1,5-benzodiazepines in high to excellent yields. The conversion proceeded successfully under ambient condition within 3 to 4 h. Thus, a 1 mmol quantity of *o*-phenylenediamine and a 2.2 mmol quantity of ketone were stirred in water (10 ml) in the presence of 10 mol% of DSA for the stipulated time at 25–30 °C; after work-up, it produced the corresponding 1,5-benzodiazepine with very good to excellent yield (Scheme 2).

Conclusion

In conclusion, an extremely efficient method has been developed for the synthesis of 3,4-dihydropyrimidin-2-ones and 1,5-benzodiazepines in water at room temperature using dodecyl sulfonic acid as a catalyst, which simultaneously catalyzes the reaction as well as solubilizes the reactants in water. This method is bestowed with several unique merits, such as high conversions, simplicity in operation, cost efficiency and use of water as a solvent, and thus significantly contributes to the practice of green chemistry.

Experimental

General procedure for the synthesis of 3,4-dihydropyrimidine-2-ones

In a 50 ml round-bottom flask, aldehyde (2 mmol), ethyl acetoacetate (2 mmol) and urea (3 mmol) were stirred in the presence of dodecyl sulfonic acid (10 mol%) in H_2O (10 ml) at the room temperature for the stipulated time. The progress of the reaction was monitored by TLC. After completion of the reaction, the solid separated was filtered, washed with water

Table 3 Dodecyl sulfonic acid catalyzed synthesis of 1,5-benzodiazepines

Entry	Diamines **5a–h**	Ketones **6a–h**	Products **7a–h**	Time/h	Yield (%)[a]
a	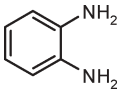	CH_3COCH_3	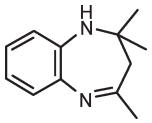	2.3	90
b	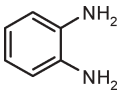	$CH_3COCH_2CH_3$	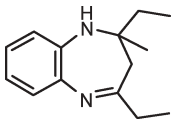	3.0	88
c	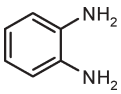	$CH_3CH_2COCH_2CH_3$	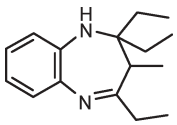	3.0	86
d	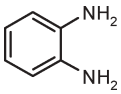	$CH_3COCH_2CH(CH_3)CH_3$	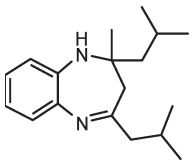	3.5	85
e	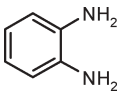	$CH_3COCH(CH_3)_2$	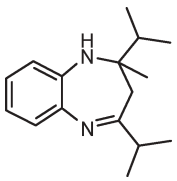	3.2	83
f	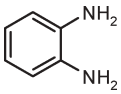	CH_3COPh	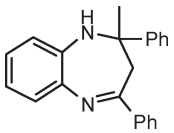	3.0	87
g	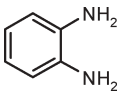	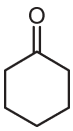	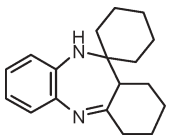	4.0	80
h	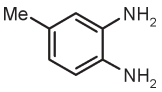	CH_3COCH_3	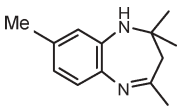	3.2	86

[a] Isolated yield. [b] stirring at 25–30 °C. [c] The structures of all the compounds were determined by using ^{1}H NMR, FT-IR, MS (*m*/*z*) and elemental analyses and they are in good agreement with the authentic samples.[10]

(5 × 10 ml), dried under vacuum and recrystallized from ethanol to afford pure product.

General procedure for the synthesis of 1,5-benzodiazepines

In a 50 ml round-bottom flask, *o*-phenylenediamine (1 mmol) and ketone (2.2 mmol) were stirred in the presence of dodecyl sulfonic acid (10 mol%) in H_2O (10 ml) at the room temperature. The reaction was monitored by TLC. After completion of the reaction, the product was extracted with ethyl acetate (2 × 25 ml), washed the organic layer with brine (2 × 15 ml), dried over Na_2SO_4 and concentrated. The product was separated and purified by column chromatography on silica gel (60–120 mesh) using an ethyl acetate/hexane mixture as the eluent to afford a pure 1,5-benzodiazepine.

Acknowledgements

The authors acknowledge the director, and the analytical division of RRL, Jorhat, Assam, India, for their help. Also, SDS and PG thank CSIR, New Delhi for the grant of fellowships.

References

1 (*a*) C.-J. Li and T.-H. Chan, *Organic Reactions in Aqueous Media*, John Wiley & Sons, New York, 1997; (*b*) *Organic Synthesis in Water*, ed. P. A. Grieco, Blackie Academic and Professional, London, 1998; (*c*) U. M. Lindstrom, *Chem. Rev.*, 2002, **102**, 2751; (*d*) S. Kobayashi and K. Manabe, *Acc. Chem. Res.*, 2002, **35**, 209.
2 S. Ribe and P. Wipf, *Chem. Commun.*, 2001, 299.
3 K. Manabe, S. Limura, X. Sun and S. Kobayashi, *J. Am. Chem. Soc.*, 2002, **124**, 11971.

4 (*a*) C. O. Kappe, *Acc. Chem. Res.*, 2000, **33**, 879; (*b*) C. O. Kappe, *Tetrahedron*, 1993, **49**, 6937.

5 (*a*) H. Schutz, *Benzodiazepines*, Springer, Heidelberg, 1982; (*b*) J. K. Lanquist, in *Comprehensive Heterocyclic Chemistry*, ed. A. R. Katritzky and C. W. Rees, Pergamon, Oxford, 1984, vol 1, p. 166.

6 (*a*) L. E. Overman, M. H. Rabinowitz and P. A. Renhowe, *J. Am. Chem. Soc.*, 1995, **117**, 2657; (*b*) L. Heys, C. G. Moore and P. J. Murphy, *Chem. Soc. Rev.*, 2000, **29**, 57; (*c*) Z. D. Arou and L. E. Overman, *Chem. Commun.*, 2004, 253.

7 (*a*) K. S. Atwal, B. N. Swanson, S. E. Unger, D. M. Floyd, S. Moreland, A. Hedberg and B. C. O'Reilly, *J. Med. Chem.*, 1991, **34**, 806; (*b*) D. Nagarathnam, S. W. Miao, B. Lagu, G. Chiu, J. Fang, T. G. Murali Dhar, J. Zhang, S. Tyagarajan, M. R. Marzabadi, F. Zhang, W. C. Wong, W. Sun, D. Tian, J. M. Wetzel, C. Forray, R. S. L. Chang, T. P. Broten, R. W. Ransom, T. W. Schorn, T. B. Chen, S. O'Malley, P. Kling, K. Schneck, R. Bendesky, C. M. Harrell, K. P. Vyas and C. Gluchowski, *J. Med. Chem.*, 1999, **42**, 4764; (*c*) M. A. Bruce, G. S. Pointdexter and G. Johnson, PCT Int. Appl. WO 98 33, 791, 1998; (*d*) T. U. Mayer, T. M. Kapoor, S. J. Haggarty, R. W. King, S. L. Schreiber and T. J. Mitchison, *Science*, 1999, **286**, 971.

8 (*a*) L. H. Sternbach, *J. Med. Chem.*, 1979, **22**, 1; (*b*) D. Römer, H. H. Büscher, R. C. Hill, R. Maurer, T. J. Petcher, H. Zeugner, W. Benson, E. Finner, W. Milkowski and P. W. Thies, *Nature*, 1982, **298**, 759; (*c*) V. J. Merluzzi, K. D. Hargrave, M. Labadia, K. Grozinger, M. Skoog, J. C. Wu, C. K. Shih, K. Eckner, S. Hattox and J. Adams *et al.*, *Science*, 1990, **250**, 1411.

9 (*a*) E. H. Hu, D. R. Sidler and U.-H. Dolling, *J. Org. Chem.*, 1998, **63**, 3454; (*b*) J. Lu and H. Ma, *Synlett*, 2000, 63; (*c*) B. C. Ranu, A. Hajra and U. Jana, *J. Org. Chem.*, 2000, **65**, 6270; (*d*) K. Ramalinga, P. Vijayalakshmi and T. N. B. Kaimal, *Synlett*, 2001, 863; (*e*) K. A. Kumar, M. Kasthuraiah, C. Reddy and C. D. Reddy, *Tetrahedron Lett.*, 2001, **42**, 7873; (*f*) C. V. Reddy, M. Mahesh, P. V. K. Raju, T. R. Babu and V. V. N. Reddy, *Tetrahedron Lett.*, 2002, **43**, 2657; (*g*) D. S. Bose, L. Fatima and H. B. Mereyala, *J. Org. Chem.*, 2003, **68**, 587; (*h*) Z.-T. Wang, L.-W. Xu, C.-G. Xia and H.-Q. Wang, *Tetrahedron Lett.*, 2004, **45**, 7951; (*i*) A. K. Bose, M. S. Manhas, S. Pednekar, S. N. Ganguly, H. Dang, W. He and A. Mandadi, *Tetrahedron Lett.*, 2005, **46**, 1901; (*j*) M. M. Heravi, K. Bakhtiari and F. F. Bamoharram, *Catal. Commun.*, 2006, **7**, 373; (*k*) A. Debache, B. Boumoud, M. Amimour, A. Belfaitah, S. Rhouati and B. Carboni, *Tetrahedron Lett.*, 2006, **47**, 5697; (*l*) A. Dondoni and A. Massi, *Tetrahedron Lett.*, 2004, **42**, 7975; (*m*) S. Palaniappan and A. John, *J. Mol. Catal. A: Chem.*, 2005, **233**, 9; (*n*) G. Sabitha, K. B. Reddy, J. S. Yadav, D. Shailaja and K. S. Sivudu, *Tetrahedron Lett.*, 2005, **46**, 8221; (*o*) Y. Ma, C. Qian, L. Wang and M. Yang, *J. Org. Chem.*, 2000, **65**, 3864; (*p*) R. Varala, M. M. Alam and S. R. Adapa, *Synlett*, 2003, 67; (*q*) W. Su, J. Li, Z. Zheng and Y. Shen, *Tetrahedron Lett.*, 2005, **46**, 6037; (*r*) M. Gohain, D. Prajapati and J. S. Sandhu, *Synlett*, 2004, 235; (*s*) X. Zhang, Y. Li, C. Liu and J. Wang, *J. Mol. Catal. A: Chem.*, 2006, **253**, 207.

10 (*a*) J. A. L. Herbert and H. Suschitzky, *J. Chem. Soc., Perkin Trans. 1*, 1974, 2657; (*b*) H. R. Morales, A. Bulbarela and R. Contreras, *Heterocycles*, 1986, **24**, 135; (*c*) M. S. Balakrishna and B. Kaboudin, *Tetrahedron Lett.*, 2001, **42**, 1127; (*d*) B. Kaboadin and K. Navace, *Heterocycles*, 2001, **55**, 1443; (*e*) M. Pozarentzi, J. S. Stephanatou and C. A. Tsoleridis, *Tetrahedron Lett.*, 2002, **43**, 1755; (*f*) B. P. Bandgar, S. V. Bettigeri and N. S. Joshi, *Synth. Commun.*, 2004, **34**, 1447; (*g*) J. S. Yadav, B. V. S. Reddy, N. lingaiah and P. S. Saiprasad, *Synthesis*, 2004, 901; (*h*) J. S. Yadav, B. V. S. Reddy, S. Praveenkumar and K. Nagaiah, *Synthesis*, 2005, 480; (*i*) B. Das, R. Ramu, B. Ravikanth and V. Reddy, *J. Mol. Catal. A: Chem.*, 2006, **246**, 76; (*j*) R. Varala, R. Enugala, S. Nuvula and S. R. Adapa, *Synlett*, 2006, 1009; (*k*) M. A. Pasha and V. P. Jayashankara, *Heterocycles*, 2006, **68**, 1017; (*l*) R. Kumar, P. Chaudhary, S. Nimesh, A. K. Verma and R. Chandra, *Green Chem.*, 2006, 519; (*m*) M. Curini, F. Epifano, M. C. Marcotullio and O. Rosati, *Tetrahedron Lett.*, 2001, **42**, 3193; (*n*) S. K. De and R. A. Gibbs, *Tetrahedron Lett.*, 2005, **46**, 1811; (*o*) D. V. Jarikote, S. A. Siddiqui, R. Rajagopal and K. V. Srinivasan, *Tetrahedron Lett.*, 2003, **44**, 1835.

11 (*a*) M. Boruah and D. Konwar, *Synlett*, 2001, **6**, 795; (*b*) M. Boruah and D. Konwar, *J. Org. Chem.*, 2002, **67**, 7138; (*c*) P. Gogoi, G. K. Sarmah and D. Konwar, *J. Org. Chem.*, 2004, **69**, 5153; (*d*) P. Gogoi, P. Hazarika and D. Konwar, *J. Org. Chem.*, 2005, **70**, 1934.

Synthesis of symmetrical or asymmetrical urea compounds from CO_2 *via* base catalysis

Angelica Ion,[a] Vasile Parvulescu,[b] Pierre Jacobs[a] and Dirk De Vos*[a]

Received 29th August 2006, Accepted 31st October 2006
First published as an Advance Article on the web 8th November 2006
DOI: 10.1039/b612403h

Using Cs^+ base catalysts and *N*-methylpyrrolidone as the solvent, both symmetrical and asymmetrical urea derivatives are prepared in good yields directly from CO_2 and amines, in the absence of any dehydrating agents.

Introduction

Substituted urea derivatives are an important class of carbonyl compounds. They find widespread applications as plant protecting agents, in pharmaceutical and dye chemistry, as plasticizers or stabilizers, as antioxidants in gasoline or as additives in the production of aminoplastics.[1] Special interest in these compounds has recently arisen since several substituted ureas have been used for brain cancer treatment, or were proven to possess a marked inhibitory effect on HIV protease enzyme.[2] Currently these compounds are synthesized using highly toxic phosgene. Several successful non-phosgene routes have also been studied. Typically, amines may react with compounds like isocyanates, formamides, or carbamates; or the amine can be oxidatively carbonylated with carbon monoxide, in the presence of transition metal catalysts like Pd,[3] Ru,[4] Au,[5] Co,[6] Ni,[7] or W.[8] An alternative is the direct carbonylation of amines by carbon dioxide, which is environmentally particularly attractive: CO_2 is a renewable, abundant, cheap, and non-toxic source of functional carbon units.

Although CO_2 is a relatively inert molecule, it is commonly known that it easily combines with amines to afford the corresponding carbamic acids at room temperature and atmospheric pressure.[9] This step occurs almost spontaneously, but the further transformation of carbamic acids into ureas normally requires quite drastic conditions (200 °C, and CO_2 pressures higher than 100 atm),[10] or the presence of stoichiometric amounts of bases such as NEt_3,[11] or DBU.[12] Since the reaction is limited by the thermodynamic equilibrium, additional stoichiometric amounts of dehydrating agents such as dicyclohexylcarbodiimide,[11] Me_3NSO_3,[12] or diphenylphosphite[13] are necessary. Ureas have also been prepared catalytically in fair yields using ruthenium complexes in the presence of toxic propargylic alcohols[14] or Ph_3SbO/P_4S_{10}.[10] Unwanted side products are formed in such approaches, like, in the latter case, H_2S. Recent progress has been made in the synthesis of urea compounds by the reaction of CO_2 with primary amines in ionic liquids in the presence of CsOH at 170 °C and 60 atm CO_2.[15] Although the dialkylureas are obtained in modest to excellent yields, the reaction requires quite expensive ionic liquids. Moreover, the ionic liquids might not be stable at the high temperatures needed to activate CO_2.[16]

Herein we report that both symmetrical and asymmetrical urea derivatives can be efficiently synthesized in good yields using base catalysts in the presence of *N*-methylpyrrolidone (NMP) as the solvent and CO_2 as a carbonyl source, with water as the only by-product (Scheme 1):

Results and discussion

Catalysts for preparation of symmetrical dialkylureas

The choice of a base catalyst is not easy, since many of the known basic materials would instantly lose their most active sites under a CO_2 atmosphere or upon gradual water formation. Nevertheless, good catalytic activity was uncovered by screening alkali catalysts (Table 1). 2-Heptylamine was chosen as a model substrate and NMP as a solvent. The reactions were conducted in the absence of any dehydrating agent. The reaction did not proceed significantly in the absence of a catalyst. Within the series of alkali carbonates, the activity of the catalysts increases in going from Na^+ to Cs^+ as the counterion for carbonate (entries 2, 3, 4, 6). With Cs_2CO_3, 50% yield of *N*,*N*′-di-2-heptylurea is easily achieved after 24 h (entry 7). The urea was identified by GC-MS and ^1H NMR. Additionally, the formation of water was quantified using Karl Fischer titrations, and this was evidence of the formation of one mole of water per mole of urea. Once the proper cation was identified, the next step was to investigate the influence of the anion. Fluoride as a catalytic anion, *e.g.* in CsF, works well (entries 12, 13), but unsatisfactory results are again obtained when F^- is combined with Na^+ or K^+ (entries 10, 11). Chloride as a counterion for caesium gives a very ineffective catalyst (entry 14). With CsOH (entry 15), results are similar as with Cs_2CO_3. Probably CsOH is transformed to Cs_2CO_3 under the reaction conditions. Summarizing, among the catalysts tested, CsF and Cs_2CO_3 gave the best results. Even 0.005 g Cs_2CO_3 catalyst (0.23 mole %) is still quite effective (entry 8). The limited effect of the amount of catalyst suggests that the catalyst may partially dissolve at the high reaction temperature, the activity being determined by the catalyst solubility. However, there is a clear beneficial effect of increasing the

[a]*Catholic University of Leuven, Centre for Surface Science and Catalysis, Kasteelpark Arenberg 23, 3001, Leuven, Belgium. E-mail: dirk.devos@biw.kuleuven.be; Fax: 32 1632 1998; Tel: 32 1632 1639*
[b]*University of Bucharest, Department of Catalysis, B-dul R. Elisabeta 4-12, 030016, Bucharest, Romania. E-mail: v_parvulescu@chem.unibuc.ro; Fax: 40 2131 59249; Tel: 40 2141 00241*

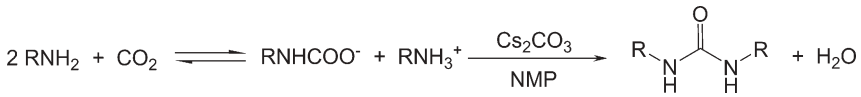

Scheme 1

amount of solid catalyst (entries 6, 8 and 9). Suitable catalysts might also be found in the series of the alkaline earth catalysts, such as $SrCO_3$ (entry 16).

Reaction conditions

In order to select the optimum reaction conditions, experiments focused on the effect of the solvent, reaction temperature, time and CO_2 pressure. The main results are presented in Table 2. Several organic solvents were screened (entries 1–5), and it became evident that the carbonylation proceeds well in *N*-methylpyrrolidone (NMP), rather than in an apolar solvent such as decane. When other amides like dimethylformamide (DMF) were used, an important side product formation was observed because DMF is not inert in the reaction conditions. On the contrary, NMP proved to be very stable; neither in ^{1}H NMR nor in GC-MS analysis, was evidence for its decomposition found. The enhanced stability of NMP in comparison with DMF is likely due to its cyclic nature. Other basic solvents were tested as well, such as acetonitrile or pyridine; however, the results were far inferior to those obtained in NMP. At first sight, there is no direct correlation between these results and solvent parameters such as the dielectric constant ε_r, the dipole moment μ or the solvent basity B_j.[17] A crucial effect is obviously the CO_2 solubility in the solvents, either at 25 °C when the reactor is initially pressurized and saturated with 25 atm of CO_2, or at the reaction temperature of 170 °C. NMP experiences a volumetric expansion of ~30% when exposed to 25 atm of CO_2 at 25 °C,[18] corresponding to a molefraction x_{CO_2} = 0.24. However, similar mole fractions are found in literature data for binary mixtures of CO_2 and acetonitrile or decane.[19] It seems that differences in molar CO_2 reactor content at the cold start of the reaction are minor. Higher temperatures decrease the CO_2 concentration in solution, but these decreases are expected to be parallel for all solvents. Nevertheless, the exceptional properties of NMP are not so surprising: first, this solvent has been used for absorption of CO_2, in combination with amines, which form a carbamic acid with CO_2. For such combined physical and chemical trapping of CO_2, NMP is an excellent choice, as it not only absorbs the CO_2, but also stabilizes the ionic intermediates of the chemisorption.[20] Secondly, several cases are known in which amide solvents like NMP give rise to high basic catalytic activity, for instance in the base-catalyzed alkylation of acetylides.[21]

The effect of the temperature and reaction time can be observed from the same Table 2. As can be expected, a sufficient reaction temperature, *e.g.* of 170 °C, is required for the reaction to proceed to high conversion within reasonable time. For higher temperatures, the yield decreased again (entries 6–8). Such a maximum is reminiscent of the thermal synthesis of urea from CO_2 and NH_3.[1] In such reactions, the initial formation of the ionic carbamate is highly exothermic, while the dehydration to urea is endothermic. As the overall process is exothermic, a shift of the equilibrium to the left with temperature is reasonable. By increasing reaction times and/or the amount of catalyst, a maximum yield of 65% was eventually obtained, which likely corresponds to the equilibrium position (entries 9–11). Within the boundaries tested, the initial carbon dioxide pressure had a small effect (entries 1, 12, 13).

Table 1 Catalytic formation of *N*,*N*′-di-2-heptylurea from 2-heptylamine and CO_2[a]

Entry	Amine	Catalyst	Yield (%)
1	2-Heptyl	None	5
2	2-Heptyl	Na_2CO_3	22
3	2-Heptyl	K_2CO_3	20
4	2-Heptyl	Rb_2CO_3	32
5[b]	2-Heptyl	Rb_2CO_3	47
6	2-Heptyl	Cs_2CO_3	37
7[b]	2-Heptyl	Cs_2CO_3	50
8[c]	2-Heptyl	Cs_2CO_3	35
9[d]	2-Heptyl	Cs_2CO_3	42
10	2-Heptyl	NaF	5
11	2-Heptyl	KF	7
12	2-Heptyl	CsF	35
13[b]	2-Heptyl	CsF	63
14	2-Heptyl	CsCl	1.5
15	2-Heptyl	CsOH	30
16[b]	2-Heptyl	$SrCO_3$	56
17[e]	n-Butyl	Cs_2CO_3	60
18[f]	n-Butyl	Cs_2CO_3	60

[a] Conditions: 0.05 g catalyst, 25 atm CO_2, 6.67 mmoles 2-heptylamine, 1.5 ml NMP, 10 ml autoclave, 170 °C, 4 h. [b] 24 h. [c] 0.005 g catalyst. [d] 0.25 g catalyst. [e] 0.25 g catalyst, 25 atm CO_2, 10 mmoles n-butylamine, 1.5 ml NMP, 10 ml autoclave, 170 °C, 4 h. [f] Re-use of the catalyst of entry 9, 25 atm CO_2, 10 mmoles n-butylamine, 1.5 ml NMP, 10 ml autoclave, 170 °C, 4 h.

Reaction scope

In these optimized conditions, the synthesis of other symmetrical ureas was successfully achieved starting from various

Table 2 Optimization of the reaction conditions[a]

Entry	Time/h	Solvent	*T*/°C	p_{CO_2}/atm	Yield (%)
1	4	NMP	170	25	37
2	4	n-Decane	170	25	0
3	4	THF	170	25	1
4	4	CH_3CN	170	25	0
5	4	Pyridine	170	25	3
6	24	NMP	130	25	10
7	24	NMP	170	25	50
8	24	NMP	200	25	38
9	8	NMP	170	25	49
10	48	NMP	170	25	57
11[b]	48	NMP	170	25	66
12	4	NMP	170	16	31
13	4	NMP	170	21	33

[a] Conditions: 0.05 g Cs_2CO_3, 6.67 mmoles 2-heptylamine, 1.5 ml solvent, 10 ml autoclave. [b] 0.25 g Cs_2CO_3.

Table 3 Synthesis of symmetrical ureas with or without cocatalysts[a]

Entry	Amine	Co-catalyst	Yield (%)[b]
1	n-Butyl	—	16
2[c]	n-Butyl	—	74
3	n-Butyl	Bu_4NBr	29
4[c]	n-Butyl	Bu_4NBr	83
5	n-Hexyl	—	31
6[c]	n-Hexyl	—	82
7	n-Hexyl	Bu_4NBr	31
8[c]	n-Hexyl	Bu_4NBr	82
9[c]	n-Heptyl	—	76
10[c]	n-Octyl	—	74
11[c]	2-Octyl	—	37
12[c]	Benzyl	—	30[d]
13[c]	t-Butyl	—	7
14	2-Heptyl	Bu_4NBr	57
15	2-Heptyl	Bu_4NI	42
16	2-Heptyl	CTAB	51
17	2-Heptyl	Me_4NBr	39
18	2-Heptyl	DMAP	56
19	2-Heptyl	PPh_3	47

[a] Conditions: 0.05 g Cs_2CO_3, 0.05 g co-catalyst, 25 atm CO_2, 6.67 mmoles 2-heptylamine (6.67 mmoles n-hexylamine, 10 mmoles n-butylamine), 1.5 ml NMP, 10 ml autoclave, 170 °C, 4 h. [b] The urea selectivity amounted to 100% in all cases, except when mentioned otherwise. [c] 24 h. [d] Amine conversion = 45%; urea selectivity = 66%.

linear amines (Table 3). Compared with the branched 2-heptylamine, the linear amines were considerably more reactive. The high conversions obtained in Table 3 likely correspond to the reaction equilibrium, *e.g.* 74% for n-butylamine (entry 2), 82% for n-hexylamine (entry 6), 76% for n-heptylamine (entry 9) and 74% for n-octylamine (entry 10). This equilibrium position was proven by performing the reverse reaction, starting from equimolar amounts of isolated *N*,*N*′-dibutylurea and water, using the same catalyst and in the same conditions. After 24 h at 170 °C, 24% of urea is transformed back to the amine, which confirms the previously determined equilibrium position. Results with the branched 2-octylamine are similar as for 2-heptylamine (entry 11). In all these reactions, the selectivity amounted to 100%, *i.e.* the urea is the only product formed. An exception is benzylamine, from which the urea was formed with a selectivity of only 66% (entry 12). Side products like *N*-benzylidene-benzylamine and benzylisocyanate were formed. Low yields were obtained from the sterically hindered primary amine t-$BuNH_2$ (entry 13). No urea compounds compounds were obtained starting from secondary or aromatic amines, *e.g.* *N*-methylbutylamine or aniline.

Use of co-catalysts

The equilibrium can be attained more quickly by adding co-catalytic compounds. A series of ammonium salts and some bases, such as 4-dimethylaminopyridine (DMAP) or PPh_3 were tested in the urea formation from 2-heptylamine (Table 3, entries 14–19). Particularly quaternary ammonium compounds give good results. Using Bu_4NBr and Cs_2CO_3, a 57% yield of *N*,*N*′-di-(2-heptyl)urea was achieved in only 4 h. The quaternary ammonium compounds probably stabilize the carbamate intermediate ($RNHCOO^-$) or other anionic reaction intermediates.[22]

Table 4 Synthesis of asymmetric urea derivatives from *N*-methylbutylamine (NMBA) and various primary amines[a]

Entry	Amine	Catalyst	Amine/NMBA molar ratio	C (%)[b]	S (%)[c]
1	n-Butylamine	Cs_2CO_3	1 : 1	63	40
2	n-Butylamine	Cs_2CO_3	1 : 2	74	76
3	n-Butylamine	Cs_2CO_3	1 : 3	83	95
4	n-Butylamine	CsF	1 : 3	52	73
5	2-Heptylamine	Cs_2CO_3	1 : 3	50	68
6	n-Hexylamine	Cs_2CO_3	1 : 3	64	67
7	n-Octylamine	Cs_2CO_3	1 : 3	63	67

[a] Conditions: 0.05 g catalyst, 25 atm CO_2, 1.5 ml NMP, 10 ml autoclave, 170 °C, 24 h. [b] Conversion of the primary amine. [c] Selectivity for the asymmetrical urea; the only side product is the symmetrical *N*,*N*′-dialkylurea derived from the primary amine.

Synthesis of asymmetrical dialkylureas

In order to prepare asymmetrical urea compounds, several primary amines were reacted with *N*-methylbutylamine (NMBA) in the presence of carbon dioxide and different base catalysts (Table 4). As secondary amines alone do not form urea compounds in these conditions, the only side product is the symmetrical urea derived from the primary amine. A conversion of 83% of n-butylamine (BA) and 95% selectivity for the asymmetrical product was obtained when the molar ratio of the amines (BA/NMBA) was adjusted at 1 : 3. Again Cs_2CO_3 appeared to be effective, with CsF somewhat less active and selective. Asymmetrical urea derivatives were also obtained when different other primary amines (2-heptylamine, n-hexylamine, n-octylamine) were used (entries 5–7).

Catalyst recycling and re-use

After careful cooling of the reaction mixture and centrifugation, the solid catalyst can be recovered and reused. In order to avoid any analytical interference of traces of unreacted amine or product contained within the separated catalyst, a different amine was used than in the first run. Thus Cs_2CO_3 was first used in a reaction with 2-heptylamine and then in a reaction with n-butylamine; results were compared with those of a fresh catalyst in the reaction of n-butylamine (Table 1, entries 9, 17, 18). The recycling tests were performed in the absence of a co-catalyst. The data show that the same yield of dibutylurea is obtained with a recycled catalyst as with a fresh catalyst, proving that the catalyst is precipitated after cooling to room temperature, and that the Cs_2CO_3 is not liable to deactivation.

Conclusion

In summary, we uncovered a very efficient and highly selective catalytic system for the synthesis of a large variety of both symmetrical and asymmetrical urea derivatives. The used catalysts were able to convert both linear and branched aliphatic amines to their corresponding urea derivatives in the absence of dehydrating agents. The combination of the Cs catalyst and the NMP solvent is crucial for obtaining high reactivity; omission of either or both leads to very sluggish reactions. The catalysts can be recovered and reused without activity loss, and the products can be easily isolated from the solution by precipitation with water. The present methodology

compares favorably with the existing methods for the preparation of these types of compounds.

Experimental

All reactions were carried out under pressurized CO_2 in small stainless steel reactors (10 ml). As an example, 10 mmoles of n-butylamine (0.73 g), 0.15 mmoles Cs_2CO_3 (49 mg) and 1.5 ml of NMP were charged in the reactor, and the reactor was saturated with CO_2 under a pressure of 25 atm at room temperature. The reaction was magnetically stirred and heated in the range 130–200 °C in a temperature-controlled electrical heater for 4–48 h. After heating, the reactor was cooled at room temperature (0 °C in the case of the more volatile amines) and carefully depressurized. The catalyst was separated by centrifugation from the reaction mixture. Then the supernatant was diluted in MeOH and analyzed with a HP 5890 GC (flame ionization detector), GC-MS and ^{1}H NMR. For product isolation, 5 ml water was added to the reaction mixture after catalyst centrifugation. This resulted in precipitation of the desired urea product, which could easily be isolated. GC-MS and ^{1}H NMR spectra were entirely consistent with the assigned structures. Spectroscopic data for the synthesized urea derivatives are given below:

***N*,*N*′-di(2-heptyl)urea**: GC-MS, *m*/*z*: 57 (100%), 69 (64), 100 (98), 114 (38), 167 (14), 185 (44), 256 (10);

***N*,*N*′-di(2-octyl)urea**: GC-MS, *m*/*z*: 57 (62%), 70 (81), 114 (100), 128 (32), 199 (43), 227 (7), 241 (7), 255 (5), 284 (11);

***N*,*N*′-dibutylurea**: GC-MS, *m*/*z*: 57 (100%), 74 (53), 87 (29), 101 (45), 115 (4), 129 (22), 143 (13), 157 (11), 172 (45);

***N*,*N*′-dihexylurea**: GC-MS, *m*/*z*: 57 (100%), 85 (45), 99 (56), 115 (36), 128 (36), 143 (12), 158 (23), 185 (58), 199 (39), 228 (31);

***N*,*N*′-diheptylurea**: GC-MS, *m*/*z*: 57 (100%), 86 (25), 101 (34), 116 (53%), 142 (45), 185 (10), 199 (59), 213 (49), 227 (19), 241 (6), 256 (38);

***N*,*N*′-dioctylurea**: GC-MS, *m*/*z*: 57 (100%), 69 (54), 85 (26), 99 (71), 112 (33), 130 (56), 157 (28), 171 (14), 185 (14), 199 (8), 213 (40), 227 (35), 241 (19), 255 (16), 269 (5), 284 (24);

***N*,*N*′-dibenzylurea**: GC-MS, *m*/*z*: 79 (21%), 91 (54), 106 (100), 149 (17); 240 (21);

***N*,*N*′-di(t-butyl)urea**: GC-MS, *m*/*z*: 58 (100%), 157 (8), 172 (3);

***N*-Butyl-*N*′-methylbutylurea**: GC-MS, *m*/*z*: 57 (100%), 72 (13), 88 (15), 101 (9), 114 (37), 143 (22), 157 (2), 186 (19);

***N*-Hexyl-*N*′-methylbutylurea**: GC-MS, *m*/*z*: 57 (100%), 70 (9), 88 (32), 99 (19), 114 (64), 128 (14), 143 (5), 157 (5), 171 (17), 185 (5), 214 (26);

***N*-2-heptyl-*N*′-methylbutylurea**: GC-MS, *m*/*z*: 57 (67%), 70 (25), 84 (15), 98 (15), 114 (70), 140 (100), 157 (29), 168 (13), 228 (3);

***N*-Octyl-*N*′-methylbutylurea**: GC-MS, *m*/*z*: 57 (100%), 88 (30), 99 (30), 114 (57), 128 (11), 156 (12), 171 (5), 199 (7), 242 (11).

Acknowledgements

Angelica Ion is grateful to the K.U. Leuven Research Fund for a doctoral fellowship. This work was performed in the frame of a Bilateral Agreement Flanders/Romania.

References

1 *Ullmann's Encyclopedia of Industrial Chemistry*, 6th edn, electronic version, Wiley VCH, Weinheim, Germany, 2000.
2 G. Bartolo, G. Salerno, R. Mancuso and M. Costa, *J. Org. Chem.*, 2004, **69**, 4741; A. Estevez-Souza, K. Pissinate, M. da Graca Nascimento, N. F. Grynberg and A. Echevaria, *Bioorg. Med. Chem.*, 2006, **14**, 492.
3 I. Chiarotto and M. Feroci, *J. Org. Chem.*, 2003, **68**, 7137; M. Gasperini, F. Ragaini, C. Remondini, A. Caselli and S. Cenini, *J. Organomet. Chem.*, 2005, **690**, 4517; I. Pri-Bar and H. Alper, *Can. J. Chem.*, 1990, **68**, 1544; F. Shi, Y. Q. Deng, T. L. SiMa and H. Z. Yang, *Tetrahedron Lett.*, 2001, **42**, 2161.
4 S. A. R. Mulla, C. V. Rode, A. A. Kelkar and S. P. Gupte, *J. Mol. Catal. A: Chem.*, 1997, **122**, 103.
5 F. Shi and Y. Q. Deng, *J. Catal.*, 2002, **211**, 548.
6 E. Bolzacchini, S. Meinardi, M. Orlandi and B. Rindone, *J. Mol. Catal. A: Chem.*, 1996, **111**, 281.
7 P. Giannoccaro, C. F. Nobile, R. N. Mastrorilli and N. Ravasio, *J. Organomet. Chem.*, 1991, **419**, 251.
8 J. E. McCusker, F. Qian and L. McElwee-White, *J. Mol. Catal. A: Chem.*, 2000, **159**, 11; J. E. McCusker, J. Logan and L. McElwee-White, *Organometallics*, 1998, **17**, 4037; J. E. McCusker, A. D. Main, K. S. Johnson, C. A. Grasso and L. McElwee-White, *J. Org. Chem.*, 2000, **65**, 5216.
9 E. M. Hampe and D. M. Rudkevich, *Tetrahedron*, 2003, **59**, 9619.
10 R. Nomura, Y. Hasegawa, M. Ishimoto, T. Toyosaki and H. Matsuda, *J. Org. Chem.*, 1992, **57**, 7339. Note that 1,2-diamines can be converted in rather mild conditions to the imidazolones in moderate conditions (60 atm CO_2, 150 °C), even without a catalyst; see: B. M. Bhanage, S. Fujita, Y. Ikushima and M. Arai, *Green Chem.*, 2003, **5**, 340. However, acyclic ureas cannot be produced this way; see Table 1, entry 1.
11 H. Ogura, K. Takeda, R. Tokue and T. Kobayashi, *Synthesis*, 1978, 394.
12 C. F. Cooper and S. J. Falcone, *Synth. Commun.*, 1995, **25**, 2467.
13 N. Yamazaki, F. Higashi and T. Iguchi, *Tetrahedron Lett.*, 1974, **13**, 1191.
14 J. Fournier, C. Bruneau, P. H. Dixneuf and S. Lecolier, *J. Org. Chem.*, 1991, **56**, 4456.
15 F. Shi, Y. Q. Deng, T. L. SiMa, J. J. Peng, Y. L. Gu and B. T. Qiao, *Angew. Chem.*, 2003, **115**, 3379.
16 M. J. Earle, J. M. S. S. Esperanca, M. A. Gilea, J. N. Canongia Lopez, L. P. N. Rebelo, J. W. Magee, K. R. Seddon and J. A. Widegren, *Nature*, 2006, **439**, 831.
17 C. Reichardt, *Solvents and Solvent Effects in Organic Chemistry*, VCH, Weinheim, 1990, p. 408.
18 R. Rajasingam, L. Lioe, Q. T. Pham and F. P. Lucien, *J. Supercrit. Fluids*, 2004, **31**, 227.
19 J. P. Passarello, S. Benzaghou and P. Tobaly, *Ind. Eng. Chem. Res.*, 2000, **39**, 2578; T. S. Reighard, S. T. Lee and S. V. Olesik, *Fluid Phase Equilib.*, 1996, **123**, 215.
20 P. D. Vaidya and V. V. Mahajani, *Ind. Eng. Chem. Res.*, 2005, **44**, 1868.
21 L. A. Oparina, S. I. Shaikhudinova, L. N. Parshina, O. V. Vysotskaya, Th. Preiss, J. Henkelmann and B. A. Trofimow, *Russ. J. Org. Chem.*, 2005, **41**, 656.
22 R. N. Salvatore, F. Chu, A. S. Nagle, E. A. Kapxhiu, R. M. Cross and K. W. Jung, *Tetrahedron*, 2002, **58**, 3329; M. Yoshida, N. Hara and S. Okuyama, *Chem. Commun.*, 2000, 151.

Effect of ionic liquids on epoxide hydrolase-catalyzed synthesis of chiral 1,2-diols

Cinzia Chiappe,*[a] Elsa Leandri,[a] Bruce D. Hammock*[b] and Christophe Morisseau[b]

Received 22nd August 2006, Accepted 30th October 2006
First published as an Advance Article on the web 14th November 2006
DOI: 10.1039/b612106c

Ionic liquids (ILs) offer new possibilities for epoxide hydrolase (EH) catalyzed resolution of epoxides and for synthesis of chiral 1,2-diols. Soluble EHs from cress and mouse (csEH and msEH) and microsomal EH from rat (rmEH) were tested in several ILs. For all the enzymes tested, higher enantioselectivities were obtained in [bmim][$N(Tf)_2$] and [bmim][PF_6]. The optimized amount of water for EH activity in these ILs was established. Classical problems arising from low solubility of epoxides in water or from the high tendency of the oxirane ring to undergo chemical hydrolysis were avoided using these new media.

Introduction

Due to their chemical versatility, enantiopure epoxides and vicinal diols are extensively employed as useful building blocks for the synthesis of bioactive compounds in the pharmaceutical and agrochemical industries.[1] An emerging approach involves the use of cofactor-independent epoxide hydrolases, which allow the preparation of these compounds under mild conditions.[2–4] These enzymes have long been known in mammalian systems, and stereochemical studies have shown that the reaction catalyzed by EHs generally proceeds with a high product and/or substrate enantioselectivity.[5,6] However, the interest of the synthetic chemist towards the application of these biocatalysts has only recently increased, since it has been shown that (i) these enzymes are ubiquitous in nature (they have been detected in plants, fungi, microorganisms) and therefore they are easily accessible;[7] (ii) EHs may be cloned, modified and expressed in cells or microorganisms;[8] (iii) racemic epoxides can be resolved on a preparative scale.[9] This latter aspect is surely important from a synthetic point of view, particularly for industrial applications; however, only a few examples have been reported using two-phase reactors.[9] Generally, a bio-catalytic approach allows only the transformation of small amounts of substrate per litre of solution, due to the low solubility and/or stability of many organic compounds in the aqueous buffer solutions used for the reactions. In order to overcome these drawbacks, non-conventional media such as organic co-solvents, and organic–aqueous two-phase systems have been used in several biocatalyzed reactions.[9] However, many common solvents are toxic, and activity and selectivity of the enzymes are generally reduced in non-aqueous media, limiting their use.[10] The use of organic solvents might be particularly important in the case of epoxides, which easily undergo spontaneous hydrolysis in the presence of water. This process not only depletes the substrate (reducing the overall yield) but it also affects the enantiomeric purity of the product. Chemical hydrolysis gives generally the same diol arising from enzymatic reaction, but in a racemic mixture. There are exceptions where chemical hydrolysis leads to extensive rearrangement and/or polymerization of the substrate. In contrast to other enzymatic systems, however, only a few examples of the use of epoxide hydrolases in organic solvents or in two phase systems have been reported, most likely due to the instability of these enzymes in non-natural media.[11] Recently, we showed that soluble epoxide hydrolases are able to perform resolution processes in a very efficient and enantioselective manner in some ionic liquids (ILs),[12] although organic solvents (*e.g.* methyl *tert*-butyl ether and *tert*-butanol) completely deactivate the same enzymes. The term ionic liquids identifies a large class of organic salts, liquid at or near room temperature, which have emerged recently as alternative green media for biotransformations, using both whole cell systems and isolated enzymes.[13] The use of ionic liquids has shown many advantages with respect to conventional organic solvents, such as a better enzyme stability, substrate and/or product selectivity and suppression of unwanted side reactions.[14] Moreover, as solvents for chemical reactions, ILs exhibit excellent physico-chemical properties, in particular they are able to dissolve polar and non-polar organic, inorganic and polymeric materials; they have a high thermal stability and they lack significant vapor pressure.[15] Finally, all the physico-chemical properties of ILs can be modified by altering the cation or anion, and in principle the best IL may be designed for each specific reaction system.

As part of our research program, we became interested in ionic liquids as alternative solvents for biotransformations using epoxide hydrolases (EHs) as catalyst. Here, we report our more recent results on the hydrolysis of racemic and meso epoxides (some of these substrates easily undergo spontaneous hydrolysis in buffer solution) catalyzed by different EHs in several ionic liquids.

[a]*Dipartimento di Chimica Bioorganica e Biofarmacia, via Bonanno 33, 56126, Pisa, Italy. E-mail: cinziac@farm.unipi.it; Fax: +39 50 2219660; Tel: +39 50 2219669*
[b]*Department of Entomology & Cancer Research Center, University of California, Davis, CA, 95616, USA. E-mail: bdhammock@ucdavis.edu*

Experimental

The ^{1}H and ^{13}C NMR spectra were obtained in $CDCl_3$ with a Bruker AC 200 instrument using TMS as the internal reference. GC analyses were performed using a Carlo Erba HRGC 5300 instrument. HPLC analyses were performed on a Waters 600E instrument equipped with a Varian Prostar 325 detector.

Chemicals and enzymes

Racemic 3,3-dimethyl-1,2-butene oxide (**1**), cyclopentene oxide (**3**) and cyclohexene oxide (**5**) were purchased from Aldrich. 4-*tert*-Butylstyrene oxide (**7**), α-methylstyrene oxide (**9**) and dihydronaphthalene oxide (**13**) were prepared from the corresponding olefins by oxidation with *m*-chloroperbenzoic acid–KF complex, as previously reported.[16] 4-Chlorostyrene oxide (**11**) was prepared by oxidation with *m*-chloroperbenzoic acid in dichloromethane. The corresponding diols were synthesized by acid catalyzed hydrolysis (0.1 N $HClO_4$) from the corresponding epoxides. [bmim][BF_4], [emim][$EtSO_4$] (ECOENG 212) and [mmim][Me_2PO_4] (ECOENG 1111P) were purchased from Solvent Innovation (GMBH). [bmim][PF_6], [bmim][Tf_2N], [bmim][BOB] and [bmpyrr][Tf_2N] were prepared following reported procedures.[17] Attention was paid to the elimination of bases and Cl^- ions which may be present in the solvents as impurities. The purity of imidazolium salts was always checked by measuring the absorption spectra between 240 and 400 nm. Purified [bmim]$^+$ salts (containing $Cl^- < 0.1$ ppm) have practically no absorption band in the 250–300 nm region.[18] After drying (2 h at 80 °C under vacuum), the amount of water in the ILs was determined by the Karl–Fisher technique using an apparatus composed of a stand titrator and a coulometer. The water content of dried ILs ranged from 150 to 350 ppm. The water activity (a_w) was measured with an a_w measuring instrument from DELTA Instrument (Trieste, Italy). Measurements were carried out by placing the sensor into the open end of 5 mL glasses vials at 37 °C, until constant readings were obtained. All samples were previously equilibrated for 24 h.

The recombinant soluble and microsomal epoxide hydrolase enzymes of mouse, cress and rat were prepared and purified as previously described.[7d,19] Recombinant cDNA of each enzyme was cloned into baculovirus expression system. *Trichoplusia ni* high five cell cultures were transfected with prepared recombinant baculovirus in order to express the desired enzyme and subsequently were purified from cell lysate using affinity chromatography.

Enantioselectivity assays

Analysis conditions. The enantiomeric composition of residual epoxides **7**, **9** and **13** was determined by ^{1}H NMR after addition of the resolving agent, Europium tri[3-heptafluoropropylhydroxymethyle)-(+)camphorate] (Aldrich), whereas the enantiomeric composition of all the other epoxides were determined by GC on a chiral 30 m Chiradex G-TA (ASTEC) column (helium flow 50 KPa, with evaporator and detector set at 200 °C) at the following temperatures: **1**, 45 °C; **11**, 100 °C. The enantiomeric composition of diols **8** and **10** were determined by ^{1}H NMR after addition of the resolving agent, Europium tri[3-heptafluoropropylhydroxymethyl)-(+)camphorate] (Aldrich), whereas that of diol **12** by HPLC on a Daicel Chiralcel OD-H column, using hexane-2-propanol (98 : 2) as solvent (solvent flow, 0.5 mL min^{-1}). The enantiomeric excesses of all the other diols were determined by GC on a chiral 30 m Chiradex G-TA (ASTEC) column (helium flow 50 KPa, with evaporator and detector set at 200 °C) at the following conditions: diol **2**, 80 °C for 10 min, at a rate of 4 °C min^{-1}, 120 °C for 10 min; diol **4** (as trifluoroacetyl derivative), 100 °C; diol **6** (as trifluoroacetyl derivative), 85 °C; diol **14** (after transformation into the corresponding 1,2-dimethyl ether), 170 °C. The absolute configurations of the excess enantiomers were determined on the basis of their optical rotation values. The enantiomeric ratios (E_S and E_P) were calculated using the conversion rate (c) and either the substrate e.e. (ee(S)) or the product e.e. (ee(P)) using the following equations.[20]

$$E_S = \ln[(1 - c)(1 - ee(S))]/\ln[(1 - c)(1 + ee(S))]$$

$$E_p = \ln[(1 - c)(1 + ee(P))]/\ln[(1 - c)(1 - ee(S))]$$

Incubation procedures with mouse and cress sEH and rat mEH. Selection of ionic liquids. Epoxide **1** (150 μmol) and epoxide hydrolase (cress sEH 3.1 mg; mouse sEH 2,8 mg; rat mEH 19 mg) were mixed with ionic liquid (2 mL) or buffer solution (Tris-HCl, pH = 7.4) and the resulting mixture was stirred at 37 °C. After 3 h, the reaction mixture was first extracted with hexane (5 times with 4 mL portion). The combined hexane phases were analyzed by GC on a chiral column, after addition of cyclopentanone as an internal standard, to determine the conversion and the e.e. of the remaining substrate. The ionic liquid was then extracted with ethyl ether (5 times with 4 mL portion) and the combined ethereal phases, containing the formed diol **2**, were analyzed by GC on the same chiral column. Control experiments carried out without enzyme or using a deactivated preparation showed that the spontaneous hydrolysis did not contribute to diol formation under the conditions reported here. Finally, after extraction of the remaining epoxide and resulting diol, the ionic liquids were filtered, washed and dried under vacuum at 80 °C for 2 h and reused. The water content of the dried ILs, determined by Karl–Fisher titration ranged from 150–350 ppm. When purified enzyme was used the amount of water was around 1% while in the case of crude extracts it was around 10%.

Incubation of epoxides 3 and 5 with rat mEH in [bmim][PF_6]. Epoxide **3** or **5** (250 μmol) and rat mEH (4 × 19 mg: each portion added every 12 h) were added to [bmim][PF_6] (2 mL), and the resulting mixture was stirred at 37 °C for 48 h until TLC analysis (hexane–ethyl acetate, 80 : 20) demonstrated the disappearance of epoxides **3** or **5**. The resulting *trans*-diol **4** or **6** was extracted with ethyl ether (5 times with 4 mL portion) and analyzed by GC after conversion to the corresponding bis-trifluoroacetyl derivatives.

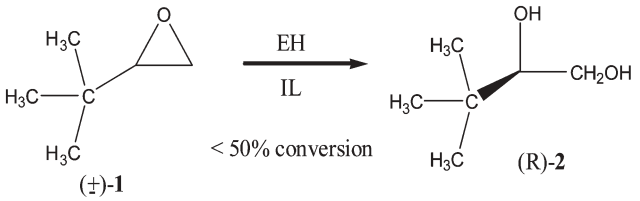

Scheme 1 EH catalyzed hydrolysis of racemic **1**.

Incubation of epoxides 7, 9 and 13. Aryl substituted epoxides **7** or **9** or **13** (400–600 μmol) were incubated at 37 °C in [bmim][PF_6] (4 mL) using microsomal and soluble epoxide hydrolase (cress sEH 10 mg; mouse sEH 9.6 mg; rat mEH 36 mg) as biocatalyst. The reactions, stopped at prefixed times (1–3 h) by filtration of the enzyme, were first extracted with hexane (5 times with 4 mL portion). The combined hexane phases were analyzed by GC, HPLC or NMR, as reported above, to determine the conversion and the e.e. of the unreacted substrate. The ionic liquid was then extracted with ethyl ether (5 times with 4 mL portion) and the combined ethereal phases, containing the formed diols, were analyzed by GC, HPLC or NMR. Blank experiments carried out without enzyme or using a deactivated preparation showed that the spontaneous hydrolysis did not contribute to diol formation under the incubation conditions.

Result and discussion

Seven different ionic liquids [bmim][PF_6], [bmim][Tf_2N], [bmim][BF_4], [bmpyr][$N(Tf_2)$], [bmim][Bob], [emim][$EtSO_4$], [mmim][Me_2PO_4] (where emim = 1-ethyl-3-methylimidazolium, bmim = 1-butyl-3-methylimidazolium, mmim = 1,3-dimethylimidazolium, bmpyr = butylmethyl pyrrolidinium, PF_6 = hexafluorophosphate, Tf_2N = bis(trifluoromethylsulfonyl)imide, BF_4 = tetrafluoroborate, $EtSO_4$ = ethylsulfate, Me_2PO_4 = dimethylphosphate, [BOB] = bis[oxalate(2-)]-borate]) were used as solvents to investigate the influence of these media on epoxide hydrolase activity to hydrolyze racemic 3,3-dimethyl-1,2-butene oxide (**1**) (Scheme 1), under water controlled conditions (around 10% when crude enzyme extracts were used; around 1% when the purified enzyme was used).

The efficiency of each conversion was evaluated on the basis of the conversion and the enantiomeric excess of the remaining epoxide **1** and resulting diol **2**, after 3 h. Both of these parameters were evaluated by GC, using a chiral column. The data reported in Table 1 show that three of the investigated ILs ([bmim][BOB], [bmim][$EtSO_4$] and [mmim][Me_2PO_4]) are not suitable for this kind of reaction. Epoxide **1** probably reacts with the anion of these ionic liquids to give one or more addition products, which have not been isolated. The enzymatic hydrolysis is able to compete with this process only in the case of [mmim][Me_2PO_4]; in this solvent, we detected small amounts of pure (*R*)-**2**. In the other ionic liquids, having $[BF_4]^-$ $[PF_6]^-$ or $[Tf_2N]^-$ as anion, the biocatalyzed reactions were dependent on the structure of the cation and anion, and on enzyme source. Higher conversions and enantioselectivities were generally found in [bmpyr][$N(Tf)_2$] and [bmim][PF_6], two hydrophobic ILs. It is worth noting that, in all examined ILs (in which it was possible to isolate the diol **2**) the reaction

Table 1 Hydrolysis of 3,3-dimethyl-1,2-butene oxide (**1**) catalyzed by crude cress, mouse soluble and rat microsomal EH (csEH, msEH, rmEH) or purified csEH in ionic liquids[a]

Solvent		Conv. (%)[b]	Residue (*S*)-**1** e.e. (%)	E_S	Formed (*R*)-**2** e.e. (%)	E_P
[bmim][PF_6]	csEH	24	30	52[c]	>98	>100
[bmim][Tf_2N]		35	54	>100	>98	>100
[bmim][BF_4]		16	18	>100	>98	>100
[bmpyr][Tf_2N]		25	35	>100	>98	>100
[bmim][BOB]		—[d]				
[mmim][Me_2PO_4]		—[e]				
[emim][$EtSO_4$]		—[f]				
[bmim][PF_6]	msEH	25	34	>100	>98	>100
[bmim][Tf_2N]		36	55	>100	>98	>100
[bmim][BF_4]		10	11	>100	>98	>100
[bmpyr][Tf_2N]		39	63	>100	>98	>100
[bmim][BOB]		—[d]				
[mmim][Me_2PO_4]		—[e]				
[emim][$EtSO_4$]		—[f]				
[bmim][PF_6]	Purified csEH	8		n.d.[g]	>98	>100
[bmim][Tf_2N]		13		n.d.	>98	>100
[bmim][BF_4]		5		n.d.	>98	>100
Tris-HCl	rmEH	20	24	>100	>98	>100
[bmim][PF_6]		10	10	21[c]	>98	>100
[bmim][Tf_2N]		10	11	>100	>98	>100
[bmpyr][Tf_2N]		20	24	>100	>98	>100
[bmim][BOB]		—[d]				
[mmim][Me_2PO_4]		—[e]				
[emim][$EtSO_4$]		—[f]				

[a] In typical analytical experiments, the enzymatic reactions were performed with a solution containing substrate (0.15 mmol) and enzyme (cress sEH 3.1 mg; mouse sEH 2.8 mg; rat mEH 19 mg) in solvent (2 mL). [b] Conversions were calculated on the basis of the unreacted epoxide and formed diols. The values matched within 5%. [c] Considering the error on conversion, the value may be >100. [d] Neither unreacted epoxide, nor the resulting diol were recovered from this IL. [e] Conversions calculated on the basis of the residue epoxide were higher than 80%. Only traces of formed diols were however detected. [f] Conversions calculated on the basis of the residue epoxide were higher than 80%. No diol was however detected. [g] n.d.: not determined.

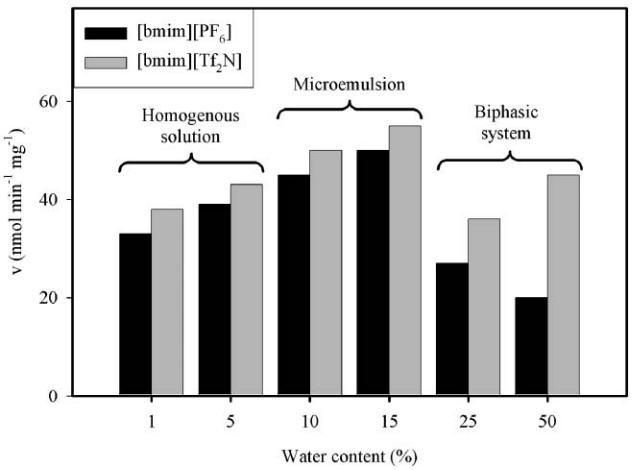

Fig. 1 The effect of water on the csEH catalyzed hydrolysis of β-methylstyrene oxide in IL–water mixtures. Black, [bmim][PF_6]–water mixtures. Grey,[bmim][Tf_2N]–water mixtures.

proceeded with a complete substrate enantioselectivity to give a pure diol of *R* configuration and an enantio-enriched epoxide of *S* configuration (before 50% conversion), in agreement with the enzyme's behavior previously observed in buffer solution.[21]

The water content of the reaction medium generally plays an important role in enzymatic catalysis, since it affects the flexibility of the proteins, a factor determining enzyme activity and selectivity.[22] In the case of EH catalyzed hydrolysis of epoxides, water is also a reactant. In neat ionic liquid, no activity was observed at all when lyophilized EH from *Aspergillus niger* was used, underlying the need for reactive water. To investigate the influence of water, we selected two ionic liquids from our first experiment, [bmim][PF_6] and [bmim][$N(Tf)_2$]. Using purified cress soluble epoxide hydrolase as catalyst and *trans*-β-methylstyrene oxide as substrate (*trans*-β-methylstyrene oxide is a typical substrate for this enzyme) we determined the enzymatic activity in the presence of different amounts of water (1, 5, 10, 15, 25 and 50%), starting from a homogeneous solution (below 5%), going to a biphasic system (above 25%) and passing through a microemulsion, (around 10–15%) as evidenced by the opalescent aspect of the mixture.

As shown in Fig. 1, in both ILs the enzyme activity varies with the water content; the higher activity being found around 10–15%. The apparent activity decrease observed at the higher water percentages, may be attributed to the biphasic system characterizing these latter conditions. Because water activity a_w is considered a more precise parameter to compare dependence of the enzyme's activity on the amount of water present in the incubation medium,[23] we determined a_w values for the employed mixtures ILs–wet csEH, corresponding to a IL : water ratio around 90 : 10 v/v.

The a_w values for the examined mixtures csEH-[bmim][PF_6], csEH-[bmim][Tf_2N], csEH-[bmim][BF_4] and csEH-[bmpyr][Tf_2N] were 0.80, 0.82, 0.84 and 0.84, respectively. These values and conditions are very similar to those found to provide mandelate racemase and penicillin G amidase activity in ILs.[24]

Considering the promising results and optimized conditions obtained for the hydrolysis of epoxide **1**, we then examined the behavior of other substrates in these reaction conditions. In particular, we investigated the enantioselective production of diols from simple *meso*-epoxides, such as cyclopentene oxide (**3**) and cyclohexene oxide (**5**) by mEH (Scheme 2) and from aryl substituted epoxides (Scheme 3).

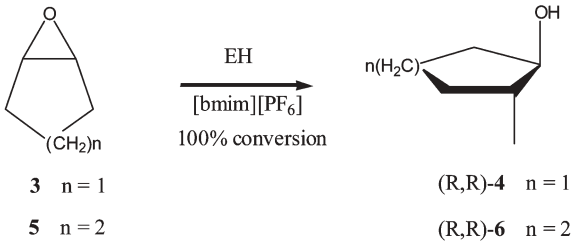

3 n = 1 **5** n = 2 (R,R)-**4** n = 1 (R,R)-**6** n = 2

Scheme 2 EH catalyzed hydrolysis of *meso*-epoxides.

Examples of desymmetrization of *meso*-epoxides are scarce.[25] Epoxides **3** and **5** (0.25 mmol) and mEH (4 × 19 mg) were suspended in 5 μl of phosphate buffer; each portion (added at intervals of 12 h) were incubated in 2 mL of [bmim][PF_6] at 37 °C for 48 h, until no epoxide was detected. Although on the basis of the data reported in Table 1 the best IL seems to be [bmpyr][Tf_2N], in this screening it was replaced with [bmim][PF_6], since this latter IL is less expensive and the products were more easily recovered. Pure *trans*-(*R*,*R*)-diols **4** and **6** (e.e. ⩾ 98) were isolated in quantitative yield. It is interesting to note that, the e.e. of diols **4** and **6** obtained from the mEH catalyzed hydrolysis of epoxides **3** and **5** in [bmim][PF_6] are significantly higher than those previously reported for the reaction carried out in buffer Tris-HCl solution (**4**, 90%; **6**; 76%).[25a] In the aqueous medium, at least for epoxide **5**, an e.e. around 90% was obtained working under highly dilute conditions.[26] Control experiments had shown that in buffer solution at pH 7.4, epoxide **5** is partially converted to its vicinal diol **6** *via* an oxirane ring opening reaction with water, and the contribution of this spontaneous reaction, which proceeds without enantioselectivity, increases with the substrate concentration. The high e.e. found in [bmim][PF_6], working at relatively high substrate concentrations (0.12 M) and in the presence of *ca.* 12% of water, highlights the ability of the IL to reduce the non-enzymatic

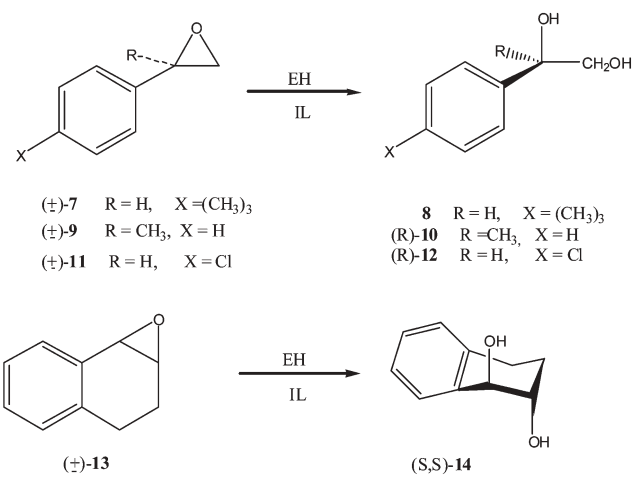

(±)-**7** R = H, X = $(CH_3)_3$
(±)-**9** R = CH_3, X = H
(±)-**11** R = H, X = Cl

8 R = H, X = $(CH_3)_3$
(R)-**10** R = CH_3, X = H
(R)-**12** R = H, X = Cl

(±)-**13** (S,S)-**14**

Scheme 3 EH catalyzed hydrolysis of racemic aryl substituted epoxides.

Table 2 Hydrolysis of 4-tert-butylstyrene oxide (**7**), α-methylstyrene oxide (**9**), dihydronaphthalene oxide (**13**) catalyzed by csEH, msEH, rmEH in [bmim][PF6] (in the presence of *ca.* 10% of water) at 37 °C[a]

Substrate		Conv (%)[b]	Residue epoxide e.e (%, abs. conf.)	E_S	Diol	Formed diol e.e. (%, abs. conf.)	E_P
7	csEH	29	10	1.8	**8**	20, (R)	1.6
	msEH	25	10	2.0		20, (R)	1.6
	rmEH	50	20	1.8		22, (R)	1.9
9	csEH	35	20,(S)	1.1	**10**	62, (R)	5.9
	msEH	30	16,(S)	2.5		30, (R)	2.0
	rmEH	33	10,(S)	1.7		20, (R)	1.6
13	csEH	10	2	1.5	**14**	80, (1S,2S)	9.8
	msEH	<1	0				
	rmEH	20	16, (1S,2R)	5.3		63, (1S,2S)	5.1

[a] In typical analytic experiments, the enzymatic reactions were performed with a solution containing substrate (0.4–0.6 mmol), enzyme (cress sEH 10 mg; mouse sEH 9.6 mg; rat mEH 36 mg) in solvent (4 mL). [b] Conversions were calculated on the basis of the unreacted epoxide and formed diols. The values matched within 5%.

hydrolysis. In ILs, water-sensitive catalysts and chemical reactions are less affected by the presence of water, compared with the situation in organic solvents, because water dispersed throughout the IL cannot act like bulk water.[15g]

To investigate in more detail the possibility of the hydrolysis of water sensitive epoxides in ionic liquids we performed the incubations of three aryl substituted oxiranes, 4-*tert*-butylstyrene oxide (**7**), α-methylstyrene oxide (**9**), and 1,2-dihydronaphthalene oxide (**13**) in [bmim][PF_6] (in the presence of *ca.* 10% of water) using soluble and microsomal epoxide hydrolases (Scheme 3).

Results are reported in Table 2. As expected, product and substrate enantioselectivity of all three aryl substituted epoxides depended on the enzyme source, being generally low with the murine soluble enzyme and relatively high with the cress soluble EH and rat microsomal EH.

In aqueous buffer solution, the product enantioselectivity characterizing the mammalian mEH catalyzed hydrolysis of terminal racemic epoxides is considered to be the outcome of the two selective processes: (i) a substrate enantioselectivity, arising from a different affinity of the two epoxide enantiomers for the enzyme active site; associated with (ii) a high regioselectivity. The enzymatic attack is highly preferential (or even absolute) at the less substituted carbon. In the case of terminal epoxides, therefore, hydrolysis involves retention of configuration at the stereogenic centre and the e.e. of the product is a function of the substrate enantioselectivity and of the conversion. The e.e. of diols **8** and **10**, although low, correlate with the e.e. of the corresponding epoxides and with the percent of conversion; the reaction occurs with high regioselectivity but with moderate substrate enantioselctivity.[27] The regioselectivity of mEH, a feature probably arising from the mechanism of hydrolysis (nucleophilic attack of an aspartate carboxylic anion on an enzymatically activated epoxide, but without the formation of a true carbonium ion),[28] seems to not be affected by the IL.

At variance, the rmEH hydrolysis of 1,2-dihydronaphthalene oxide (**13**) proceeds with a significant substrate enantioselectivity, resulting in the corresponding *trans*-diol of (1*S*,2*S*) configuration, by formal water attack at the benzylic carbon of the (1*R*,2*S*)-enantiomer. In agreement with the proposed topology of the active site, the enantiomer preferentially hydrolyzed is that bearing the phenyl ring on the right back side, when the oxirane ring is oriented with the oxygen upward, as reported in Scheme 4.

In aqueous buffer solution, it is more difficult to generally rationalize the enantioselectivity of the sEH catalyzed processes. These enzymes show the potential to convert both substrate enantiomers through two processes having different regioselectivity.[6,29] As a consequence, the product enantioselectivity is not only a function of the substrate enantioselectivity and the conversion, but also of the ratio of retention to inversion for each enantiomer. Moreover, many sEH enzymes were found to be regioselective at the benzylic oxirane carbon, supporting the proposed mechanism in which one or more tyrosine residues in the site active of the enzyme act as general acid catalysts in the alkylation half reaction.[6] The moderate e.e. characterizing diol **8** and epoxide **7** evidences the lack of enantioselectivity of both the msEH and csEH, analogous to the behavior observed with mEH (Table 2).

On the other hand, the significant e.e. of diol **10**, obtained from csEH hydrolysis of **9**, is reasonably consistent with a regioselective attack at the terminal carbon. The tertiary benzylic position should not be reactive towards the nucleophilic attack due to the steric hindrance. Related to the hydrolysis of this substrate, it is also worth noting that the high enantioselectivity found in the csEH catalyzed hydrolysis of

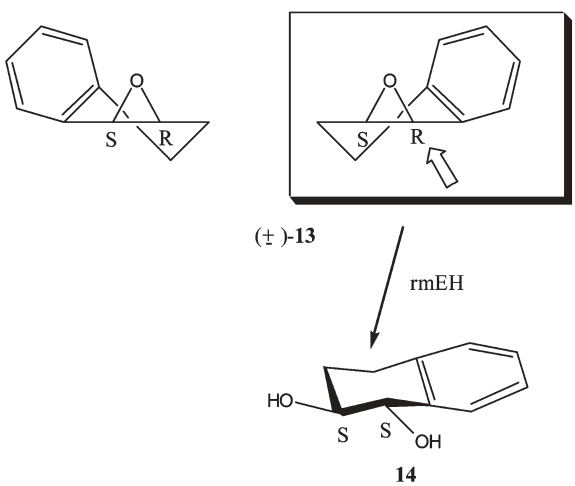

Scheme 4 Preferential pathway in the mRH catalyzed hydrolysis of racemic **13**.

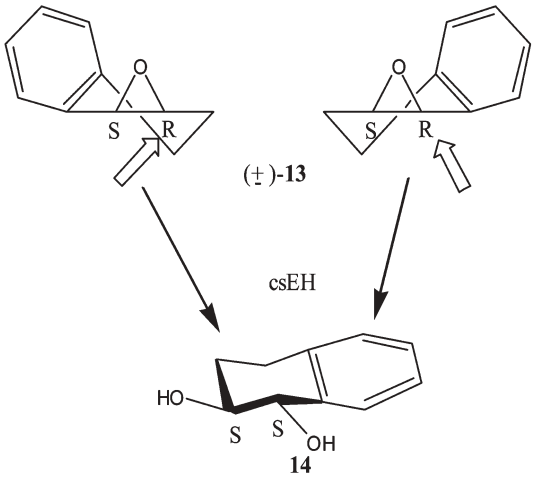

Scheme 5 Hydrolysis pathway for the cress sEH catalyzed hydrolysis of racemic **13**.

α-methylstyrene oxide (**9**) shows that ILs can be efficiently used to perform the hydrolysis of water sensitive epoxides at high substrate concentration (0.1–0.2 M) without the competition of the non-enzymatic process, which generally occurs without any stereoselectivity. Moreover, α-methylstyrene is prone to dimer formation under acidic conditions.

Finally, a comment concerning the sEH catalyzed hydrolysis of epoxide **13** is necessary. Whereas the mammalian enzyme (msEH) hydrolyses epoxide **13** at a negligible rate, csEH more efficiently catalyzes the oxirane ring opening. Moreover, the high product enantioselectivity is associated with a completely non-selective hydrolysis of the two enantiomers of racemic epoxide **13**. In analogy with the hydrolysis of meso epoxides, the oxirane ring opening of both enantiomers occurs selectively at the same configured carbon (in this case the (*R*) carbon) to give the corresponding (*S*,*S*) diol with a very high enantiomeric excess. The csEH catalyzed hydrolysis of this substrate is an enantioconvergent process, arising from the different regioselectivity characterizing the oxirane ring opening of each enantiomer (Scheme 5). The fact that E_P is much larger than E_S (Table 2) illustrates the opposite regioselectivity of csEH for both enantiomers of **13**.

Ultimately, to verify the general applicability of ILs in EH catalyzed reactions we performed the hydrolysis of 4-chlorostyrene oxide (**11**, 0.6–0.7 mmol) using a commercial EH from *Aspergillus niger* (2.5 mg) in "wet" [bmim][PF_6] (6 mL), after addition of 5, 10 or 15% of water. The higher conversion (around 25%) has been obtained in the presence of 15% of water. The percentage of hydrolysis was comparable to that characterizing the reaction in Tris-HCl buffer solution (28%). Enantiomerically pure (*R*) diol **12** was obtained both in buffer solution and in [bmim][PF_6]. In [bmim][PF_6] the epoxide **11** was completely soluble and even higher concentrations may be used, supporting a synthetic application of the enzymatic hydrolysis.

Conclusions

In summary, we have shown that ionic liquids not bearing nucleophilic anions can be used effectively for the enzymatic hydrolysis of epoxides catalyzed by EHs. Soluble EHs from cress and mouse, and microsomal EH from rat are able to catalyzed the hydrolysis of racemic and meso epoxides in several ILs in the presence of water (around 10%). The optimized amount of water has been established. Problems arising from low solubility of epoxides in water or from the tendency of oxirane rings to undergo chemical hydrolysis have been avoided using these new media, resulting in more enantioselective reactions.

Acknowledgements

This was supported by grants from MIUR, NIEHS (# R37-ES02710), NIEHS Center (# P30-ESO5707), and NIH/NIEHS Superfund Basic Research program (# P42-ES04699).

References

1 P. S. Savle, M. J. Lamoreaux, J. F. Berry and R. D. Gandour, *Tetrahedron: Asymmetry*, 1998, **9**, 1843–1846.
2 A. Steinreiber and K. Faber, *Curr. Opin. Biotechnol.*, 2001, **12**, 552–558.
3 A. Archelas and R. Furstoss, *Curr. Opin. Chem. Biol.*, 2001, **5**, 112–119.
4 V. J. Archer, *Tetrahedron*, 1997, **53**, 15617–15662.
5 C. Chiappe, G. Cordoni, G. Lo Moro and C. D. Palese, *Tetrahedron: Asymmetry*, 1998, **9**, 341–350.
6 K. C. Williamson, C. Morisseau, J. E. Maxwell and B. D. Hammock, *Tetrahedron: Asymmetry*, 2000, **11**, 4451–4462.
7 (*a*) W. Kroutil, M. Mischitz and K. Faber, *J. Chem. Soc., Perkin Trans. 1*, 1997, 3629–3636; (*b*) P. Moussou, A. Archelas, R. Baratti and R. Furstoss, *J. Org. Chem.*, 1998, **63**, 3532–3537; (*c*) C. A. G. M. Weijers, A. L. Botes, M. S. Van Dick and M. De Bont, *Tetrahedron: Asymmetry*, 1998, **9**, 467–473; (*d*) C. Morisseau, J. K. Beetham, F. Pinot, S. Debernard, J. W. Mewman and B. D. Hammock, *Arch. Biochem. Biophys.*, 2000, **387**, 321–332.
8 (*a*) A. Stapleton, J. K. Beetham, F. Pinot, J. E. Garbarino, D. R. Rockhold, M. Friedman, B. D. Hammock and W. R. Belknap, *Plant J.*, 1994, **6**, 251–258; (*b*) L. Zhao, E. J. Mathur, D. Weiner, T. Richardson, A. Milan, M. J. Burk, B. Han and J. M. Short, *US Pat.*, 6979733B2, 2005.
9 (*a*) C. Morisseau, H. Nellaiah, A. Archelas, R. Furstoss and J. C. Baratti, *Enzyme Microb. Technol.*, 1997, **20**, 446–452; (*b*) K. M. Manoj, A. Archelas, J. Baratti and R. Furstoss, *Tetrahedron*, 2001, **57**, 695–701; (*c*) N. Monfort, A. Archelas and R. Furstoss, *Tetrahedron*, 2004, **60**, 601–605.
10 (*a*) A. M. P. Koshinen and A. M. Klibanov, *Enzymatic Reactions in Organic Media*, Blackie Academic & Professional, Glasgow, United Kingdom, 1996; (*b*) K. Faber, *Biotransformation in Organic Chemistry*, Springer, Berlin, Germany, 3rd edn, 1997; (*c*) A. M. Klibanov, *Trends Biotechnol.*, 1997, **15**, 97–101.
11 (*a*) W. J. Choi, E. Y. Lee, S. J. Yoon, S.-T. Yang and C. Y. Choi, *J. Biosci. Bioeng.*, 1999, **88**, 339–341; (*b*) M. Cleij, A. Archelas and R. Furstoss, *Tetrahedron: Asymmetry*, 1998, **9**, 1839–1842; (*c*) P.-F. Gong and J.-H. Xu, *Enzyme Microb. Technol.*, 2005, **36**, 252–257.
12 C. Chiappe, E. Leandri, S. Lucchesi, D. Pieraccini, B. D. Hammock and C. Morisseau, *J. Mol. Catal. B: Enzym.*, 2004, **27**, 243–248.
13 (*a*) S. G. Cull, J. D. Holbrey, V. Vargas-More, K. R. Seddon and G. Ley, *J. Biotechnol. Bioeng.*, 2000, **69**, 227; (*b*) R. M. Lau, F. van Rantwijk, K. R. Seddon and R. A. Sheldon, *Org. Lett.*, 2000, **2**, 4189–4191; M. Erbeldinger, A. J. Mesiano and A. Russell, *J. Biotechnol. Prog.*, 2000, **16**, 1131; (*c*) T. Itoh, E. Akasaki, K. Kudo and S. Shirakami, *Chem. Lett.*, 2001, 262; (*d*) S. Park and R. J. Kazlauskas, *J. Org. Chem.*, 2001, **66**, 8395–8401; (*e*) S. H. Schöfer, N. Kaftzik, P. Wassersheid and U. Kragl, *Chem. Commun.*, 2001, 425–426; (*f*) K. W. Kim, B. Song and M. J. Kim, *Org. Lett.*, 2001, **3**, 1507–1509; (*g*) S. J. Nara, J. R. Harjani and M. M. Salunkhe, *Tetrahedron Lett.*, 2002, **43**, 2979–2982; (*h*) P. Lozano, T. De Diego, D. Carrié, M. Vaultier and J. L. Iborra, *J. Mol. Catal. B: Enzym.*, 2003, **21**, 9–13; (*i*) N. Kaftzik,

P. Wassersheid and U. Kragl, *Org. Process Res. Dev.*, 2002, **6**, 553–557; (*j*) J. Howarth, P. James and J. Dai, *Tetrahedron Lett.*, 2001, **42**, 7517–7519; (*k*) J. Howarth, P. James and J. Day, *Tetrahedron*, 2001, **42**, 7517; (*l*) T. Kitazume, Z. Jiang, K. Kasai, Y. Mihara and M. J. Suzuki, *Fluorine Chem.*, 2003, **121**, 205; (*m*) R. P. Gaisberger, M. H. Fechter and H. Griengl, *Tetrahedron: Asymmetry*, 2004, **15**, 2959; (*n*) M. Matsumoto, K. Mochizuki, K. Fukunishi and K. Kondo, *Sep. Purif. Technol.*, 2004, **40**, 97; (*o*) T. Matsuda, Y. Yamagishi, S. Koguchi, N. Iwai and T. Kitazume, *Tetrahedron Lett.*, 2006, **47**, 4619.

14 (*a*) U. Kragl, M. Eckstein and N. Kaftzik, *Curr. Opin. Biotechnol.*, 2002, **13**, 565–571; (*b*) F. van Rantwijk, R. M. Lau and R. A. Sheldon, *Trends Biotechnol.*, 2003, **21**, 131–138; (*c*) S. Park and R. J. Kazlauskas, *Curr. Opin. Biotechnol.*, 2003, **14**, 432–437; (*d*) T. Itoh, E. Akasaki and Y. Nishimura, *Chem. Lett.*, 2002, 154; (*e*) T. Itoh, Y. Nishimura, N. Ouchi and S. Hayase, *J. Mol. Catal. B: Enzym.*, 2003, **26**, 41; (*f*) T. Itoh, S. Han, Y. Matsushita and S. Hayase, *Green Chem.*, 2004, **6**, 437; (*g*) C. Chiappe, L. Neri and D. Pieraccini, *Tetrahedron Lett.*, 2006, **47**, 5089.

15 (*a*) J. D. Holbrey and K. R. Seddon, *Clean Prod. Process.*, 1999, **1**, 223–236; (*b*) M. J. Earle and K. R. Seddon, *Pure Appl. Chem.*, 2000, **72**, 1391–1398; (*c*) T. Welton, *Chem. Rev.*, 1999, **99**, 2071–2083; (*d*) P. Wasserscheid and W. Keim, *Angew. Chem., Int. Ed.*, 2000, **39**, 3773–3789; (*e*) R. A. Sheldon, *Chem. Commun.*, 2001, 2399–2407; (*f*) H. Olivier-Bourbigou and L. Magna, *J. Mol. Catal. A: Chem.*, 2002, **182**, 419–437; (*g*) J. Dupont, R. F. de Souza and P. A. Z. Suarez, *Chem. Rev.*, 2002, **102**, 3667–3692.

16 G. Bellucci, G. Catelani, C. Chiappe and F. D'Andrea, *Tetrahedron Lett.*, 1994, **35**, 8433–8436.

17 (*a*) J. Fuller, R. T. Carlin, H. C. De Long and D. Haworth, *J. Chem. Soc., Chem. Commun.*, 1994, 299–300; (*b*) L. Cammarata, S. G. Kazarian, P. A. Salter and T. Welton, *Phys. Chem. Chem. Phys.*, 2001, 5192–5200; (*c*) C. Chiappe, D. Pieraccini and P. Saullo, *J. Org. Chem.*, 2003, **68**, 6710–6715; (*d*) C. Jork, C. Kristen, D. Pieraccini, A. Stark, C. Chiappe, Y. A. Beste and W. Arlt, *J. Chem. Thermodyn.*, 2005, **37**, 537–558.

18 I. Billard, G. Moutiers, A. El Azzi, C. Gaillard, C. Mariet and J. Lützenkinchen, *Inorg. Chem.*, 2003, **42**, 1726–1733.

19 D. F. Grant, D. H. Stroms and B. D. Hammock, *J. Biol. Chem.*, 1993, **268**, 17628–17633.

20 C.-S. Chen, Y. Fujimoto, G. Girdaukas and C. J. Sih, *J. Am. Chem. Soc.*, 1982, **104**, 7294–7299.

21 (*a*) G. Bellucci, C. Chiappe, L. Conti, F. Marioni and G. Pierini, *J. Org. Chem.*, 1989, **54**, 5978–5983; (*b*) G. Bellucci, C. Chiappe, F. Marioni and M. Benetti, *J. Chem. Soc., Perkin Trans. 1*, 1991, 361–362.

22 S. Clark, *Philos. Trans. R. Soc. London, Ser. B*, 2004, **359**, 1299–1307.

23 R. H. Valivety, P. J. Halling and A. R. Macrae, *Biochem. Biophys. Acta*, 1992, **1118**, 218–222.

24 (*a*) N. Kaftzik, W. Kroutil, K. Faber and U. Kragl, *J. Mol. Catal. A: Chem.*, 2004, **214**, 107–112; (*b*) A. Basso, S. Cantone, P. Linda and C. Ebert, *Green Chem.*, 2005, **7**, 671–676.

25 (*a*) G. Bellucci, I. Capitani, C. Chiappe and F. Marioni, *J. Chem. Soc., Chem. Commun.*, 1989, 1170–1171; (*b*) L. Zhao, B. Han, Z. Huang, M. Miller, H. Huang, D. S. Malashock, Z. Zhu, A. Milan, D. E. Robertson, D. P. Weiner and M. J. Burk, *J. Am. Chem. Soc.*, 2004, **126**, 11156–11157.

26 G Bellucci, C. Chiappe and F. Marioni, *J. Chem. Soc., Perkin Trans. 1*, 1989, 2369–2373.

27 Similar enantiomeric ratios can be calculated from the remaining substrate (ES) or formed product (EP).

28 (*a*) C. Morisseau and B. D. Hammock, *Annu. Rev. Pharmacol. Toxicol.*, 2005, **45**, 311–333; (*b*) K. H. Hopmann and F. Himo, *Chem.–Eur. J.*, 2006, **12**, 6898.

29 G Bellucci, C. Chiappe, A. Cordoni and F. Marioni, *Tetrahedron Lett.*, 1994, **35**, 4219–4222.

Supported choline chloride/urea as a heterogeneous catalyst for chemical fixation of carbon dioxide to cyclic carbonates

Anlian Zhu, Tao Jiang,* Buxing Han,* Jicheng Zhang, Ye Xie and Xiumin Ma

Received 24th August 2006, Accepted 31st October 2006
First published as an Advance Article on the web 13th November 2006
DOI: 10.1039/b612164k

In this work, the catalytic efficiency of ionic liquid (IL) choline chloride/urea supported on molecular sieves for the reactions of CO_2 and epoxides was studied under different conditions. It was demonstrated that this biodegradable and green catalyst is very active and selective, and choline chloride and urea showed a synergetic effect in promoting these reactions. After reaction, the solid catalyst and the products could be separated easily because the IL was insoluble in the products, and the catalyst was reusable. The origin of the high catalytic efficiency and the reaction mechanism were also discussed.

Introduction

Chemical fixation of CO_2 is of great importance in connection with the development of environmentally benign processes, and there are many possibilities for using CO_2 as a safe and cheap C_1 source in organic synthesis.[1–3] The formation of cyclic carbonates *via* cycloaddition of CO_2 with epoxides is one of the attractive routes for chemical fixation of CO_2 because the cyclic carbonates have shown interesting applications as polar aprotic solvents, precursors for polycarbonate materials, and intermediates in organic synthesis.[4,5] Numerous catalysts have been developed to catalyze these reactions, including alkali metal salts (alone[6] or in combination with hydrogen bond donor phenol[7] or supported on solid support[8]), MgO[9] or calcined hydrotalcites,[10] Schiff base,[11] transition-metal complexes,[12–15] ion-exchange resins,[16] and ionic liquids (ILs).[17] However, in most cases, organic solvents are used in the reactions or work-up procedures and the products are commonly isolated from the reaction systems by distillation. Recently, supported ILs[18,19] were reported to be effective catalysts for cyclic carbonate synthesis, but the procedure to prepare catalyst is relatively complicated. In addition, large excess of CO_2 was used in many protocols, which in fact acts as the reactant as well as co-solvent. Therefore, it is still desirable to explore a highly efficient, easily separating and recyclable catalyst system for this transformation.

In recent years, utilization of ILs in chemical synthesis has received great attention due to their unusual properties compared with traditional molecular solvents, such as undetectable vapor pressure, wide liquid temperature range, special solubility for many organic or inorganic compounds, and the feasibility for designing.[20] Besides the traditional imidazolium-based ILs, many functional ILs have also been synthesized and utilized in catalysis,[21] adsorbing acid gases,[22] and processing of cellulose[23] *etc.* However, the toxicology of ILs remains unclear and further studies are required to assess their sustainability.[24,25] Avalos *et al.*[26] believed that green alternatives for traditional ILs would be composed of biodegradable constituents and exhibit high thermal and chemical stabilities. One of these is the deep eutectic mixture based on choline chloride (CH, Scheme 1).[27] The CH/urea (Scheme 1) eutectic mixture has been used as the solvent and the template for the synthesis of microporous crystalline zeolites.[28] Choline chloride plus Lewis acid has been used as the catalyst for Diels–Alder reactions,[29] Fischer indole annulation[30] and selective acylation of primary hydroxyl groups in cellulose.[31] The mixture of CH with urea showed a deep eutectic effect when the ratio of CH to urea is 1 : 2, and its melting point (12 °C) is much lower than those of CH and urea due to the hydrogen bonding between the halide anion and urea. The special composition and interaction led to very poor solubility of this IL in polar aprotic solvent and apolar solvents. Recently, the bifunctional catalyst based on urea has found great potential in organic synthesis due to its strong ability to form hydrogen bonds,[32] and urea and other functional catalytic centers show a synergetic effect for some reactions.

CH/urea is an IL, and both of the components, CH and urea, have the ability to form hydrogen bonds. Therefore, the IL may exhibit a synergetic effect on catalytic activity for some reactions. To our knowledge, this cleaner IL has not been used as catalyst or solvent in organic synthesis. In present work, we carried out the cycloaddition reactions of epoxides with CO_2 promoted by CH/urea supported on molecular sieves. The results show that the IL is very active and selective for the reactions, and the reactions can be conducted with little excess of CO_2, which is economically favorable and the reactions can be truly solvent free processes. The insoluble nature of the IL in the reactants and products makes separation of product

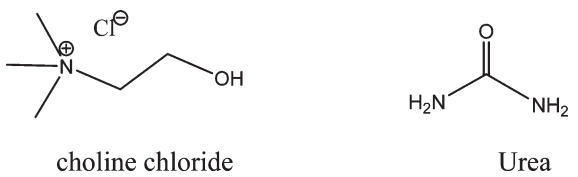

Scheme 1 The structures of choline chloride and urea.

Beijing National Laboratory for Molecular Sciences (BNLMS), Centre for Molecular Science, Institute of Chemistry, Chinese Academy of Sciences, Beijing, 100080, China. E-mail: Jiangt@iccas.ac.cn; Hanbx@iccas.ac.cn; Fax: 86-10-62562821

much easier. In addition, the catalyst can be prepared by simple impregnation.

Results and discussion

The activity of different catalysts was tested using the reaction of propylene oxide (PO) and CO_2, and the results are summarized in Table 1. Obviously, urea or the molecular sieves alone showed little activity for this reaction (entries 1, 4). Choline chloride (CH) could catalyze this reaction effectively (entry 2), but some by-products were produced, and our experiments showed that the resulting mixture was very dark and the yield was only 85% after 10 h. It is interesting that combination of choline chloride and urea (CHCl·2urea) led to much higher conversion with 99% yield (entry 3), and that the IL immobilized on molecular sieves also gave satisfactory results in relatively short reaction time (entry 5), and the separation procedure was very simple. The effect of the amount of CO_2 was also studied using the supported catalyst. The difference in reaction rate was not considerable as the ratio of CO_2 to PO was changed in the range of 1.14–1.86 (entries 7–10). In all of these reaction conditions, quantitative conversion of PO with high cyclic carbonates selectivity was reached. However, when the ratio was increased to 2.45, the reaction was sluggish and 9 h were required to complete the reaction (entries 5, 6). Decrease in catalyst amount also reduced the reaction rate, but reaction selectivity was not changed (entry 11). Fig. 1 illustrates the effect of temperature on this reaction in the range of 80–130 °C. The results suggested that the optimized reaction temperature was 110 °C.

Table 1 Coupling of CO_2 and propylene oxide catalyzed by different catalysts under various conditions[a]

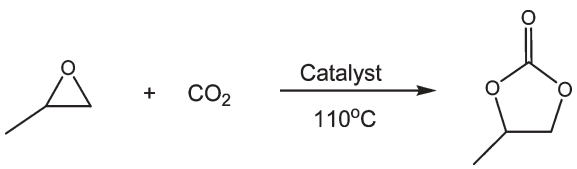

Entry	Catalysts	Ratio of CO_2/substrate	Reaction time/h	Yields[b] (%)
1	Urea	2.42	14	9
2	CH	2.45	10	85
3	IL (CH/urea)	2.45	10	99
4	Molecular sieves	2.29	10	8
5	SIL[c]	2.45	9	99
6	SIL[c]	2.47	5	75
7	SIL[c]	1.86	4	99
8	SIL[c]	1.67	4	99
9	SIL[c]	1.49	5	98
10	SIL[c]	1.14	5	98
11	SIL[c,d]	1.74	6	96
12	SIL[c] (2nd)	1.59	5	98
13	SIL[c] (3rd)	1.90	5	99
14	SIL[c] (4th)	1.42	5	97
15	SIL[c] (5th)	1.56	5	98

[a] Typical reaction conditions: a stainless steel reactor of 11 ml, 41 mmol PO with 1% catalyst, all the reactions were conducted at 110 °C. [b] The yields was calculated from the ratio of PC to PO, the amount of PC was determined from GC using acetophenone as the internal standard. [c] SIL refers to the IL supported on molecular sieves. [d] The catalyst was 0.5% of PO.

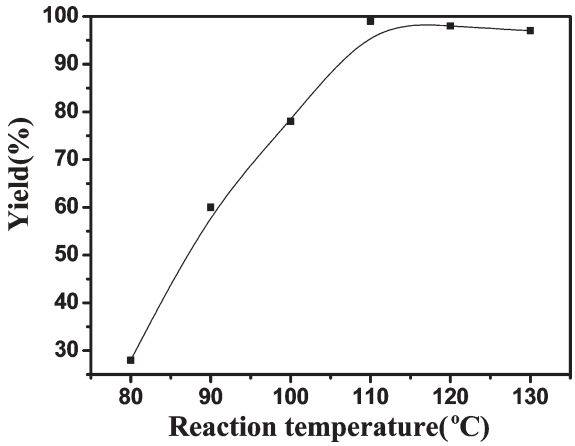

Fig. 1 The dependence of yield of PC on reaction temperature (other reaction conditions were the same as that of entry 8 in Table 1).

The reusability of the supported catalyst was also studied with the catalyst used in entry 8 and the results are also summarized in Table 1 (entries 11–15). Obviously, the catalyst did not lose catalytic activity after 5 runs.

The above results indicated that CH/urea immobilized on molecular sieves was an effective catalyst for the cyclic addition reaction of propylene oxide and CO_2 in solvent free conditions. Under the optimized reaction conditions, the reactions of other epoxides with CO_2 were also examined and the results are summarized in Table 2. All the reactions could be complete in less than 5 h except cyclohexene oxide, which needs 22 h to reach 80% yield due to the higher hindrance originated from the two rings. The selectivity of the reactions to the cyclic carbonates was almost 100%, and epichlorohydrin (entry 2), for which the selectivity was 92%.

It has been suggested by Huang and Shi[7] that the chlorine ions can open the epoxy ring when the ring was activated through the forming of hydrogen bonding with phenol. In our catalysis systems, the co-existence of chlorine and the hydrogen bonding donors have shown the synergetic effect on the reactions. The possible mechanism is suggested and shown schematically in Scheme 2. The chlorine anion (combining with two urea molecules[27b]) of the IL opens the epoxy ring, which is activated by the choline cation through hydrogen bonding, to give the intermediate. Then, the intermediate further reacts with CO_2 to form the corresponding cyclic carbonate and regenerate the catalyst (Scheme 2). The synergistic effect of the cation and the anion of the IL is perhaps the main reason for the high catalytic activity of the catalyst. The effect of urea can be attributed to its interaction with chloride anion. The existence of urea decreases the strength of interaction between the chlorine anion and epoxides, which leads to higher selectivity.

Conclusions

In conclusion, the greener and biodegradable IL CH/urea supported on molecular sieves can efficiently catalyze the reactions of epoxides and CO_2 to form cyclic carbonates with high conversion and selectivity without any co-solvents. The

Table 2 Reactions of different epoxides with CO_2 in the presence of IL/molecular sieves[a]

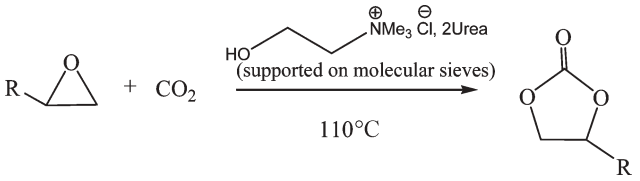

Entry	Epoxides	Products	Reaction time/h	Yield (%)
1	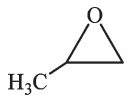	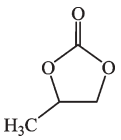	5	99
2	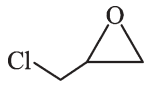	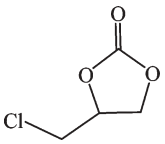	4	92
3	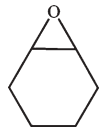	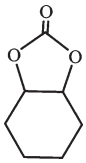	22	80
4	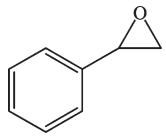	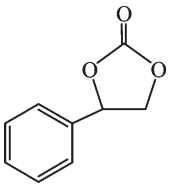	5	95
5	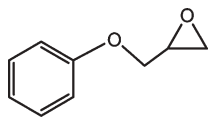	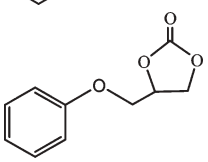	3	99

[a] Reaction conditions: epoxide 41 mmol; (IL on molecular sieves)/epoxide = 1 mol%; molar ratio of CO_2: epoxide = 1.5–1.87); reaction temperature 110 °C.

reactions can be made complete with a little excess quantity of CO_2. The catalyst is easy to prepare and can be reused at least five times without noticeable decrease in activity. This greener catalyst has potential application for synthesizing cyclic carbonates from CO_2 and epoxides.

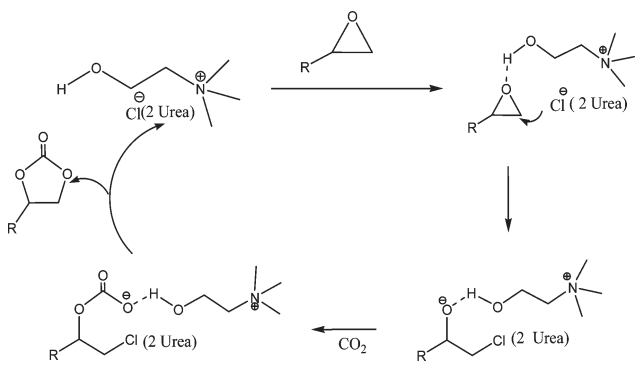

Scheme 2 The plausible reaction mechanism for the cycloaddition of epoxides with CO_2 catalyzed by choline chloride/urea.

Experimental

Materials

CO_2 was supplied by Beijing Analytical Instrument Factory with a purity of 99.995%. Propylene oxide, epichlorohydrin, choline chloride, and urea were A.R. grade and produced by Beijing Chemical Plant. Other epoxides were purchased from ACROS ORGANICS. Molecular sieves (Si/Al = 1 : 1) with a porous diameter of 6.7 nm were employed, and the surface area and pore volume (determined by nitrogen adsorption) were 520 $m^2\ g^{-1}$ and 0.87 $cm^3\ g^{-1}$, respectively. Styrene oxide was purified by distillation and other chemicals were used as received.

Preparation of catalyst

The IL CH/urea was prepared according to the procedures reported in literature[27b] simply by heating mixture of choline chloride and urea with a molar ratio of 1 : 2 at 80 °C until a homogeneous liquid was formed. The immobilization of the IL was performed by impregnation of the molecular sieves in the IL using methanol as the solvent at room temperature under stirring. The weight ratio of the IL and methanol was 1 : 6, and that of the molecular sieves to the IL was 2 : 1. The methanol was evaporated under vacuum to obtain the supported white powder catalyst.

Procedures for cycloadditions

All the reactions were conducted in an 11 ml stainless steel reactor equipped with a magnetic stirrer and an electrical heater. The reactor was first loaded with suitable amounts of epoxide and catalyst and then sealed. After the temperature of the reactor reached the required value, CO_2 was charged into the reactor by a sample bomb of 30 ml. The amount of CO_2 loaded was known by the mass difference of the sample bomb before and after charging CO_2. A Mettler MP1200 balance with the accuracy of ± 0.001 g was used for the mass determination, and minimum amount of CO_2 charged in each reaction was 2.3 g in our experiments. Therefore, the accuracy was sufficient. The reaction was monitored by the pressure variation. The pressure gauge was composed of a pressure transducer (FOXBORO/ICT Model 93) and an indicator. Its accuracy was ± 0.025 MPa in the pressure range 0–20 MPa. After the pressure became constant, the reactor was rapidly cooled with ice water and depressurized by releasing the gas slowly through an absorbing tube (which was also put in the ice bath) containing *N*,*N*-dimethyl formamide to capture the reactants and products entrained by CO_2. After depressurization was completed the reactor was opened and *N*,*N*-dimethyl formamide in the absorbing tube and internal standard acetophenone were added into the reactor. The catalyst was separated from the reaction mixture through filtration. The reaction mixture for the reaction of CO_2 and PO was analyzed with a gas chromatography (GC, Agilent 4890D) equipped with a flame-ionized detector using acetophenone as the internal standard. The purity and structure of the product

obtained at some typical experimental conditions were also checked by NMR and GC-MS methods, and no by-product was detected. The products of other epoxides were analyzed at room temperature on a Bruker 400 MHz NMR spectrometer using $CDCl_3$ as the solvent.

Acknowledgements

We sincerely acknowledge the financial supports from National Natural Science Foundation of China (20332030, 20473105).

References

1 D. H. Gibson, *Chem. Rev.*, 1996, **96**, 2063.
2 M. Shi and Y. M. Shen, *Curr. Org. Chem.*, 2003, **7**, 37.
3 C. S. Song, *Catal. Today*, 2006, **115**, 2.
4 P. G. Jessop, T. Ikariya and R. Noyori, *Chem. Rev.*, 1999, **99**, 475.
5 S. J. Zhang, Y. H. Chen, F. W. Li, X. M. Lu, W. B. Dai and R. Mori, *Catal. Today*, 2006, **115**, 61.
6 M. Kihara, N. hara and T. Endo, *J. Org. Chem.*, 1993, **58**, 6198.
7 J.-W. Huang and M. Shi, *J. Org. Chem.*, 2003, **68**, 6705.
8 T. Zhao, Y. Han and Y. Sun, *Phys. Chem. Chem. Phys.*, 1999, **12**, 3047.
9 T. Yano, H. Matsui, T. Koike, H. Ishiguro, H. Fujihara, M. Yoshihara and T. Maeshima, *Chem. Commun.*, 1997, 1129.
10 K. Yamaguchi, K. Ebitani, T. Yoshida, H. Yoshida and K. Kaneda, *J. Am. Chem. Soc.*, 1999, **121**, 4526.
11 (*a*) T. Aida and S. Inoue, *J. Am. Chem. Soc.*, 1983, **105**, 1304; (*b*) Y. M. Shen, W. L. Duan and M. Shi, *Eur. J. Org. Chem.*, 2004, **14**, 3080.
12 W. N. Sit, S. M. Ng, K. Y. Kwong and C. P. Lau, *J. Org. Chem.*, 2005, **70**, 8583.
13 J. L. Jiang, F. Gao, R. Hua and X. Qiu, *J. Org. Chem.*, 2005, **70**, 381.
14 H. S. Kim, J. J. Kim, S. D. Lee, M. S. Lah, D. Moon and H. G. Jang, *Chem. Eur. J.*, 2003, **9**, 678.
15 S. D. Allen, D. R. Moore, E. B. Lobkovsky and G. W. Coates, *J. Am. Chem. Soc.*, 2002, **124**, 14284.
16 Y. Du, F. Cai, D.-L. Kong and L.-N. He, *Green Chem.*, 2005, **7**, 518.
17 (*a*) H. Kawanami, A. Sasaki, K. Matsui and Y. Ikushima, *Chem. Commun.*, 2003, 896; (*b*) H. Z. Yang, Y. L. Gu, Y. Q. Deng and F. Shi, *Chem. Commun.*, 2002, 274; (*c*) H. B. Xie, S. H. Li and S. B. Zhang, *J. Mol. Catal. A: Chem.*, 2006, **250**, 30; (*d*) H. B. Xie, H. F. Duan, S. H. Li and S. B. Zhang, *New J. Chem.*, 2005, **29**, 1199.
18 L.-F. Xiao, F.-W. Li, J.-J. Peng and C.-G. Xia, *J. Mol. Catal. A: Chem.*, 2006, **253**, 265.
19 T. Takahashi, T. Watahiki, S. Kitazume, H. Yasuda and T. Sakakura, *Chem. Commun.*, 2006, 1664.
20 (*a*) R. Sheldon, *Chem. Commun.*, 2001, 2399; (*b*) J. Dupont, R. F. de Souza and P. A. Z. Auarez, *Chem. Rev.*, 2002, **102**, 3667.
21 (*a*) A. L. Zhu, T. Jiang, D. Wang, B. X. Han, L. Liu, J. Huang, J. C. Zhang and D. H. Sun, *Green Chem.*, 2005, **7**, 514; (*b*) S. Z. Luo, X. L. Mi, L. Zhang, S. Liu, H. Xu and J. P. Cheng, *Angew. Chem., Int. Ed.*, 2006, **45**, 3093.
22 W. Wu, B. Han, H. Gao, Z. Liu, T. Jiang and J. Huang, *Angew. Chem., Int. Ed.*, 2004, **43**, 2415.
23 (*a*) R. P. Swatloski, S. K. Spear, J. D. Holbrey and R. D. Rogers, *J. Am. Chem. Soc.*, 2002, **124**, 4974; (*b*) R. C. Remsing, R. P. Swatloski and G. Moyana, *Chem. Commun.*, 2006, 1271.
24 (*a*) M. T. Garcia, N. Gathergood and P. J. Scammells, *Green Chem.*, 2005, **7**, 9; (*b*) R. P. Swatloski, J. D. Holbrey and R. D. Rogers, *Green Chem.*, 2003, **5**, 361; (*c*) B. Jastorff, R. Störmann, J. Ranke, K. Mölter, F. Stock, B. Oberheitmann, W. Hoffmann, J. Hoffmann, M. Nüchter, B. Ondruschka and J. Filser, *Green Chem.*, 2003, **5**, 136.
25 A recent study points to potential damage by ionic liquids to the aquatic environment, even at lower exposure concentrations than other organic pollutants; see: C. Pretti, C. Chiappe, D. Pieraccini, M. Gregori, F. Abramo, G. Monni and L. Intorre, *Green Chem.*, 2006, **8**, 238.
26 M. Avalos, R. Babiano, P. Cintas, J. L. Jiménez and J. C. Palacios, *Angew. Chem., Int. Ed.*, 2006, **45**, 3904.
27 (*a*) A. P. Abbott, G. Capper, D. L. Davies, H. L. Munro, R. K. Rasheed and V. Tambyrajah, *Chem. Commun.*, 2001, 2010; (*b*) A. P. Abbott, G. Capper, D. L. Davies, R. K. Rasheed and V. Tambyrajah, *Chem. Commun.*, 2003, 70; (*c*) A. P. Abbott, G. Capper, D. L. Davies and R. K. Rasheed, *Chem. Eur. J.*, 2005, **10**, 3769; (*d*) A. P. Abbott, D. Boothby, G. Capper, D. L. Davies and R. K. Rasheed, *J. Am. Chem. Soc.*, 2004, **126**, 9142.
28 E. R. Cooper, C. D. Andrews, P. S. Wheatley, P. B. Webb, P. Wormald and R. E. Morris, *Nature*, 2004, **430**, 1012.
29 A. P. Abbott, G. Capper, D. L. Davies, R. K. Rasheed and V. Tambyrajah, *Green Chem.*, 2002, **4**, 24.
30 R. C. Morales, V. Tambyrajah, P. R. Jenkins, D. L. Davies and A. P. Abbott, *Chem. Commun.*, 2004, 158.
31 A. P. Abbott, T. J. Bell, S. Handa and B. Stoddart, *Green Chem.*, 2005, **7**, 705.
32 (*a*) D. Menche, J. Hassfeld, J. Li, G. Menche, A. Ritter and S. Rudolph, *Org. Lett.*, 2006, **8**, 741; (*b*) L. Shi, X. W. Wang, C. A. Sandoval, M. X. Li, Q. Y. Qi, Z. T. Li and K. L. Ding, *Angew. Chem., Int. Ed.*, 2006, **45**, 4108; (*c*) S. B. Tsogoeva, D. A. Yalalov, M. J. Hateley, C. Weckbecker and K. Huthmacher, *Eur. J. Org. Chem.*, 2005, **70**, 4995; (*d*) M. S. Taylor and E. N. Jacobsen, *Angew. Chem., Int. Ed.*, 2006, **45**, 1520.

Improved methanol tolerance during Novozym435-mediated methanolysis of SODD for biodiesel production

Wei Du, Li Wang and Dehua Liu

Received 20th September 2006, Accepted 30th October 2006
First published as an Advance Article on the web 14th November 2006
DOI: 10.1039/b613704k

SODD is proposed here as a sort of feedstock for biodiesel production. During lipase-catalyzed alcoholysis of soybean oil deodorizer distillate (SODD) for biodiesel production, lipase expressed higher tolerance to methanol compared to that with refined soybean oils as the feedstock, and much a faster reaction rate could be obtained. Further study showed that free fatty acid contained in SODD was the major factor contributing to the improvement of lipase tolerance to methanol. It was further demonstrated that the improved methanol tolerance was related to the hydrophobicity of the reactants (log $P_{reactant}$), the lower the |log $P_{reactant}$ − log $P_{interface}$|, the higher the lipase tolerance to methanol that could be achieved. The highest biodiesel yield of 95% could be achieved by adding a 3 Å molecular sieve as an adsorbent into the system to control the by-product water.

Introduction

Biodiesel is gaining more and more importance as an attractive fuel due to the depleting fossil fuel resources. Chemically, biodiesel is monoalkyl esters of long chain fatty acids derived from renewable feed stock like vegetable oils and animal fats. Generally speaking, biodiesel can be produced by transesterification, in which oil or fat is reacted with a monohydric alcohol in presence of a catalyst. Utilization of lipase as a catalyst for biodiesel production is a clean technology due to its non-toxic and environmentally friendly nature and requires mild operating conditions compared with chemical methods.[1–5] However, there are two bottlenecks in enzymatic approaches for biodiesel production: one is the relatively high cost of lipase and its short operational life caused by the negative effects of excessive methanol and by-product glycerol.[6–8] Some efforts have been made to reduce the negative effect and some satisfactory results have been achieved.[9–12]

Another bottleneck for lipase-catalyzed biodiesel production is the high cost of the feedstock. Producing biodiesel from vegetable oils and greases directly is obviously not competitive. Some waste oils have been tried for biodiesel production and it has been found that waste oils usually gave much lower biodiesel yield compared to that with refined oils as the feedstock, which was thought to be caused by other ingredients, apart from triglycerides, contained in waste oils.[13–16]

Soybean oil deodorizer distillate (SODD) is an important by-product in the refining process of soybean oil, and the quantity of SODD accounts for 0.3–0.5% of the oil feedstock. SODD usually contains tocopherols (3–12%) (mainly γ-isomer), triglycerides (45–55%), free fatty acids (FFA, 25–35%), sterols (7–8%), hydrocarbons and other impurities. Traditionally SODD is adopted as the feedstock for high purity production of sterols and tocopherols.[17–19] Since SODD contains quite a large number of ingredients (TAG and FFA) which can be transformed to biodiesel, it is also very promising for the production of biodiesel. However, almost no related research on lipase-catalyzed transesterification of SODD for biodiesel production was reported. In this paper, SODD has been adopted as the feedstock for biodiesel production and the role of FFA contained in SODD on lipase-mediated methanolysis has been studied systematically.

Department of Chemical Engineering, Tsinghua University, Beijing, 100084, China

Materials and methods

Materials

Novozym435 (from *Candida antarctica*) was purchased from Novo Nordisk (Denmark). SODD (triglyceride: 60%, FFA: 28%, vitamin E: 6%) was obtained locally. Palmitic acid methyl ester, stearic acid methyl ester, oleic acid methyl ester, linoleic acid methyl ester, linolenic acid methyl ester, arachidic acid methyl ester, eicosane acid methyl ester, docosane acid methyl ester and heptadecanoic acid methyl ester were bought from Sigma and were chromatographically pure. All other chemicals were obtained commercially and were of analytical grade.

Methanolysis of SODD for biodiesel production

Methanolysis reactions were carried out in a 50 ml shaking flask, maintained in a rotary shaker at 150 rpm and the temperature was kept at 40 °C. Samples (100 μL) were taken from the reaction mixture at specified times and centrifuged to obtain the upper layer. 5 μL of the upper layer, 300 μL of heptadecanoic acid methyl ester (which served as the internal standard) and 300 μL ethanol (which served as solvent) were precisely measured and mixed thoroughly for gas chromatographic analysis.

Biodiesel yield (ME%) was calculated as the percentage of the actual amount of methyl ester detected in the reaction process divided by the theoretical quantity of methyl ester.

GC method for ME analysis

Biodiesel yield in the reaction mixture was analyzed on a GC-14B gas chromatograph equipped with FFAP capillary column (0.32 mm × 25 m) and FID detector. The column temperature was kept at 150 °C for 0.5 min, raised to 250 °C at 15 °C min^{-1} and maintained at this temperature for 6 min. The temperatures of the injector and detector were set at 245 °C and 250 °C, respectively.

Results

Effect of methanol to SODD molar ratio on lipase-catalyzed methanolysis

With some triglycerides, such as soybean oils, as the feedstock for biodiesel production, it has been reported that more than 1.5 molar methanol present in the reaction system would lead to serious loss of lipase activity.[1–9] However, during Novozym435-catalyzed methanolysis of SODD for biodiesel production, it was been observed that lipase could still maintain high activity even with more than 3 molar methanol (equivalent to the SODD molar value) existing in the system. When the ratio of methanol to SODD was 3.6, a biodiesel yield of 61% could be achieved, as shown in Fig. 1.

The stability of the lipase was studied further, and during this study the lipase was reused directly for the next batch reaction. And as can be seen from Fig. 2 there was almost no loss in lipase activity detected even after being reused for 10 batches.

It has been well demonstrated that lipase would lose its activity in the presence of too much methanol existing in a solvent-free system and lipase expressed relatively poor stability.[2–10] However, the above study showed that lipase could not only maintain relatively high activity, but also better stability in catalyzing SODD methanolysis for biodiesel production, even with 3 molar methanol present in the system.

Some ingredients contained in SODD might contribute to the improvement of lipase tolerance to methanol as well as the enhancement of lipase stability. Apart from triglycerides, SODD contains some other ingredients, such as FFA, vitamin E and sterols (the quantity of these ingredients has been measured and stated in the Materials and methods). The effect of vitamin E and sterols on lipase-catalyzed methanolysis of refined soybean oils was further studied and the possibility of these two minor ingredients contributing to the above mentioned improvement could be ruled out (detailed data not shown here). Since the major difference between refined soybean oil and SODD is the relatively high content of FFA, the effect of free fatty acid on lipase-catalyzed methanolysis was further explored.

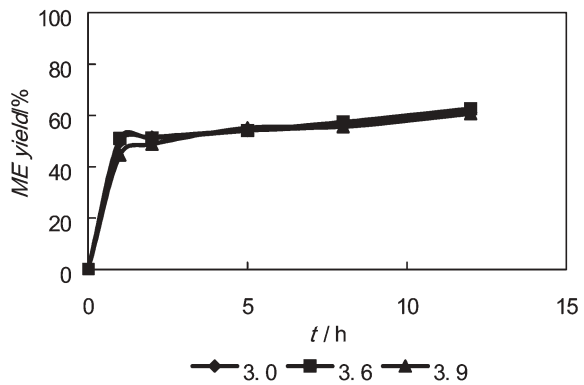

Fig. 1 Effect of methanol to SODD molar ratio on lipase-catalyzed methanolysis. *Reaction conditions*: 4% Novozym435 based on SODD weight, 40 °C, 150 rpm.

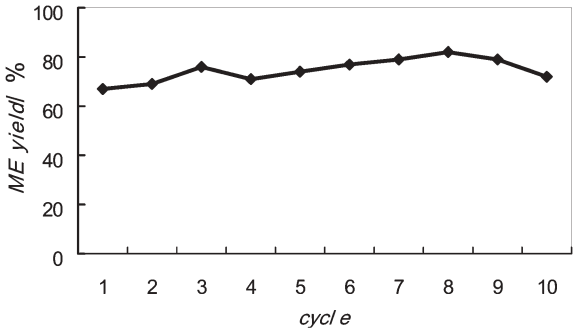

Fig. 2 Operational stability of the lipase. *Reaction conditions*: 4% molar ratio of methanol to SODD 3, 4% Novozym435 based on SODD weight, 40 °C, 150 rpm, each cycle 24 h.

Effect of FFA on lipase tolerance to methanol

To study the effect of FFA on the tolerance of lipase to methanol, different amounts of oleic acid were added into refined soybean oils (keeping the total weight as a constant, 10 g). Within the range studied (FFA amount ranging from 5% to 100%, based on refined soybean oil weight), it was noticed that faster reaction rates could be obtained with higher FFA content existing in the system, which was in agreement with some other reports.[15,16] What's more, it was also observed that the more FFA that was contained in the feedstock, the higher the lipase tolerance to methanol (Fig. 3).

It seemed that FFA did have some relationship with lipase tolerance to methanol (the lipase tolerance to methanol was defined as the critical molar ratio of methanol to oil at which lipase activity beginning to decrease). A complementary study showed that lipase tolerance to methanol had an almost linear relationship to FFA content (Fig. 4).

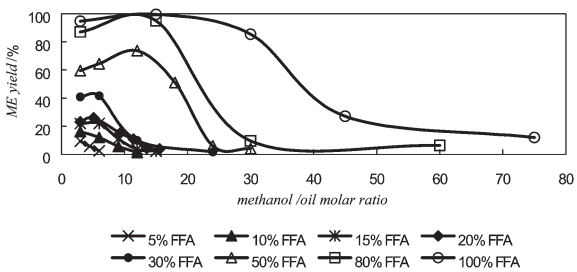

Fig. 3 Effect of FFA on lipase-catalyzed methanolysis for biodiesel production. *Reaction conditions*: 2% Novozym 435 based on oil weight, 40 °C, 150 rpm, 11 h

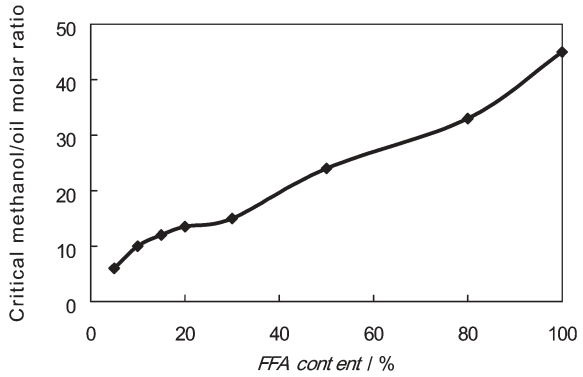

Fig. 4 The relationship of FFA with critical molar ratio of methanol to oil. *Reaction conditions*: 2% Novozym435, 40 °C, 150 rpm.

Effect of adsorbents on the methanolysis of SODD

Since there is some FFA contained in SODD, water will be produced as one of the by-products, and too much water will not only influence the equilibrium, but also might make the lipase aggregating, leading to a loss in lipase activity. Therefore adsorbents were adopted to adsorb the by-product water during the reaction process.

A 3 Å molecular sieve was introduced to adsorb the by-product water produced from the esterification of FFA with methanol. It was found that adding 10 fold of a 3 Å molecular sieve (based on the maximum water calculated from FFA) into the system from the beginning of the reaction, the highest biodiesel yield of 95% could be achieved (Fig. 5).

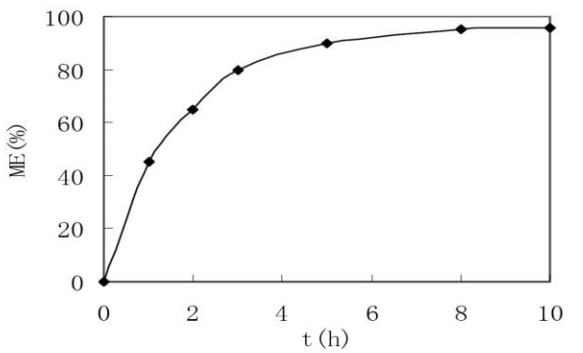

Fig. 5 Biodiesel production with 3 Å molecular sieve as the adsorbent. *Reaction conditions*: 4% Novozym435 based on SODD weight, 40 °C, 150 rpm, molar ratio of methanol to SODD 3.9, 10 fold 3 Å molecular sieve based on the maximal water weight (calculated from FFA).

Discussion

It has been well demonstrated that excessive methanol would deactivate the lipase seriously during lipase-mediated methanolysis of renewable oils for biodiesel production in solvent-free systems. However, in this study it was found that with SODD as the oil feedstock for biodiesel production, a higher lipase tolerance to methanol could be observed, and further study showed that this was due to the existence of FFA contained in SODD.

Table 1 Log *P* value of different ingredients involved in SODD methanolysis

	Water	Methanol	Oleic acid	Trioleicglyceride
Log *P*	−1.44	−0.75	7.87	25.43

Lanne reported that there was some influence of the log *P* value of the reaction medium on the reaction rate (log *P* is defined as the logarithm of the partition coefficient in an octanol–water two-phase system). They also found that the lower the $|\log P_{\text{interface}} - \log P_{\text{substrate}}|$ or the higher the $|\log P_{\text{continuous phase}} - \log P_{\text{substrate}}|$ was, the easier/faster the reaction proceeded.[20,21] In this study, lipase-catalyzed methanolysis of SODD for biodiesel production was carried out in a solvent-free system, and the log *P* of reactants was proposed here to analyze the improved lipase tolerance to methanol. Since the reactants include triglycerides, FFA and methanol, therefore the log P_{reactant} was calculated according to the semiempirical formula: $\log P_{\text{mixture}} = x_1 \log P_1 + x_2 \log P_2 + x_3 \log P_3$, where x_1, x_2 and x_3 stand for the molar percentage of each reactant.[20] Here x_1, x_2 and x_3 stand for the molar ratio of methanol, free fatty acid and triglycerides, respectively. The interface of the lipase was supposed to be a layer of water, therefore the log *P* value of the interface was supposed to be that of water, and the log *P* values of different ingredients are listed in Table 1.

It was demonstrated above that the more FFA that was contained in the oils, the higher the lipase tolerance to methanol (Fig. 3 and Fig. 4). Table 2 gives the log *P* values of reactant with varied amounts of FFA, and the values of $|\log P_{\text{interface}} - \log P_{\text{reactant}}|$ were also calculated accordingly. It could be seen that the higher the content of FFA contained in the feedstock for biodiesel production, the lower the value of $|\log P_{\text{interface}} - \log P_{\text{reactants}}|$ calculated. This was in agreement with our above research, where more FFA contained in feedstock not only resulted in a faster reaction rate, but also higher tolerance of the lipase to methanol.

Theoretically speaking, solid acid also can be used as the catalyst for biodiesel production with oil feedstocks containing much FFA. However, there are some obvious disadvantages associated with using a solid acid as the catalyst compared to lipase as the catalyst for transformation of such oils. Firstly, with solid acid as the catalyst for biodiesel production, a much higher temperature is needed, usually more than 65 °C, and therefore more energy is required. Secondly, since 65 °C is above the boiling point of methanol, methanol vapor will be formed during the process, so the reaction has to be carried out

Table 2 Effect of FFA on the value of $|\log P_{\text{interface}} - \log P_{\text{reactants}}|$

FFA%	x_{methanol}	x_{TGA}	$x_{\text{oleic acid}}$	$\log P_{\text{reactants}}$	$\lvert\log P_{\text{interface}} - \log P_{\text{reactants}}\rvert$
0	0.75	0.25	0	5.79	7.23
25	0.67	0.17	0.17	5.02	6.46
50	0.6	0.1	0.3	4.42	5.86
75	0.55	0.04	0.41	3.83	5.27
100	0.5	0	0.5	3.43	4.87

under some pressure and this will impose much higher requirements for the facilities. Thirdly, acid catalyst will have some corrosive influence, therefore much higher requirements are needed for the reactor and other related facilities. Fourthly, with solid acid catalyst, too much methanol is needed for the transformation. Usually, if the molar ratio of methanol to oils is over 10, then much higher energy and efforts are needed to recover the surplus methanol. Finally, in order to reuse the solid acid catalyst, some complicated regeneration process is needed. However, when lipase is used as the catalyst, lipase can be reused directly without any pretreatment and regeneration process, which can really make the whole process green.

Conclusion

SODD was adopted as the feedstock for lipase-mediated methanolysis for biodiesel production in a solvent-free system and it was demonstrated that FFA contained in SODD contributed to the improved methanol tolerance of the lipase. Further studies showed that the lower the value of $|\log P_{\text{reactant}} - \log P_{\text{interface}}|$, the higher the lipase tolerance to methanol. Much higher biodiesel yield could be achieved when an adsorbent 3 Å molecular sieve was introduced into the reaction system to adsorb the by-product water produced from the esterification of FFA and methanol.

References

1 B. Selmi and D. Thomas, Immobilized lipase-catalyzed ethanolysis of sunflower oil in a solvent-free medium, *J. Am. Oil Chem. Soc.*, 1998, **75**(6), 691–695.
2 W. Du, Y. Y. Xu, D. H. Liu and Z. B. Li, Study on acyl migration in immobilized lipozyme TL-catalyzed transesterification of soybean oil for biodiesel production, *J. Mol. Catal. B: Enzym.*, 2005, **37**(1–6), 68–71.
3 M. Iso, B. Chen, M. Eguchi, T. Kudo and S. Shrestha, Production of biodiesel fuel from triglycerides and alcohol using immobilized lipase, *J. Mol. Catal. B: Enzym.*, 2001, **16**(1), 53–58.
4 J. S. Yang, G. J. Jeon, B. K. Hur and J. W. Yang, Enzymatic methanolysis of castor oil for the synthesis of methyl ricinoleate in a solvent-free medium, *J. Microbiol. Biotechnol.*, 2005, **15**(6), 1183–1188.
5 Ö. Köse, M. Tüter and H. A. Aksoy, Immobilized *Candida antarctica* lipase-catalyzed alcoholysis of cotton seed oil in a solvent-free medium, *Bioresour. Technol.*, 2002, **83**(2), 125–129.
6 Y. Watanabe, Y. Shimada, A. Sugihara, H. Noda, H. Fukuda and Y. Tominaga, Continuous production of biodiesel fuel from vegetable oil using immobilized *Candida antarctica* lipase, *J. Am. Oil Chem. Soc.*, 2000, **77**(4), 355–360.
7 M. Soumanou Mohamed and T. Bornscheuer Uwe, Improvement in lipase-catalyzed synthesis of fatty acid methyl esters from sunflower oil, *Enzyme Microb. Technol.*, 2003, **33**, 97–103.
8 Y. Watanabe, Y. Shimada, A. Sugihara and Y. Tominaga, Enzymatic conversion of waste edible oil to biodiesel fuel in a fixed-bed bioreactor, *J. Am. Oil Chem. Soc.*, 2001, **78**(7), 703–707.
9 Y. Y. Xu, W. Du and D. H. Liu, Study on the kinetics of enzymatic interesterification of triglycerides for biodiesel production with methyl acetate as the acyl acceptor, *J. Mol. Catal. B: Enzym.*, 2005, **32**(5–6), 241–245.
10 T. W. Tan, K. L. Nie and F. Wang, Production of biodiesel by immobilized Candida sp lipase at high water content, *Appl. Biochem. Biotechnol.*, 2006, **128**(2), 109–116.
11 W. Du, Y. Y. Xu and D. H. Liu, Comparative study on lipase-catalyzed transformation of soybean oil for biodiesel production with different acyl acceptors, *J. Mol. Catal. B: Enzym.*, 2004, **30**, 125–129.
12 Y. Y. Xu, W. Du, J. Zeng and D. H. Liu, Conversion of soybean oil to biodiesel fuel using lipozyme TL IM in a solvent-free medium, *Biocatal. Biotransform.*, 2004, **22**(1), 45–48.
13 Z. F. Chen, H. Wu and M. H. Zong, Transesterification of waste oil with high acid value to biodiesel catalyzed by immobilized lipase, *Chin. J. Catal.*, 2006, **27**(2), 146–150.
14 R. Alcantara, J. Amores, L. Canoira, E. Fidalgo, M. J. Franco and A. Navarro, Catalytic production of biodiesel from soy-bean oil, used frying oil and tallow, *Biomass Bioenergy*, 2000, **18**(6), 515–527.
15 Y. Watanabe, P. Pinsirodom, T. Nagao, T. Kobayashi, Y. Nishida, Y. Takagi and Y. Shimada, Production of FAME from acid oil model using immobilized *Candida antarctica* lipase, *J. Am. Oil Chem. Soc.*, 2005, **82**(11), 825–831.
16 A. V. Tomasevic and S. S Siler-Marinkovic, Methanolysis of used frying oil, *Fuel Process. Technol.*, 2003, **81**(1), 1–6.
17 Y. Shimada, S. Nakai and M. Suenaga, et al., Facile purification of tocopherols from soybean oil deodorizer distillate in high yield using lipase, *J. Am. Oil Chem. Soc.*, 2000, **77**(10), 1009–1013.
18 S. Ghosh and D. K. Bhattacharyya, Isolation of tocopherol and sterol concentrate from sunflower oil deodorizer distillate, *J. Am. Oil Chem. Soc.*, 1996, **73**(10), 1271–1274.
19 Y. Watanabe, T. Nagao, Y. Hirota, M. Kitano and Y. Shimada, Purification of tocopherols and phytosterols by a two-step in situ enzymatic reaction, *J. Am. Oil Chem. Soc.*, 2004, **81**(4), 339–345.
20 C. Laane, S. Boeren, K. Vos and C. Veeger, Rules for optimization of biocatalysis in organic solvents, *Biotechnol. Bioeng.*, 1987, **30**(1), 81–87.
21 R. Hilhorst, R. Spruijt, C. Laane and C. Veeger, Rules for the regulation of enzyme activity in reserved micelles as illustrated by the conversion of apolar steroids by 20β-hydroxysteroid dehydrogenase, *Eur. J. Biochem.*, 1984, **144**, 459–466.

Investigation of aqueous biphasic systems formed from solutions of chaotropic salts with kosmotropic salts (salt–salt ABS)

Nicholas J. Bridges, Keith E. Gutowski and Robin D. Rogers*

Received 11th August 2006, Accepted 10th November 2006
First published as an Advance Article on the web 30th November 2006
DOI: 10.1039/b611628k

A study of salt–salt aqueous biphasic systems (ABS) was conducted to increase our understanding of solutions of kosmotropic *vs*. chaotropic salts, especially since most ionic liquids (ILs) fall within the latter class. The salting-out strength of the kosmotropic salts follows the well established Hofmeister series, as observed in polymer–salt ABS, and can be directly related to the ions' Gibbs free energies of hydration (ΔG_{hyd}). Most currently studied ILs are designed to have chaotropic cations and are thus salted-out by kosmotropic salts. Here, we describe the phase diagrams for imidazolium-, pyridium-, and quaternary ammonium- and phosphonium-based chloride salts (all chaotropic salts) salted-out by K_3PO_4, K_2HPO_4, K_2CO_3, KOH, and $(NH_4)_2SO_4$ (all kosmotropic salts). The Gibbs free energy of methylene transfer (ΔG_{CH_2}) was also determined for 1-butyl-3-methylimidazolium chloride ([C_4mim]Cl)/K_3PO_4, K_2HPO_4, and K_2CO_3 ABS. The latter results are in the range of an ethanol–water to a chloroform–water system, and can be controlled predominately by the system composition.

Introduction

Since most current liquid–liquid (l–l) separations involve at least one aqueous phase, water-immiscible organic diluents are commonly used in industry and modern research.[1] Mainly comprised of volatile organic compounds (VOCs), these diluents are widely used because they have well established research procedures, protocols, availability, and a long tradition of use.[2] As environmental concerns about VOCs increase there is a growing interest in finding ''greener'' replacement solvents for l–l separations, both in industry and academia. Lately, systems based on polymers or ionic liquids (ILs—by definition salts which have melting points less than 100 °C) have received attention since both can exhibit negligible vapor pressures.

One of the common polymers studied is poly(ethylene glycol) (PEG) because it is non-volatile, widely available, inexpensive, and included on the FDA's GRAS list (compounds generally recognized as safe).[3] Shorter PEG polymers ($M < 600$) are hygroscopic and miscible in water at all ratios, while longer PEGs have a more limited, but still high solubility in water (60% for PEG-2000 at 20 °C). PEG-based systems can only be a viable substitute for VOCs in l–l extractions after the PEG has been ''salted-out'' through the use of inorganic salts.[4–6] The addition of a kosmotropic (water-structuring) salt to aqueous solutions of high molecular weight PEGs can result in the formation of aqueous biphasic systems (ABS). ABS are comprised of two immiscible aqueous phases with variable concentrations of the solutes. Though these PEG–salt ABS are more complicated than the VOC–water systems, they have been shown to be effective for separation of organics,[6] metals,[7] and biological compounds.[8,9]

Department of Chemistry and Center for Green Manufacturing, The University of Alabama, Box 870336, Tuscaloosa, AL 35487-0336, USA. E-mail: RDRogers@bama.ua.edu

Another alternative to VOCs are ILs which have the flexibility to be designed either as hydrophobic or hydrophilic salts. Because ILs are ionic, hydrophobic IL–aqueous separations are complex with the potential for different mechanisms such as anion exchange, cation exchange, and ion-pairing.[10–12] Thus, ILs may participate directly in the separation mechanism, but can also be tuned *via* different cation and anion combinations to allow for several different separation techniques.

Currently, hydrophobic ILs usually contain expensive fluorinated ions which raises the cost of the IL and environmental concern. There are many more, inexpensive, hydrophilic ILs, however, these hydrophilic ILs can not be used directly in a l–l separation with water due to their solubility. Recently, we,[13] and others,[14–19] have investigated hydrophilic ILs mixtures with aqueous solutions of kosmotropic salts to form salt–salt ABS.

In 1888, Hofmeister established the strength of salts used to salt-out egg proteins and this is now commonly referred to as the ''Hofmeister series'', an ordering of the salts from kosmotropic to chaotropic.[20] A thermodynamic approach, utilizing the Gibbs free energy of hydration, ΔG_{hyd}, to quantify this series has been developed.[21,22] ΔG_{hyd} is the change in free energy from an isolated naked ion in the gas phase to the aqueous solvated ion in solution. Kosmotropic ions have a large negative ΔG_{hyd}, due to the resulting structured water 'lattice' around the ion,[23] while chaotropic ions have smaller negative or even positive values for ΔG_{hyd}.[21] Recent computational techniques have also been used to predict and improve the accuracy of the ΔG_{hyd} for the proton[24] and hydroxide ions,[25] as well as other ions.[26]

ILs tend to be chaotropic salts, that is they have depressed melting points as a result of low symmetry ions which contain charge delocalization, and weak directional intermolecular interactions. Such salts should be water-destructuring and

thus, capable of being salted-out by kosmotropic salts. In order to learn more about the generality and design of such salt–salt ABS, we have investigated the phase diagrams of several commonly used IL–salt ABS. Here we report these results and compare the relative phase divergence for three systems based on the Gibbs free energy of methylene transfer (ΔG_{CH_2}) between the phases.

Experimental

Chemicals

Tetra-*n*-butylammonium chloride ($N_{4444}Cl$) and tetra-*n*-butylphosphonium chloride ($P_{4444}Cl$) were purchased from Fluka (Seelze, Germany) and used as received. 1-Chlorobutane, pyridine, K_3PO_4, K_2HPO_4, K_2CO_3, $(NH_4)_2SO_4$, and KOH were purchased from Aldrich (Milwaukee, WI) and used as received. 1-Methylimidazole was purchased from Aldrich and freshly distilled before use. 1,2-Dimethylimidazole was washed with hexane, melted, recrystallized by quickly cooling, washed again with hexane, and dried under vacuum before use. DI water was obtained with a commercial deionizer (Culligan, Northbrook, IL) with a conductivity around 1.0 μS.

1-Butyl-3-methylimidazolium chloride ([C_4mim]Cl) and 1-butyl-2,3-dimethylimidazolium chloride ([C_4mmim]Cl) were synthesized with 5% molar excess of 1-chlorobutane added to the appropriate imidazole base and refluxed for one week. *N*-Butylpyridinium chloride ([C_4py]Cl) was synthesized *via* reaction of pyridine with 5% molar excess of 1-chlorobutane followed by reflux for a week. These ILs are solid at room temperature and were dried on a high vacuum line for at least 12 h at 60–70 °C.[27] The purity of the ILs was verified through ^{1}H NMR. Water content was measured through Karl–Fisher titration and any residual water in the chaotropic salts was used in constructing the phase diagrams.

Phase diagrams

The binodals were determined through cloud point titration[28] at ambient temperature using aqueous inorganic salt (K_3PO_4, K_2HPO_4, K_2CO_3, KOH, and $(NH_4)_2SO_4$) stock solutions of 40% by weight and variable aqueous concentrations of chaotropic salts ([C_4mim]Cl, [C_4mmim]Cl, [C_4py]Cl, $N_{4444}Cl$, and $P_{4444}Cl$) solutions. Drop-wise addition of water or salt solution to a monophasic (clear) solution was followed by vortexing, and time to settle. Upon settling, if a cloudy solution formed (which would yield a biphasic solution if allowed to completely separate), the cloud point was deemed reached and the concentration of all components noted *via* mass of all solutions added. This was continued until enough points were measured for an accurate binodal. All measurements were taken as weight percent and converted to molality.

An empirical mathematical model developed by Merchuk *et al.*[29] was used to fit the binodal using eqn 1:

$$y = M_1 \exp^{\left[\left(M_2 x^{0.5}\right) + \left(M_3 x^3\right)\right]} \quad (1)$$

The tie line lengths (TLLs), which measure the relative divergence in the two phases, were measured with the equation for a line between the upper and lower composition points using the procedure outlined in Merchuk *et al.*[29]

Partitioning and ΔG_{CH_2} calculations

Methanol-^{14}C and *n*-butanol-^{14}C were purchased from Aldrich and diluted in methanol and *n*-butanol, respectively. *N*-Pentanol-^{14}C and *n*-propanol-^{14}C were purchased from American Radiochemical Company, Inc. (St. Louis, MO) and diluted in an appropriate amount of *n*-pentanol and *n*-propanol, respectively.

All salt–salt ABS were prepared by mixing equal volumes of variable aqueous concentrations of the chaotropic salt with 40% w/w aqueous solution of the kosmotropic salt and allowed to stand for a minimum of 12 h. Equal volume aliquots (1 mL) of top and bottom phases were combined in a fresh vial then spiked with the appropriate ^{14}C-labeled alcohol. The biphasic system was vortexed for 1 min followed by centrifugation for 1 min. This was repeated twice, then equal aliquots (100 μL) of each phase were diluted in 5 mL of scintillation cocktail, Fisher (Fairlawn, NJ) ScintiSafe Econol. Samples were counted on a Packard Tri-Carb 1900TR liquid scintillation counter. The kosmotropic phase disengaged from the cocktail in less than 3 h. To ensure accurate counting, count times were shortened to 5 min per sample, and all samples were vortexed within 1 h of being counted to ensure proper mixing of the aqueous samples with the scintillation cocktail. Since equal volumes were counted, the distribution ratios were defined as in eqn 2:

$$D = \frac{[\text{Chaotropic upper phase}]_{cpm}}{[\text{Kosmotropic lower phase}]_{cpm}} \quad (2)$$

All radiotracer work was conducted in duplicate under the same conditions, and the relative error between duplicates was less than 5%. The relative error is smaller than the data points in the figures, thus not included in the subsequent figures.

Results and discussion

Phase diagrams

The previously reported [C_4mim]Cl–K_3PO_4 phase diagram[13] has been converted to units of molality and is shown in Fig. 1. The binodal separates the two phase region, located above the binodal, from the monophasic region, which lies between the binodal and the origin. The phase composition of a biphasic system can be determined by the tie line, any system located on any point along a single tie line will phase separate into compositions designated by the intersecting points of the tie line with the binodal. The phase ratio can be derived from the inverse lever rule.

In the [C_4mim]Cl–K_3PO_4 ABS, there are four different ions (two cations and two anions) in solution. The concentrations of $[C_4mim]^+$, Cl^-, and PO_4^{-3} were measured radioanalytically and that of the K^+ ion was calculated based on maintaining electroneutrality of individual phases (Fig. 2). Upon phase separation these ions partition to one of the two phases while maintaining electroneutrality. The most chaotropic ion of each type partitions to the upper phase. As the TLL increases, the bottom phase becomes increasingly kosmotropic; the phase

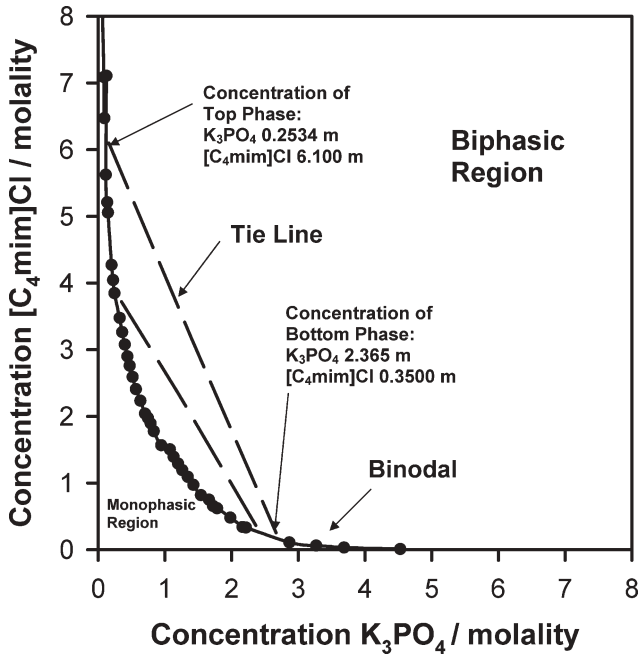

Fig. 1 The phase diagram for $[C_4mim]Cl–K_3PO_4$ illustrating the binodal (—) and the tie lines (---). (The data from ref. 13 were converted to units of molality for this depiction of the phase diagram.)

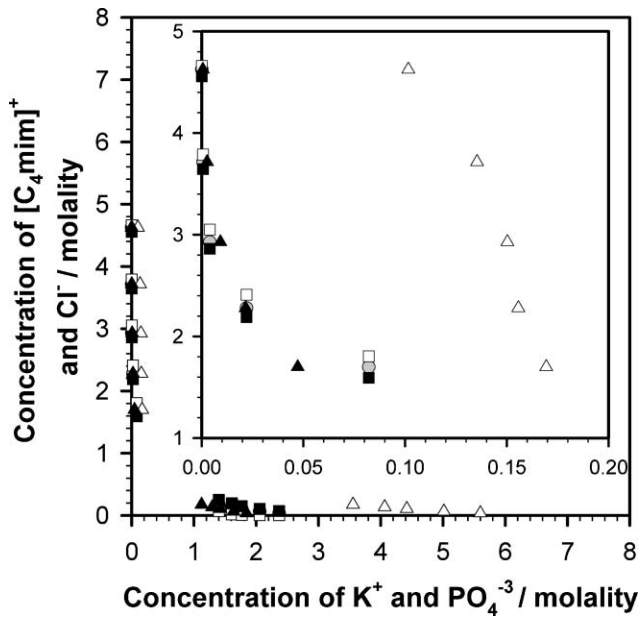

Fig. 2 Ion concentrations in the $[C_4mim]Cl–K_3PO_4$ system with respect to the binodal (grey circle) *via* cloud point titration: (□) $[C_4mim]^+$; (■) Cl^-; (Δ) K^+; (▲) PO_4^{-3}.

becoming more structured, and thus causing a greater degree of chaotropic ion transfer to the upper phase. The increased water structuring of the kosmotropic phase decreases the difference in the distribution ratios between $[C_4mim]^+$ and Cl^-. The overall deviations are small enough that cloud-point titration and interpretation of the results based on salt concentrations rather than ion concentrations yields an operationally sufficient representation of the concentration of the ions present at any tie line.

As the TLL increases, the concentrations of the ions increase and there is less water to completely hydrate the ions, thus cation–anion interactions begin to dominate. The strength or time scale of these interactions has not been investigated here, but previous literature notes that cation–anion interactions of aqueous solvated $[C_4mim]Cl$ occur at concentrations greater than 0.9 molal.[30]

The phase diagrams can be used to illustrate the differences in anion kosmotropicity for salting-out a single chaotropic pair. In Fig. 3(a), four different kosmotropic salts (K_3PO_4, K_2HPO_4, K_2CO_3, and KOH) were used to salt-out $[C_4mim]Cl$. The observed shifts in the binodals follow the Hofmeister series for the strength of the kosmotropic salts: $K_3PO_4 > K_2HPO_4 > K_2CO_3 \gg KOH$. Use of the most kosmotropic salt, K_3PO_4 (ΔG_{hyd} of $PO_4^{-3} = -663$ kcal mol^{-1}) results in a binodal closest to the origin, meaning less salt is needed to form an ABS. This is the same order as determined by comparing the ions' ΔG_{hyd} (Table 1). (In PEG–salt ABS,[31] the kosmotropic anion is predominately responsible for the observed effect, while the cation has a measurable, but much smaller, effect on the salting-out strength.[7])

Fig. 3(b) illustrates the binodals for $[C_4mmim]Cl$ with the same four salts and the same trend is observed with salting-out strength decreasing in the order $K_3PO_4 > K_2HPO_4 > K_2CO_3 \gg KOH$. There is little overall difference in the amount of kosmotropic salt needed when comparing the two imidazolium-based ILs, except for KOH.

Investigation of $N_{4444}Cl$ with the five kosmotropic salts (Fig. 3(c)) provides results which also follow the Hofmeister series: salting-out strength decreasing in the order, $K_3PO_4 > K_2HPO_4 > K_2CO_3 \gg (NH_4)_2SO_4 \gg KOH$. In most cases investigated here, $(NH_4)_2SO_4$ forms a precipitate, NH_4Cl, before reaching the critical concentration, thus there are sulfate data only with $N_{4444}Cl$. Unlike the two imidazolium salt phase diagrams, the relative differences in the salting-out abilities of the K_3PO_4, K_2HPO_4, and K_2CO_3 salts are suppressed in the $N_{4444}Cl$ system, due to an increased chaotropicity of the N_{4444}^+ ion (confirmed by location of the binodals for this salt closer to the origin). An exception was found for $(NH_4)_2SO_4$ where a common ion effect was observed due to the similarities between the N_{4444}^+ and the NH_4^+ ions, thus requiring more salt than predicted by ΔG_{hyd}.

In Fig. 4(a), five different chaotropic chloride salts ($P_{4444}Cl$, $N_{4444}Cl$, $[C_4py]Cl$, $[C_4mmim]Cl$, and $[C_4mim]Cl$) are compared using the strongest kosmotropic salt studied, K_3PO_4, to determine the order of chaotropicity of the cations. From the insert in Fig. 4(a), a small difference in $P_{4444}Cl$ and $N_{4444}Cl$ can be seen and is due to the slight increase in hydrophobicity of the slightly larger phosphonium cation over the ammonium cation. There is also only a small, if any, difference when using similar imidazolium salts except with KOH where the lack of an acidic C2-H in $[C_4mmim]^+$ appears to make a difference (see below).

Though the differences in some cases are small, an overall chaotropic order can be established: $P_{4444}Cl > N_{4444}Cl \gg [C_4py]Cl \gg [C_4mmim]Cl \cong [C_4mim]Cl$. This ordering is due to the increased chaotropic nature of the salts due to the chemical differences in the cations. The two quaternary onium salts have highly shielded charges, located mostly on the heteroatom

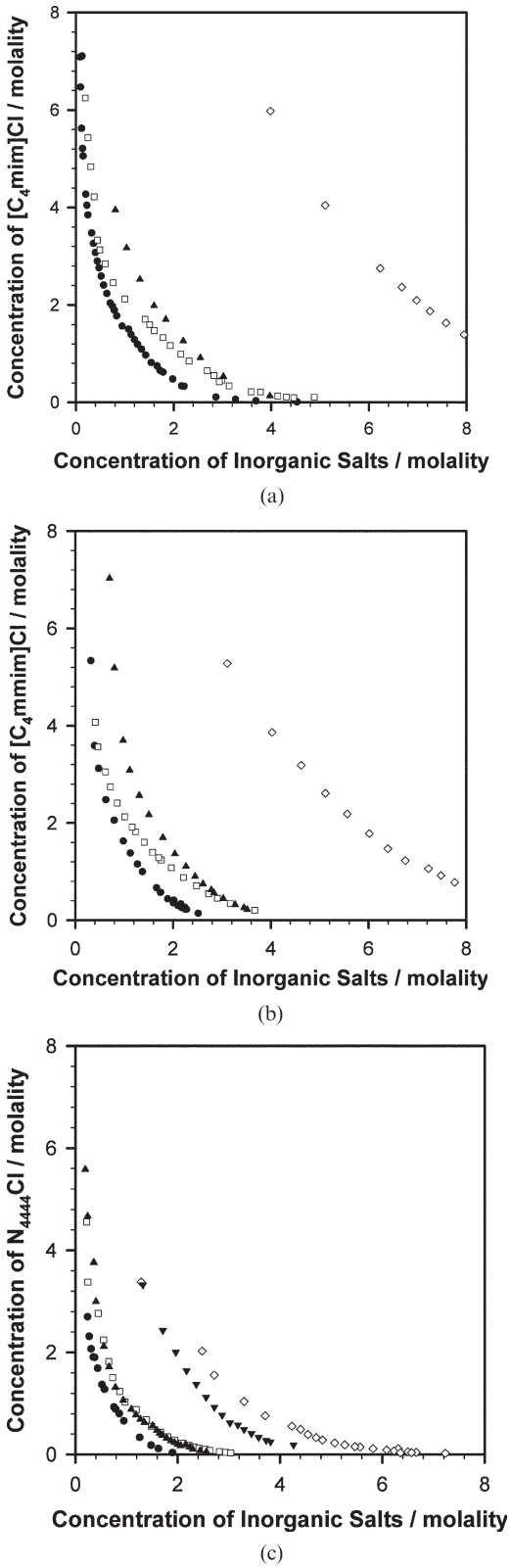

Fig. 3 Phase diagrams of (a) [C_4mim]Cl, (b) [C_4mmim]Cl, and (c) N_{4444}Cl with (●) K_3PO_4, (□) K_2HPO_4, (▲) K_2CO_3, (▼) $(NH_4)_2SO_4$, and (◇) KOH.

surrounded by four butyl chains. The [C_4py]Cl has less shielding when compared to the quaternary salts, but the charge is mostly located on the nitrogen which is shielded with the single butyl chain. The imidazolium salts have charge diffuse cations, which lead to the depressed melting points. The charge is dispersed between the two nitrogen atoms and the C2 carbon, thus exposing the charge to the solvent and allowing for more interactions between the cation and water. The interactions lead to a relative increase in the structuring of the water which is characteristic of kosmotropic salts.

Table 1 A selected list of ΔG_{hyd} for both inorganic cations and anions illustrating the kosmotropic and chaotropic salts. The ions in bold are those used in this paper[21,22]

Cation	ΔG_{hyd}/kcal mol^{-1}	Anion	ΔG_{hyd}/kcal mol^{-1}
H^+	−252(−263)[24]	ClO_4^-	−51.1
Cs^+	−61.7	TcO_4^-	−60.0
Rb^+	−67.1	**Cl^-**	**−82.9**
NH_4^+	**−69.8**	**OH^-**	**−104(−104)**[25]
K^+	**−72.7**	F^-	−114
Na^+	−89.6	CrO_4^{2-}	−229
Li^+	−115	**SO_4^{2-}**	**−261**
Fe^{2+}	−446	SO_3^{2-}	−311
Cu^{2+}	−482	**CO_3^{2-}**	**−353**
Al^{3+}	−1083	**PO_4^{3-}**	**−663**

Further investigation of phase diagrams for N_{4444}Cl, [C_4mmim]Cl, and [C_4mim]Cl vs. K_2HPO_4 and K_2CO_3 are shown in Fig. 4(b) and 4(c). The results are similar with chaotropicity increasing N_{4444}Cl ≫ [C_4mmim]Cl ≅ [C_4mim]Cl. This is the same trend observed with K_3PO_4.

KOH is the least kosmotropic salt and thus the binodals (Fig. 4(d)) are observed much farther to the right. As seen previously, N_{4444}Cl is the most chaotropic salt and this binodal is furthest to the left (it is the easiest to salt-out). The binodals for [C_4mmim]Cl and [C_4mim]Cl, however, show a degree of separation with chaotropicity increasing [C_4mmim]Cl > [C_4mim]Cl. The only difference between the two imidazolium salts is the lack of an acidic proton on C2 in [C_4mim]Cl, yet this has a significant effect on the phase diagram.

It was observed that the rate of decomposition of both of these imidazolium ILs is accelerated once the ABS is formed, perhaps due to the concentrating of the IL once phase separation has occurred. [C_4mim]Cl decomposes at a rate on the order of a few minutes, while the [C_4mmim]Cl takes over 12 h before noticeable decomposition. Longer TLLs accelerate the decomposition (color change from clear to yellow and, if allowed to proceed, to a black liquid with a pungent smell). This increased decomposition in the [C_4mim]Cl system is presumably due to the attack of the hydroxide anion at the C2 hydrogen.

Partitioning and ΔG_{CH_2}

Potential application of these salt–salt ABS requires a comparison to traditional VOC–water systems. Linear solvent free-energy relationships (LSER) and Gibbs free energies of methylene transfer (ΔG_{CH_2}) have been used for such comparison in the investigation of PEG–salt ABS.[32] Here, we have chosen ΔG_{CH_2} to probe the relative phase divergence as a function of kosmotropic salt and TLL. ΔG_{CH_2} has been used in organic–water, polymer–polymer ABS, and polymer–salt ABS as a way to compare these different systems in a quantitative way, allowing for direct correlation.

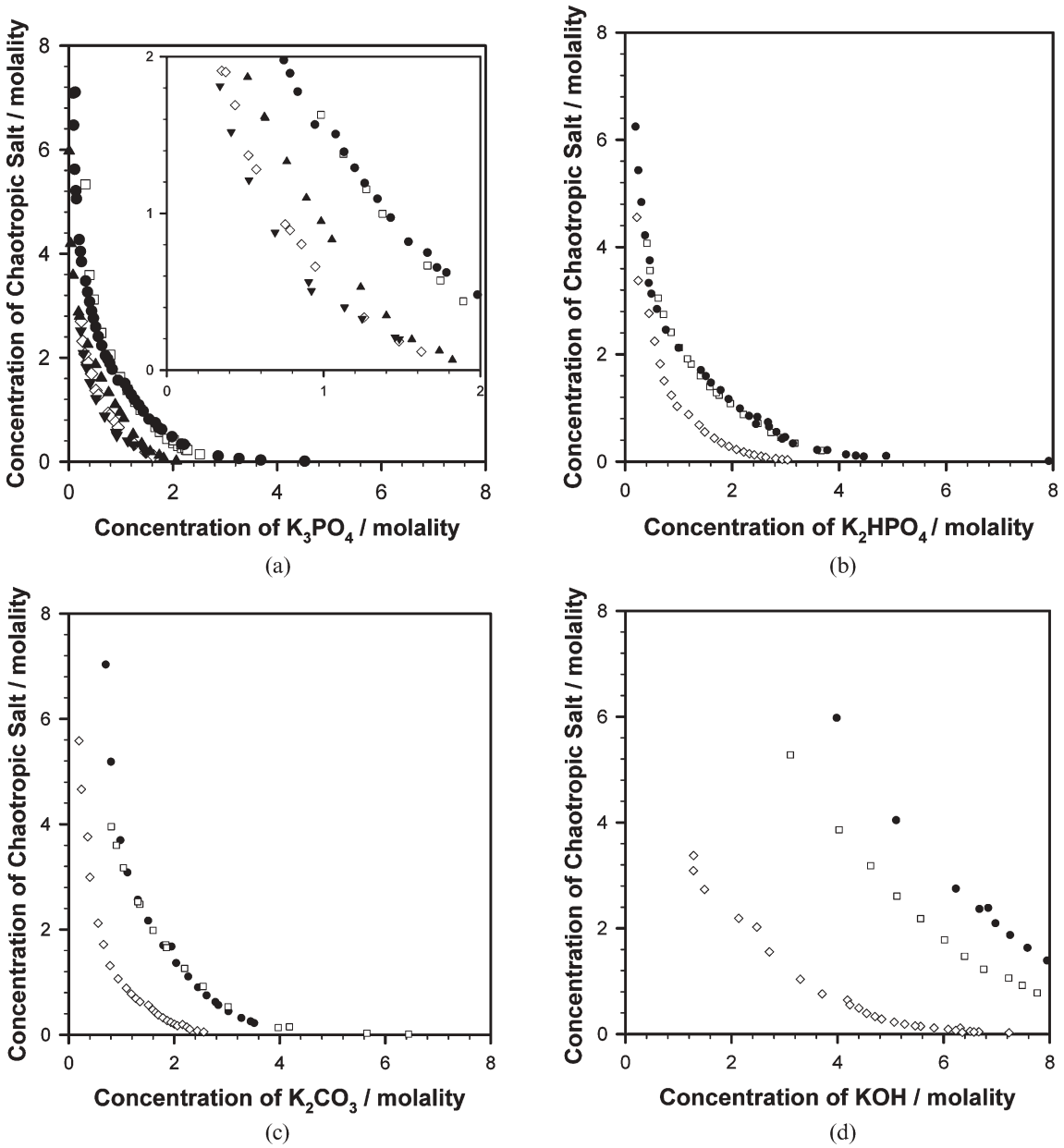

Fig. 4 Phase diagrams of (a) K_3PO_4, (b) K_2HPO_4, (c) K_2CO_3, and (d) KOH with (●) [C_4mim]Cl, (□) [C_4mmim]Cl, (▲) [C_4py]Cl, (◇) N_{4444}Cl, and (▼) P_{4444}Cl.

ΔG_{CH_2} does not measure the relative polarity of the system, but rather the free energy for cavity formation. It can be calculated from partitioning data for a series of linear alcohols,[33] for example, the data depicted in Fig. 5, which shows the distribution ratios of methanol, ethanol, propanol, butanol, and pentanol between the phases of [C_4mim]Cl–K_3PO_4 ABS at five different TLLs.

The data in Fig. 5 are also instructive with regard to the tunability of ABS. At any given TLL, the more hydrophobic the solute, the greater its distribution to the upper, more chaotropic phase. Thus, ln D for the straight chain alcohols increases methanol < ethanol < propanol < butanol < pentanol. It is also noticeable, however, that as TLL is increased the resolution between hydrophobic solutes increases. That is the distribution ratios for more hydrophobic solutes increase with increasing TLL at a greater rate than those for less hydrophobic solutes. Since TLL can be carefully controlled simply *via* changing the composition of the system, ABS allow for fine tuning separations, a feature not normally associated with the use of VOCs in l–l separations.

Each of the TLL relationships in Fig. 5 can be described by eqn 3:

$$\ln D = C + En_c \quad (3)$$

where D is the distribution ratio (also equivalent to K, or equilibrium constant), C is a constant related to the hydration properties of the phases, n_c refers to the number of carbons in the alkyl chain of the partitioned alcohols, and E is the slope of

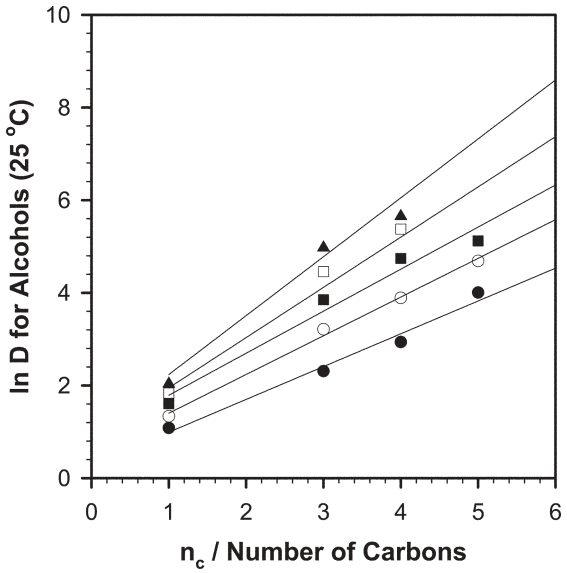

Fig. 5 Natural logarithm of the partition coefficients for straight chained alcohols (n_c) between the phases of the [C_4mim]Cl–K_3PO_4 ABS at variable TLLs (in molality): (●) TLL = 2.58; (○) TLL = 4.12; (■) TLL = 5.39; (□) TLL = 6.85; (▲) TLL = 8.66. (Pentanol was not measured at the two longer TLLs due to the high errors associated with the distribution ratios in these two systems.)

the line represented by ln D for the series of alcohols at a particular TLL. ΔG_{CH_2} is calculated by eqn 4:

$$\Delta G_{CH_2} = -RTE \quad (4)$$

where R is the universal gas constant, T is the absolute temperature (Kelvin), and E is the slope from eqn 3.[34–36]

In Fig. 6, three different salt–salt ABS ([C_4mim]Cl salted-out by K_3PO_4, K_2HPO_4, or K_2CO_3) are compared. Changes in ΔG_{CH_2} are related to the TLL, which supports the idea that

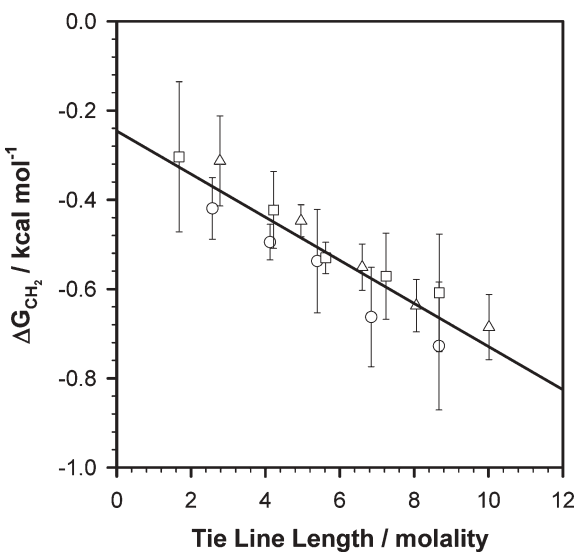

Fig. 6 ΔG_{CH_2} for three salt–salt ABS at variable TLLs: (○) [C_4mim]Cl–K_3PO_4; (□) [C_4mim]Cl–K_2HPO_4; (Δ) [C_4mim]Cl–K_2CO_3.

TLL can be used to describe phase divergence and relative hydrophobicity within a system. Because ΔG_{CH_2} is a measure of cavity formation for an additional methylene group, the decrease in the ΔG_{CH_2} as the TLL increases implies that the kosmotropic phase becomes more structured (harder to form a cavity) as the concentration of kosmotropic salt increases. At the same time, the top phase becomes more chaotropic leading to a more destructured phase, thus allowing for easier cavity formation and transfer of the alcohol. By varying the TLL, a range of ΔG_{CH_2} values from −0.304 to −0.728 kcal mol^{-1} are attainable. These values are comparable to ethanol–water (−0.388 kcal mol^{-1}) through chloroform–water (−0.731 kcal mol^{-1}) systems. With shorter TLL, much smaller differences can be obtained, up to the system's critical point.

The salt–salt ABS studied here are similar to PEG–salt ABS in the sense that the relative divergence of the system is controlled mostly by the salt concentrations, directly affecting the TLL. In Fig. 7, ΔG_{CH_2} for the three imidazolium-based salt–salt ABS are plotted with nine different PEG–salt ABS for comparison. In all of the systems, there are differences in the ΔG_{CH_2} values with different kosmotropic salts (as evidenced by the different slopes). The large difference in the slopes between salt–salt and PEG–salt ABS may be due to differences in the nature of the uncharged PEG compared to the [C_4mim]$^+$ cation. The large size of a PEG molecule (PEG-2000 has an average of 45 ethylene oxide units per polymer chain) provides greater phase divergence in response to the kosmotropic salts due to the larger cavity size needed to encompass PEG-2000 compared to the smaller, charged imidazolium cations. A charged species will also inherently have interactions with water due to coulombic forces, decreasing ΔG_{hyd}, thus making the species more kosmotropic than a neutral molecule.

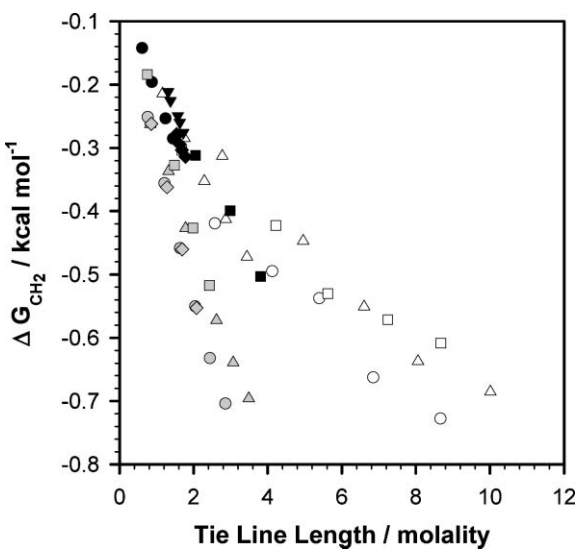

Fig. 7 Comparisons of ΔG_{CH_2} for three salt–salt ABS and nine PEG–salt ABS: (○) [C_4mim]Cl–K_3PO_4; (□) [C_4mim]Cl–K_2HPO_4; (Δ) [C_4mim]Cl–K_2CO_3; (grey circle) PEG-2000–K_3PO_4; (grey diamond) PEG-3400–K_3PO_4; (grey square) PEG-1000–K_3PO_4 (grey triangle) PEG-2000–K_2CO_3; (▲) PEG-2000–$(NH_4)_2SO_4$; (■) PEG-2000–Na_2SO_4; (●) PEG-2000–Li_2SO_4; (◆) PEG-2000–$ZnSO_4$; (▼) PEG-2000–$MnSO_4$. (All PEG data were plotted with data from ref. 37.)

Conclusions

The ability to form salt–salt ABS allows for hydrophilic ILs to be used in aqueous separation systems, opening the door to multiple uses (*e.g.*, metathesis, separation of biological species or inorganics, *etc.*). It has been demonstrated here that as previously observed with PEG–salt ABS, the Hofmeister series can be used to grade the kosmotropic salts' (K_3PO_4, K_2HPO_4, K_2CO_3, KOH, and $(NH_4)_2SO_4$) ability to salt-out various chaotropic salts ([C_4mim]Cl, [C_4mmim]Cl, [C_4py]Cl, N_{4444}Cl, and P_{4444}Cl). Interestingly, such phase diagrams should also provide a method to grade the chaotropicity of IL salts, as observed here where the chaotropicity decreased in the order $P_{4444}Cl > N_{4444}Cl \gg [C_4py]Cl \gg [C_4mmim]Cl \cong [C_4mim]Cl$. Such empirically derived parameters may also aid in the search for new IL-forming ions.

The tunability of these systems is apparent from the ability to change the ΔG_{CH_2} between the co-existing phases simply by changing the concentrations of the ions, thus changing the TLL. This feature of salt–salt ABS provides additional operational diversity (and complexity) to these systems compared to traditional l–l separations. Nonetheless, much additional work is needed to fully define salt–salt ABS and provide more operational control, before such systems will see useful technological implementation.

Acknowledgements

This research is supported by the US Department of Energy Environmental Management Science Program (Grant DE-FG02-05ER63989) and Division of Chemical Sciences, Geoscience, and Bioscience, Office of Basic Energy Sciences, Office of Science, (Grant DE-FG02-96ER14673).

References

1 R. D. Noble and R. Agrawal, *Ind. Eng. Chem. Res.*, 2005, **44**, 2887.
2 *Solvent Extraction Principles and Practice 2nd Edition*, ed. J. Rydberg, M. Cox, C. Musikas and G. Choppin, Marcel Dekker, New York, 2004.
3 D. Herold, K. Keil and D. E. Burns, *Biochem. Pharmacol.*, 1989, **38**, 73.
4 F. E. Bailey, Jr., *Poly(Ethylene Oxide)*, Academic Press, New York, 1976.
5 J. G. Huddleston, H. D. Willauer, S. T. Griffin and R. D. Rogers, *Ind. Eng. Chem. Res.*, 1999, **38**, 2523.
6 R. D. Rogers, H. D. Willauer, S. T. Griffin and J. G. Huddleston, *J. Chromatogr., B: Biomed. Appl.*, 1998, **711**, 255.
7 R. D. Rogers and C. B. Bauer, *J. Chromatogr., B: Biomed. Appl.*, 1996, **680**, 237.
8 F. Tjerneld and H. O. Johansson, *Int. Rev. Cytol.*, 2000, **192**, 137.
9 J. Chen, S. K. Spear, J. G. Huddleston and R. D. Rogers, *Green Chem.*, 2005, **7**, 64.
10 M. L. Dietz and J. Dzielawa, *Chem. Commun.*, 2001, 2124.
11 M. L. Dietz, J. Dzielawa, I. Laszak, B. A. Young and M. P. Jensen, *Green Chem.*, 2003, **5**, 682.
12 M. P. Jensen, J. Dzielawa, P. Richet and M. L. Dietz, *J. Am. Chem. Soc.*, 2002, **124**, 10664.
13 K. E. Gutowski, G. A. Broker, H. D. Willauer, J. G. Huddleston, R. P. Swatloski, J. D. Holbrey and R. D. Rogers, *J. Am. Chem. Soc.*, 2003, **125**, 6632.
14 M. Lucas, *J. Inorg. Nucl. Chem.*, 1970, **32**, 3692.
15 Y. Anzai and Y. Akama, *Bunseki Kagaku*, 2003, **52**, 337.
16 Y. Akama, M. Ito and S. Tanaka, *Talanta*, 2000, **53**, 645.
17 C. He, S. Li, H. Liu, K. Li and F. Liu, *J. Chromatogr., A*, 2005, **1082**, 143.
18 Y. Akama and A. Sali, *Talanta*, 2002, **57**, 681.
19 T. C. Franklin and S. B. Benson, *J. Chem. Educ.*, 1986, **63**, 821.
20 F. Hofmeister, *Arch. Exp. Pathol. Pharmakol.*, 1888, **24**, 247.
21 Y. Marcus, in *Ion Properties*, Marcel Dekker, New York, 1997.
22 Y. Marcus, *J. Chem. Soc., Faraday Trans.*, 1991, **87**, 2995.
23 H. O. Johnansson, G. Karlström and F. Tjerneld, *Macromolecules*, 1993, **26**, 4478.
24 C. G. Zhan and D. A. Dixon, *J. Phys. Chem. A*, 2001, **105**, 11534.
25 C. G. Zhan and D. A. Dixon, *J. Phys. Chem. A*, 2002, **106**, 9737.
26 G. Hummer, L. R. Pratt and A. E. Garcia, *J. Phys. Chem.*, 1996, **100**, 1206.
27 J. G. Huddleston, A. E. Visser, W. M. Reichert, H. D. Willauer, G. A. Broker and R. D. Rogers, *Green Chem.*, 2001, **3**, 156.
28 K. P. Ananthapadmanabhan and E. D. Goddard, *J. Colloid Interface Sci.*, 1986, **113**, 294.
29 J. C. Merchuk, B. A. Andrews and J. A. Asenjo, *J. Chromatogr., B: Biomed. Appl.*, 1998, **711**, 285.
30 K. Miki, P. Westh, K. Nishikawa and Y. Koga, *J. Phys. Chem. B*, 2005, **109**, 9014.
31 J. G. Huddleston, H. D. Willauer and R. D. Rogers, *J. Chem. Eng. Data*, 2003, **48**, 1230.
32 H. D. Willauer, J. G. Huddleston and R. D. Rogers, *Ind. Eng. Chem. Res.*, 2002, **41**, 2591.
33 B. Y. Zaslavsky, L. M. Miheeva and S. V. Rogoshin, *Biochim. Biophys. Acta*, 1978, **510**, 160.
34 B. Y. Zaslavsky, L. M. Miheeva, N. N. Mestechkina and S. V. J. Rogozhin, *J. Chromatogr.*, 1982, **253**, 139.
35 B. Y. Zaslavsky, L. M. Miheeva and S. V. J. Rogozhin, *J. Chromatogr.*, 1981, **212**, 13.
36 B. Y. Zaslavsky, N. D. Gulaeva, E. A. Djafarov, E. A. Masimov and L. M. Miheeva, *J. Colloid Interface Sci.*, 1990, **137**, 147.
37 H. D. Willauer, PhD thesis, the University of Alabama, 2001.

Highly efficient [2,3]-sigmatropic rearrangement of sulfur ylide derived from Rh(II) carbene and sulfides in water

Mingyi Liao and Jianbo Wang*

Received 4th September 2006, Accepted 23rd November 2006
First published as an Advance Article on the web 11th December 2006
DOI: 10.1039/b612743f

The Doyle–Kirmse reaction, namely the [2,3]-sigmatropic rearrangement of sulfonium ylides generated from transition metal carbenoids and sulfides has been, for the first time, carried out in water.

Introduction

Since their discovery in the late 1960s,[1] the [2,3]-sigmatropic rearrangements of sulfonium ylides have received considerable attention because of their applications in organic synthesis and their probable involvement in biochemical processes.[2] The most common method for sulfonium ylide generation involves the removal of a proton from a sulfonium salt with a strong base.[2a] However, a more direct method makes use of the reaction between a carbene (or carbenoid) and a sulfide. Although suitable for ylide formation, carbenes generated photochemically and thermally from diazo compounds are relatively indiscriminate.[3] The potentially more general catalytic approach to carbenoid generation began to evolve with the use of transition metal-catalyzed reactions of diazo compounds. The [2,3]-sigmatropic rearrangement of sulfonium ylides generated from transition metal carbenoids and sulfides, known as the Doyle–Kirmse reaction, is a powerful method for C–C bond formation (Scheme 1).[4] Therefore, many metal catalysts, such as $Rh_2(OAc)_4$, $Cu(acac)_2$, $[Ru^{II}(TTP)(CO)]$ and $dppeFeCl_2$, were developed to catalyze this reaction.[2,5]

However, the Doyle–Kirmse reaction is always performed in dry organic solvent under inert atmosphere due to the high reactivity of the metal carbenoid intermediates. To the best of our knowledge a metal-catalyzed Doyle–Kirmse reaction in water has not been reported. Water, as the most inexpensive and environmentally benign solvent, has been widely used for organic reactions in the past decade.[6] More recently, a few examples demonstrated that the reactions involving metal carbenoid intermediates, such as cyclopropanation, intramolecular C–H insertion and intermolecular N–H insertion of diazo carbonyl compounds, can be carried out in aqueous conditions.[7] Here we report a highly efficient [2,3]-sigmatropic rearrangement of sulfur ylides derived from Rh(II) carbene and sulfides in water.

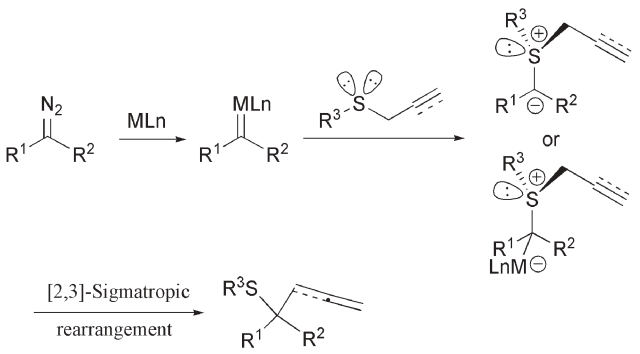

Scheme 1

Results and discussion

First, diazo compound **1a** and sulfide **2a** were used as the substrates to optimize the reaction conditions (Table 1). When we treated **1a** and **2a** in 5 mL tap water in the presence of 10 mol% $CuSO_4{\cdot}5H_2O$ at ambient temperature, the reaction proceeded very slowly and **1a** disappeared after 72 h. [2,3]-sigmatropic rearrangement product **3a** was isolated in 31% yield (entry 1). Then a variety of metal salts were explored as catalysts. $Fe(NO_3)_3$, $MnCl_2$, $CoCl_2$ and $NiBr_2$ did not catalyze this reaction under the same conditions (entries 2–5). Use of

Table 1 Effect of the catalysts on the reaction of **1a** and **2a** in water[a]

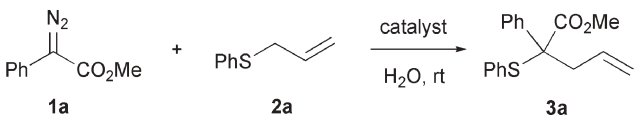

1a **2a** **3a**

Entry	Catalyst	Reaction time/h	Yield (%)[b]
1	$CuSO_4{\cdot}5H_2O$	72	31
2	$Fe(NO_3)_3$	30	—
3	$MnCl_2$	30	—
4	$CoCl_2$	24	—
5	$NiBr_2$	24	—
6	CuOTf	38	trace
7	$Cu(acac)_2$	72	trace
8	$CuSO_4{\cdot}5H_2O$[c]	72	trace
9	$Rh_2(OAc)_4$[d]	3	91
10[e]	$Rh_2(OAc)_4$[d]	5	93

[a] Reaction conditions: **1a** (0.2 mmol), **2a** (0.3 mmol), 10 mol% catalyst, 5 mL tap water. [b] Isolated yields after column chromatography. [c] 10 mol% sodium dodecylbenzenesulfate was added. [d] 0.5 mol% catalyst was used. [e] The reaction was carried out in deionized distilled water.

Beijing National Laboratory of Molecular Sciences (BNLMS), Green Chemistry Center (GCC) and Key Laboratory of Bioorganic Chemistry and Molecular Engineering of Ministry of Education, College of Chemistry Peking University, Beijing, 100871, China. E-mail: wangjb@pku.edu.cn; Fax: +8610-62751708; Tel: +8610-62757248

10 mol% CuOTf or $Cu(acac)_2$ as catalyst led to very low conversions of the starting materials (entries 6 and 7). Considering the low solubility of the substrates **1a** and **2a** in water, a surfactant was introduced. However, when the reaction was carried out in the presence of a catalytic amount of $CuSO_4 \cdot 5H_2O$ and sodium dodecylbenzenesulfate (SDBS) in water, the result was even worse (entry 8). Considering the "on-water effect" proposed by Sharpless and co-workers,[8] we conceived another possibility to solve this problem by using a less water-soluble catalyst. Thus, Rh(II) carboxylates were applied. To our delight, **3a** was obtained in 91% yield within 3 h when the reaction was catalyzed by a catalytic amount of $Rh_2(OAc)_4$ (entry 9). Although $Rh_2(OAc)_4$ is actually quite soluble in water, the sulfide could coordinate to the rhodium atom, and thus the catalyst might be pulled into organic phase. As a result, the reaction could proceed effectively. For comparison, the reaction was also tested in deionized distilled water and a similar result was obtained (entry 10).

Using the optimized reaction conditions, we carried out the rhodium-catalyzed Doyle–Kirmse reaction of a variety of aryldiazoacetates (**1a–j**) and phenyl allyl sulfide (**2a**). The results were summarized in Table 2. As can be seen, in all cases [2,3]-sigmatropic rearrangement products (**3a–j**) were obtained in good to excellent yields, regardless of the position and electronic effect of the substituent in the phenyl ring. When there was a substituent in the ortho position, the yield decreased to some extent (entries 2 and 8). **1j** (Ar = 1-naphthyl) was also suitable for this reaction (entry 10). Notably, most aryldiazoacetates are solid except **1a**, **1f** and **1j**. **1b** can dissolve in phenyl allyl sulfide, **2a** and other solid substrates were dissolved in a tiny amount of organic solvent (most cases in toluene) before they were subjected to the reaction.

As an extension of the approach, the reaction of aryldiazoacetates and phenyl propargyl sulfide **4a** was then examined. Surprisingly, when we treated **1a** and **4a** in the presence of a catalytic amount of $Rh_2(OAc)_4$ in water, the reaction proceeded very slowly and was completed in about 4 days to afford [2,3]-sigmatropic rearrangement product **5a** in only 74% yield. A hydrophobic Rh(II) catalyst was then considered. We were delighted to find that the reaction proceeded smoothly and finished within 14 h when catalyzed by dirhodium(II) octanoate, $Rh_2(Oct)_4$. Allene derivative **5a** was formed in 93% yield. Subsequently, the reaction condition was applied to **1b–h, j** (Table 3). The reaction worked well and the corresponding rearrangement products **5b–h, j** were all obtained in high yields.

In addition, α-diazoacetophenone, **6**, as substrate was also tested for the Doyle–Kirmse reaction. **6** reacted with **2a** or **4a** and afforded the corresponding rearrangement product in moderate yield under identical reaction conditions (Scheme 2). The low yield obtained may be due to the easy dimerization of **6** as well as the instability of the rearrangement product. Moreover, it should be noted that the reaction of **6** and **4a** in water was much faster than in CH_2Cl_2.

Since the pioneering work of Uemura *et al.* in 1995,[9] asymmetric catalysis in [2,3]-sigmatropic rearrangement of sulfur ylides has attracted considerable attention.[10] Considering the difference between organic solvents and water, we conceived that the enantioselectivity of the asymmetric catalytic [2,3]-sigmatropic rearrangement of sulfur ylides might be improved when carrying out the reaction in water. Thus, diazo compound **1g** and allyl 2-chlorophenyl

Table 2 Reaction of **1a–j** and **2a** catalyzed by $Rh_2(OAc)_4$ in water[a]

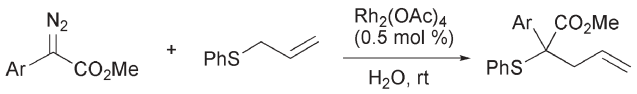

1a-j **2a** **3a-j**

Entry	Substrate **1** (Ar=)	Reaction time/h	Yield (%)[b]
1	**a**, C_6H_5	3	91
2	**b**, *o*-ClC_6H_4	3	82
3	**c**, *m*-ClC_6H_4[c]	4	92
4	**d**, *p*-ClC_6H_4[c]	16	92
5	**e**, *p*-BrC_6H_4[c]	1	92
6	**f**, *m*-$MeOC_6H_4$	1.5	97
7	**g**, *p*-$MeOC_6H_4$[c]	0.75	96
8	**h**, 2,4-$Cl_2C_6H_3$[c]	6	82
9	**i**, 3,4-$Cl_2C_6H_3$[d]	3	93
10	**j**, 1-naphthyl	5	89

[a] Reaction conditions: **1a–j** (0.2 mmol), **2a** (0.3 mmol), 0.5 mol% $Rh_2(OAc)_4$, 5 mL tap water. [b] Isolated yields after column chromatography. [c] The substrate was dissolved in 0.1 mL toluene. [d] The substrate was dissolved in 0.3 mL CH_2Cl_2.

Table 3 Reaction of **1a–h, j** and **4a** catalyzed by $Rh_2(Oct)_4$ in water[a]

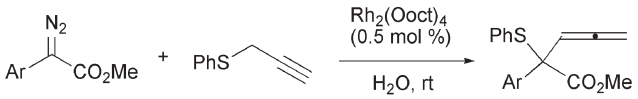

1a-h, j **4a** **5a-h, j**

Entry	Substrate **1** (Ar=)	Reaction time/h	Yield (%)[b]
1	**a**, C_6H_5	14	93
2	**b**, *o*-ClC_6H_4	8	88
3	**c**, *m*-ClC_6H_4[c]	4	95
4	**d**, *p*-ClC_6H_4	1.5	94
5	**e**, *p*-BrC_6H_4	4	95
6	**f**, *m*-$MeOC_6H_4$	6	96
7	**g**, *p*-$MeOC_6H_4$[c]	3	92
8	**h**, 2,4-$Cl_2C_6H_3$[c]	2	89
9	**j**, 1-naphthyl	7	87

[a] Reaction conditions: **1a–h, j** (0.2 mmol), **2a** (0.3 mmol), 0.5 mol% $Rh_2(Oct)_4$, 5 mL tap water. [b] Isolated yields after column chromatography. [c] The substrate was dissolved in 0.1 mL toluene.

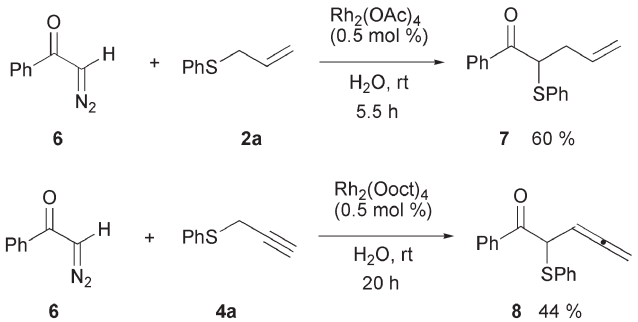

Scheme 2

Table 4 Asymmetric [2,3]-sigmatropic rearrangement of sulfur ylide in water[a]

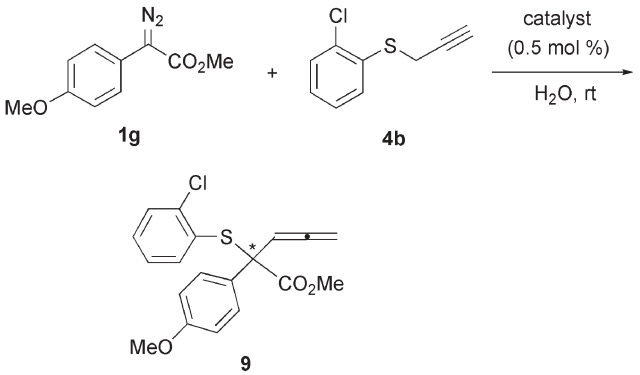

Entry	Catalyst	Reaction time/h	Yield (%)[b]	ee (%)[c]
1	Rh_2(*S*-DOSP)$_4$	0.3	93	48
2	Rh_2(*S*-TBSP)$_4$	1	91	44
3	Rh_2(*S*-BNP)$_4$	1	94	27
4	Rh_2(4*S*-MEAZ)$_4$	38	67	2
5	Rh_2(4*S*-MEOX)$_4$	160	56	2
6	Rh_2(5*S*-MEPY)$_4$	120	41	8
7	Rh_2(4*S*-MPPIM)$_4$	87 (14)[d]	42 (28)[d]	68 (47)[d]
8[e]	Rh_2(*S*-DOSP)$_4$	22	91	48

[a] Reaction conditions: **1g** (0.2 mmol) dissolved in 0.1 mL toluene, **4b** (0.3 mmol), 0.5 mol% catalyst, 5 mL tap water. [b] Isolated yields after column chromatography. [c] Enantiomeric excess values determined by chiral HPLC. [d] The data in parentheses refers to the reaction in toluene. [e] The reaction was carried out at 0 °C.

sulfide **4b** were chose as the substrates to screen the chiral rhodium(II) catalysts (Table 4). When catalyzed by Rh_2(*S*-DOSP)$_4$,[11] Rh_2(*S*-TBSP)$_4$[11] or Rh_2(*S*-BNP)$_4$[12] in water, the reaction proceeded efficiently to give the allenic product in excellent yield. Unfortunately, the enantioselectivity was lower than that performed in toluene (entries 1–3).[10e] A lower temperature significantly slowed down the reaction rate, while the enantioselectivity remained the same (entry 8). Using Rh_2(4*S*-MEAZ)$_4$,[13] Rh_2(4*S*-MEOX)$_4$,[14] Rh_2(5*S*-MEPY)$_4$[15] or Rh_2(4*S*-MPPIM)$_4$[16] as catalyst, the reaction proceeded much more slowly. Rh_2(4*S*-MEAZ)$_4$, Rh_2(4*S*-MEOX)$_4$ and Rh_2(5*S*-MEPY)$_4$ showed low enantioselectivities, whereas Rh_2(4*S*-MPPIM)$_4$ gave the best result (entries 4–7). Since an improvement in enantioselectivities was often observed in toluene media, the reaction catalyzed by Rh_2(4*S*-MPPIM)$_4$ in toluene was also tested. Although the reaction proceeded much faster, both yield and enantioselectivity decreased (entry 7 in parentheses). Other chiral catalysts may be employed to improve the enantioselectivity. This work is still under investigation in our laboratory. The results obtained so far demonstrate that aqueous media does not significantly improve the enantioselectivity in this type of reaction.

Conclusions

In conclusion, we have demonstrated that [2,3]-sigmatropic rearrangement of sulfur ylide generated through Rh(II) carbene and allyl and propargyl sulfides can be efficiently carried out in an aqueous suspension. We consider that this is an example of an "on-water" reaction.

Experimental

Caution: All diazo compounds are highly toxic or presumed to be toxic. Diazo compounds are potentially explosive. They should be handled with care in a well-ventilated fumehood.

General

^{1}H NMR and ^{13}C NMR were measured at 300 MHz and 75 MHz on Varian Mercury 300 spectrometers or at 200 MHz and 50 MHz on Varian Mercury 200 spectrometers. IR spectra were recorded with a Nicolet AVATAR 330 FT-IR infrared spectrometer. Mass spectra were obtained on a VG ZAB-HS mass spectrometer. Elemental analysis was carried out at Elementar Vario EL Instrument. Column chromatography was performed on 200–300 mesh silica gel (Yantai, China) employing a petroleum ethyl acetate mixture (distilled prior to use) as eluent. All solvents were distilled prior to use.

General procedure for the reaction of diazo compound and allyl sulfide catalyzed by $Rh_2(OAc)_4$ in water. Diazo compounds **1a–j**, **6** (0.2 mmol) and sulfide **2a** were charged in a 25 mL round bottomed flask, 5 mL tap water was added followed by $Rh_2(OAc)_4$ (0.001 mmol), the mixture was stirred at room temperature until complete disappearance of the diazo substrate. The reaction mixture was then extracted with CH_2Cl_2, dried over anhydrous Na_2SO_4 and concentrated under vacuum. The residue was purified on a silica gel column (petroleum ether–EtOAc, 15 : 1–50 : 1) to afford the products **3a–j**, **7**.

Methyl 2-(2-chlorophenyl)-2-(phenylthio)pent-4-enoate (3b). 82%; IR (neat) 3074, 2948, 1732, 1438, 1228 cm^{-1}; ^{1}H NMR (300 MHz, $CDCl_3$) δ 2.82–2.90 (m, 1 H), 3.02–3.10 (m, 1 H), 3.61 (s, 3 H), 5.03–5.11 (m, 2 H), 5.81–5.94 (m, 1 H), 7.14–7.42 (m, 9 H); ^{13}C NMR (75 MHz, $CDCl_3$) δ 39.9, 52.5, 63.4, 118.8, 126.1, 128.5, 128.8, 129.4, 129.5, 130.2, 130.8, 132.5, 133.6, 136.9, 137.3, 171.2; EI-MS (*m*/*z*, relative intensity): 332 (M^+, 12), 291 (20), 223 (44), 163 (36), 155 (40), 128 (72), 109 (28), 71 (100). Anal. calcd for $C_{18}H_{17}ClO_2S$: C, 64.95; H, 5.15. Found: C, 64.93; H, 5.07.

Methyl 2-(3-chlorophenyl)-2-(phenylthio)pent-4-enoate (3c). 92%; IR (neat) 3076, 2950, 1732, 1438, 1215 cm^{-1}; ^{1}H NMR (300 MHz, $CDCl_3$) δ 2.77–2.91 (m, 2 H), 3.70 (s, 3 H), 5.04–5.15 (m, 2 H), 5.82–5.95 (m, 1 H), 7.14–7.36 (m, 9 H); ^{13}C NMR (75 MHz, $CDCl_3$) δ 40.6, 52.8, 64.0, 119.2, 125.7, 127.6, 127.7, 128.6, 129.2, 129.5, 130.1, 132.6, 134.0, 136.8, 141.8, 171.7; EI-MS (*m*/*z*, relative intensity): 332 (M^+, 33), 291 (31), 223 (73), 191 (36), 163 (83), 155 (74), 128 (82), 109 (35), 71 (100), 59 (49). Anal. calcd for $C_{18}H_{17}ClO_2S$: C, 64.95; H, 5.15. Found: C, 65.00; H, 5.23.

Methyl 2-(4-chlorophenyl)-2-(phenylthio)pent-4-enoate (3d). 92%; IR (neat) 2950, 1729, 1494, 1474, 1219 cm^{-1}; ^{1}H NMR (300 MHz, $CDCl_3$) δ 2.77–2.90 (m, 2 H), 3.69 (s, 3 H), 5.03–5.14 (m, 2 H), 5.81–5.95 (m, 1 H), 7.16–7.35 (m, 9 H); ^{13}C NMR (75 MHz, $CDCl_3$) δ 40.6, 52.7, 63.8, 119.1, 128.1, 128.6, 128.9, 129.4, 130.3, 132.7, 133.3, 136.8, 138.3, 171.8; EI-MS (*m*/*z*, relative intensity): 332 (M^+, 16), 291 (8), 223 (96), 191

(33), 163 (84), 155 (94), 128 (100), 109 (46), 71 (95), 59 (66). Anal. calcd for $C_{18}H_{17}ClO_2S$: C, 64.95; H, 5.15. Found: C, 64.84; H, 5.12.

Methyl 2-(4-bromophenyl)-2-(phenylthio)pent-4-enoate (3e). 92%; IR (neat) 3076, 2949, 1731, 1489, 1217 cm^{-1}; ^1H NMR (300 MHz, $CDCl_3$) δ 2.77–2.90 (m, 2 H), 3.69 (s, 3 H), 5.04–5.14 (m, 2 H), 5.81–5.94 (m, 1 H), 7.15–7.43 (m, 9 H); ^{13}C NMR (75 MHz, $CDCl_3$) δ 40.6, 52.7, 63.9, 119.2, 121.5, 128.6, 129.3, 129.4, 130.2, 131.1, 132.7, 136.8, 138.8, 171.8; EI-MS (*m*/*z*, relative intensity): 376 (M^+, 13), 267 (82), 235 (25), 199 (54), 129 (70), 128 (100), 109 (27), 71 (67). Anal. calcd for $C_{18}H_{17}BrO_2S$: C, 57.30; H, 4.54. Found: C, 57.25; H, 4.55.

Methyl 2-(3-methoxyphenyl)-2-(phenylthio)pent-4-enoate (3f). 97%; IR (neat) 2950, 2836, 1731, 1257, 1215 cm^{-1}; ^1H NMR (300 MHz, $CDCl_3$) δ 2.77–2.93 (m, 2 H), 3.69 (s, 3 H), 3.74 (s, 3 H), 5.04–5.14 (m, 2 H), 5.85–5.98 (m, 1 H), 6.78–6.88 (m, 3 H), 7.16–7.33 (m, 6 H); ^{13}C NMR (75 MHz, $CDCl_3$) δ 40.5, 52.6, 55.2, 64.3, 112.8, 113.4, 118.7, 119.7, 128.4, 128.9, 129.2, 130.5, 133.0, 136.7, 141.2, 159.2, 172.1; EI-MS (*m*/*z*, relative intensity): 328 (M^+, 11), 287 (5), 219 (90), 187 (24), 159 (100), 151 (50), 109 (21), 71 (31). Anal. calcd for $C_{19}H_{20}O_3S$: C, 69.48; H, 6.14. Found: C, 69.42; H, 6.24.

Methyl 2-(4-methoxyphenyl)-2-(phenylthio)pent-4-enoate (3g). 96%; IR (neat) 2951, 2837, 1731, 1512, 1252 cm^{-1}; ^1H NMR (300 MHz, $CDCl_3$) δ 2.76–2.92 (m, 2 H), 3.69 (s, 3 H), 3.80 (s, 3 H), 5.03–5.13 (m, 2 H), 5.84–5.98 (m, 1 H), 6.79–6.88 (m, 2 H), 7.17–7.33 (m, 7 H); ^{13}C NMR (75 MHz, $CDCl_3$) δ 40.6, 52.6, 55.2, 63.9, 113.3, 118.6, 128.4, 128.6, 129.1, 130.8, 131.7, 133.3, 136.8, 158.7, 172.4; EI-MS (*m*/*z*, relative intensity): 328 (M^+, 0.4), 219 (28), 180 (30), 159 (20), 121 (100), 91 (10), 77 (14), 51 (8). Anal. calcd for $C_{19}H_{20}O_3S$: C, 69.48; H, 6.14. Found: C, 69.35; H, 6.28.

Methyl 2-(2,4-dichlorophenyl)-2-(phenylthio)pent-4-enoate (3h). 82%; IR (neat) 3074, 2944, 1736, 1471, 1216 cm^{-1}; ^1H NMR (300 MHz, $CDCl_3$) δ 2.84 (dd, J = 14.4, 7.8 Hz, 1 H), 3.02 (ddt, J = 14.4, 6.6, 1.5 Hz, 1 H), 3.58 (s, 3 H), 5.02–5.12 (m, 2 H), 5.78–5.92 (m, 1 H), 7.14–7.43 (m, 8 H); ^{13}C NMR (75 MHz, $CDCl_3$) δ 39.9, 52.5, 63.0, 119.1, 126.2, 128.6, 129.7, 130.0, 130.4, 130.6, 132.1, 133.9, 134.4, 135.8, 137.3, 170.8; EI-MS (*m*/*z*, relative intensity): 366 (M^+, 13), 325 (10), 257 (39), 189 (33), 162 (30), 128 (40), 109 (54), 71 (100). Anal. calcd for $C_{18}H_{16}Cl_2O_2S$: C, 58.86; H, 4.39. Found: C, 58.82; H, 4.48.

Methyl 2-(3,4-dichlorophenyl)-2-(phenylthio)pent-4-enoate (3i). 93%; IR (neat) 3077, 2951, 1732, 1474, 1217 cm^{-1}; ^1H NMR (300 MHz, $CDCl_3$) δ 2.81–2.89 (m, 2 H), 3.70 (s, 3 H), 5.04–5.16 (m, 2 H), 5.79–5.92 (m, 1 H), 7.14–7.38 (m, 8 H); ^{13}C NMR (75 MHz, $CDCl_3$) δ 40.6, 52.8, 63.4, 119.5, 127.1, 128.7, 129.7, 129.8, 129.9, 131.5, 132.1, 132.3, 136.8, 140.0, 171.3; EI-MS (*m*/*z*, relative intensity): 366 (M^+, 23), 325 (14), 257 (86), 225 (33), 189 (78), 162 (52), 109 (34), 71 (100). Anal. calcd for $C_{18}H_{16}Cl_2O_2S$: C, 58.86; H, 4.39. Found: C, 58.87; H, 4.34.

Methyl 2-(1-naphthyl)-2-(phenylthio)pent-4-enoate (3j). 89%; IR (neat) 3053, 2949, 1731, 1438, 1214 cm^{-1}; ^1H NMR (300 MHz, $CDCl_3$) δ 2.95–3.11 (m, 2 H), 3.56 (s, 3 H), 5.07–5.17 (m, 2 H), 6.05–6.17 (m, 1 H), 6.89–6.92 (m, 2 H), 7.04–7.10 (m, 2 H), 7.20–7.28 (m, 3 H), 7.46–7.56 (m, 2 H), 7.75–7.78 (m, 1 H), 7.86–7.89 (m, 1 H), 8.19–8.22 (m, 1 H); ^{13}C NMR (75 MHz, $CDCl_3$) δ 41.2, 52.6, 63.9, 118.6, 124.2, 124.5, 125.3, 125.4, 126.1, 128.2, 129.1, 129.2, 129.3,130.5, 131.0, 133.1, 134.2, 134.9, 137.2, 173.3; EI-MS (*m*/*z*, relative intensity): 348 (M^+, 4), 239 (25), 207 (12), 179 (100), 165 (17), 109 (4), 71 (8), 43 (13). HRMS calcd for $C_{22}H_{20}O_2S$: 348.1184; Found: 348.1185.

1-Phenyl-2-(phenylthio)pent-4-en-1-one (7). 60%; IR (neat) 3075, 1678, 1439, 1240 cm^{-1}; ^1H NMR (300 MHz, $CDCl_3$) δ 2.54–2.64 (m, 1 H), 2.71–2.81 (m, 1 H), 4.50 (dd, J = 8.1, 6.6 Hz, 1 H), 5.06–5.16 (m, 2 H), 5.82–5.96 (m, 1 H), 7.24–7.38 (m, 5 H), 7.42–7.48 (m, 2 H), 7.54–7.59 (m, 1 H), 7.91–7.95 (m, 2 H); ^{13}C NMR (75 MHz, $CDCl_3$) δ 35.0, 50.7, 117.7, 128.5, 128.6, 128.8, 128.9, 131.4, 133.1, 134.7, 134.8, 136.0, 195.1; EI-MS (*m*/*z*, relative intensity): 268 (M^+, 21), 163 (100), 159 (26), 135 (56), 109 (31), 105 (82), 77 (71), 51 (22). Anal. calcd for $C_{17}H_{16}OS$: C, 76.08; H, 6.01. Found: C, 76.20; H, 6.07.

General procedure for the reaction of diazo compound and propargyl sulfide catalyzed by $Rh_2(Ooct)_4$ in water. Diazo compounds **1a–h, j**, **6** (0.2 mmol) and sulfide **4a** (0.3 mmol) were charged in a 25 mL round bottomed flask, 5 mL tap water was added followed by $Rh_2(Ooct)_4$ (0.001 mmol), the mixture was stirred at room temperature until complete disappearance of the diazo substrate. The reaction mixture was then extracted with CH_2Cl_2, dried over anhydrous Na_2SO_4 and concentrated under vacuum. The residue was purified on a silica gel column (petroleum ether–EtOAc, 15 : 1–50 : 1) to afford the products **5a–h, j**, **8**.

Methyl 2-(2-chlorophenyl)-2-(phenylthio)penta-3,4-dienoate (5b). 88%; IR (neat) 3061, 2948, 1954, 1734, 1232 cm^{-1}; ^1H NMR (300 MHz, $CDCl_3$) δ 3.51 (s, 3 H), 4.70 (d, J = 6.6 Hz, 2 H), 5.96 (t, J = 6.6 Hz, 1 H), 7.22–7.43 (m, 8 H), 7.95–7.98 (m, 1 H); ^{13}C NMR (75 MHz, $CDCl_3$) δ 52.6, 63.7, 78.9, 93.8, 126.1, 128.5, 129.0, 129.6, 130.3, 130.4, 130.9, 134.1, 136.8, 137.0, 169.9, 207.8; EI-MS (*m*/*z*, relative intensity): 330 (M^+, 3), 295 (25), 263 (20), 221 (100), 189 (43), 127 (53), 109 (61), 65 (34). Anal. calcd for $C_{18}H_{15}ClO_2S$: C, 65.35; H, 4.57. Found: C, 65.34; H, 4.72.

Methyl 2-(3-chlorophenyl)-2-(phenylthio)penta-3,4-dienoate (5c). 95%; IR (neat) 3060, 2950, 1955, 1733, 1232 cm^{-1}; ^1H NMR (300 MHz, $CDCl_3$) δ 3.69 (s, 3 H), 4.76 (d, J = 6.6 Hz, 2 H), 5.73 (t, J = 6.6 Hz, 1 H), 7.21–7.48 (m, 9 H); ^{13}C NMR (75 MHz, $CDCl_3$) δ 53.0, 63.9, 79.1, 93.5, 126.4, 127.9, 128.4, 128.5, 129.2, 129.4, 130.9, 133.9, 136.7, 140.8, 170.6, 208.3; EI-MS (*m*/*z*, relative intensity): 330 (M^+, 5), 263 (9), 221 (100), 189 (88), 162 (31), 142 (29), 127 (34), 109 (37), 59 (28). Anal. calcd for $C_{18}H_{15}ClO_2S$: C, 65.35; H, 4.57. Found: C, 65.52; H, 4.63.

Methyl 2-(4-bromophenyl)-2-(phenylthio)penta-3,4-dienoate (5e). 95%; IR (neat) 2950, 1955, 1732, 1486, 1232 cm^{-1}; ^1H NMR (300 MHz, $CDCl_3$) δ 3.68 (s, 3 H), 4.74 (d, J = 6.6 Hz, 2 H), 5.73 (t, J = 6.6 Hz, 1 H), 7.21–7.46 (m, 9 H); ^{13}C NMR

(75 MHz, $CDCl_3$) δ 52.9, 63.8, 79.1, 93.6, 121.9, 128.5, 129.3, 129.9, 131.0, 136.6, 137.9, 170.7, 208.2; EI-MS (*m*/*z*, relative intensity): 374 (M^+, 5), 315 (6), 265 (100), 235 (72), 186 (94), 155 (88), 142 (60), 127 (74), 109 (69), 59 (34). Anal. calcd for $C_{18}H_{15}BrO_2S$: C, 57.61; H, 4.03. Found: C, 57.66; H, 4.07.

Methyl 2-(3-methoxyphenyl)-2-(phenylthio)penta-3,4-dienoate (5f). 96%; IR (neat) 2950, 1955, 1732, 1599, 1229 cm^{-1}; ^1H NMR (300 MHz, $CDCl_3$) δ 3.69 (s, 3 H), 4.69–4.80 (m, 2 H), 5.75 (t, J = 6.6 Hz, 1 H), 6.80–6.84 (m, 1 H), 7.02–7.07 (m, 2 H), 7.20–7.38 (m, 6 H); ^{13}C NMR (75 MHz, $CDCl_3$) δ 52.9, 55.2, 64.3, 78.8, 93.7, 113.2, 113.9, 120.3, 128.4, 129.0, 129.1, 131.5, 136.6, 140.3, 159.2, 171.1, 208.3; EI-MS (*m*/*z*, relative intensity): 326 (M^+, 8), 294 (7), 217 (58), 185 (100), 164 (26), 115 (29), 110 (36), 29 (31). Anal. calcd for $C_{19}H_{18}O_3S$: C, 69.91; H, 5.56. Found: C, 69.86; H, 5.63.

General procedure for the reaction of 1g and 4b catalyzed by chiral Rh(II) complex in water. Diazo compound **1g** (0.2 mmol) and sulfide **4b** (0.3 mmol) were charged in a 25 mL round bottomed flask, 5 mL tap water was added, followed by the chiral Rh(II) complex (0.001 mmol), the mixture was stirred at room temperature until complete disappearance of the diazo substrate. The reaction mixture was then extracted with CH_2Cl_2, dried over anhydrous Na_2SO_4 and concentrated under vacuum. The residue was purified on a silica gel column (petroleum ether–EtOAc, 15 : 1) to afford the product **9**. The enantiomeric excess value determined by chiral HPLC: Chiracel OJ-H; hexane–iso-propanol = 70 : 30.

Acknowledgements

The project is generously supported by Natural Science Foundation of China (Grant No. 20572002, 20521202, 20225205, 20390050) and the Ministry of Education of China (Cheung Kong Scholars Program). We thank Professor M. P. Doyle (University of Maryland, USA) for the gift of the chiral Rh(II) catalysts.

References

1 (*a*) J. E. Baldwin, R. E. Hackler and D. P. Kelley, *J. Am. Chem. Soc.*, 1968, **90**, 4758; (*b*) G. M. Blackburn, W. D. Ollis, C. Smith and I. O. Sutherland, *Chem. Commun. (London)*, 1968, 186; (*c*) J. E. Baldwin, R. E. Hackler and D. P. Kelley, *Chem. Commun. (London)*, 1968, **537**, 538.
2 For reviews in the area, see: (*a*) B. M. Trost and L. S. Melvin, Jr., *Sulfur Ylides*, Academic Press, New York, 1975, ch. 7; (*b*) E. Vedejs, *Acc. Chem. Res.*, 1984, **17**, 358; (*c*) M. P. Doyle, M. A. McKervey and T. Ye, *Modern Catalytic Methods for Organic Synthesis with Diazo Compounds*, Wiley-Interscience, New York, 1998; (*d*) A.-H. Li, L.-X. Dai and V. K. Aggarwal, *Chem. Rev.*, 1997, **97**, 2341; (*e*) M. P. Doyle and D. C. Forbes, *Chem. Rev.*, 1998, **98**, 911; (*f*) O. M. Hodgson, F. Y. T. M. Pierard and P. A. Stupple, *Chem. Soc. Rev.*, 2001, **30**, 50.
3 W. Ando, *Acc. Chem. Res.*, 1977, **10**, 179.
4 (*a*) W. Kirmse and M. Kapps, *Chem. Ber.*, 1968, **101**, 994; (*b*) M. P. Doyle, J. H. Griffin, M. S. Chinn and D. van Leusen, *J. Org. Chem.*, 1984, **49**, 1917.
5 (*a*) D. S. Carter and D. L. Van Vranken, *Org. Lett.*, 2000, **2**, 1303; (*b*) C.-Y. Zhou, W.-Y. Yu, P. W. H. Chan and C.-M. Che, *J. Org. Chem.*, 2004, **69**, 7072.
6 For recent reviews, see: (*a*) U. M. Lindstrom, *Chem. Rev.*, 2002, **102**, 2751; (*b*) R. Breslow, *Acc. Chem. Res.*, 2004, **37**, 471; (*c*) C.-J. Li, *Chem. Rev.*, 2005, **105**, 3095; (*d*) C.-J. Li and L. Chen, *Chem. Soc. Rev.*, 2006, **35**, 68.
7 (*a*) R. P. Wurz and A. B. Charette, *Org. Lett.*, 2002, **4**, 4531; (*b*) N. R. Candeias, P. M. P. Gois and C. A. M. Afonso, *Chem. Commun.*, 2005, 391; (*c*) N. R. Candeias, P. M. P. Gois and C. A. M. Afonso, *J. Org. Chem.*, 2006, **71**, 5489; (*d*) J. M. Antos and M. B. Francis, *J. Am. Chem. Soc.*, 2004, **126**, 10256.
8 S. Narayan, J. Muldoon, M. G. Finn, V. V. Fokin, H. C. Kolb and K. B. Sharpless, *Angew. Chem., Int. Ed.*, 2005, **44**, 3275.
9 Y. Nishibayashi, K. Ohe and S. Uemura, *J. Chem. Soc., Chem. Commun.*, 1995, 1245.
10 (*a*) T. Fukuda, R. Irie and T. Katsuki, *Tetrahedron*, 1999, **55**, 649; (*b*) D. W. McMillen, N. Varga, B. A. Reed and C. King, *J. Org. Chem.*, 2000, **65**, 2532; (*c*) S. Kitagaki, Y. Yanamoto, H. Okubo, M. Nakajima and S. Hashimoto, *Heterocycles*, 2001, **54**, 623; (*d*) X. Zhang, Z. Qu, Z. Ma, W. Shi, X. Jin and J. Wang, *J. Org. Chem.*, 2002, **67**, 5621; (*e*) X. Zhang, M. Ma and J. Wang, *Tetrahedron: Asymmetry*, 2003, **14**, 891; (*f*) X. Zhang, M. Ma and J. Wang, *Chin. J. Chem.*, 2003, **21**, 878; (*g*) M. Ma, L. Peng, C. Li, X. Zhang and J. Wang, *J. Am. Chem. Soc.*, 2005, **127**, 15016.
11 (*a*) H. M. L. Davies and D. K. Hutcheson, *Tetrahedron Lett.*, 1993, **34**, 7243; (*b*) H. M. L. Davies, P. R. Bruzinski, D. H. Lake, N. Kong and M. J. Fall, *J. Am. Chem. Soc.*, 1996, **118**, 6897.
12 M. C. Pirrung and J. Zhang, *Tetrahedron Lett.*, 1992, **33**, 5987.
13 M. P. Doyle, S. B. Davies and W. Hu, *Org. Lett.*, 2000, **2**, 1145.
14 M. P. Doyle, A. B. Dyatkin, M. N. Protopopova, C. I. Yang, C. S. Miertschin, W. R. Winchester, S. H. Simonsen, V. Lynch and R. Ghosh, *Recl. Trav. Chim. Pays-Bas*, 1995, **114**, 163.
15 M. P. Doyle, W. R. Winchester, J. A. A. Hoorn, V. Lynch, S. H. Simonsen and R. Ghosh, *J. Am. Chem. Soc.*, 1993, **115**, 9968.
16 M. P. Doyle, Q.-L. Zhou, C. E. Raab, G. H. P. Roos, S. H. Simonsen and V. Lynch, *Inorg. Chem.*, 1996, **35**, 6064.

Environmental Science Books

Issues in Environmental Science & Technology

Series Editors:
R E Hester and R M Harrison
Format: **Hardback**
Price: **£45.00**
RSC Member Price: **£29.25**

Written by leading experts, this series presents a multidisciplinary approach to pollution and the environment. Focussing on the science and broader issues including economic, legal and political considerations.

Chemicals in the Environment Assessing and Managing Risk Vol. No. 22

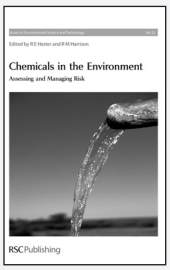

Beginning with a review of the current legislation, the books goes on to discuss scientific and technical issues relating to chemicals in the environment and future developments.
2006 | xvi+158 pages | ISBN-10: 0 85404 206 7
ISBN-13: 978 0 85404 206 7

Sustainability in Agriculture Vol. No. 21

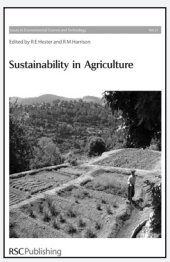

Discusses the key factors impacting on global agricultural practices including fair trade, the use of pesticides, GM products and government policy.

2005| xiv+130 pages | ISBN-10: 0 85404 201 6
ISBN-13: 978 0 85404 201 2

Alternatives to Animal Testing Vol. No. 23

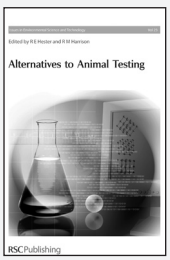

Provides an up-to-date discussion on the development of alternatives to animal testing including; international validation, safety evaluation, alternative tests and the regulatory framework.
2006 | xii+118 pages | ISBN-10: 0 85404 211 3
ISBN-13: 978 0 85404 211 1

Practical Environmental Analysis 2nd Edition

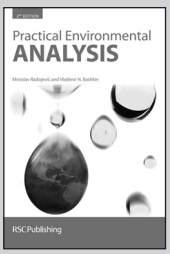

By *M Radojevic and V N Bashkin*
A new edition textbook providing an-up-to date guide to practical environmental analysis. Ideal for students and technicians as well as lecturers wishing to teach the subject.

Hardback | 2006 | xxiv+458 pages | £39.95 | RSC member price £25.75 | ISBN-10: 0 85404 679 8 | ISBN-13: 978 0 85404 679 9

Clean Energy (RSC Clean Technology Monographs)

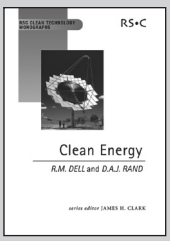

By *R M Dell* and *D A J Rand*
Series Editor *J H Clark*
Covering a broad spectrum of energy problems, this highly accessible book discusses in detail strategies for the world's future energy supply.

Hardback | 2004 | xxxvi+322 pages | £89.95 | RSC Member Price £58.25 | ISBN-10: 0 85404 546 5| ISBN-13: 978 0 85404 546 4

An Introduction to Pollution Science

By *R M Harrison*
A student textbook looking at pollution and its impact on human health and the environment. Covering a wide range of topics including pollution in the atmosphere, water and soil, and strategies for pollution management.

Hardback | 2006 | ca xii+322 pages | £24.95 | RSC Member Price £16.50 | ISBN-10: 0 85404 829 4 | ISBN-13: 978 0 85404 829 8

Water Contamination Emergencies Enhancing Our Response

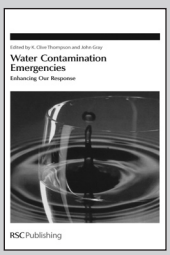

By *J Gray* and *K C Thompson*
A look at the impact and response of contaminated water supplies including the threat of chemical, biological, radiological and nuclear (CBRN) events.

Hardback | 2006 | x+372 pages | £99.95 | RSC Member Price £64.75 | ISBN-10: 0 85404 658 5| ISBN-13: 978 0 85404 658 4

RSC Publishing **www.rsc.org/books**

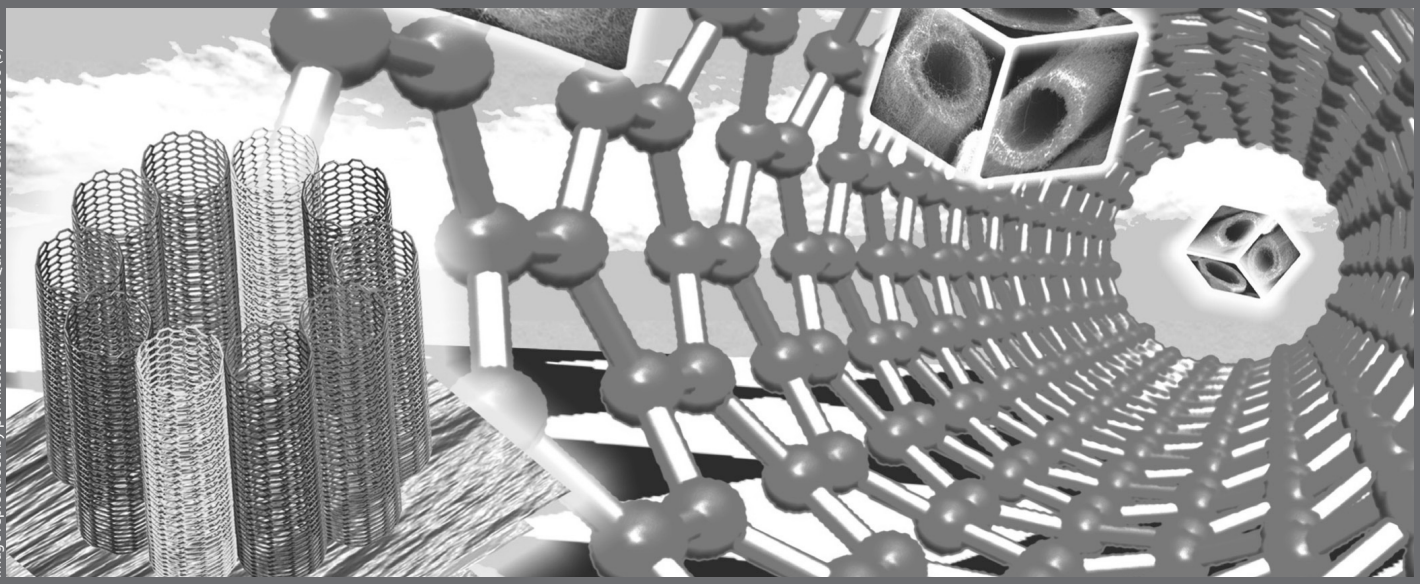

ChemComm

A leading international journal for the publication of communications on important new developments in the chemical sciences.

- Weekly publication
- Impact factor: 4.426
- Rapid publication – typically 60 days
- 3 page communications – providing authors with the flexibility to develop their results and discussion
- More than 40 years publishing excellent research
- High visibility – indexed in MEDLINE

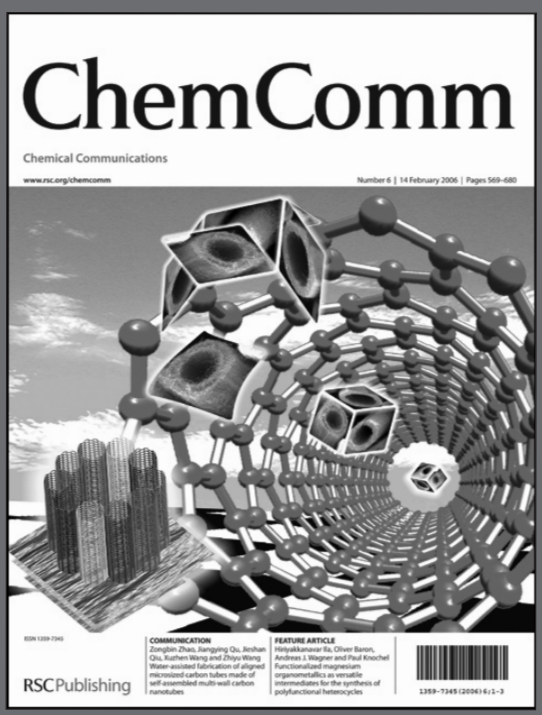

RSC Publishing

www.rsc.org/chemcomm

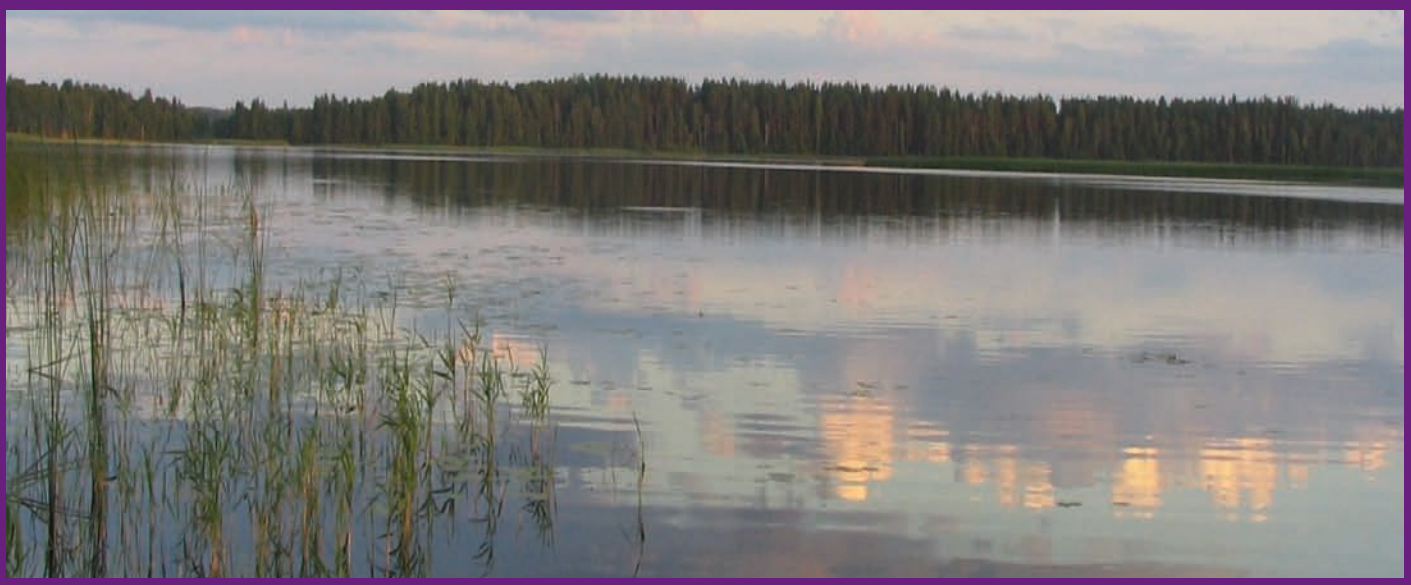

Image reproduced by permission of Ainis Pivoras, *J. Environ. Monit.* 2006, **8**(3)

Journal of Environmental Monitoring

Comprehensive, high quality coverage of multidisciplinary, international research relating to the measurement, pathways, impact and management of contaminants in all environments.

- Dedicated to the analytical measurement of environmental pollution
- Assessing exposure and associated health risks
- Fast times to publication
- Impact factor: 1.578
- High visibility - cited in MEDLINE

RSC Publishing

www.rsc.org/jem